Modeling and Mapping of MaeLa Refugee Camp Water Supply

by

Navid Rahimi

B.Sc., Civil Engineering
University of Virginia, 2007

SUBMITTED TO THE DEPARTMENT OF CIVIL AND ENVIRONMENTAL ENGINEERING IN PARTIAL FULFILLMENT OF THE REQUIREMENTS FOR THE DEGREE OF

MASTER OF ENGINEERING IN CIVIL AND ENVIRONMENTAL ENGINEERING
AT THE
MASSACHUSETTS INSTITUTE OF TECHNOLOGY

JUNE 2008

Signature of Author _____
Department of Civil and Environmental Engineering
May 19, 2008

Certified by _____
Peter Shanahan
Senior Lecturer, Civil and Environmental Engineering

Accepted by _____
Daniele Veneziano
Professor, Civil and Environmental Engineering
Chairman, Departmental Committee for Graduate Students

MODELING AND MAPPING OF MAELA REFUGEE CAMP WATER SUPPLY SYSTEM

By

NAVID RAHIMI

Submitted to the Department of Civil and Environmental Engineering
on May 19, 2008 in partial fulfillment of the requirements of
the degree of Master of Engineering in Civil and Environmental Engineering

ABSTRACT

This thesis describes the development and use of a model, using the EPANET computer code, to simulate the three-hour intermittent MaeLa refugee camp water supply.

In coordination with Aide Médicale Internationale, a field survey and pressure, flow and salt tracer testing were conducted as a basis to model the water distribution system in MaeLa, Thailand. The collected data was assembled in EPANET and controls were added to best represent the functioning of the water system and to simulate the calibration tests. The model simulated field parameters successfully despite inaccuracies in elevation due to imprecise instrumentation. The model served as a tool to further understand the dynamics of the system such as mixing in the supply tanks, connections between subsystems and system controls.

The distribution model was used to evaluate three alternative scenarios to improve system performance. The objective of the first and second scenario was to increase the flow rate at taps of low supply; the third scenario aimed at adding taps to parts of the camp without easy access to running water. The first scenario consisted in opening valves to connect subsystems: it increased the flow rate at taps of large supply more so than at taps of low supply. This scenario was not recommended because it would quickly drain parts of the water supply. The second scenario consisted in adding connecting pipes between subsystems of high pressure and those of low pressure. It was recommended because it would increase the flow rate of low and medium supply taps. For the third scenario, areas of the camp without easy access to water were defined by using the result of mapping the current system and the population distribution in a Graphical Information System software. These new taps were successful in providing water to these areas without significantly affecting the rest of the system. An additional recommendation for increasing the water supply in the camp was found from analyzing tank level: because tanks would not drain by the end of the distribution period, it was recommended that the period of water supply be increased from 3 hour periods to 4½ hours.

Further study is recommended for improving the elevation accuracy of the model, running more calibration studies and running an optimization model for maximizing water supply.

Thesis Supervisor: Peter Shanahan

Title: Senior Lecturer, Department of Civil and Environmental Engineering

ACKNOWLEDGMENTS

I have never been keen on acknowledgments: the issue to me is the implication that I have achieved something great. Sitting in front of a computer for countless hours is not an accomplishment in of itself; standing up to that knowledge to use it at the service of humankind is where the task takes its full meaning. I am asking that this thesis not be viewed as an end but as a mean.

I would like to thank my family for constantly supporting me, though not always sure what it is that I do. Thank you to Peter Shanahan, my advisor, for all the time and energy dedicated to this work. Thank you to the AMI-Thailand staff for giving me the opportunity to contribute to such a tremendous project.

Author contact: navidrahimi9@gmail.com

Table of Contents

INTRODUCTION

The present thesis is offered in fulfillment of the requirements of the Master of Engineering degree in Environmental Engineering offered by the Massachusetts Institute of Technology.

MaeLa refugee camp is located along the border of Thailand and Myanmar and the current water distribution system is overseen by Aide Médicale Internationale (AMI). After conducting a water assessment to trace cholera outbreaks, Daniele Lantagne from the Center for Disease Control and Prevention (CDC) recommended a collaboration between the M.I.T. Master of Engineering Program and AMI to work on a comprehensive study of the existing water supply and distribution system. Navid Rahimi, Mary Harding and Katherine Vater collaborated on both the distribution modeling and water quality aspects of this project.

The following work focuses on the water supply system, its modeling and mapping. It was motivated by the need to develop analysis tools to identify areas of improvements and a further understanding of the complexities of this water distribution system which supplies drinking water to close to 50,000 individuals. AMI is currently planning an expansion in the geographical coverage of the water system, and a modeling tool would provide predictions of the performance of the system if new taps were added to portions of the system. It would also allow testing potentially superior designs of the piping system layout or increasing the system volumetric capacity.

This work is closely related to the mapping of the distribution system conducted by Mary Harding (2008). The objective is that results from the modeling analysis could be transferred to the Geographical Information System interface to run further analyses. Then, questions of water supply per person per day, or water collection travel time could be answered. This project is also conducted in the context of the hand-over of responsibilities between AMI and another NGO, Solidarites. As such, the model needs to be clearly laid out, easily accessible and transferable.

The project setting including a presentation of the situation at the camp and its water supply is presented in Chapter 2. Chapter 3 describes the methodology used in the field work followed by a description of the modeling work including the assumptions made on issues such as intermittent distribution and a technical background on modeling. Chapter 4 presents the results of the work such as analysis of the calibration tests, the determination of emitter coefficients, dispersion calculations, mixing models used for the tanks and more. Chapter 5 consists of a discussion of these results, the weaknesses of the model, and recommendations for further work.

I. PROJECT SETTING

This chapter is the result of a collaboration between Katherine Vater, Mary Harding and Navid Rahimi.

I.1 THE THAILAND – MYANMAR BORDER

MaeLa camp is a refuge for thousands of people seeking protection from persecution in Myanmar. Ongoing turmoil shapes the lives of the people within the camp. In addition to being aware of why and under what conditions people are living in these camps, the climate and geography of the region are vital to understanding the available water resources.

I.1.A Politics

In September 1988 a military junta took control in Burma killing as many as 10,000 people (Lansner, 2006). The military regime has placed restrictions on work and civil liberties and has become increasingly brutal, especially towards ethnic minorities. As a result, a large number of people from Myanmar have fled to escape poverty or persecution. It is estimated that the largest number, about 2 million people, have migrated into Thailand, although the exact numbers are unknown. Of these, about 140,000 reside in United Nations (UN) sanctioned camps and 500,000 are registered migrant workers. The rest remain unregistered and attempt to stay unnoticed to avoid being deported back across the border (Fogarty, 2007).

Wages in Myanmar are not sufficient to meet the basic needs of most families. Acquiring legal working papers in Thailand allows migrants to work for one year and gives them a better chance of receiving at least the minimum wage and decent working conditions upon arrival. Many Thai business owners rely on illegal workers for an unending supply of cheap labor. In Mae Sot, the closest city to the MaeLa camp, it is estimated that around 50% of the 80,000 Myanmar people have papers (McGeown, 2007). Illegal residents are often forced to pay bribes to Thai authorities. In many cases, a migrant detained by Thai authorities is dropped on the other side of the border and can merely pay a small bribe to the Myanmar guard to return again to Thailand. When reported to the Myanmar government, however, heftier fines must be paid in order to avoid jail time (McGeown, 2007).

Much of the challenge for these migrants stems from the fact that Thailand is not a signatory of the UN Refugee Convention. As such, the government only grants asylum to those fleeing combat

as opposed to those fleeing human rights violations (Refugees International, 2007). This makes the situation complicated as the UN-sanctioned camps along the border are officially called temporary shelters by the Thai government, while in reality many families have lived in these camps for more than 20 years. It is the intention of the Thai government that the residents either return to Myanmar or move on and repatriate to another nation. It is illegal, yet common practice, for camp residents to work in the surrounding Thai towns. They will generally try to find whatever day labor is available and send money earned back to Myanmar to provide for remaining family members (D. Lantagne, personal communication, October 19, 2007).

Native hill tribes, which historically lived impartially across Northern Thailand and what is now Myanmar, make up a large majority of the resettling group. The Karen, Karenni, Shan, and Mon are the main tribes that are being driven from their homes by the Myanmar military (McGeown, 2007). Within Myanmar there is some resistance from the Karen National Liberation Army (KNLA) which is fighting for an independent Karen state. There were additional rebel armies, but over the past 20 years most have agreed to ceasefires with the military junta. Many of the refugees in the camps in Thailand are sympathetic to the KNLA, and some have even served in it (McGeown, 2007).

The Karen believe strongly in the value of family. As a result, decisions to leave the camps and repatriate are difficult and must be made as a family. Generally, the teenagers and young adults who have lived most of or all of their lives inside the camp want to repatriate elsewhere while older generations hope to return to Burma if it is restored (D. Lantagne, personal communication, October 19, 2007).

I.1.B Economy

As described above, there is a significant amount of poverty in Myanmar as a result of the military junta's overbearing controls and inefficient economic policies. Inconsistent exchange rates and a large national deficit create an overall unstable financial atmosphere (CBS, 2007). Although difficult to accurately assess, it is estimated that the black market and border trade could encompass about half of the country's economy. Importing many basic commodities is banned by the Myanmar government and exportation requires time and money (McGeown, 2007). Timber, drugs, gemstones and rice are major imports into Thailand while fuel and basic consumer goods such as textiles and furniture are returned (CBS, 2007).

By night, the Moei River, which divides the two countries, is bustling with illicit activity. Through bribing several officials, those who ford the river are able to earn a modest profit (for

example around 2 USD for a load of furniture) and provide a service to area merchants and communities. Thailand benefits from a robust gemstone business that draws dealers from all over the world. The Myanmar mine owners would get a fraction of the profit by dealing directly with the government (McGeown, 2007).

I.1.C Climate in Northern Thailand

The Tak region of northern Thailand is characterized by a tropical climate with wet and dry seasons (UN Thailand, 2006; ESS, 2002). The rainy season lasts from June to October, followed by a cool season until February. The weather turns hot and sunny between March and May (UN Thailand, 2006). The northern region of Thailand has an average temperature of 26ºC although there is significant variation over the year due to elevation differences. Typical temperatures range from 4ºC to 42ºC (Thailand Meterological Department in ECC, 2002). The average annual rainfall in Mae Sot, Thailand is 2100 millimeters (mm) (GOSIC, 1951-2007), and Figure 1-1 shows the monthly rainfall averages over the past 56 years. June through October is the rainy season when more than 85% of the 2100 mm falls.

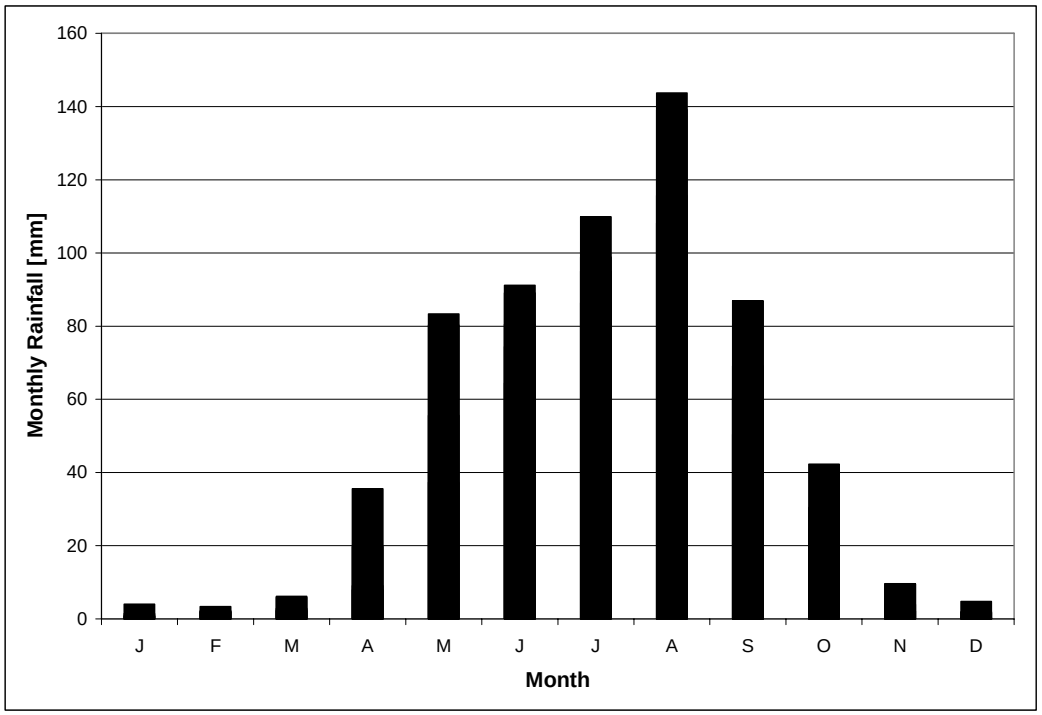

Figure 1-1: Average Monthly Rainfall for Mae Sot, Thailand (GOSIC, 2007).

I.2 MAELA CAMP

The MaeLa camp is a refuge for people seeking protection from the Myanmar government and from warfare along the Thailand-Myanmar border (McGeown, 2007). The camp is run by the United Nations High Commissioner on Refugees and has existed since 1984 (TBBC, No Date).

I.2.A Location and Demographics

MaeLa is located near 16º30'N and 98º30'E in the northern region of Thailand about ten kilometers from the border with Myanmar (TBBC, No Date). The camp location is shown by the red circle in Figure 1-2. MaeLa is home to about 45,000 refugees, mainly of the Karen ethnic minority (UNHCR, 2007; TBBC, No Date). There are reportedly more than six million Karen people living in Myanmar and about 400,000 living in Thailand (KarenPeople, 2004). These numbers may not account for the approximately 150,000 Karen refugees living in refugee camps in Thailand (UNHCR, 2007).

Figure 1-3 shows the relative populations, ethnicities, and age demographics of the UN refugee camps in Thailand. MaeLa is the largest camp with about half of its population 18-59 years old and one-third 5-17 years old.

Figure 1-2: Location of MaeLa Refugee Camp (Maps-Thailand, 2006)

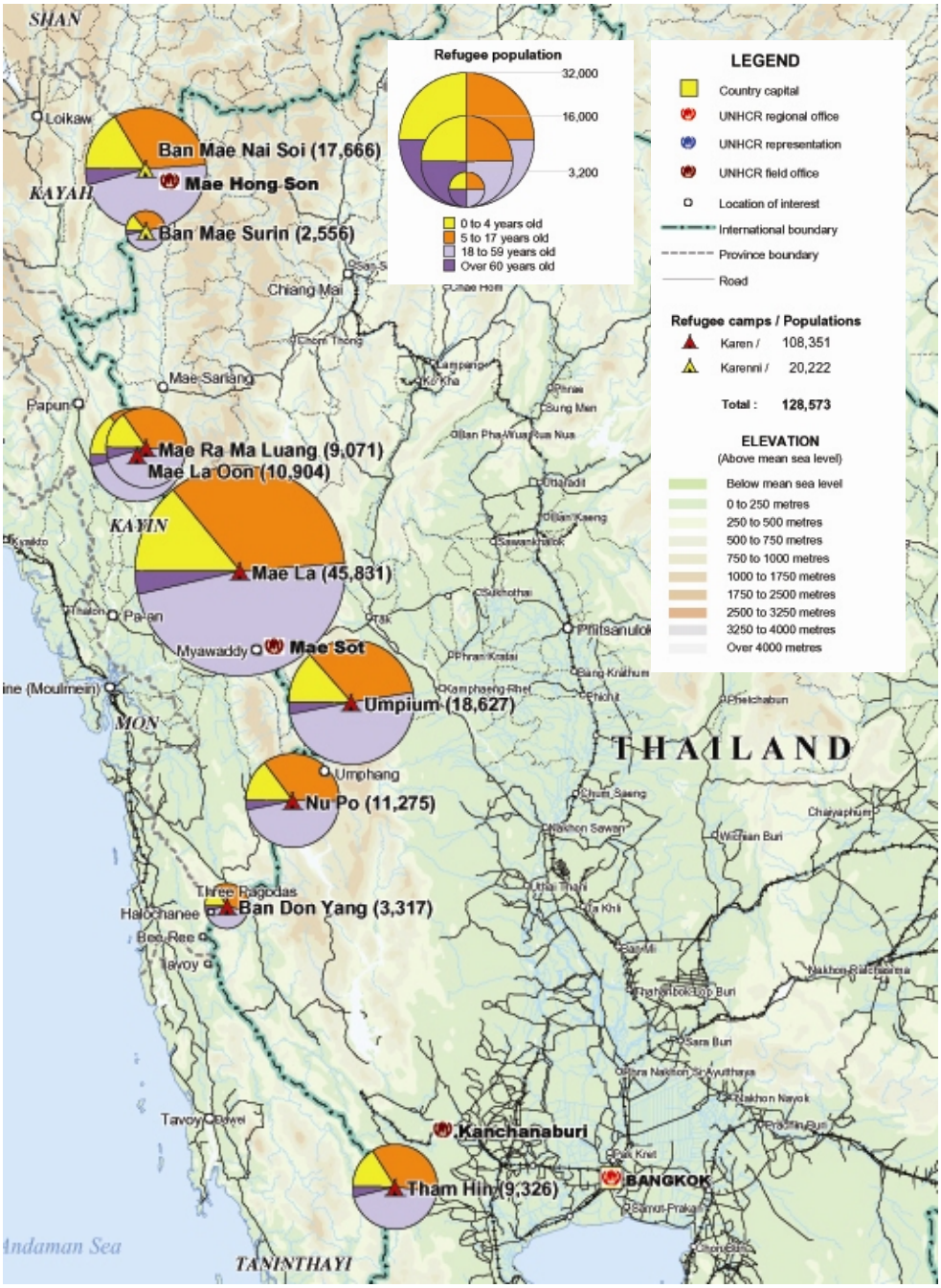

Figure 1-3: UN Refugee Camp Populations and Demographics (UNHCR, 2006).

The camp is located in a valley surrounded by two ridges rising about 300 meters above the camp. These hills are distant extremities of the Himalayan mountain range which is mainly located northwest of Thailand. A UN-protected road links the camp with the nearest Thai city of Mae Sot, which has a population of about 40,000 Thai and an unofficial count of about 80,000 illegal Burmese

residents (TBBC, No Date; Brinkhoff, 2007; McGeown, 2007). Mae Sot is an hour away from MaeLa by car. The nearest larger city is Tak; Bangkok is about 500 kilometers southeast of Mae Sot (Google, 2007). The key features of the camp including pumps, storage tanks and some springs are shown in Figure 1-4, which is an image from Google Earth (with data from Lantagne, 2007).

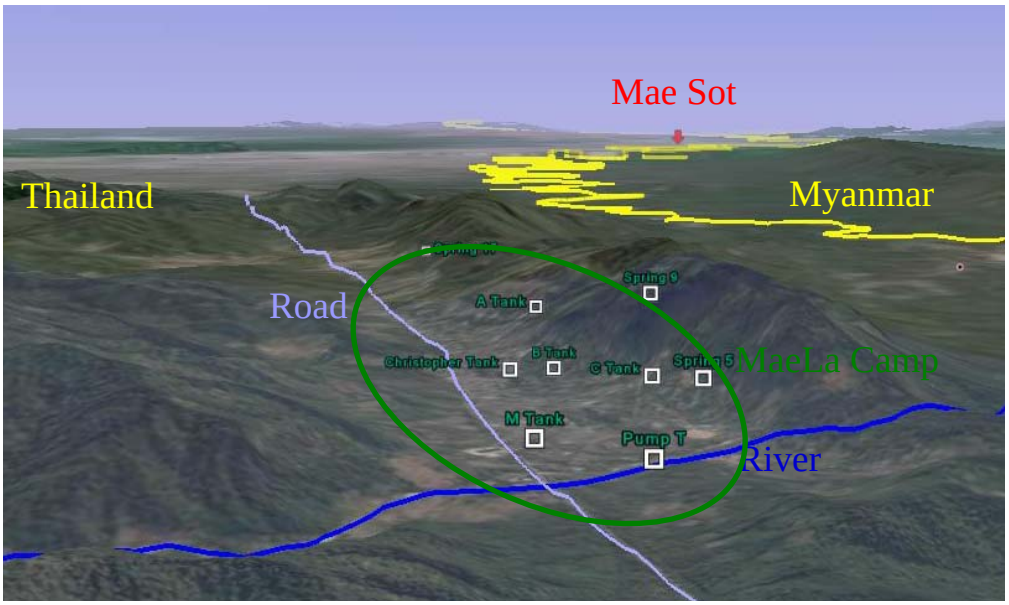

Figure 1-4: MaeLa Location, looking southeast.

I.2.B AMI & Solidarites

Created in 1979, AMI works to restore systems related to people's health. Currently they have approximately 25 projects in 9 countries. The projects are related to improving drinking water access, education, healthcare, and job opportunities; and resisting religious, sexual and ethnic discrimination (AMI, 2007b).

In 1995, AMI took over healthcare and some water and sanitation services for MaeLa and two other camps in the region from Medecins Sans Frontieres (Polprasert et al., 2006). Maintaining and running the water supply system of the MaeLa camp is a major component of AMI's involvement. A team of about 30 AMI employees and camp residents work each day to ensure camp residents have access to clean water. Between August and December 2008, AMI will turn over their water responsibilities to Soldarités, the NGO currently responsible for the camp's waste disposal (F. Pascal, personal communication, October 30, 2007). Having one NGO responsible for both the

water and sanitation is logical. The two systems are linked as drinking water quality is affected greatly by waste contamination and having the two systems coordinate should increase overall health (Polprasert et al., 2006).

I.3 MAELA WATER RESOURCES

I.3.A Water Supply and Use

The water sources in MaeLa are surface water from a river, naturally flowing springs, groundwater wells and boreholes. The river runs east-west, cross-cutting the end of the ridges that border the camp. The springs are located at higher elevations along the western ridge while rope-pump wells and boreholes are located at low elevations in the housing area of the camp. An example of a rope-pump well is shown in Figure 1-5. It is an improved water source by UN definition, but some of the wells are contaminated by sewerage (D. Lantagne, personal communication, October 19, 2007). The water supply can be divided into drinkable water, that from the distribution system which originates from springs and the river, and non-drinkable water. The rope-pump wells, boreholes and other alternate sources of water are not within the scope of this thesis. The thesis deals with distribution of the drinkable water from tanks to public taps.

Figure 1-5: Typical rope-pump well
(Lantagne, 2007)

Most of the spring- and all of the river-supplied water is only available during three-hour blocks each morning and afternoon. Once water reaches the public taps, residents fill containers until the entire volume of water has been collected. Figure 1-6 shows the available water volume for the first seven months of 2006 by month and source – the river water is called pumped water.

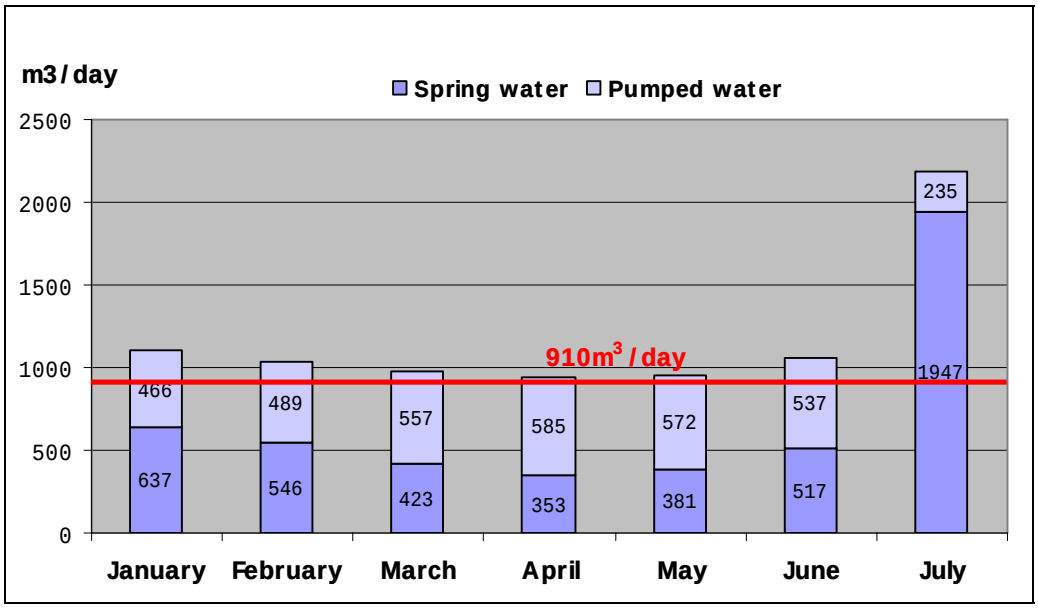

Figure 1-6: Division of Flow Volume from Storage Tanks by Source (Brizou, 2006).

People store their water in containers on their porches and in their homes. An example of this is shown in Figure 1-7. If water goes unused, it is discarded and the containers are refilled the following day (Lantagne, personal communication, October 19, 2007). This makes understanding the water balance and actual demand of the camp difficult, because not all the water collected is used. To resolve this problem, it is assumed that the water supply is pressure-driven rather than demand-driven as discussed later.

Figure 1-7: Water Storage Containers on Porch (Lantagne, 2007).

Infrastructure is not the only necessary step to promote the distribution of clean, safe drinking water. Safe water storage and improved sanitation infrastructure are an important part of disease reduction, as much as clean water (Wagner and Lanoix, 1959; Alekal et al., 2005). Although these aspects are outside the scope of this work, they must be part of the total community health plan.

I.3.B Water System

Water in MaeLa comes from a range of sources, not all of which are maintained by AMI. Water from the springs and river is treated and made available through public tap stands. Other sources of water are available, but the quality is not as good as the water from the taps (Lantagne, 2007). The scope of this thesis includes the river and spring water and particularly the distribution system which conveys it to the users.

a. Layout

The MaeLa distribution system provides water to around 45,000 people. It was developed incrementally as the camp population grew. This explains the heterogeneous character of the system through which water is supplied from open boreholes, rope-pump wells, and the tap distribution system. The distribution system, which is supplied by multiple sources, is fragmented and has a variety of pipe sizes and lengths.

AMI funded most of the water system with a total of 17 boreholes, 63 rope-pump wells and 152 tap stands. Some spring connections supplying a minority of taps are isolated and run straight from spring to tap without affecting the central distribution system. This thesis does not address these connections and focuses instead on the major parts of the distribution system. It is estimated that tap stands provides the majority of the water supply (Lantagne, 2007). The water is free for residents of the camp. Both AMI and the users would like to improve accessibility, quality and quantity of the supply. The locations of the various sources are shown in Figure 1-8.

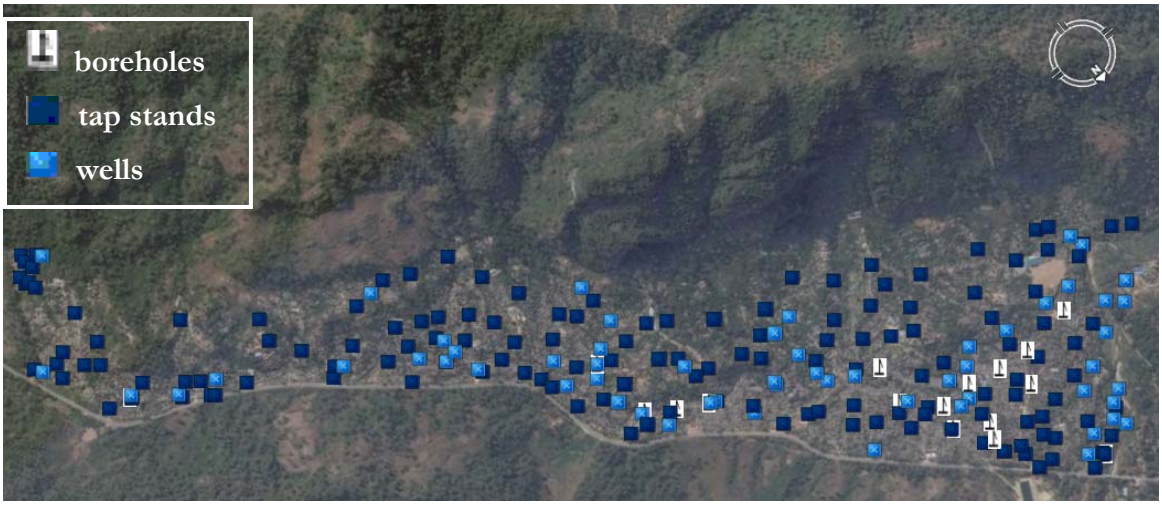

Figure 1-8: Distribution of boreholes, rope-pump wells and tap stands (Lantagne, 2007)

The tap distribution system provides water to over three-fourths of the population (Lantagne, 2007). The system is supplied by the adjacent river to the northwest of the camp, and a series of springs found in the hills to the southwest. Water is pumped from the river and naturally flows from the springs into storage tanks, where water is treated and released to the pipes, reaching the taps solely by gravity. It should be noted that even though some private standpipes exist (such as those for the school or the hospital), the vast majority of the standpipes shown in Figure 1-8 are public. The tanks are open twice a day to provide water at the standpipes, for 3 hours each from 6 to 9 AM and 3 to 6 PM. Figure 1-9 illustrates the layout of the storage tanks, springs, and pumps.

There are six major tanks: A Tank, B Tank, C Tank, Christopher Tank, MOI Tank and Spring 17 Tank which give rise to six mostly independent systems. The MOI and C Tanks are the largest tanks, with the MOI Tank providing water to the densely populated north corner. C Tank connects to Spring 8 to distribute water west and to Springs 6 and 7 to distribute water east. Spring 17 Tank collects water from Spring 17, located to the southeast of the camp, out of the range of Figure 1-9.

Spring 14 supplies water to a limited number of taps and connects to the A-Tank distribution system to supplement it during the rainy season. Each system covers a certain portion of the camp.

Figure 1-10 is a comparison of the flow from the different tanks from January to October 2007. Generally the flow is reduced entering the rainy season. It is clear that C Tank (CT) and MOI Tank have the largest flows, at approximately 200 cubic meters per day. A Tank (AT), B Tank (BT), Christopher Tank (CH) and Spring 17 Tank (17) have about half that flow volume.

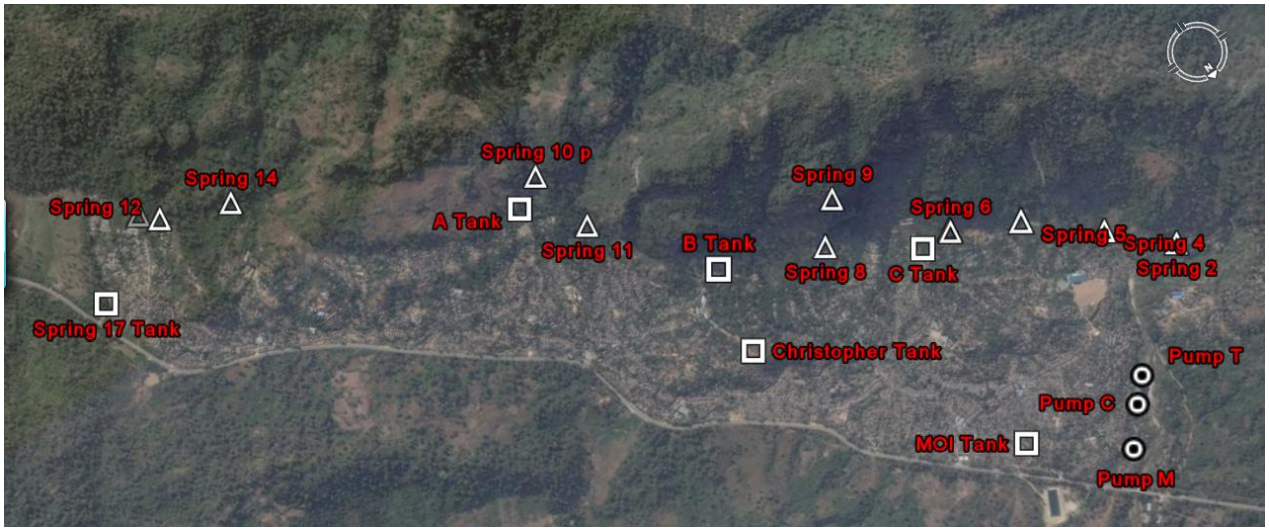

Figure 1-9: Storage tanks, springs and pumps (Lantagne, 2007)

There are a total of 13 springs that provide water to the system. Springs 10 and 17 have the largest flow volumes throughout most of the year. Some springs connect to one of the main tanks' systems, while others flow directly into distribution pipes. These isolated springs include: Springs 15 and 12, which join to supply water to the south-east area; Spring 11 in the central area; Spring 2 for the south-west area; and the smallest springs, 5 and 4, nearest the river. These springs are not included in the model. Only Springs 17, 6 and 7, 8 and 14 are considered which connect to major systems. Each spring also possesses its own small distribution tank called a ring tank because it is made out of a certain number of concrete rings of 1.13 meter inner diameter and 0.4 meter height.

Figure 1-11 compares the flow volumes for the different springs in 2007. The sources have been organized by geographic location from the river side (northwest) to Spring 17 (southeast). Springs 2, 4 and 5 were grouped because they are isolated systems near the river. Springs 6, 7 and 8 were grouped because they all connect to C tank system. Springs 12 and 15 are grouped because they flow down the same distribution pipes.

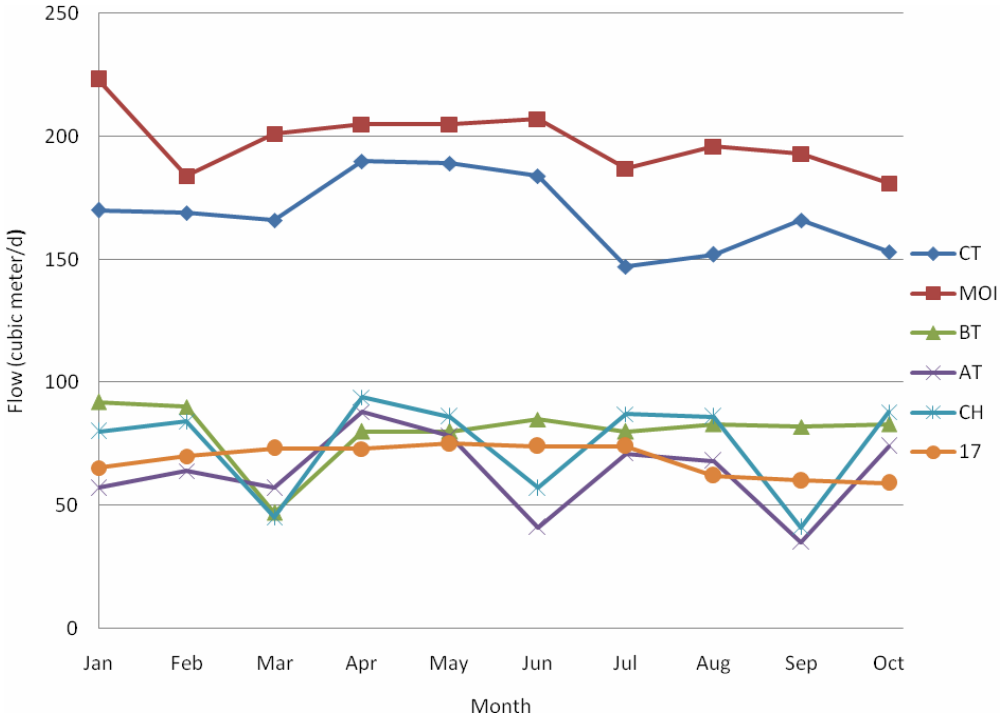

Figure 1-10: Average monthly flow from tanks in 2007 (AMI, 2007).

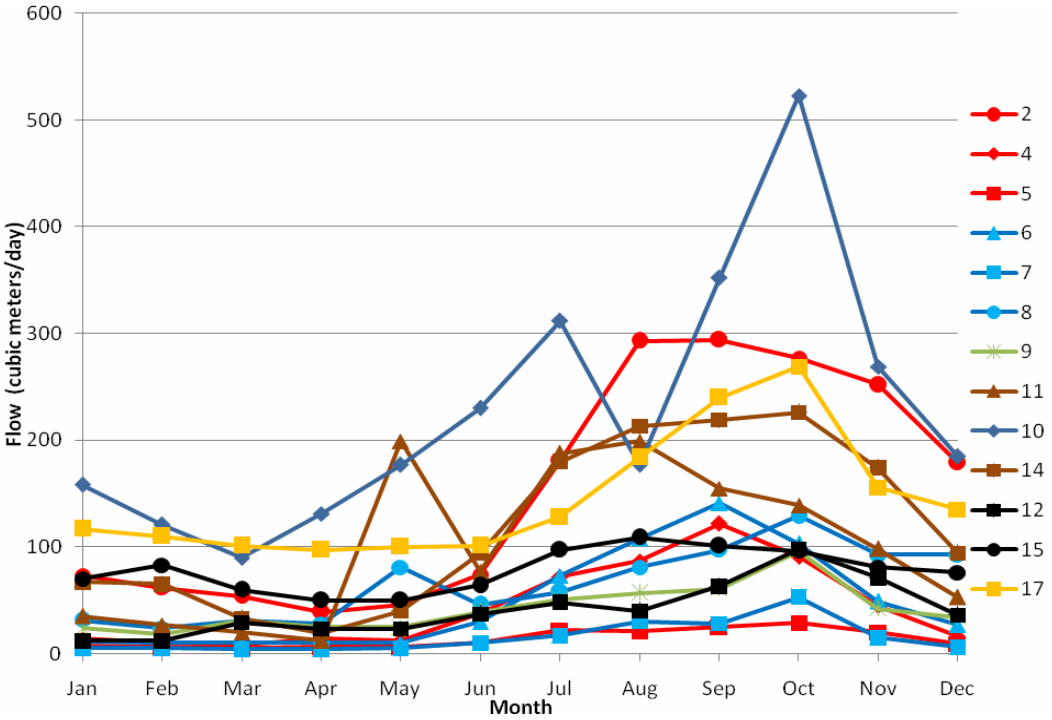

Figure 1-11: Spring Flow in 2007.

One of the general trends deduced from the graph is an increase in flow volumes from the dry season (February) to the rainy season (August) with a delay of about two months. Notice that Springs 10, 17, 2, 11 and 14 provide a larger volume than the rest of the sources, but only Springs 17 and 14 is included in the model out of these, in addition to Springs 6,7 and 8.

Secondary tanks are not represented in Figure 1-9. These consist of storage tanks used for special facilities and include the MaeLa 1 and 2 office ring tanks, the buddhist temple ring tanks and the Tuberculosis Village (TB Village) ring tank. These tanks, except the one for the TB Village, are filled during the distribution period to the same as public taps connected to the same distribution system. The TB Village ring tank on the other hand receives water that is pumped from Spring 17 Tank in order to start full during the distribution periods. This does not affect the level of the Spring 17 Tank since it is supplied by a constantly streaming spring.

Another characteristic of the system is the seasonal variation of supply. The dry and rainy seasons cause lower or higher flow from the springs, which might reduce the need and costs associated to pumping water from the river. In addition, there are valves between systems which are opened and closed depending on the needs of the system. For example, the Spring 17 subsystem may be able to supply water to the periphery of the Christopher Tank subsystem when Spring 17 is running high and vice-versa. The Spring 6/7 system may also supplement edges of the MOI subsystem just as the Spring 14 system may supplement the A Tank subsystem. The model however assumes that all these valves are closed (as it was the case during the dry season) and that the major tanks as well as spring tanks start full during distribution. These assumptions may be modified however to simulate the varying pumping and distribution decisions.

There are three pumps used to drive the river water to tanks: Tim Pump, Christopher Pump and MOI Pump. The flows associated with each pump are shown in Figure 1-12. Tim Pump drives river water to tanks A, B, C and Christopher; Christopher Pump to Christopher Tank and MOI Tank; and MOI Pump to MOI Tank as well as recently, on an intermittent basis, to a storage pond.

The general trend of pumping is similar to that of the tanks. A lower pumping rate is noted entering the rainy season because more water is available from the springs, so there is less need to pump water from the river.

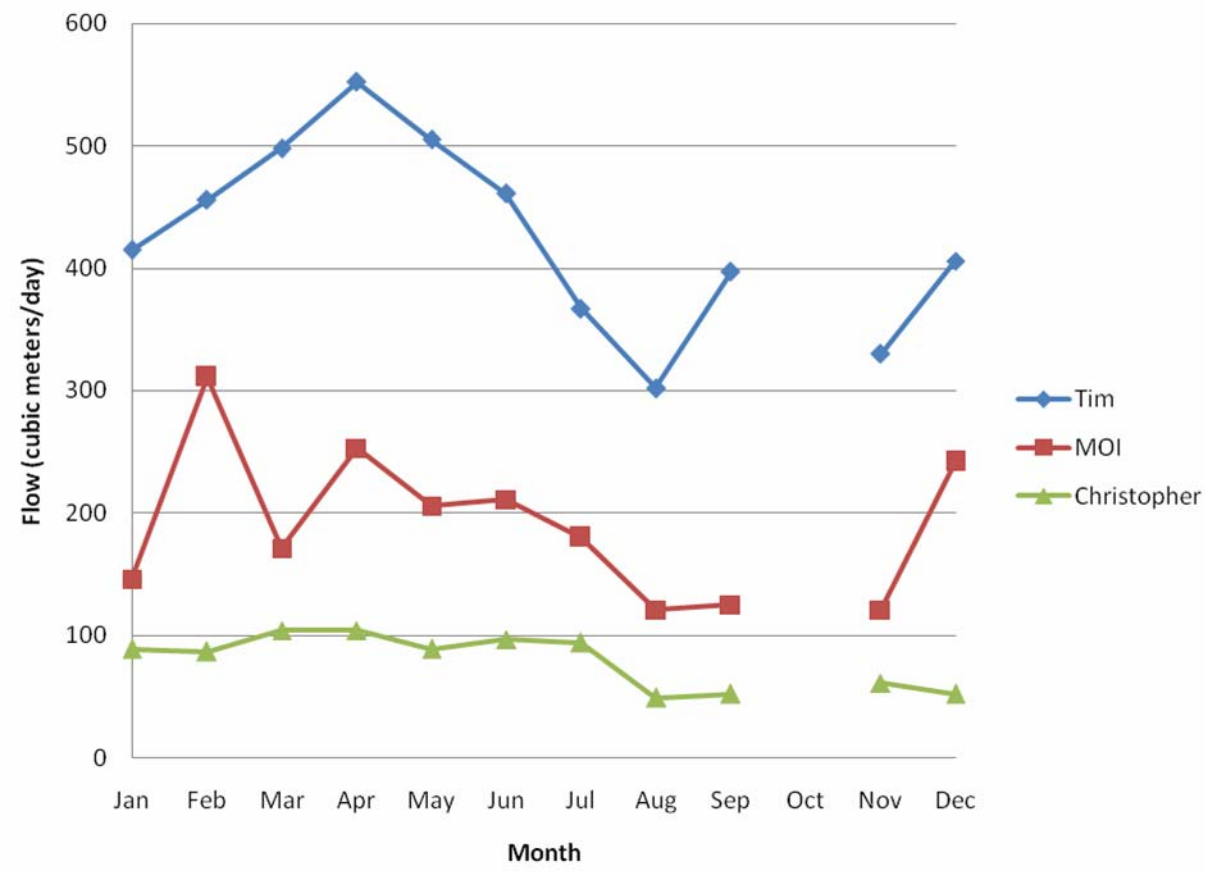

Figure 1-12: Pump usage by flow rate for 2007.

b. Treatment

Currently, the main treatment for the river and spring water is disinfection by chlorination; some of the springs also have roughing filters. Chlorine is a common disinfectant for treatment of water against disease-causing bacteria. According to Lantagne (2007), the distribution system had sufficient disinfection at the tap stands in August 2007.

II METHODOLOGY

II.1 FIELD WORK

The first few days were dedicated to setting the goals of our mission in accordance to the needs of AMI and with the help of our advisor, Peter Shanahan. After getting an introduction to the present situation of the water system through meetings and a tour of the camp, we agreed that the scope of our work would be twofold: it would consist of surveying the water-supply system, followed by running calibration tests whose results could be used to verify our future model. AMI put all the necessary man-power and facilities at our disposal.

II.1.A Surveying

The scope of our surveying efforts was limited to the system from tanks to public taps. We focused on the major systems: MOI, Christopher Tank (CHT), A Tank (AT), B Tank (BT), C Tank (CT), and Spring 17 Tank (S17) and their related springs, Spring 6 and 7 (S67), Spring 8 (S8) and Spring 14 (S14). The TB Village system was also included as part of the S17 subsystem.

The goal of our surveying efforts was to collect the necessary data to construct the water distribution model. As material, we had at our disposition a handheld Garmin E-trex Vista Global Positioning System (GPS) device (with accuracy in the range of 15 meters in the X-Y dimension) and a Bushnell Yardage ProSport 450 laser range finder (with 1 meter accuracy). The GPS was setup with the appropriate projection of World Geodetic System (WGS) 84, Zone 47 North, corresponding to the MaeLa camp and UTM coordinates. The data collected included GPS coordinates of about 140 tap stands, 140 valves, and 350 tee and reduction joints with a description of their diameter, the time at which they were collected, the number of taps at each stand, a rating of use as large (for public taps) or small (for private use or latrines for example) and brand. We also adopted a nomenclature describing these objects: a tap is defined with T#-system, a valve is V#-system, a tee-joint is JT#-system, a reduction joint is J#-system, and the few major bends were qualified as B#-system.

The lengths of pipes and their diameters were measured using the laser range finder and taking notes of the lengths, diameters and their layout in a field notebook. About 500 pipes were surveyed this way. We have then adopted the nomenclature of System-# to recognize pipes.

Elevation measurement accuracy data was an issue throughout the surveying process. It was particularly important considering that elevation is one of the most crucial factors for determining the water pressure at different points in the system. The handheld GPS possessed an integrated altimeter, which measured temperature and pressure to determine elevation. We realized however that elevation could vary by up to 50 meters throughout the day. It was thought that by taking a reference point multiple times a day, we would be able to determine through interpolation the elevations. This process revealed itself less than accurate however, because the variation of temperature was not linear throughout the day and depended on other factors such as humidity and cloud coverage.

Fortunately, Dr. Bunlur Emaruchi from Mahidol University in Bangkok, contracted by AMI, shot aerial photographs and ran a differential GPS survey to obtain a digital elevation model (DEM) of the area. We hence decided that elevation data from the surveyed points would be obtained from Dr. Emaruchi's contour map and DEM.

An integral part of the surveying process was obtaining the data from AMI staff and asking questions multiple times in different ways to make sure the information was not lost in translation. We obtained information on dimensions of the different tanks, the logistical functions of the system such as what valves are open or closed, and what tanks flow to which spring ring-tank, the level of tank-filling before distribution and more.

II.1.B Calibration

The first two weeks of our project were dedicated to surveying the camp site. Calibration tests were run in the last week of the field work with the purpose of testing the field data against calculated data from the model.

We chose three different types of calibration tests: pressure, flow and salt tracer tests at specific taps. Unfortunately, calibration data for every single tap could not be measured within the time constraints. The chosen taps covered all the major subsystems; they usually were large use taps at the edges of the subsystems. Both morning and afternoon distribution periods were used to run all of the tests, with half the systems tested in the morning and the other half in the afternoon.

Pressure tests were run by first using a 10-bar pressure gage, and then a 3-bar pressure gage (which was more in the range of the values measured around the camp). I conducted the first set of tests personally at T25-MOI, T24-MOI, T23-MOI, T16-S17, T4-BT and T5-AT during the morning distribution period using the 10-bar pressure gage and recording the time of measurement. The

second set of measurements was run by an AMI staff member in the afternoon using the 3-bar pressure gage at T6-CH, T7-CH, T10-CH, T10-AT, T5-AT, T6-AT, T8-CT, T7-CT, T13-S17, T10-BT, T3-BT, T12-MOI and T11-MOI. The pressure gages were brought back to M.I.T. and calibrated against known pressures to check the accuracy of the measured data.

Flow tests were conducted by using a watch and measuring the time it took to fill a 20-liter bucket (volume of the bucket was verified by field checking). The taps tested were also divided between the morning and afternoon distribution periods and were tested once an hour during distribution. Simultaneously, samples to be tested for salt concentration were collected in zip-lock bags at each tap every 15 minutes throughout distribution. A total of 18 taps were tested: T2-AT, T16-S17, T7-MOI, T25-MOI, T10-AT, T7-S8, T10-BT, T3-CH, T7-BT, T3-S67, T8-CT, T4-CT, T10-CH, T4-BT, T18-MOI, T8-AT, T12-MOI and TB5-S17. T16-S17 had to be re-tested because the piping system broke in the morning.

To run these flow tests and collect water samples, we had at our disposal a staff of 18 AMI staff members. A training session was run before the testing day to explain the purpose of both tests, provide the material and record sheets to run the tests, run some demonstrations, and specify logistical issues such as having all the taps open during collection and flow testing in order not to tie up the tap stands (flow measurements would then be multiplied by the number of taps to get the total outflow rates). The 18 individuals were divided into groups of two (for double-checking and procedural facility), testing 9 taps in the morning and 9 taps in the afternoon.

To run the salt tracer test, we first calibrated our conductivity meter, a Hanna Model HI9812, against known concentrations of salts. To do so, we first measured the background conductivity level for water collected at a rope pump, which happened to be around 530 μS/cm. Taking into account the maximum measurable level of 2000 μS/cm for our meter, we were aiming to increase the measurement to around 1500 μS/cm. Hence adding 10 grams of salt in 15 liters of water would yield an increase of 667 mg/L in salt concentration, which, with a conversion factor of 0.67 from conductivity (μS/cm) to total dissolved solids (mg/L) at a standard temperature of 20 degrees Celsius and pH of around 7, should yield a total conductivity of 1515 μS/cm (Eaton et al., 2005). After full mixing of the bucket, we found measurements from 1400 to 1600 μS/cm which is in the correct ball park (considering an accuracy of 10 μS/cm for our conductivity meter).

In order to decide the appropriate level of increase in salt concentration in the system, we aimed to be at 80 percent of the taste threshold. This precaution was to ensure that the experiment did not interfere with the drinking and cooking habits of the users of the system. The EPA has set a level of

250 mg/L of chloride concentration as the taste threshold for its secondary maximum contaminant levels (U.S. EPA, 2007). With the margin of safety used, we decided to aim for an increase in conductivity of about 300 μS/cm for each of the major systems assuming complete mixing. This would require about 1 kg salt input for 5 cubic meters of water (leading to 298.5 μS/cm). After buying the appropriate number of 1 kg bags of salt, we verified the mass of each bag and realized that the true mass of the salt bags was actually 583 grams which would then actually amount to an increase in 174 μS/cm for each of the systems.

After calculating the appropriate number of bags for each of the tanks, we met with the tank managers to hand them the appropriate amount of salt for their tank and explained they should add the salt half an hour after the start of the distribution. We also provided them a bucket in which to dilute the salt as they were pouring it and advised them to pour it in the middle of the tank to best approximate complete mixing. We have estimated the rate of pouring to be around 1 bag per minute or 583,000 mg/min. The salt tracer test provided a third check of the system as well as useful information on the mixing at the tanks, the dispersion throughout the pipe systems, and verification of the time of travel and lengths of pipes.

II.2 DISTRIBUTION SYSTEM MODELING

Following data collection, including geographic position of system components and calibration data, this next section discusses the hydraulics and water quality dynamics of the system model. A distribution network model provides a tool to understand the chemical distribution and hydraulic characteristics of the system. Generally, a model, along with other studies, can help in many areas including chlorine residual analysis, disinfection by-product growth analysis, consumer exposure assessment, pipe cleaning and replacement schedules, and pumping energy and cost analysis.

This analysis will provide a necessary tool that will help better understand current water flow in MaeLa and a means to answer questions of how the system can be modified and expanded to better suit the needs of the camp.

II.2.A Technical Background

The components and processes of a water distribution system including hydraulic and water quality concepts are described in this section.

a. Definitions

A water distribution system is principally made of links and nodes. Links are pipe sections which can contain valves, bends and pumps. The nodes can be categorized as junction nodes, which join pipes and are the points of input or output of flow, and fixed-grade nodes such as tanks and reservoirs with fixed pressure and elevation.

As defined in water distribution system models, reservoirs are nodes that represent infinite sources or sinks of water, such as lakes. Tanks are nodes with fixed storage capacity and varying volumes during distribution. Pumps are devices that impart energy to water thereby increasing its head. Valves limit the pressure or flow at points in the system. These components are illustrated in figure 2-1.

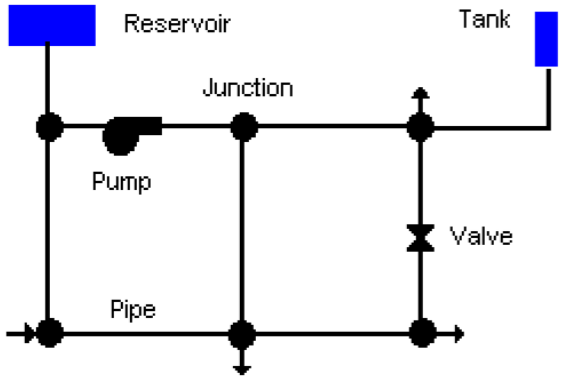

Figure 2-1: Physical components of a distribution system (Rossman, 2000)

A loop is a sub-component of a distribution system: it consists of an entity made of nodes all connected through links. It is an important component of a model because mass in and out of a loop can be accounted for and used to solve for flows.

b. Hydraulics Modeling

The two fundamental concepts of distribution network hydraulics are conservation of mass and energy. For energy, the Bernoulli equation states that the sum of the elevation, pressure and velocity heads between two points must be constant. Due to losses because of friction during flow through the pipe, this equation does not hold precisely in practice. Frictional head loss is accounted for with head loss factors typically based on the Hazen-Williams, Chezy-Manning or Darcy-Weisbach equations.

Head loss can be described as

$$h_l = Aq^B \tag{2-1}$$

where A is the resistance coefficient, B is the flow exponent and q is the flow rate. Table 2-1 illustrates the different formulas used to account for head losses. Notice that each of them contains a friction or roughness coefficient.

Table 2-1: Pipe head loss formulas for full flow (flow rate in cfs and head in ft) (Rossman, 2000)

Formula	*Resistance Coefficient (A)*	*Flow Exponent (B)*
Hazen-Williams	$4.727\ C^{-1.852}\ d^{-4.871}\ L$	1.852
Darcy-Weisbach	$0.0252\ f(\varepsilon,d,q)d^{-5}L$	2
Chezy-Manning	$4.66\ n^2\ d^{-5.33}\ L$	2

Notes: C = Hazen-Williams roughness coefficient
ε = Darcy-Weisbach roughness coefficient (ft)
f = friction factor (dependent on ε, d, and q)
n = Manning roughness coefficient
d = pipe diameter (ft)
L = pipe length (ft)
q = flow rate (cfs)

Conservation of mass dictates that flows are equal for pipes in series and they are summed for pipes in parallel. Head losses, on the other hand, are summed for pipes in series and assumed equal at nodes that join pipes in parallel.

Equations can be categorized into loop and node equations. Among loop equations, mass continuity takes the form of

$$\Sigma Q_{in} - \Sigma Q_{out} = Q_e \tag{2-2}$$

where Q_{in} is the inflow, Q_{out} is the outflow and Q_e is the external flow into or out of the system at each node. Energy conservation is written as

$$\Delta E = \Sigma h_l - \Sigma E_p \tag{2-3}$$

where ΔE is the difference in energy grade, h_l are losses considering pipe length, diameter, roughness and minor losses, and E_p is the pump head. Node equations expand the mass continuity equations to

express discharge in terms of head difference between nodes a and b (H_a-H_b) and resistance of the pipeline (K_{ab}):

$$Q_{ab} = [(H_a - H_b)/K_{ab}]^{1/n} \quad (2\text{-}4)$$

where n is selected depending on the head loss equation (Viessman and Hammer, 1998).

The single path adjustment method described by Hardy-Cross is best known for solving loop equations. It consists in making an initial guess of flow rates that satisfy continuity at each node, followed by computing flow correction factors for each loop to satisfy the energy equation. Through iteration, improved solutions are found until the average correction factor is within acceptable limits. The most widely used algorithm for solving node equations is the single-node adjustment method also described by Hardy-Cross. A grade is assumed for each junction node, followed by computation of a grade adjustment factor to satisfy continuity and through iteration improved solutions are found until a specified convergence criterion is met (Viessman and Hammer, 1998).

c. Water Quality Modeling

Water quality modeling uses the flow results from the hydraulics calculations and concepts of reaction kinetics to track the concentration of a substance through the system. The processes of advective transport in pipes, mixing at pipe junctions and mixing in storage facilities dictate the concentrations throughout the system.

Advective transport is the bulk movement of chemicals with the carrier fluid. This transport process may occur while the substance is reacting (either growing or decaying) at some given rate. It is represented by

$$\frac{dC_i}{dt} = -u_i \frac{dC_i}{dx} + rC_i \quad (2\text{-}5)$$

where C_i = concentration in pipe i as a function of distance x and time t, u_i = flow velocity in pipe i and r = rate of reaction.

Mixing at junctions is often taken to be complete and instantaneous. Thus, with link j and an external source connecting at node k to flow into link i,

$$C_{i/x=0} = (\Sigma Q_j C_{j/x=L} + Q_{k,ext} C_{k,ext}) / (\Sigma Q_j + Q_{k,ext}) \quad (2\text{-}6)$$

where i = link with flow from node k, $C_{i/x=0}$ = concentration at the start of link i, ${}_jC_{j/x=L}$ = concentration at distance L in link j, L = length of link j, Q_j = flow in link j, $Q_{k,ext}$ = external source flow entering the network at node k and $C_{k,ext}$ = concentration of the external flow entering at node k.

Storage facilities are also often assumed to be completely mixed, and the concentration throughout the tank is a combination of that of the current contents and that of entering water. The internal concentration could also be changing due to reactions. This process is represented by

$$\frac{d(V_s C_s)}{dt} = \sum Q_i C_i - \sum Q_j C_s + r C_s \quad (2\text{-}7)$$

where V_s = volume in storage at time t, C_s = concentration within the storage facility, Q_i = flows into the facility, C_i = concentration of flow into facility, Q_j = withdrawal flows from the facility, r = rate of reaction (Rossman, 2000).

Chemical reactions are accounted for in the above equations with a chemical rate of reaction r. These reactions can be categorized as either occurring within the bulk flow or through interaction with the material along the pipe wall. The main parameters for modeling bulk flow reaction rate are the reactant concentration C, the limiting concentration C_L, the bulk reaction rate coefficient K_b and the reaction order n. They come together in the general expression

$$R = K_b(C_L - C)C^{(n-1)} \text{ for } n>0 \text{ and } K_b>0 \quad (2\text{-}8)$$

or

$$R = K_b(C - C_L)C^{(n-1)} \text{ for } n>0 \text{ and } K_b<0 \quad (2\text{-}9)$$

Hence, bulk flow reaction rates can be modeled as any n-order reaction and be linked to concentration.

Pipe wall reactions can occur as the chemical species transported react with materials such as corrosion products or biofilm that are on or close to the wall. These reaction rates can be modeled based on the surface area per unit volume within a pipe, the wall reaction rate coefficient K_w, the reactant concentration C and the order of reaction n. These factors come together in

$$R = (A/V)K_w C^n = (2/R)K_w C^n \quad (2\text{-}10)$$

Often, a Lagrangian time-based transport algorithm is used to track water quality as water moves along pipes and mixes at junctions. A Lagrangian transport algorithm summarizes the dynamics of the system: it updates water quality in each segment by any reaction that took place, then blends waters with those that flow into the segment from leading segments or outside sources and finally calculates concentration of new segments to which water flows (Rossman, 2000).

II.2.B EPANET

EPANET is a computer program that simulates hydraulic and water quality behavior within pressurized pipe networks. It was developed for the Environmental Protection Agency, and presents the great advantage of being available on the internet free of charge. This enhances its suitability for the context of the hand-over between AMI and Solidarites, making such a model more easily accessible and transferable. It can model networks of pipes, nodes, pumps, valves, storage tanks and reservoirs and tracks the flow of water in each pipe, the pressure at each node, the height of water in each tank, and the concentration of a chemical in the network during a time-stepped simulation. As an illustration, Figure 2-2 shows the representation of the B Tank system in EPANET.

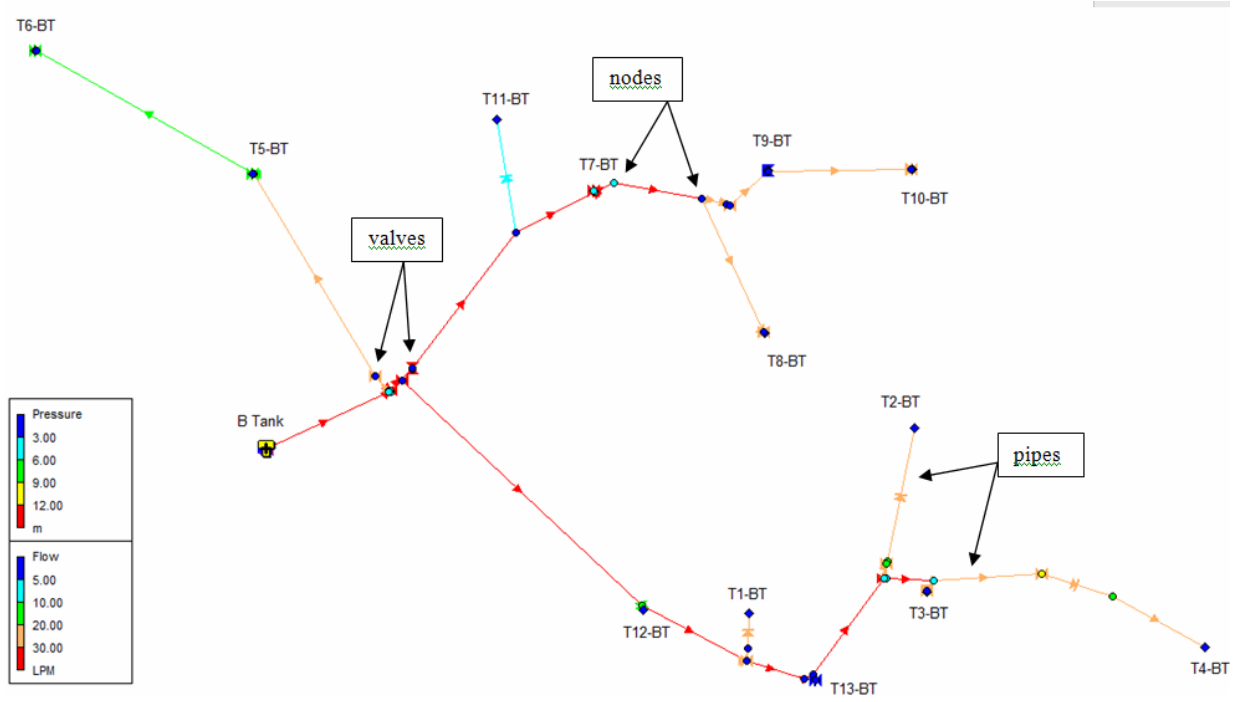

Figure 2-2. B Tank subsystem represented in EPANET

Some of the key hydraulic capabilities of EPANET include no size limitations on the network, time-varying demand or controls (e.g. opening and closing valves), simulating a pressure-driven node using the concept of emitter coefficient as discussed later, handling multiple head-loss equations, and pump operation control (e.g. based on tank water levels). The program also sends warning messages which point out changes in the system such as negative pressures occurring in the system.

No model can perfectly reflect the underlying system but these capabilities enhance the realism of the simulation (Rossman, 2000).

EPANET is able to model the movement and fate of non-reactive or reactive material, such as the growth of disinfection by-products or the decay of chlorine residual. These reactions can be modeled to any n order of reaction in the bulk of the fluid and Michaelis-Menton decay kinetics are supported. EPANET can also model reactions occurring with the pipe wall material as a zero-order or first-order reaction. Since pipe roughness is often related to a reaction rate coefficient, if desired a link can be made during the simulation. By specifying molecular diffusivity, EPANET can account for mass transfer limitations in moving reactants and products between the bulk flow and the wall. These features could reveal themselves useful in future chlorine analysis but they were not used for this thesis. The program also provides four types of models to characterize mixing in storage tanks: complete mixing, two-compartment mixing, and horizontal first-in first-out (FIFO) and vertical last-in first-out (LIFO) plug-flow models depending on the particular circumstances simulated (Rossman, 2000).

An important scenario that often occurs in situations of crisis is that of intermittent flow. EPANET assumes a constantly pressurized system, with instantaneously full pipes at the start of distribution. Hence, relatively significant discrepancies could arise between the model and the actual dynamics of the system and these are discussed in the following section.

II.2.C INTERMITTENT FLOW

Intermittent flow is a major characteristic of this system and a factor that cannot easily be accounted for with the modeling software. The major issues concerning intermittent flow are now discussed.

a. Major Issues

This sub-section is the result of a collaboration with Mary Harding.

Hydraulics

There are a limited number of studies to understand the effect of the non-ideal but widely utilized intermittent water supply (IWS).

Water supply for eight hours or less is generally considered sufficient for a community. Whereas in a typical continuous system the demand dictates the system flow, an intermittent system is driven

by the supply available at collection sites (Batish, 2003). Since users will normally draw all the water available at a node, the available pressure determines the amount of water as opposed to the amount desired by the user.

An interesting effect of a limited supply system is that a consumer will generally withdraw as much water as is available and store excess in the home. This behavior is especially visible when distribution is from public stand pipes where there is no individual cost to collecting water. When new water becomes available the stored water is likely to be disposed of so the consumer always stores the "freshest" water (Batish, 2003).

Unlike typical demand driven systems, an IWS can shift in space and time between demand- and pressure-dominant system. How this affects water quality and hydraulics is not well known (Sashikumar et al., 2003). One field observation is that the Hazen-Williams C value varies by over 25% for pipes. While it is commonly understood that the roughness factor in pipes can change over the lifetime of the pipe (on the order of tens of years), an intermittent system can see such variation within hours. One suggested cause for the variation is the presence of air pockets created during stagnation periods (Sashikumar et al., 2003). Air pockets can cause head loss to increase by nearly 45%. Before the air is gradually driven out with the flow in the system, there is increased head loss in air pocket presence creating an effectively lower C value (Sashikumar et al., 2003).

Additionally, higher than typical peak load factors can be present in an IWS. The peak factor is the design flow rate divided by the average flow rate. If, for example, the supply of water occurs only once every two days, and consumption is then averaged over the entire period, these averages are much lower than the actual rates observed when the system is active. The decreased average flow rate results in a much higher than typical peak factor. In a study of four cities in India, the peak load factor was 6.4 for IWS versus 3.06 for continuous water supply (CWS) (Andey & Kelkar, 2007). In data collected from Bangalore city, peak load factors above 10 were noted in several cases, while the corresponding pipe velocities remained mostly below 1.5 m/sec (Sashikumar et al., 2003). In this case the load factors are artificially high as compensation for minimal distribution time but do not represent a great strain on the system.

Pressures were also found to decrease by about 50% under IWS as opposed to CWS within the various systems in the study of cities in India (Andey & Kelkar, 2007). This decreased pressure creates undesirable effects on water quality discussed subsequently.

Distribution loss is the difference between the amount of water supplied by the system and the amount of water accounted for as having reached consumers. While loss typically arises from leakage and poor connections, in an IWS unauthorized connections to the system are more common and may account for greater distribution loss. Unauthorized connections can occur in continuous water systems as well, and proper leak detection and system awareness is necessary to ensure that the designed supply reaches the consumer.

Consumer satisfaction regarding IWS is highly dependent on the community's situation. While over three quarters of the population in one Indian city reported three hours per day an adequate supply, in another city over three quarters of the population found five hours per day unsatisfactory (Andey & Kelkar, 2007). This difference was attributed to a large rooftop storage capacity on homes in the first city that made the shorter access time viable.

Water Quality

As a result of the various issues concerning intermittent water flow including high peak factors, the presence of air in the system, and a need to store water in the home, specific water quality concerns arise. In particular, concerns specific to intermittent supply include (Coelho et al., 2003):

1. Groundwater ingress while unpressurized (not as relevant in the above-ground MaeLa system)
2. Biofilm detachment from increased pressure and velocity peaks
3. Microbial re-growth during stagnation
4. Bacterial growth and contamination of stored water

Andey and Kelkar (2007) found that fecal coliform was not present more than 90% of the time for a CWS. With intermittent flow, however, the fecal coliform was absent only 24 to 73% of the time. The samples were taken at the pump, and it is not clear which of the first three concerns listed above was most responsible for these results, or if there was some other reason, or, reasonably likely, if it was some combination.

During a controlled study of an IWS in Lebanon, an increase in bacterial plate count was found between two points separated by 1 km. The increase was statistically significant and it is possible that bacteria re-growth is responsible for the increase (Tokajian & Hashwa, 2003). When the distribution system is not pressurized, groundwater from the surrounding area can infiltrate the pipes. The amount and severity of problems associated with groundwater ingress will depend on the amount of time the system is unpressurized and the degree to which the infiltrating groundwater is contaminated. This particularly creates problems in regions where wastewater is not well contained or controlled. Leaking wastewater pipes and poorly constructed or maintained latrines, septic tanks or soakaways near water distribution pipes create contamination. Since intermittent supply is often a result of a lack of financing or infrastructure, the corresponding wastewater systems are not normally ideal.

Higher than typical pressure and velocity peaks within IWS systems can cause biofilms to detach from pipe walls and enter the drinking water. Biofilms are known to exist in water systems and can be used as a final method of treatment before reaching the consumer. Water quality tests do not analyze the microbial cells that make up the biofilm since they are left to accumulate (Coelho et al., 2003). Figure 2-3 presents results from Coelho et al. that illustrate the so called "first flush" phenomenon. This is commonly accounted for in applications such as rooftop rainwater harvesting. The water that first comes to the tap after a period of rest in this case has significantly higher heterotrophic plate count (HPC), which is a representation of the amount of bacteria present. Residual chlorine levels are also shown to be reduced during the time that water that has been idle in the system.

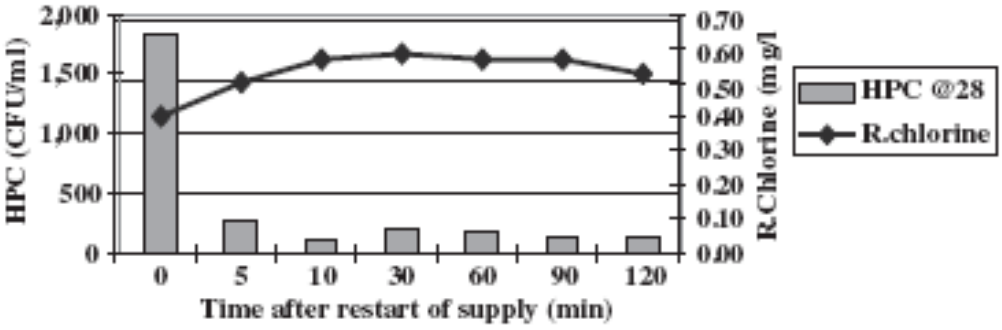

Figure 2-3: First flush effect shown by heterotrophic bacteria (Coehlo et al., 2003).

One seemingly simple potential solution that would address the higher level of contamination in the "first flush" is that consumers could be educated regarding these harmful effects and reserve the water first collected for watering gardens or washing up. Although this is not a complete solution and ideally the consumer would discard the water entirely, in communities where demand is not met, making compromises is necessary.

b. Preliminary Data Analysis

Pressurized Pipe Assumption

A preliminary analysis was conducted to see if the assumption of pressurized flow in EPANET could apply to the system in MaeLa. With system specifications including pipe lengths and diameters, the total volume of pipe downstream of each major tank was calculated. This volume was divided by the monthly average spring and pumping flow rates for each tank in order to estimate potential fill times for the system (Figure 2-4).

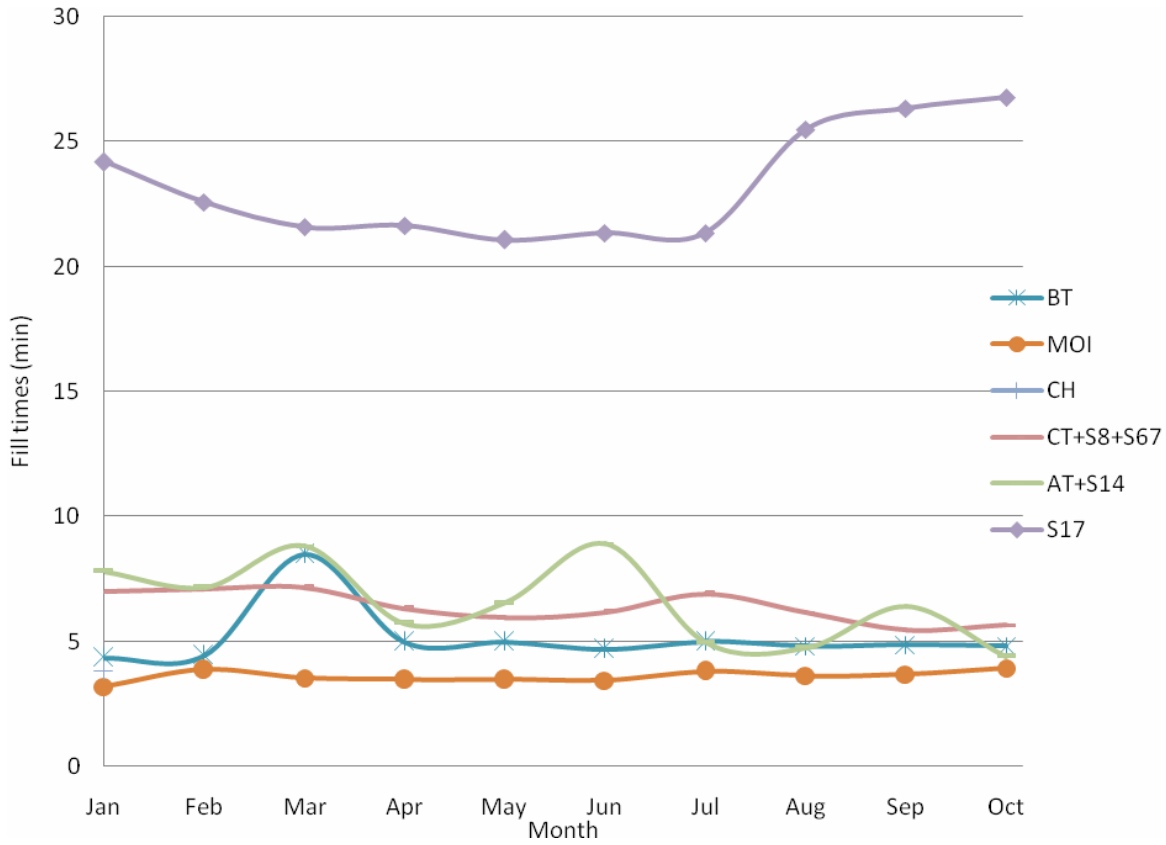

Figure 2-4: System Component Fill Times in 2007.

The data behind this plot came from the field survey of the system as well as the springs and flow data collected by AMI in 2007. Comparing fill times with the three-hour distribution time helps to get a sense of how important intermittent flow is in the system. For example, if the fill times were found to be less than 10 minutes, it is obvious that the system would act very much like a CWS and pressurized flow would dominate.

No subsystem ever takes more than 25 minutes to fill and all the subsystems except S17 have filling times less than ten minutes with MOI's particularly short filling time always under five minutes. Comparing systems in increasing order of filling times, the MOI subsystem, the largest single system in flow volumes, is the shortest closely followed by CH and BT, all generally around 5 minutes. Then come CT, combined with S6/7 and S8, and AT with S14 which are around 7 minutes. The S17 subsystem sticks out as taking the longest by far: understandably, it is the largest system in terms of length and tracks three quarters of the length of the camp along the road.

From this analysis, we can conclude that most major systems of the camp, S17 included, take at most 10 percent of the distribution time to fill the pipes; it is actually less than 5 percent for most systems. Hence, the system can be considered essentially pressurized. This conclusion is further confirmed looking at the systematic controls of the water system: at no point during the distribution are any of the tanks emptied completely. The logistics staff makes sure to pump enough water to tanks such that there would always remain some in the tank at the end of distribution which implies that pipes are essentially always under pressure.

Another subtle conclusion from the figure is that slightly longer filling times during the dry season than the rainy season suggest that flow rates are actually lower during the dry season than the rainy season. Hence it might be wise to vary the assumptions made during modeling (i.e. the starting tank level or demand) depending on the period of the year.

Pressure-driven demand

A second point of analysis is whether EPANET can model the pressure-driven demand occurring in intermittent flow. Because of the limited supply, demand does not so much depend on consumer usage as much on the pressure that exists in the system (Batish, 2003). Public taps in MaeLa are left fully open during the distribution period and queues are formed to collect the water in buckets and other containers. Figure 2-5 is a photograph of one of these tap stands during distribution.

Figure 2-5. Public Tap Stand during Distribution

EPANET can model emitters, which are devices such as nozzles or sprinklers associated with nodes that discharge to the atmosphere. They are considered properties of junctions and not separate components. Such a device can also simulate a tap that is fully open throughout distribution and whose flow depends on the pressure at the tap. The flow rate is determined from the pressure through the expression

$$Q = Cp^{\gamma} \tag{2-11}$$

where Q is the flow rate in units liters per minute, C is the emitter coefficient in units of liters/minute/meter$^{\gamma}$, p is the pressure in meters and γ is the pressure exponent.

Virtually all the taps present at public stands are ½-inch SANWA taps. Figure 2-6 illustrates the relationship between flow rate and pressure for this tap. Note that the pressure here is different than the pressure available in the piping system: it is actually the pressure measured at the tap while the tap is flowing. Ideally this pressure should be zero and flow out of the tap should only be a function of the energy available and not of the tap. Depending on the emitter coefficient and exponent, this graphic illustrates how much friction plays a role in limiting the flow out of a SANWA tap.

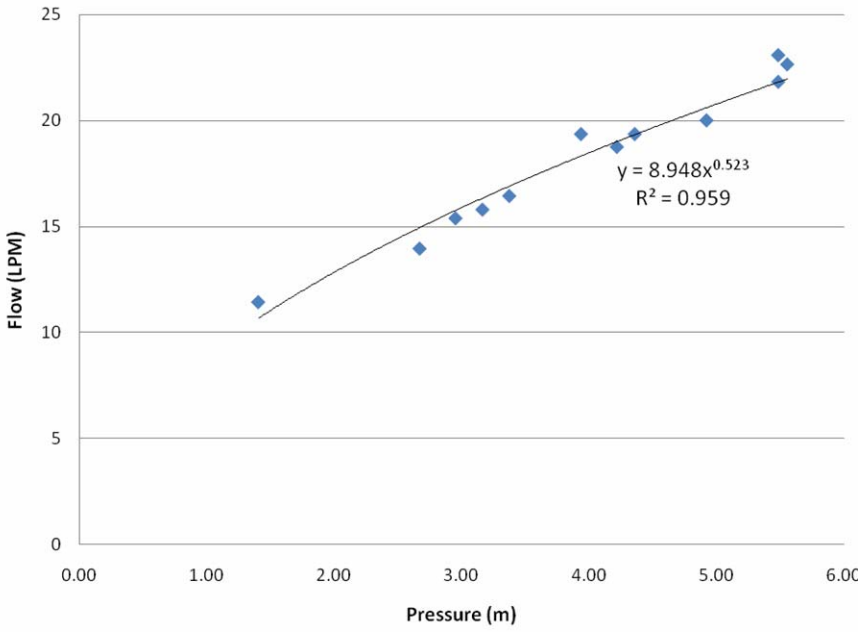

Figure 2-6. Flow versus pressure of half-inch SANWA tap

These results were found from testing a half-inch SANWA faucet in an M.I.T. laboratory. The setup consisted of a flexible pipe connected to the highest flow faucet in the laboratory, which was then joined hermetically to a tee to with a pressure gage and the faucet such that readings of pressure could be made as the water flows through the SANWA faucet. Care was taken to hermetically seal all connections using pipe glue when necessary to prevent water from escaping the setup or air from entering. The range of readings however was limited by the range of the pressure gage, the laboratory faucet's maximum output flow, and the minimum flow needed to keep the system under pressure. But considering the consistency of data readings, with an R-squared value very close to 1 (0.959), and the fact that a wide range of common pressure usage was tested, these results are deemed reliable.

Hence, the relation $Q = 8.948p^{0.523}$ relates flow and pressure in a half-inch SANWA faucet. The pressure exponent coefficient is 0.523 and the emitter coefficient is 8.948 liters/minute/meter$^{0.523}$. It is not a linear relationship in that the incremental flow out of the tap decreases as pressure out of the tap increases because of increased friction.

The emitter function produces negative demand in the model whenever a nodal pressure becomes negative (Bentley, 2006). This is not the case in reality, since water is not injected into the system when the tap runs dry. Fortunately, this should not be a major issue in the MaeLa simulations because neither tanks nor sources run completely dry. We have also further prevented such

problems in the model by inserting control valves associated with pipes just before taps to allow flow in one direction only in the model.

II.2.D DATA ASSEMBLY

The following section describes the process of putting together the water distribution model in EPANET from the raw data collected in the field. The first step in starting the model is to set up some important parameters which define the input values used by the software.

a. Initial Setup

Throughout the process, International System Units (SI units) have been used. To request the use of these units in EPANET, the user chooses SI flow unit under the hydraulics option. I have selected liters per minute for the model, which also defines all other units using the SI system. Hence lengths, pressures, head, elevation, and diameter of tanks are taken as meters. Diameters of pipes are defined as millimeters, and selecting mg/L in the quality options also defines source injections in mg/minute. The Hazen-Williams equation was chosen for determining head-loss. Further setup of the interface for analysis is discussed in the next section.

To expedite the entry process, an EPANET input template is produced by exporting an empty network. This text file is imported to Microsoft Excel (using tab delimited import for example) or some other sophisticated software to facilitate data entry.

Dr. Bunlur Emaruchi, from Mahidol University in Bangkok, provided an aerial photograph of the camp with contour lines, which is a useful basemap for the system to check the accuracy of the components' location and to orient the system. The file's resolution was first reduced to make it more manageable for the computer to handle. It was then set up as a backdrop and geo-referenced by setting the image lower left and upper right corner coordinates in UTM coordinates under the backdrop section of the EPANET template file. The file source was specified as program input, as well as the units of meters for UTM coordinates and no offset.

b. Data Entry

The locations of specific system features included in EPANET were determined in the field using GPS. The GPS data gathered consists of latitude, longitude, and elevation from the altimeter (which was not used). These locations were mapped in the WGS 84, 47 North coordinates. The identifications (ID) of the points and their X-Y coordinates are copied under the coordinates section and the Digital Elevation Model (DEM) is used to estimate the elevation of each point.

The ID of all data points, except those of tanks, are copied into the junctions section of the EPANET inputs as well as the elevation data gathered from the DEM. Demand at each of these nodes is defined to be zero since pressure-dependent emitters are used rather than demand-based nodes.

Taps

The different tap stands are characterized in EPANET under the emitter section. After copying tap stand IDs, emitter coefficients are assigned depending on their use. It was decided that taps of little use, such as latrines or private use taps leading to small drums or taps dedicated to specific institutions such as schools, would be assigned an emitter coefficient of zero. It could have been possible to assign a small emitter coefficient or a specific demand at the tap following a certain time pattern. However, this would have complicated the process because data is not available to specify such values adequately and these taps are insignificant in comparison to the large-use taps that are constantly open. Because tap stands have 1, 2 or 3 taps, emitter coefficients of 8.948, 17.896 and 26.844 liters/minute/meter$^{0.523}$ were assigned to each of the tap stands.

Tanks

The tanks are further defined in EPANET under the tanks section. Tanks are assumed cylindrical in EPANET: hence their height should be kept but an equivalent diameter needs to be calculated from each tank's volume. After copying the tank's ID into the section, their elevation is inputted. Their initial water level is then taken to be their height (assuming full tanks); such height was taken from the overflow to the outflow pipes, the useful height of the tank, and not from the total height. The minimum level and volume is taken to be zero and the maximum level is the same as the initial one. No volume curve is chosen since all of the tank storage volume varies linearly with height.

Pipes

In EPANET, pipes are links connecting two nodes. Inputting pipes can be done using the text or the graphical interface of EPANET. I recommend using the graphical interface with the backdrop map to verify the overall logic of the system by its location. Also, throughout the process of inputting pipes, lengths surveyed were verified against computed lengths (using the auto-length tool) to make sure the field lengths were correctly recorded. Recorded lengths were however chosen over the auto-lengths because those surveyed consisted in direct measurements using the long range finder rather than relying on GPS points of 15-meter inaccuracy. Besides, direct measurements take

into account the slope whereas the auto-length feature only provides the planar distance between two points.

As a side note, it should be noted that to write data from an Excel file into an EPANET input data file, it is necessary to first save the Excel file as a tab-delimited text file and to then copy and paste the content of the text file into an input file exported from EPANET. Otherwise, the software would not recognize the input file. Another common issue in importing network input files is the presence of apostrophes: Excel often adds apostrophes when importing text files and EPANET does not recognize files containing apostrophes.

When inputting pipes, nodes 1 and 2 need to be selected concurrently to follow the direction of the flow (else flow appears negative in EPANET's output). Pipe length and diameters are then inputted as well as roughness. A roughness of 150 was selected for the polyvinyl chloride (PVC) pipes at the camp (Briere, 1999). The pipes are fairly new but considering the stagnation periods due to the intermittent nature of the system, build-up should have made roughness rise to such levels. Minor losses are also included as part of pipes, not at the tee or elbow junctions. These minor losses were ignored and assigned a null value because errors in elevation were assumed to outweigh the minor losses sufficiently that results would not significantly vary by considering such losses.

As to the status of pipes, they were generally left with their default status of open. The exception included pipes connecting to taps or secondary tanks. These were assigned the status of control valve, letting water flow only in the direction of their first to their second node. This setting is important to avoid backwards flow from tanks whose inlets discharge above surface water or for emitter taps which would become sources in the absence of flow.

Valves

Valves and pumps are considered to be links as well in EPANET and not nodes. Hence, one could decide not to survey or input these points in the coordinates and junction sections but only under their respective sections as a component between two nodes, just like pipes. I decided against this option for the sake of better representing the model visually and to verify the accuracy of the survey as a whole. However, the task of geographically locating valves requires that a second node be created next to the valve node. These two nodes have been re-defined as V#i-system and V#j-system, between which the actual valve V#-system would be located.

It is also helpful to see the system when creating new valve nodes in order not to clash with the direction of the connecting pipes and to minimize the distance between the two valve nodes so that

the recorded lengths of pipes would still be applicable. Thus, the graphical interface might again be preferred over the text file.

Inputting valves, the first and second connecting nodes need to follow the direction of flow to avoid negative flows. The diameter is assigned the one recorded in the survey, or if unknown, the diameter of the preceding pipe. Minor losses are again ignored. The type of valve inserted is irrelevant in the majority of cases since most valves are either set to open or closed. One exception however is valves just before secondary tanks. These valves were created as modeling artifacts to simulate open-air flow of water as it cascades into the water in the tank. Here, a pressure sustaining valve is used with a setting of zero. Pressure sustaining valves maintain pressure just at a point. Hence it closes the valve if the pressure is higher downstream to prevent reverse flow and it partially opens it if the downstream pressure is below the value. With a setting of zero pressure, such a valve would simulate open flow. The pipe that connects the valve to the tank is then taken to have a large diameter and low roughness to minimize pressure and flow resistance and simulate free fall from the water outlet. The second instance when the pipe type is relevant and needs to be changed to flow control is when simulating the salt test, which will be discussed in the next section.

It is important to set the status of valves as open or closed according to their use. To set the status of valves, their IDs are copied under the status section and their status is set as open or closed. Most valves are open. The ones that are closed include such valves that could potentially connect two isolated subsystems that are in close proximity. Spring 17 and the Christopher subsystems could connect at V7-CH for example. It is also the case for Spring 6/7 and MOI which connect at V-18-5, for Spring 14 and A-Tank which connect at V-T10-AT and for Spring 17 and the TB Village which connect at V-PTB. All these valves have been assigned a closed status. Valves at the outlet of major tanks have also been assigned a closed status that would then be modified according to the hour using controls discussed in the next section. These valves include V-ATOLDout, V-17Tout, V-CTout, V-TBRINGout, V-MOITout, V-BTout , V-CHT1, V-CHT2, V-BT1, V-BT2, V-JT5-S8, V-S14RING and V-S67RING.

As the model was assembled, care was also taken to provide a brief description of tap stands (the number of taps, brand, type of use and more), and information not apparent by visual inspection (such as elbows that were a part of pipes). These appear after the semi-column in the text file. The next step after inputting the raw data into the model is to modify the EPANET setup options to prepare the model for solving hydraulic and quality equations under conditions adapted to the specific context.

II.2.E SETUP

As mentioned earlier, it is important to define the parameters on which the model is based.

a. Hydraulics, Water Quality and Time Parameters

Under hydraulics options, SI units of measurement are chosen and the the Hazen-Williams equation used to find head-loss. The specific gravity of water is set to 0.998, for average temperature of 25 degrees Celsius, and a relative viscosity of 1. The emitter coefficient is 0.52 and the bulk reaction coefficient is 0, since salt will not react in the system.

The hydraulics accuracy represents the threshold ratio of variation in total flow from one iteration to the next over total flow in the system. If this ratio is under the specified accuracy, iterations for solving the model stop. A lower value for this accuracy would give more precise results. A lower accuracy would also increase the solution time for the model, and possibly prevent the model from converging on a solution. The value of accuracy is often tweaked in the case of non-convergence. I have chosen it to be 0.03, which represents a reasonable accuracy considering the magnitude of error in the surveyed elevations. It is also preferable to set a large maximum number of trials (10,000 for example) and to select the option of continuing if the model is unbalanced (instead of stopping), since the analysis can be cancelled manually if it takes too long. The quality tolerance is another important parameter. It represents the smallest change in water quality that will cause a new parcel of water to be created. Typically, this accuracy is set at or below the detection limit. A value of 0.01 is reasonable for measurements in mg/L.

Besides hydraulics and water quality setup, time characteristics need to be set up to properly use EPANET. The duration of the simulation is one such time setting. Other parameters include the hydraulic and water quality time steps as well as time pattern and reporting time steps. A time pattern can be associated with different parameters such as chemical sources, valve controls and more. The duration of these time increments determine the time resolution for analysis, control setting and reporting. For a distribution period of 3 hours, as used at MaeLa, precise hydraulics and water quality results are needed. Hydraulics usually vary less throughout the distribution period than quality does and this is why the hydraulics time step is often set to be longer than the water quality time step to reduce computing time. Considering the subtleties of the system with its opening and closing of valves, I have chosen a short 5-minute hydraulic time step and a water quality time step of

1 minute. The latter is particularly important for updating the concentration of salt throughout the system without any time lag. These settings mean that the hydraulic state of the system and its water quality are calculated every 5 and 1 minute respectively during the modeling period; this avoids the otherwise inaccurate interpolation of results. For consistency, the reporting step and pattern time step have also been set to 5 minutes.

The distribution period practice at MaeLa consists of two periods of 3 hours per day. However the 6 to 9 AM distribution period is identical to the 3 to 6 PM period and there is no need for a re-iteration of the calculations. Henceforth most of the results will be based on the morning results. The modeling duration has however been set to 18:05 hours with a clock start time of 12:00 AM to simply illustrate a day and the change from closed tank valves to open. The afternoon distribution period is not quite representative however (because tanks are not modeled to be re-filled in between) but is used for the pressure calibration test as will be discussed later in this section.

b. Controls and Calibration

The actual opening and closing of the tank valves also need to be simulated in EPANET. This is done using the controls options. In the model simulations, the valves of all major tanks as well as the MaeLa 2 ring tank (which distributes to a public tap) open at 5:59 AM and close at 9:01 AM. The valves are initially closed and these controls represent the morning distribution. A minute less and a minute extra were chosen in order to read results at 6:00 and 9:00 AM as well to accommodate the 5-minute reporting time step.

In addition to the tank valve controls, a number of controls were added to simulate the different calibration tests conducted on the field. For example, the field pressure tests consisted in directly connecting to the faucet a flexible pipe attached to a gage. Such a methodology prevented outflow of water from the tap. In contrast, the pressures reported by EPANET during distribution are pressures at taps while the water is flowing through them. Hence controls were added in the simulation to close the faucet valves of the taps tested at specific times to simulate the same dynamics and make comparison possible. These controls were set to close the specific taps tested after the morning distribution. This precaution was taken so that the closing of taps would not affect the normal pressure and flow distribution represented in the morning period. During simulated pressure testing, no two taps within the same subsystem were set to close at the same time in order not to affect each other's pressure reading. As discussed further, the field calibration data was also

adjusted to fit the time during which this simulated testing was run, in order for EPANET to automatically compare field calibration data to calculated results.

Another artifact added to compare calculated data to calibration data was an additional virtual tank connected to each of the major tanks where the salt test was conducted. Salt tests were conducted at one of the two Christopher Tanks, the old A Tank, the MOI Tank, the Spring 17 Tank, the C Tank and one of the two B Tanks. The need for additional virtual tanks is because of the fact that EPANET cannot simulate direct addition of salt to tanks. Rather, sources of chemicals can only be added at the outlet of tanks: hence there is the need to simulate water as a carrier of chemicals flowing into the actual storage tanks. These additional salt-providing tanks were set at higher elevation than their corresponding tanks to allow water to flow from the salt tanks to the water distribution tank.

A flow control valve was added at the outlet of each of these virtual tanks. These valves limit the inflow to insignificant amounts of water in order not to change the volume of water in the major tanks or its subsequent salt concentration. They are annotated FCV-tank and limit the flow to 0.1 L per minute. A mass source was then added at the outlet of each of the virtual tanks by editing the sources section or using the source editor in the graphical interface.

The rate of mass input was made to simulate the rate of pouring of salt during the field experiment, at 583,000 mg per minute (1 bag of salt per minute). Associated with each source is also a pattern (with the corresponding tank name) that dictates the amount of time the source flow should be added. For example, 30 bags were added to the C-tank during the salt test: hence the mass source of 583,000 mg per minute was added and set to follow the CT pattern, which is a pattern created with a factor of 0 up until 6:30 (at 5-minute time steps), a factor of 1 from 6:30 to 7:00 AM, and then a return back to 0 from 7:00 AM on. This captures 30 minutes of pouring salt at a rate which amounts to the correct mass poured in the tank over the approximate time it took to pour it. The mass of salt added differs for each tank, aiming to reach an approximate increase of 116 mg/L in salt concentration. Hence appropriate patterns were also created for each of the tanks, all starting at 6:30 AM (the time instructed to start pouring salt) for the commensurate amount of time.

The pipes connecting the virtual tank to the valve and to the actual tank were chosen to have a very large diameter and a short distance to minimize the time for the salt to reach the tank and thereby simulate direct salt addition. The flow control valves should ideally be closed for all times but the source injection, but the flows are so small that it would not actually affect levels of tanks, their salt concentration or pressure.

EPANET also possesses a function to automatically compare measured calibration data to simulation results. In order to take advantage of this feature, the calibration data needs to be created or imported to EPANET. This consists in node IDs, followed by the time of the day and the particular value of the parameter measured. Calibration data from the field tests was entered for pressure, demand and water quality in the appropriate SI units. Flows recorded were those of individual faucets and they were multiplied by the number of taps, assuming equal flows, to get the total flow out of each tap stand.

For convenience, and to facilitate comparison of modeled events with actual events in the field, the three-hour distribution periods during both the morning and afternoon were treated as if they occurred between 6 am and 9 am. In actuality, the morning and afternoon distribution periods are essentially identical and the change in clock time does not alter the character of the results. As discussed above, taps were closed in the simulation following the three-hour distribution period to enable comparisons with the field pressure measurements.

Another modification made in simulating salt tests consisted in a variation of the mixing model at the tank. This issue is discussed further in Section III.2.C, which explains that the salt tests provide an understanding of the mixing patterns at the tanks. The tank mixing model was changed from the default fully-mixed assumption to a two-compartment model, made of two fully-mixed tanks, with 12 percent of total volume dedicated to the bottom tank. This second model happens to better simulate the mixing at the tanks and the rationale is explained further in Section II.2.C.

Finally, in order to be able to compare the salt field-test results directly to the calculated ones, the initial concentrations at all the points in the system were set to their respective system background concentrations found in the field salt tests. This was done by setting the initial water quality under the quality section for all of the points recorded. It avoids having to take the difference between the recorded values and their background level to compare to calculated quality results. It also gives a better understanding of the actual total dissolved solids content for the different systems in January as the system is currently functioning. This background total dissolved solids concentration would however vary with the season (because of variation in spring water input) and with the modifications in water distribution considering the inclusion of water from the reservoir.

II.2.F ASSUMPTIONS

The logistics of the system form one of the most important assumptions on which the model is based.

a. System Management Assumptions

After investigating with the AMI staff, it was found that not all compartments of the tanks were in use at the time of the field studies. The A subsystem is supplied by identical new and old tanks. AT-NEW was not functional at the time of the field analysis, and the A subsystem was solely relying on the AT-OLD tank. The valve from AT-NEW was closed in the model so that only AT-OLD would supply water to the system. It was also understood that only one of the two identical B Tank compartments was used at a time, and they would rotate for morning and afternoon distribution. At the time of the salt test and other calibration tests only one of the two identical compartments of the Christopher Tank was in use: the valve from the second compartment was closed in the model to simulate the experiment. All other compartments of tanks function as a unit and are represented as such in EPANET.

Another assumption in the model is that the water distribution starts with all major tanks full. This is the case for A, B, C, Christopher, MOI and Spring 17 tanks. All of the spring ring tanks modeled were also considered to start full, including Springs 14, 8, 6/7 ring tanks but also the TB Village ring tank which receives pumped water from the Spring 17 tank. Pumping is not modeled however and the TB and Spring 17 systems are considered separately. Also, water flowing into these major tanks is not considered. Hence even though Spring 17 actually keeps on flowing into Tank 17 during distribution, this is not taken into consideration and neither is the inflow from the other springs into their respective spring ring tanks.

Some of the reasoning behind this assumption is that, for one, modeling the flow of water from springs to the ring tanks would complicate the model significantly, especially considering that spring flows vary throughout the year. Another reason for not modeling this component of the system is the fact that pumping river water is by far the major source of water for distribution. Major tanks (besides spring ring tanks) receive virtually all of their water through pumping, except Tank 17. This pumping occurs in a short amount of time before distribution and stops while distribution is running. Comparing volumes of the tanks filled with river water versus spring water (which would include Tank 17), 75 percent of the volume is water pumped from the river. Another factor to take

into account is the fact that flow from springs is distributed throughout the 24 hours of a day, and it would not significantly change the levels of the tanks during the 3 hours of distribution.

These assumptions can be varied however as the model is refined and the system is modified. One such variation would be including sources to ring tanks and Tank 17 and modifying the output of the sources and the initial level of the tanks by season. A maximum level, as modeled here, could very well be representative of the rainy season but maybe not of the dry season. In addition, the issue of initial tank level is even more complicated than it seems. It also involves human decisions, and, even though the AMI staff was advised to pump water to fill the major tanks before tests were run, it seemed that this was not done systematically and varied not only by season but also simply by the judgment of the tank and pump manager.

Despite all of these possible nuances, it is assumed that the levels of the tanks and ring tanks will not greatly affect the pressures and flows at the taps. What varies with the size of the tanks is the time of distribution mainly and whether the system runs dry before the end of the 3-hour period. During distribution, considering the 2-meter average height of most tanks, this variation would imply at most a pressure difference of 2 meters, which is grossly exaggerated considering the head losses in the pipes and in the system. Hence, a 50 percent error in tank level would amount to an error in pressure of less than a meter. The DEM used for elevations has an error of about 1 meter elevation, and the X-Y accuracy of 15 meters makes the elevation difference a much larger source of error than the tank levels. For the same reason, the time change for the pressure and flow calibration data was assumed not to significantly affect the comparison against calculated data. Tank levels would more significantly affect the salt test because concentration is a function of volume but the AMI staff was instructed to fill the tanks as in the model for these tests.

In contrast with the major tanks, secondary tanks are assumed to be empty at the start of the simulation. This is the case for the MaeLa 1 and 2 ring tanks as well as all of the temple ring tanks. They are secondary because they are located out in the distribution system and accumulate water during the 3-hour distribution period. The accumulated water is then used at any time in smaller amounts by institutions such as the hospital or the temple. This irregular smaller distribution is not modeled. MaeLa 2 on the other hand does supply one major public tap and this flow is modeled with an opening of the MaeLa 2 valve during the hours of distribution.

b. Key Parameter Setting Assumptions

The DEM does not extend all the way to the TB Village. Hence values of elevation were taken from the altimeter data which was calibrated using a point of reference with known elevation from the DEM. This point of reference was surveyed multiple times throughout the day using the altimeter to note the differential error and this error was applied to the TB Village elevation measurements. It was assumed that these elevation measurements were within the range of acceptable data even though it is clearly not as accurate as the 1-meter resolution Digital Elevation Model.

The Hazen-Williams equation was used for head-loss calculations over Darcy-Weisbach or Chezy-Manning equations. Chezy-Manning is mainly used for open channel flows, and even though it is sometimes used for pressurized flow, it is not the most accurate. Darcy-Weisbach is more common and theoretically accurate: it uses different methods depending on the turbulence of the flow. However, Hazen-Williams is the most commonly used, particularly in the U.S.: it is empirically determined, and therefore inherently more accurate than theoretical results and has been found to cause fewer computational problems when solving hydraulics in EPANET (Rossman, 2000).

Another assumption used throughout the analysis is the fact that low-use taps have no demand whereas public taps are constantly discharging water during the distribution period. This is certainly not absolutely true in reality, but such an assumption can be justified when comparing the volumes of water used in a 3-hour distribution period for big tanks and public taps with close to constant use compared to latrines, taps of personal use and small drums. A further refinement of the model would be to include a fixed demand of water for these components of the system, and to get a better understanding of the demand variation at public taps throughout the day (at 6:00 AM versus 5:00 PM for example). The pressure and flows at taps would most likely average to similar values however.

III RESULTS

The work discussed thus far has led to the construction of a computer model designed to serve as a tool for analysis and improvement of the drinking water supply system in MaeLa. The following chapter gives a brief overview of the system and evaluates the success of this model in predicting different parameters associated with the water supply. It then provides an analysis of potential improvements of the system.

III.1 System Overview

Figure 3-1 gives a global view of the MaeLa water distribution system using the EPANET visual interface. In Figure 3-1, Bunlur Emaruchi's aerial photograph underlies the system. The road can be observed crossing the picture from the southeast tip to the northwest with the system adjacent to it. The river is situated at the northwest edge of the system and the ridge is to the southwest.

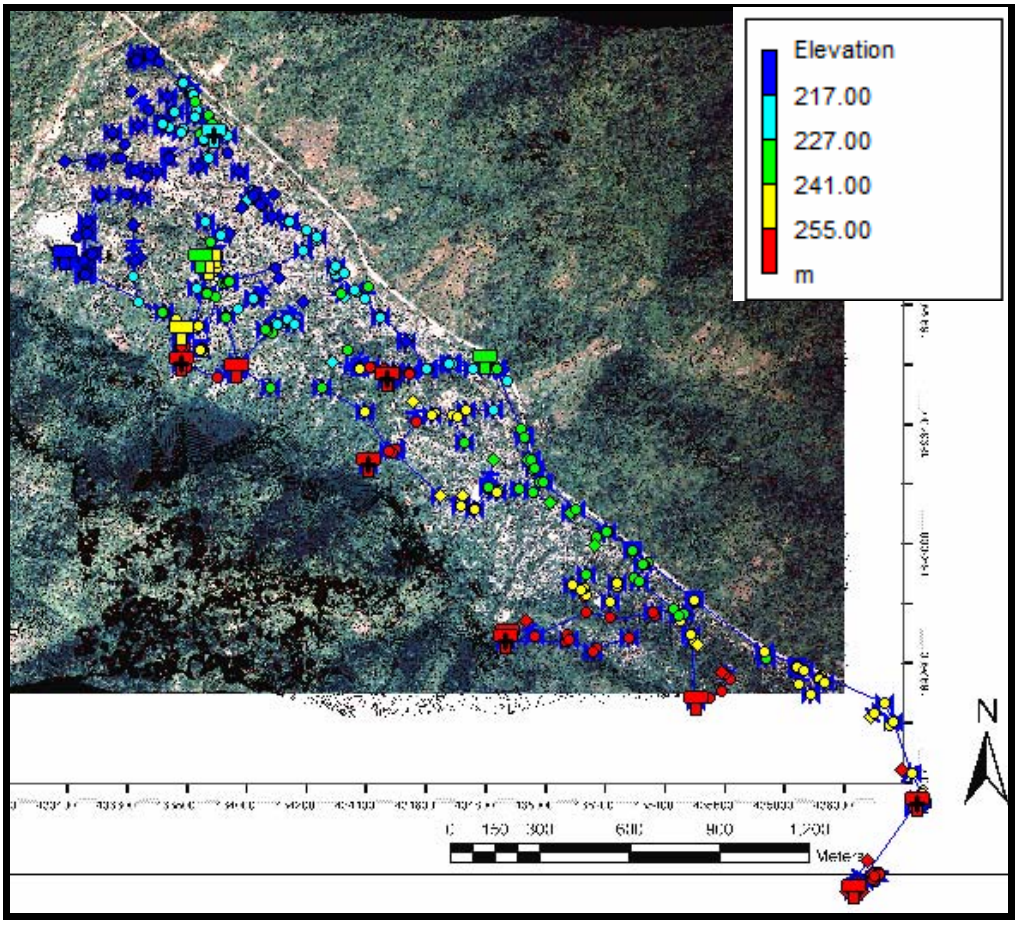

Figure 3-1. Overall view of water distribution system in EPANET

The color coding of the map symbols in Figure 3-1 represents elevation and can be read from the legend. Part of the system to the southeast is not covered by the photograph nor the DEM associated with it: elevations were determined by using calibrated altimeter readings. Major tanks as well as secondary tanks are shown as rectangular symbols on the map. The many nodes (circular symbols) represent some 140 tap stands and 350 joints and tees. Pipelines are shown as blue lines.

The skeleton of the system is shown in Figure 3-2 in the same orientation as Figure 3-1. It is made of about 500 pipes and 140 valves. The different subsystems within the overall distribution system are shown. Spring 6/7 and Spring 8 are sub-components of the C Tank system subsystem since C Tank can supply water to their ring tanks. The TB Village is a sub-component of the Spring 17 subsystem since water is pumped from Tank 17 to the TB ring tanks. As can be observed, some subsystems can potentially interconnect but the valves separating them are usually left closed: these valves are illustrated by black circles in Figure 3-2.

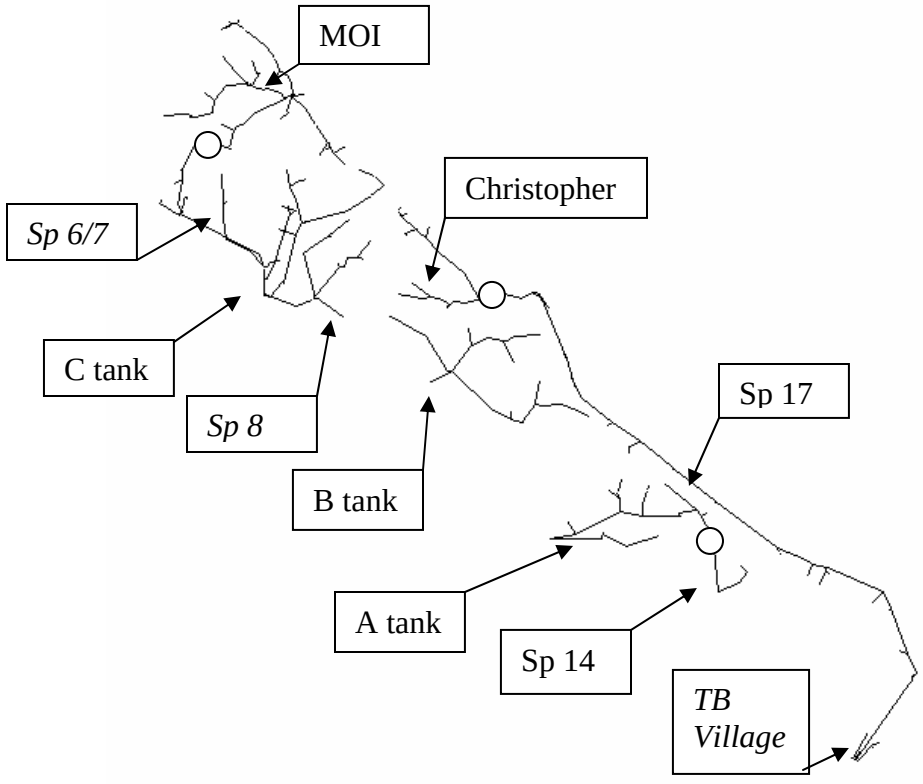

Figure 3-2. Skeleton of the water distribution system

EPANET can show pressures, demand, and water quality at different nodes as well as flows, velocities and head loss in pipes throughout the distribution period. Such results can be exported to tables and graphics or visualized on the graphical interface as illustrated in Figure 3-3. Direction of flow is shown by arrows on Figure 3-3. The figure shows large flows (red arrows) going into the MaeLa 2 ring tank which then re-distributes water to taps to its west. To the very left of the illustration, flow is coming in the opposite direction (from Christopher tank) but a valve blocks it from entering the pipes supplied by the MaeLa 2 ring tank. Many other analysis tools are available in EPANET, such as drawing contour plots of the region based on a parameter of choice, or time series plots of specific nodes. Please refer to the EPANET manual for a complete listing of capabilities.

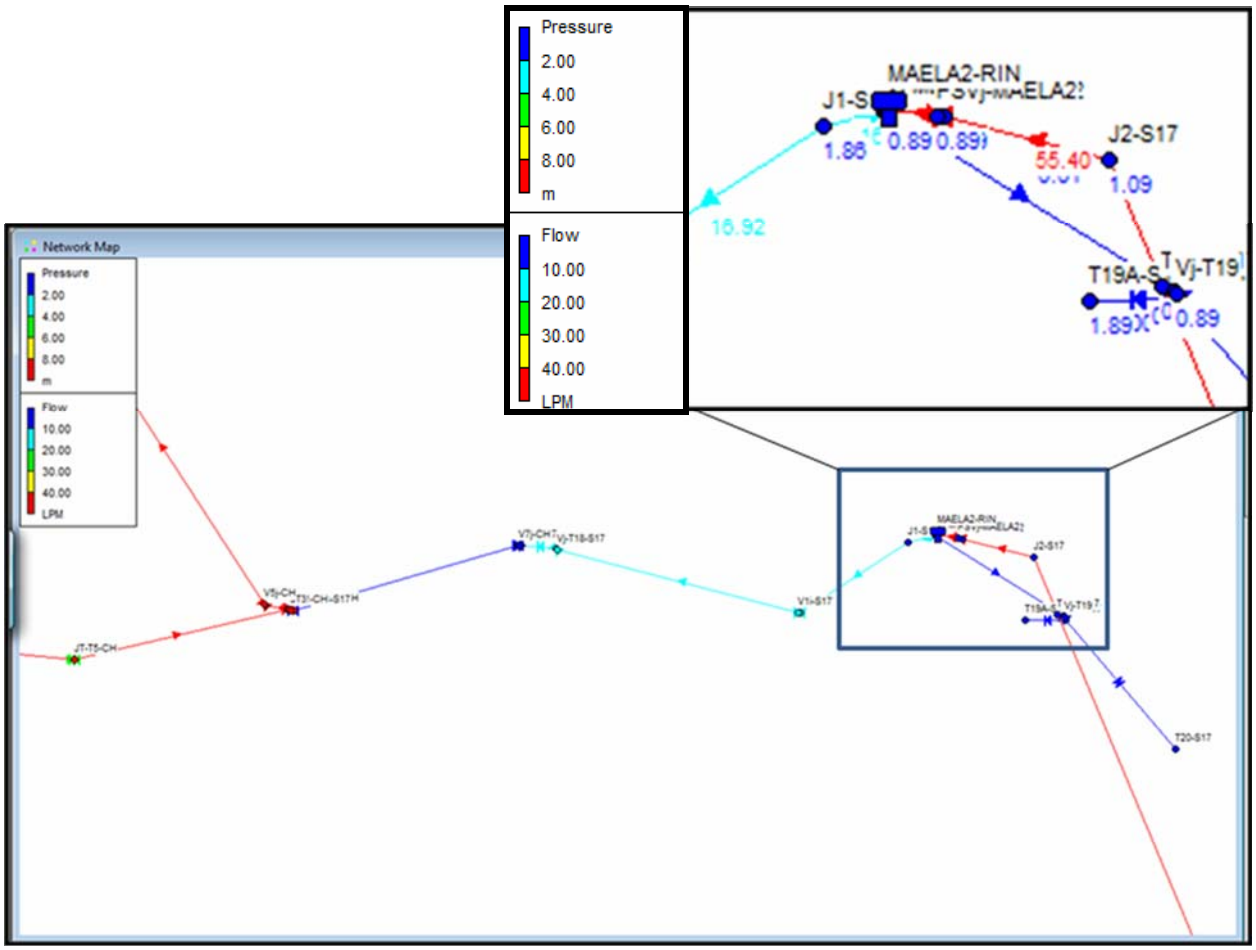

Figure 3-3. Illustration of predicted pressure and flows by the EPANET graphical interface

III.2 Calibration Results

III.2.A Pressure Calibration

Pressures were measured in the field in order to compare with the results of the distribution model. The measurements covered a wide range of subsystems and branches to get a representative sample. Figure 3-4 is a comparison plot of observed pressures versus calculated pressures at various taps throughout the system. The diagonal line on the plot represents the line of perfect correlation. Ideally all the points should align themselves on this line, meaning that all observed pressures would be equal to the computed pressures, giving a correlation coefficient of 1. The linear correlation coefficient (R) of observed versus computed pressures is calculated by EPANET at 0.60. The coefficient of determination (R^2) would only be about 0.36.

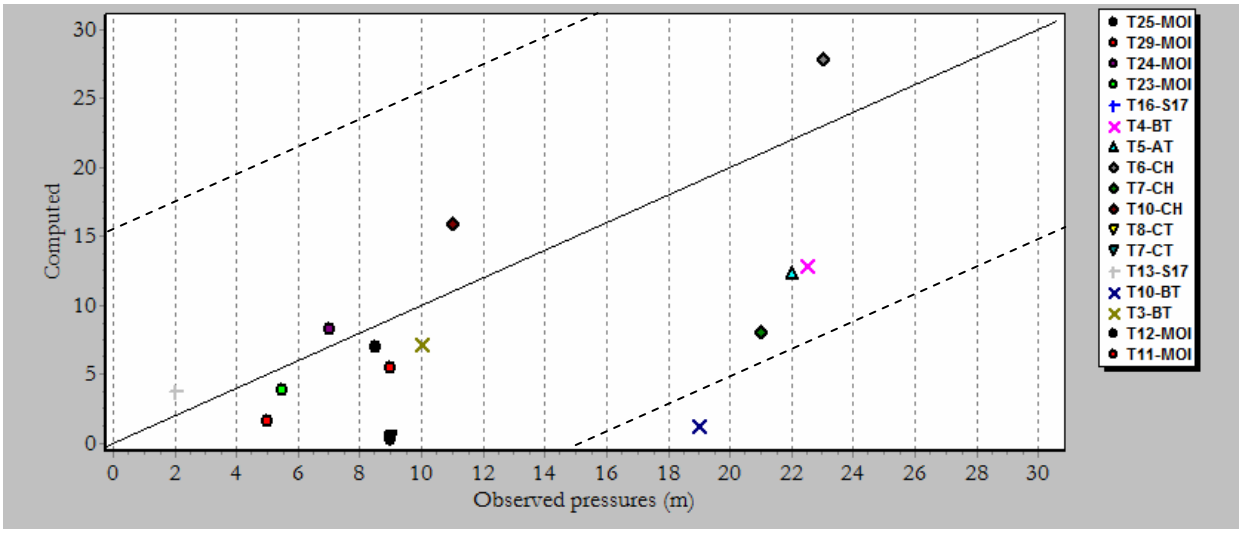

Figure 3-4. Correlation Plot for Pressure

One reassuring fact with respect to Figure 3-4 is that the discrepancy between observed and computed pressures seems to be random rather than systematic. Indeed, one can observe both over-estimates and under-estimates of calculated pressures, at all ranges, and there is no particular tendency by subsystem either. If anything, one might observe a tendency to under-estimate pressures, but considering that minor head-losses have been ignored, this fact is most likely due to the small sample size.

As mentioned previously, the likely major source of error resides in the elevation of tap stands. As indicated above, horizontal (X-Y) points are accurate within about 15 meters. This magnitude of error translates, depending on the slope, to elevation errors from 3 to up to 15 meters. The dashed lines in Figure 3-4 show ±15 meters around the perfect correlation line and give a sense of the potential magnitude of this error. All but one of the points lie within the bounds of these lines. The taps with relatively large difference between computed and observed pressures usually lie in areas of steep slope. Refer to Harding (2008) for more information on surveying errors.

III.2.B Flow Calibration

A different but related test conducted in the field was flow measurement at a number of taps covering the major subsystems. One would expect to get similar results to the pressure calibration since pressures and flows are related by the pressure-driven demand. Figure 3-5 is a comparison of observed flows versus computed flows. The observed and computed flows are clearly correlated. This relation is characterized by an R^2 value of 0.38, just slightly over that of the pressure calibration results. These similar results are to be expected because of the relation between pressure and flow. Again, the differences between computed and observed results do not follow any systematic pattern: they vary across subsystems and flow regimes. The slightly higher correlation factor might be due to the larger sample size of measured flow data compared to collected pressure measurements

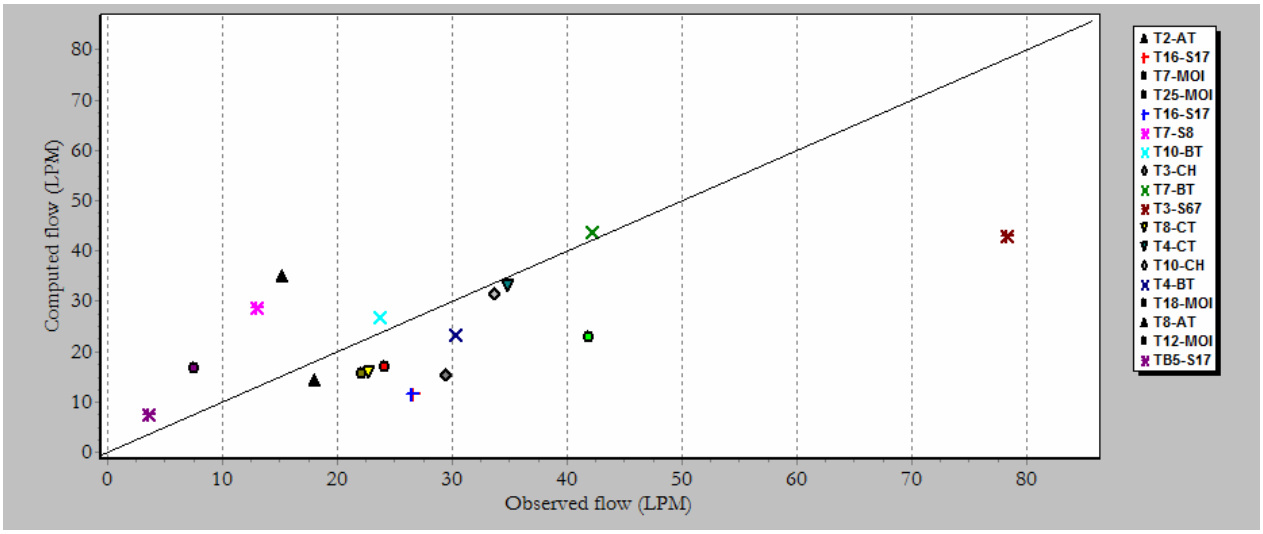

Figure 3-5. Correlation plot for flow

III.2.C Salt Tracer Tests

Another set of tests conducted in the field consisted of salt tracer tests. Unlike the pressure and flow tests, which are straightforward comparisons of computed and observed values, tracer tests can bring out other dimensions of the water distribution system. It is a method of testing for processes such as dispersion and tank mixing as well as general parameters such as the size of the system and its controls.

Using the calibration tool from EPANET, Figure 3-6 illustrates a preliminary comparison of computed versus observed salt concentration. Figure 3-6 is a bit difficult to interpret but it can be seen that the general tendency is for computed and observed data to correlate. The R^2 is 0.33 on this plot.

Several results deserve further analysis. A closer analysis shows that T10-AT (blue diamonds along the chart bottom) is not receiving any salt in the model. Computed values for taps TB5-S17 (green squares) and T7-S8 (red triangles) concentrations do not vary while observed values do. Both computed and observed values of T3-S67 (purple squares) do not vary throughout the simulation.

T10-AT's concentration does not vary in the model because this tap stand does not produce any flow in the model. It is located in a steep region of the camp and hence, a 15-meter inaccuracy in X-Y can imply an elevation difference of about 8 meters which could make the difference between predicting zero and non-zero flow.

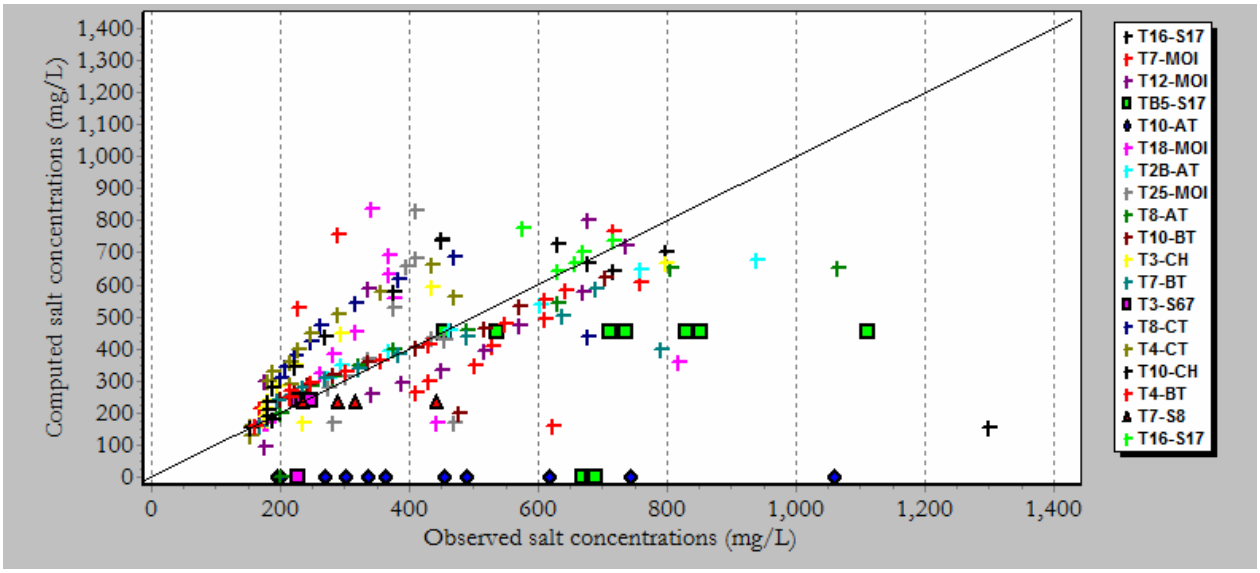

Figure 3-6. Correlation plot for salt concentrations

Figure 3-7 shows the observed and calculated concentrations at these specific taps. This graphic reveals that according to the model no salt reaches the TB Village (TB5-S17) whereas it does with observed measurements: calculated results remain at their background levels of 450 mg/L whereas this is not the case for observed measurements. The reason for this is a variation in the controls of the system. The TB ring tanks receive their supply through pumping water from Tank 17. The model assumes that this process is done outside of the distribution period. The observed salt concentration reveals that in reality, pumping occurs during distribution as well because no salt was directly injected in the TB ring tanks and these readings are instead a result of the salt injected in Tank 17.

Another observation is a variation in the observed salt concentration at T7-S8. C Tank is connected and can supply water to the Spring 8 ring tanks. The model assumes however that no water enters the Spring 8 ring tanks from the C Tank during distribution. Thus, even though salt was injected in the C Tank, calculated results show constant concentrations at background levels from the Spring 8 ring tanks. Observed measurements differ which suggests that water flows from the C Tank to the Spring 8 ring tanks during distribution.

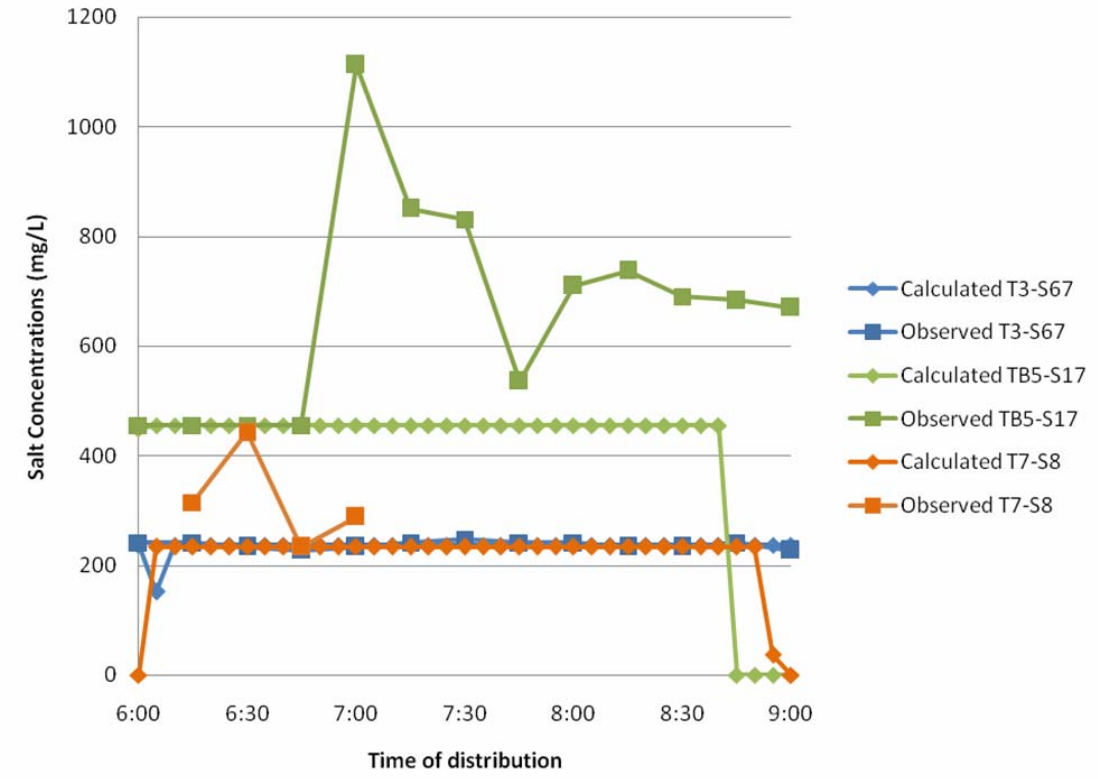

Figure 3-7. Calculated and observed salt concentrations for taps in selected subsystems

On the other hand, recordings for T3-S67 agree with the model in that they maintain background levels throughout distribution. Hence even though the C Tank is connected to the Spring 6/7 ring tanks, indeed no water from C Tank reaches the S67 ring tanks during distribution.

Omitting T10-AT and the other instances in which the model does not represent unexpected operating conditions, Figure 3-8 shows a revised correlation plot for salt concentration. With the specified revisions, the coefficient of determination (R^2) rises to 0.82, a good result. Since pipe lengths are a determinant of the start and evolution of salt concentrations through time, such satisfying results would tend to confirm the quality of the directly measured pipe lengths.

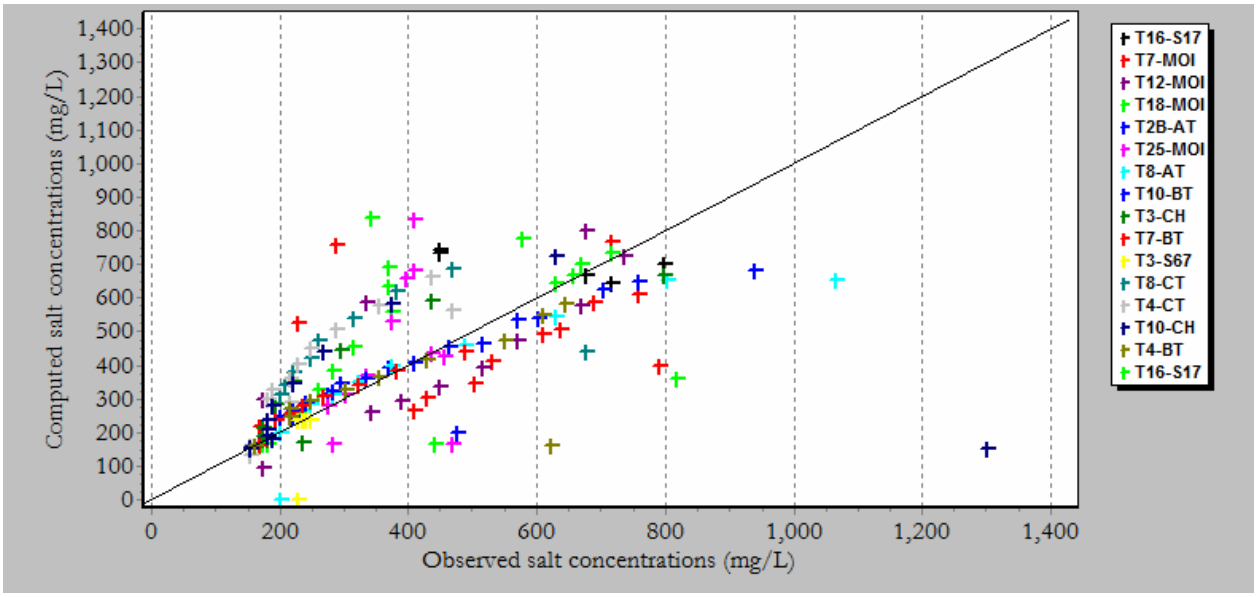

Figure 3-8. Revised correlation plot of salt concentration

The salt-tracer simulation assumes two-compartment mixing at the tanks, insignificant dispersion throughout the system, and constant salt pouring rate and pouring start time. The following discussion addresses these assumptions and takes the reader through a step-by-step analysis of the process used to reach them.

a. Dispersion Assumption

Dispersion represents the variation of velocity over the cross-section of pipes because of shear stress on the inside of the pipes. It leads to a smoothing of salt concentration results through time, with lower peaks and wider spread. As a preliminary analysis of dispersion, Figure

3-9 a, b and c provide observed measurements of salt concentrations at two taps in each of the A Tank, B Tank and Christopher Tank subsystems. These taps were chosen at two extremes of distance from the central distribution tank. The further tap is typically over twice the closer tap's distance from the central tank.

The expectation is that the further tap should have experienced more dispersion resulting in a lower peak concentration and a wider spread. Though limited by the 15-minute resolution in the field data, Figures 3-9a and b show that the further tap has a peak occurring later than the closer tap, as expected because of distance differential. However, the expected trend due to dispersion does not occur. Actually, it is even observed that further taps in two of the three subsystems present an unexpected higher peak concentration than its counterpart: this result may be due to the 15-minute resolution of the data which does not record the actual peaks at close taps. Nor is there a wider spread observed in the further taps for any of these subsystems. Hence, dispersion does not seem very probable but dispersion is further evaluated.

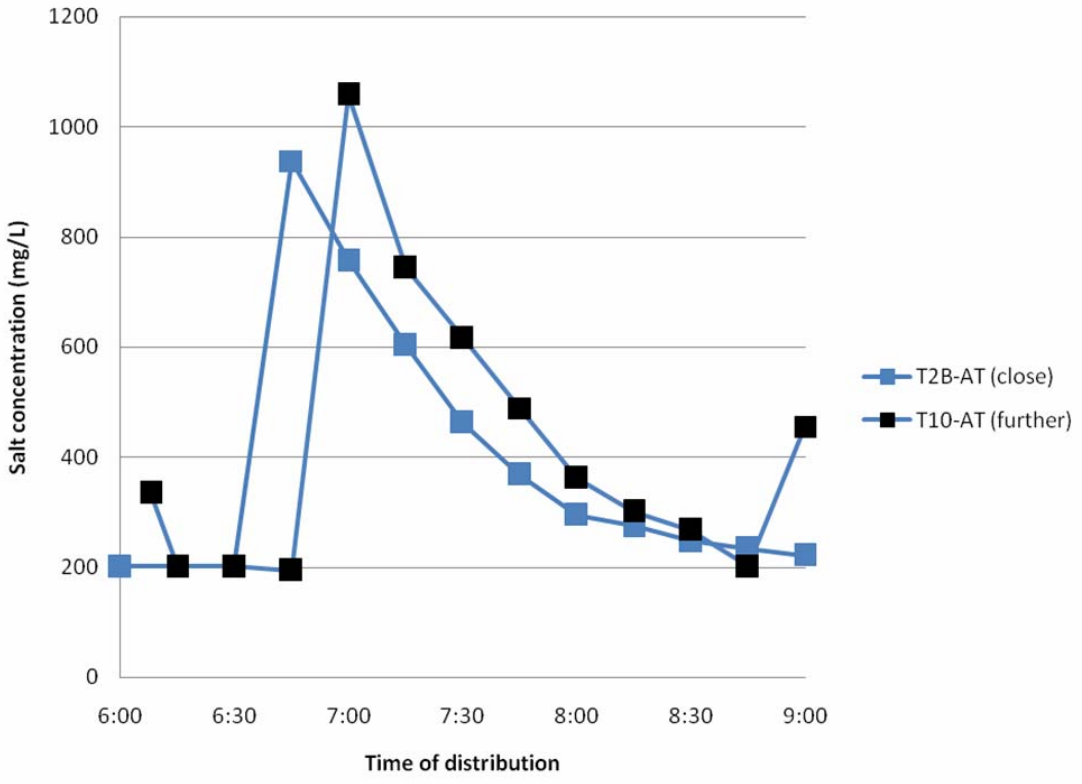

Figure 3-9a. Dispersion analysis of field results at A Tank subsystem

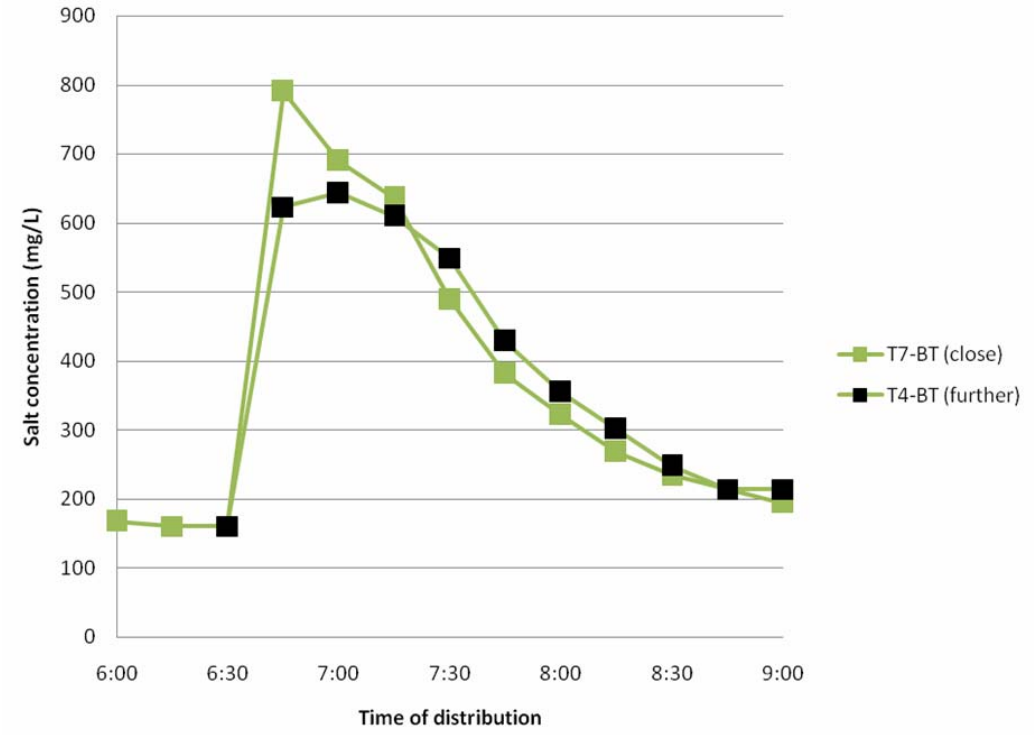

Figure 3-9b. Dispersion analysis of field results at B Tank subsystem

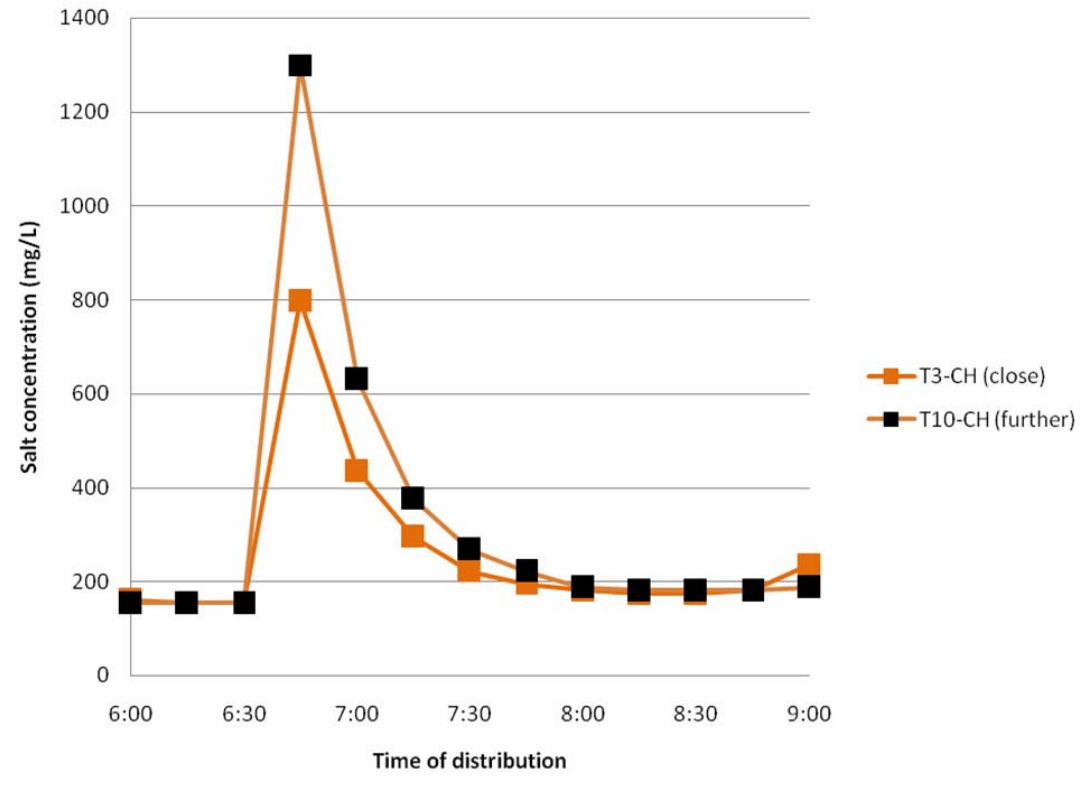

Figure 3-9c. Dispersion analysis of field results at Christopher Tank subsystem

To evaluate the magnitude of dispersion in the distribution system, the dispersion coefficient is calculated in the Spring 17 subsystem, the subsystem with the lowest water velocities, at T16-S17, one of its furthest tap at about 1,850 meters from the tank. Dispersion should be at its highest at this point since dispersion is strongly dependent on travel time.

Taylor (1954) defines the longitudinal dispersion coefficient in pipes as:

$$D = 10.1\, r\, v \tag{3-1}$$

where D is the dispersion coefficient in square meters per second, r is the radius of the pipe in meters and v is the shear velocity in meters per second. This equation characterizes dispersion for turbulent flow. The Reynolds number is the main factor in categorizing flow as turbulent or laminar: assuming a temperature of 20 degrees Celsius, the Reynolds Number was calculated to be 5.84×10^{-4} on average through this Spring 17 branch which confirms that flow is turbulent and this analysis is viable. Flow should be turbulent throughout the distribution system since the Reynolds number is proportional to the velocity in the pipes and Spring 17 is characterized by slower water velocities.

After gathering the necessary data from the Spring 17 branch analysis, the average dispersion coefficient was found from Equation 3-1 to be about 0.014 square meters per second. The longitudinal dispersion coefficient can be used to predict the distribution of mass along the pipe and is related to the variance of the mass distribution at a point in the subsystem through

$$D = \sigma / 2t \tag{3-2}$$

where D is the dispersion coefficient in square meters per second, σ is the mass variance as a function of distance is in square meters and t is the time of travel in seconds. The variance was found from the dispersion coefficient and the time of travel calculated from the distance and average velocity of water in the branch analyzed. The square root of the variance yields the standard deviation of the mass distribution at T16-S17. It was evaluated at about $\sigma = 7$ meters. Figure 3-10 shows the probability density function for mass distribution at T16-S17, after 1,850 meters of travel, with an average travel time of 30 minutes.

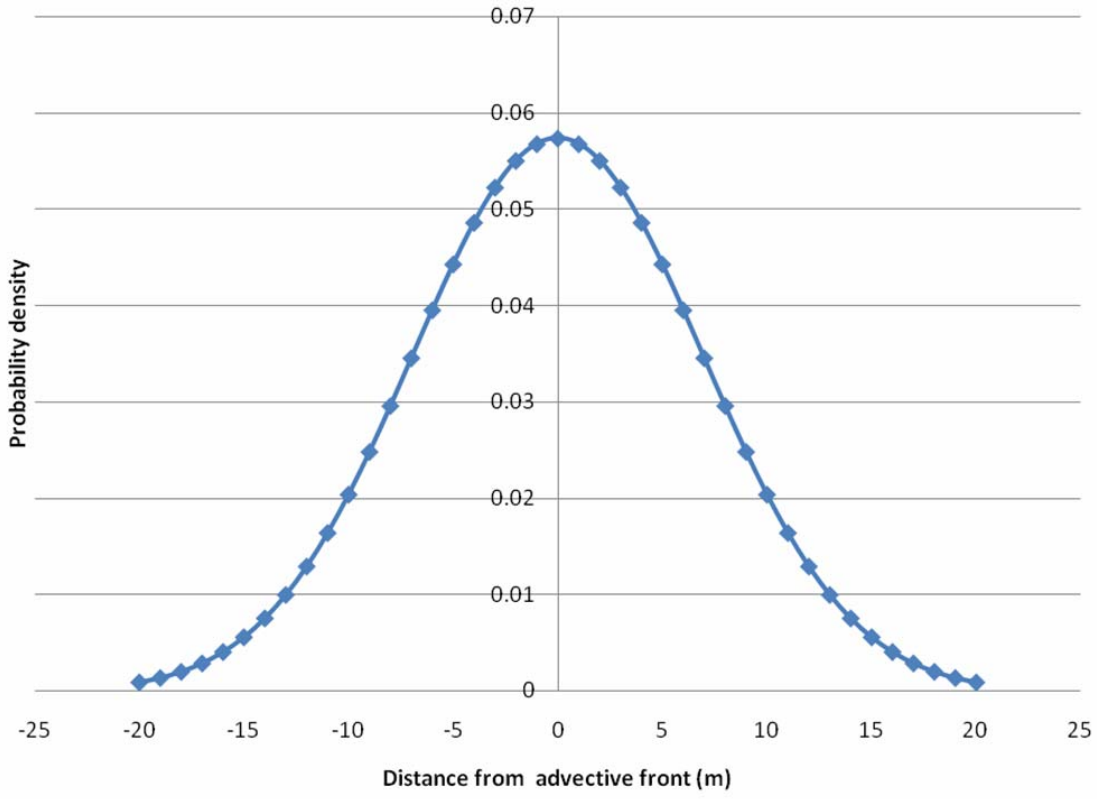

Figure 3-10. Probability density function of matter at T16-S17 as a result of dispersion

One can imagine the total area under the curve as being the total mass of salt if it were injected straight into the pipe system. This implies that at this point of relatively high dispersion, 96 percent of the matter is contained within 28 meters of the advective front. Hence considering the average velocity of water in this subsystem at about 1 m/s, the bulk of injected matter should have passed within 28 seconds. With the resolution of 15 minutes in the observed data, dispersion is not a significant factor.

b. Tank Mixing Assumption

In order to isolate variables, let us first consider salt concentration results within a single subsystem. This procedure eliminates some source of variability from this preliminary analysis since the pouring rate (and its potential variations through time) and the mixing start time is the same within a single subsystem. Figure 3-11 shows these results for the MOI subsystem with the initial default assumption of fully mixed tanks.

In analyzing salt results, one should consider time separately from concentration levels. Analyzing concentrations, the peak of the curve should be considered in relation to its breadth. Indeed, by conservation of mass, the area below the curve should be the same at the end of the analysis no matter its shape. This area is equal to the portion of the initial salt mass poured into the subsystem that is coming out of the tap, which can be calculated by multiplying the concentration by the average flow rate at the tap.

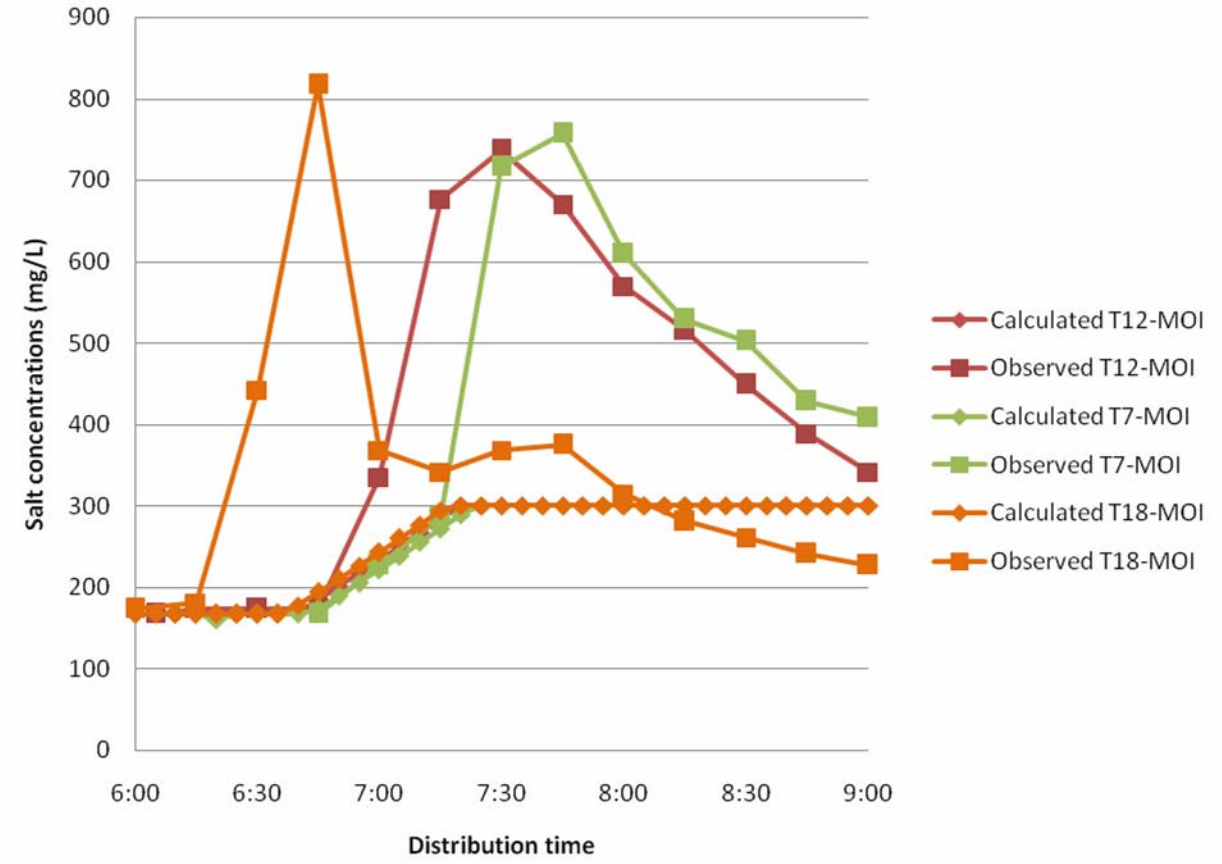

Figure 3-11. Comparison of calculated and observed salt concentration in MOI subsystem under fully-mixed tank assumption (note that calculated curves for T7-MOI, T12-MOI and T18-MOI overlap over much of the distribution time)

Figure 3-11 shows that concentration levels between observed and calculated results do not match under the assumption of fully-mixed tanks. However, though the tank has not drained fully by the end of the distribution period, it does seem that all areas under the curves (i.e., the total mass) are reaching the same value (disregarding the area under the curves that is below their background concentration level of 170 mg/L). Along the same lines, the fixed concentrations

calculated (300 mg/L) are reaching an average level of the observed concentrations. This is expected because despite possible dispersion and time delays, the average concentration of salt over a period of complete distribution should be the same at all taps within a single subsystem. Actual masses of salt at each tap stand are different however because of the variation in flow rates between taps.

The difference in observed and calculated levels of concentration cannot be attributed to human error and different pouring rates since all these results are within the same subsystem. The concentration differences are a consistent concern confirmed by the fact that all observed results reach about the same peak level of concentration and so do all calculated results. The calculated results follow a different pattern than the observed results. No peaks are observed, and the concentrations simply rise to a level that is kept constant for the rest of the distribution period. This result can be explained by the assumption that the tanks are fully mixed.

It should be pointed out that the times at which concentration starts to increase are virtually the same for calculated and observed results. Since these results are within the same subsystem and hence pouring start time is certainly the same, this correlation confirms that generally the survey of the dimensions of the system corresponds to true values and the model-field data discrepancy cannot be attributed any systematic error. Similar patterns are observed within other systems.

A fully-mixed tank implies no short-circuiting within the tank and that all mass is spread evenly within the tank and comes out at a constant concentration during distribution. Considering the results of dispersion, the concentration should reach its maximum level quickly and stay at such levels as was observed in the calculated results.

Since this was not the case in observed data, the assumption of a fully-mixed tank should be revised. In reality, there is no turbine inside the tank to mix it at a uniform concentration. Even further, salt was not sprinkled all around the tank area because of the difficulty of opening multiple sections of the concrete tank roof. The salt was poured into the center of the tank and it did not mix with the whole volume of water. Hence the salt mixed into a smaller volume of water at a higher concentration. This high-density salt water is heavier than the unsalted water and would tend to sink to the bottom of the tank. The outflow pipes are situated at the bottom of the tank and would draw water preferentially from the bottom. Thus, we anticipate there would be short-circuiting of salt through the tank.

The two-compartment model is able to simulate such processes: it separates tanks into two fully-mixed bottom and top compartments (the active and dead zone) assuming that inflow and outflow occur to and from the bottom compartment hence short-circuiting the system while the top tank remains dilute. The assumption that inflow occurs to the bottom compartment is largely correct in this analysis because salt tends to sink to the bottom of the tank. Outflow also occurs from the bottom in the real tank. The amount of water with which salt mixes (which determines the peak concentration) is set by the bottom compartment volume fraction parameter in EPANET. By mass conservation, a lower fraction would mean a higher concentration of shorter duration.

But in reality, because there is no physical separation between the top and the bottom of the tank, not all water from the bottom drains before the top layer comes into play: there is some level of water exchange and mixture from top to bottom compartments as the tank drains. This is taken into account by the model in that as the bottom compartment empties, it is replenished by the top compartment which dilutes the water quality in the outflow.

To summarize the process simulated, salt enters the bottom compartment and increases its concentration. It reaches a peak at the tank when the source input discontinues. This peak is determined both by the salt pouring rate and the size of the bottom compartment. Then as the tank drains, the top compartment (without added salt) replenishes the bottom one and dilutes its concentration no more water is available in the top compartment.

In reality, the process is not so linear because the compartments are not in fact fully-mixed. Hence water does not flow vertically and then horizontally but more diagonally. It could very well be that the introduced salt could find itself in a dead zone within the tank and would come out later. Alternatively, salt could have been poured at the front of the tank just next to the outlet and could have short-circuited quickly to the tank outlet. Generally however, the salt was poured at the center of the tank and the two-compartment model is a good working assumption.

Assuming that all major tanks in the camp follow similar mixing dynamics, an analysis of each subsystem would determine the average mixing fraction for the bottom compartment in the major tank serving that system. As discussed earlier, observed salt concentration at taps within a single subsystem show a similar evolution and peak concentration. Hence, to determine the appropriate mixing fraction, only one tap needs to be included from each subsystem. Figures 3-12 and 3-13 show measured salt concentrations at one tap in each major subsystem and the

corresponding calculated results with an initial estimated fraction of 0.2 for the bottom compartment volume.

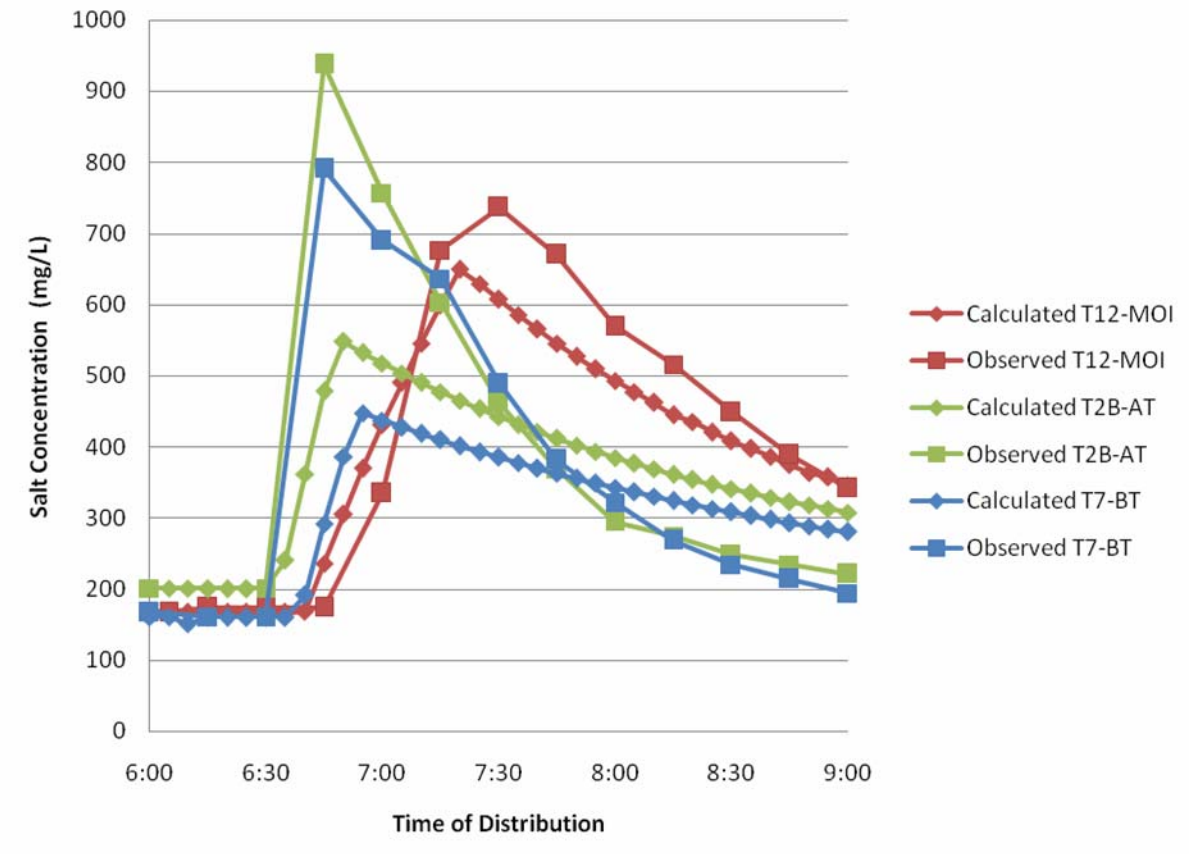

Figure 3-12. Observed and calculated concentrations in MOI Tank, A Tank and B Tank subsystems under 0.2 mixing fraction for bottom compartment

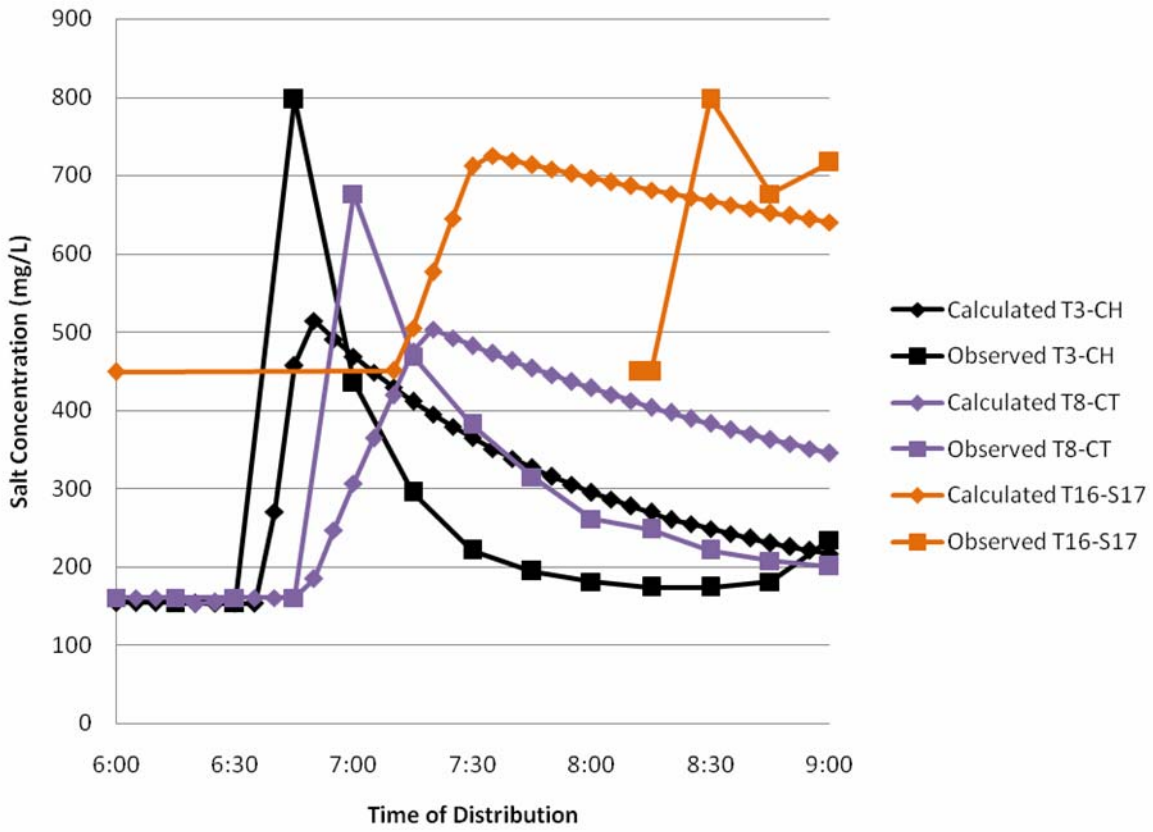

Figure 3-13. Observed and calculated concentrations in subsystems Christopher, C Tank and Spring 17 under 0.2 fraction for bottom compartment

The first observation is that observed and calculated results for all subsystems, except that of Spring 17, match in the time it takes salt to reach the taps. Assuming the technicians all poured their salt at 6:30 AM, this result again shows the validity of the physical survey of the system. A full set of observed data could not be collected for any tap at Spring 17. The main distribution pipe unfortunately broke just before data collection; flow was interrupted and restarted later.

Despite tanks not having drained fully (implying that more salt would come out) and a low resolution in the observed data, another satisfying result is that the average concentration of corresponding and calculated results is about the same. Again, this is also saying that underlying areas of corresponding calculated and observed curves are converging. Hence, assuming correct calculation of flow rates, no significant mass of salt was lost in the process of pouring. The issue is debatable for the tap in the C Tank subsystem: some salt might have been lost in the process of pouring.

One should also observe the relative magnitude of peak concentrations by subsystem within the calculated concentrations, and the relative magnitude within the observed concentrations. The evolution of concentration with time is a function of rate and quantity of salt addition and the flow rate out. The combination of different flow rates and different mass injected in each subsystem (as we were initially aiming for a fully-mixed tank) explains the different peak concentrations illustrated in the EPANET results. However, relative peak concentrations among EPANET curves and among observed results should match. For example, looking at Figure 3-12, EPANET shows a higher peak concentration for the MOI Tank subsystem tap, followed by that of the B Tank and then that in the A Tank subsystem. The observed results however show the B Tank subsystem having the highest concentration followed by A Tank and then MOI Tank. One could argue that peak differences are a result of the low data resolution but the general MOI concentration curve is flatter than expected. This is a result of a slower pouring rate at the MOI tank resulting in a lower peak and wider curve compared to other observed concentration curves.

All calculated curves are lower than the observed concentrations, which implies that a smaller mixing fraction better represents the true mixing in the tanks. A different mixing fraction could have been chosen for each of the tanks to better match their respective concentration results. However, such a solution would mask errors in the field experiment such as the slower pouring rate at the MOI Tank. A mixing fraction around 12 percent was found to achieve a better match between calculated and observed concentration curves. Figures 3-14 and 3-15 illustrate the modified results.

These modified calculated results better match the observed data. Discrepancy still remains, particularly for the taps in the MOI, C and Spring 17 Tanks for extraneous reasons mentioned earlier. Besides, these calculated results are affected by multiple uncertainties. Are all tanks following the same mixing patterns? Is the manual pouring actually kept at the same rate at each tank and within the pouring time range? Also, the flow rates calculated were shown to present uncertainties. Overall however, the assumptions are reasonable and matching the actual dynamics of the system to a satisfying degree of accuracy.

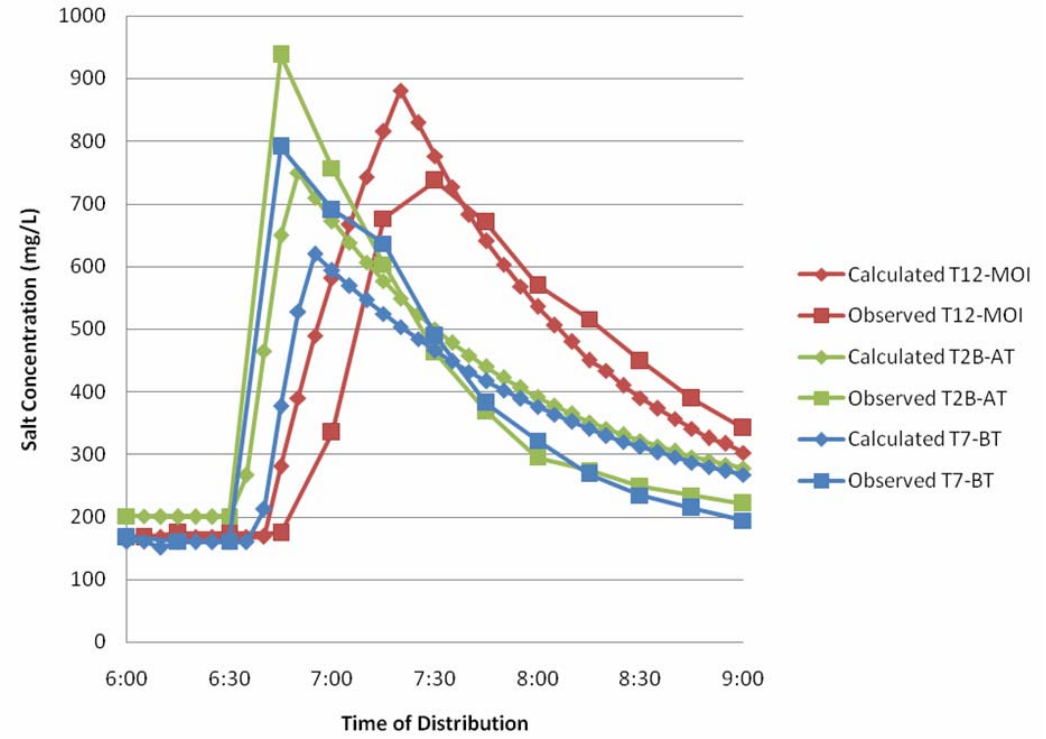

Figure 3-14. Observed and calculated concentrations in subsystems Christopher Tank, C Tank and Spring 17 Tank under 0.12 fraction for bottom compartment

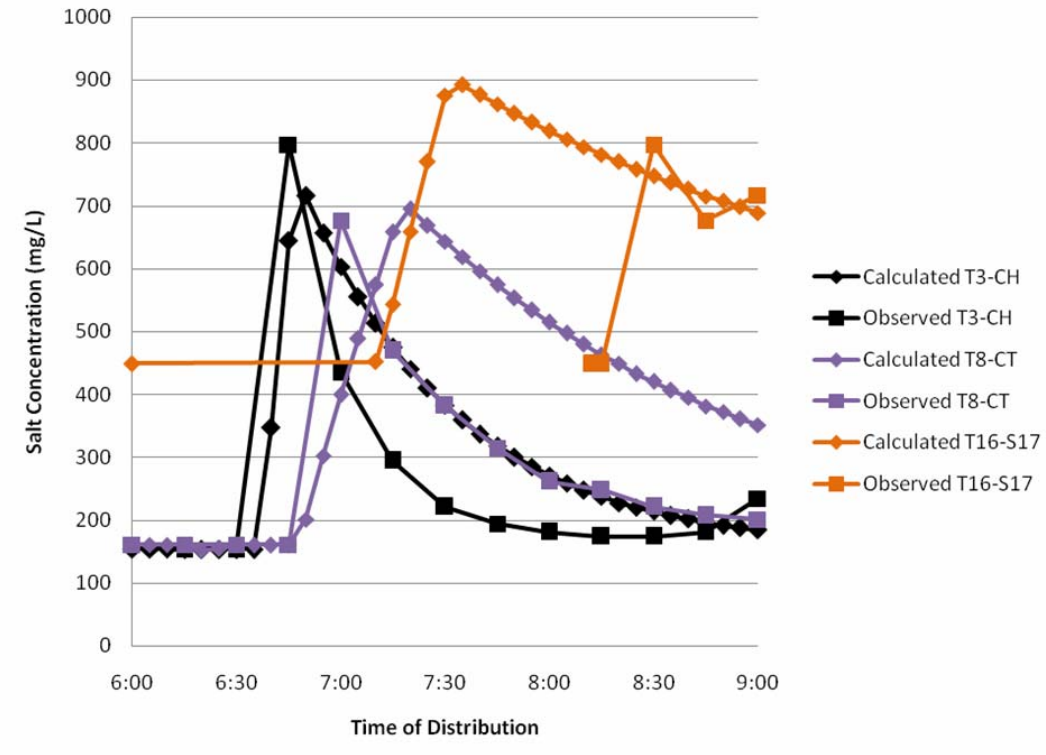

Figure 3-15. Observed and calculated concentrations in subsystems Christopher Tank, C Tank and Spring 17 Tank under 0.12 fraction for bottom compartment

III.3 Potential System Modifications

The purpose of the present model is to run various types of analyses aiming at improving the distribution system. This section evaluates simple modifications which could potentially equilibrate pressure and flow distribution. The premise is that areas of low pressure and flow need to be minimized assuming that population distribution is fairly uniform throughout the camp. It is also important to mention that generally, because of the non-linearity between pressures and flows due to the increasing friction in faucets with higher flows, re-distributing pressure allows a higher overall flow out of the system.

III.3.A Original System

Figure 3-16 is an illustration of the pressure distribution throughout the camp. The orientation of the camp is the same as in Figure 3-1 and all subsequent figures of the camp will follow the same orientation. North is upward and the river crosses the top left tip of the image while the road is adjacent to the right edge of the image. The pressure distribution is extrapolated by EPANET to areas without pipes but these areas should not distract the viewer. It should be noted that the pressure distribution is not an illustration of pressures at taps only; it includes the pressure at all different nodes in the system.

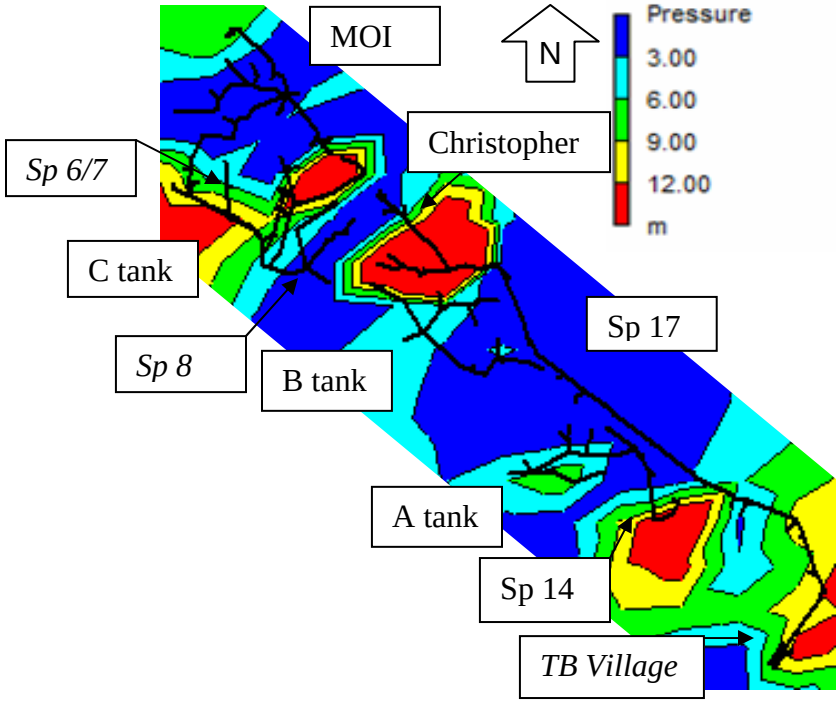

Figure 3-16. Geographical distribution of pressure in original system

There are extremes of low and high pressure throughout the camp mainly due to the topography of the area and the elevation of the distribution tanks. The Spring 17 subsystem in particular is marked by low pressure in the pipes bordering the road. The MOI subsystem could make use of higher pressures as well. On the other hand, the Christopher, C Tank and A Tank subsystems are marked by high pressures even though they also possess some low pressure areas. The objective is to convey some of the high pressure to low pressure areas.

Figure 3-16 provides a geographical analysis of the pressure distribution in the camp whereas Figure 3-17 provides more quantitative information through a frequency plot of the pressure at nodes throughout the camp. About 50 percent of the camp is marked by pressure of 3 meters or less. Considering the flow versus pressure curve of a typical SANWA tap, each tap added to the pipe system in the camp will produce about 15 liters per minute.

The pressure is only important as it creates the flow to provide water to the general camp's population. Figure 3-18 shows the geographical distribution of flow around the camp.

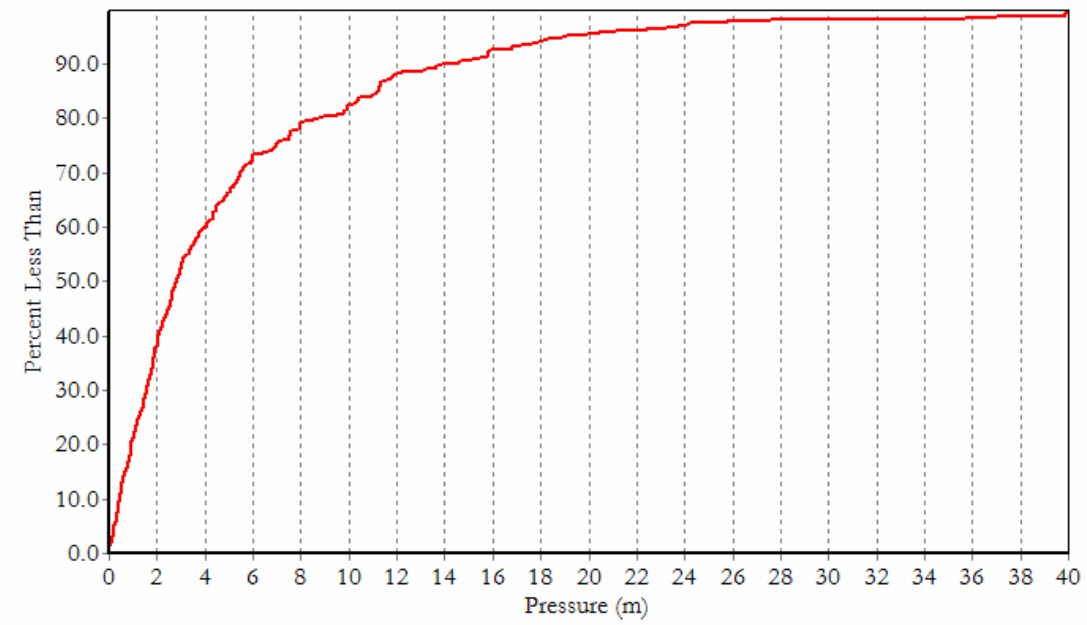

Figure 3-17. Numerical distribution of pressure in original system

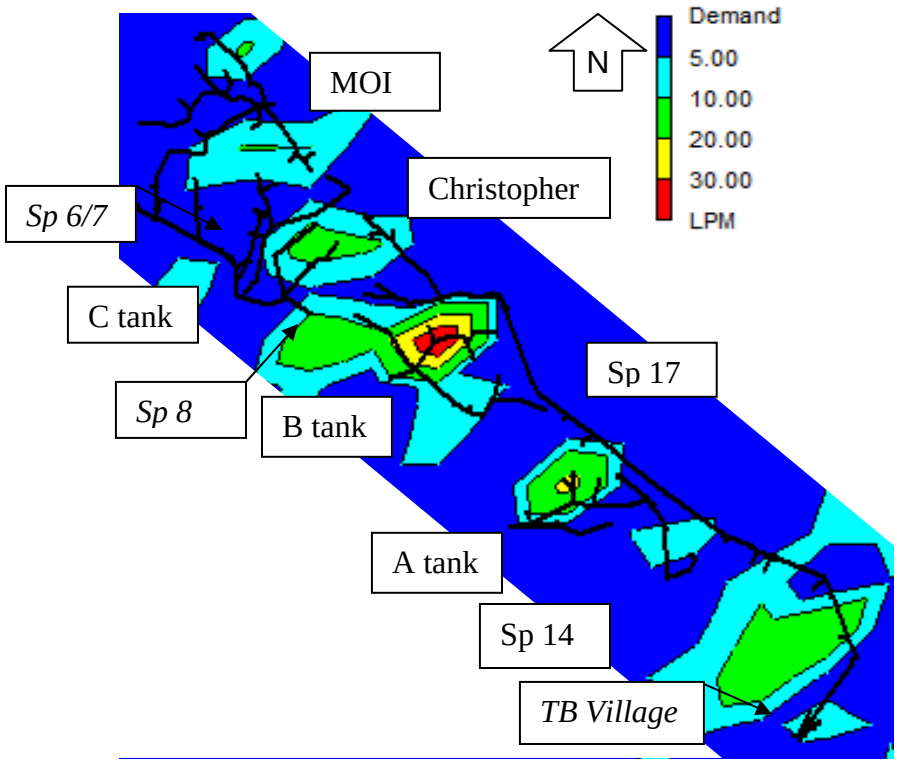

Figure 3-18. Geographical distribution of flow in original system

Comparing pressure (Figure 3-16) and flow distribution (Figure 3-18) shows that elevated flows are located in more concentrated areas than pressure: these areas are centered around the public taps. However, some extremes of the pipe system do not end in a concentrated demand area: this is either due to a flow less than 5 liters per minute (quite low), or simply because these taps have an emitter coefficient of zero because they were used minimally (e.g. latrines). These are usually non-public taps such as those for NGOs, schools or latrine and private taps or drums. Unfortunately, there are some high flow public taps not represented on the figure: some taps are calculated to have low or no flow because of the elevation error due to GPS instrumentation.

As far as distribution of water, it seems that the northern part of the camp has better access to water than the southern part. This might be because the northern part is more densely populated but people also live in the southern region and they should be provided drinkable water at a reasonable distance. This issue will be addressed later.

Figure 3-19 provides a more quantitative analysis of the demand throughout the camp. The distribution of flows in Figure 3-19 only takes into account taps with non-zero flows. About 50 percent of the taps have flows of 18 liters per minute or less. This is close to the median value of 15

liters per minute flow from a single faucet which was calculated from the pressure distribution. The median flow from Figure 3-19 is a bit higher because the system includes many tap stands with more than one faucet. Tap stands with more than one faucet have a reduced pressure at each tap but can generally discharge more than a single faucet tap stand because of the non-linear relationship between flows and pressure. The 18-liters-per-minute flow takes into account taps with more than one faucet.

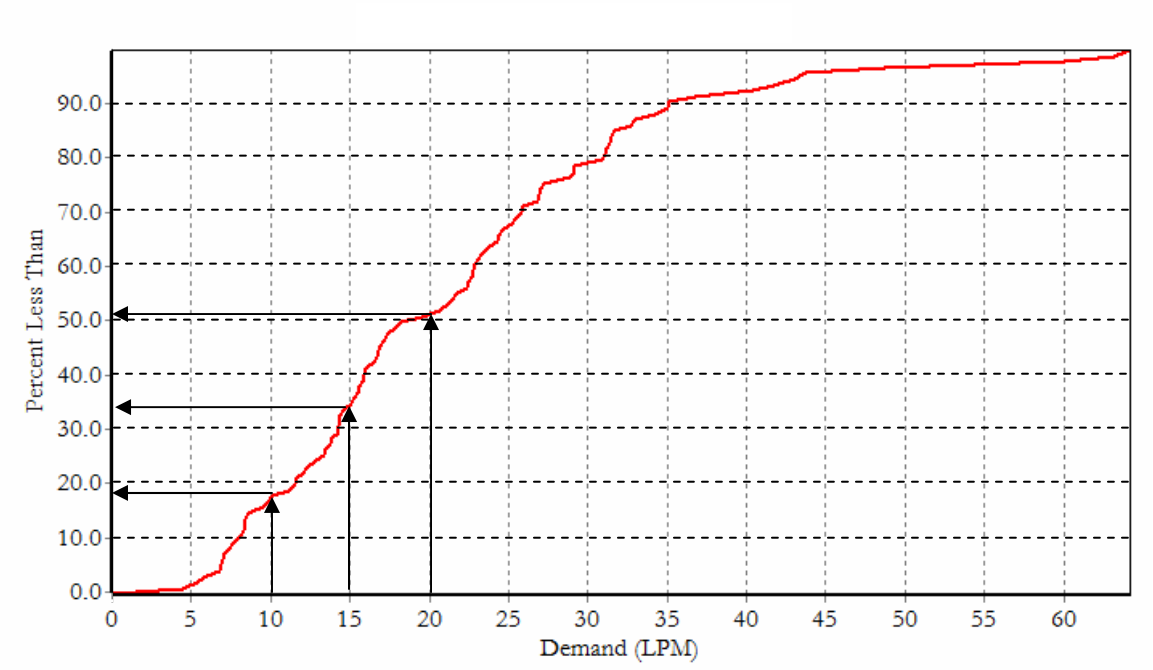

Figure 3-19. Numerical distribution of flow in original system

The lower flow portion of this distribution represent the tap stands of concern with flows that need to be increased. Currently, about 19 percent of the taps provide flows of 10 liters per minute or less, 34 percent are at flows of less than 15 liters and 51 percent at 20 liters or less.

III.3.B System Connecting Valves

Section II.2.D indicates that pipes interconnect the individual subsystems in the camp but that a closed valve usually prevents flow between subsystems. This is the case for the Spring 17 and Christopher subsystems for example, which connect at valve V7-CH, for the MOI and Spring 6/7

component of the C Tank subsystems, which connect at V-18-5, and for the Spring 14 and A Tank subsystems, which connect at V-T10-AT. One alternative to potentially distribute the pressure of the different subsystems more evenly is to open these valves. It is the simplest potential solution, which can take place immediately at no cost of material or labor, and hence deserves attention. Figure 3-20 locates these valves by white circles on the original system's pressure distribution map (to the left) and the subsequent pressure distribution with the valves opened (to the right).

Comparing pre- and post-opening of the valve, no noticeable pressure change occurred between the MOI and C tank (Spring 6/7) subsystems. Little pressure was passed on to the edge of Spring 17 subsystem from the Christopher tank subsystem, at a relatively higher altitude. The MaeLa 2 secondary collection tank, shown by a white square in Figure 3-20, is located close to the edge of the Spring 17 subsystem to collect water from the Spring 17 Tank and re-distribute it during times outside of distribution. The pressure from the Christopher tank subsystem is not distributed further in the Spring 17 subsystem mainly because it would have to go through the MaeLa 2 tank.

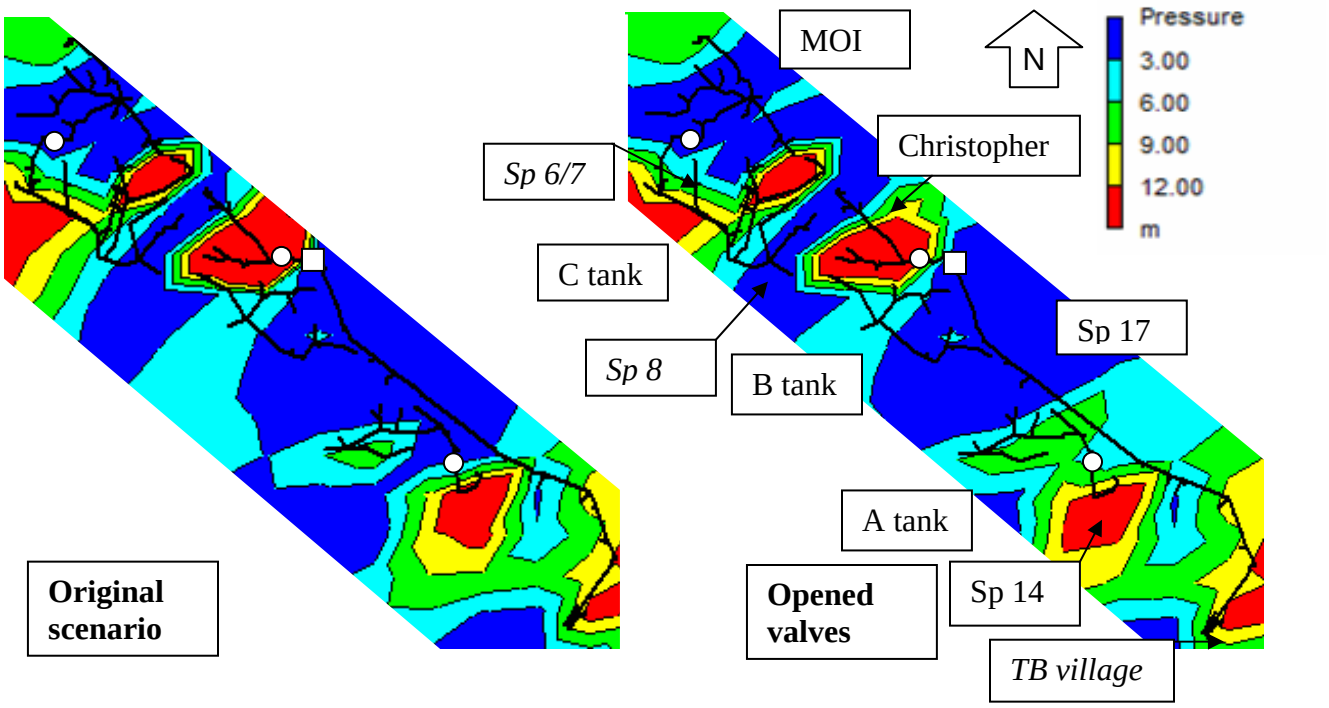

Figure 3-20. Geographical pressure distribution difference from opening system connecting valves

The effect of opening the valves in the Spring 14 and A Tank region is most interesting: the Spring 14 ring tanks have a high pressure potential because they are located at a high elevation and hence opening the valve could provide a re-distribution of this pressure to parts of the A Tank subsystem with low pressure. The catch however is that the Spring 14 water is quite limited. Hence the pressure increase only lasts for the first hour of distribution starting with full ring tanks. Then, the additional pressure to A Tank is lost as well as all pressure to the one tap supplied by the Spring 14 ring tanks. Figure 3-22 illustrates the pressure distribution after an hour of distribution. As can be seen in the circled area, pressure is no longer available at the Spring 14 subsystem because the tank is fully drained. To examine whether opening these valves is useful (particularly the Spring 14 valve), let us observe the consequences it would have on flows at taps.

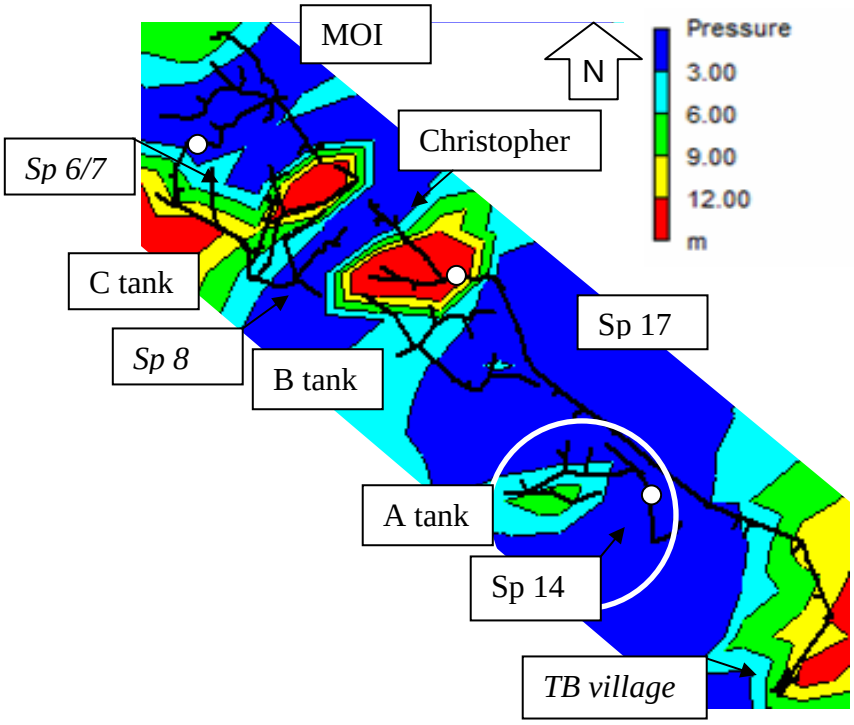

Figure 3-22. Geographical pressure distribution over 1 hour after opening system connecting valves

Figure 3-23 shows, in parts a, b, and c respectively, the original flow distribution, the distribution during the first hour of distribution with open valves, and the distribution after an hour. One of the striking observations is that there is little difference in tap flows before and after opening the valves. As expected, no difference is observed in the C Tank area. Some of the flow is re-directed from

edges of the Christopher subsystem, where it was more needed, to the edge of the Spring 17 subsystem. But there is little variation in the Spring 14 and A Tank area: the epicenter of the flow around the A Tank subsystem becomes slightly larger but the difference is minimal and irrelevant since that portion of the A Tank subsystem was already provided with a significant supply. Areas of the A Tank subsystem with lesser flow are not reached because of elevation difference among other things. Then after an hour of flow when the Spring 14 tank is empty, all flow is lost to the tap Spring 14 was supplying.

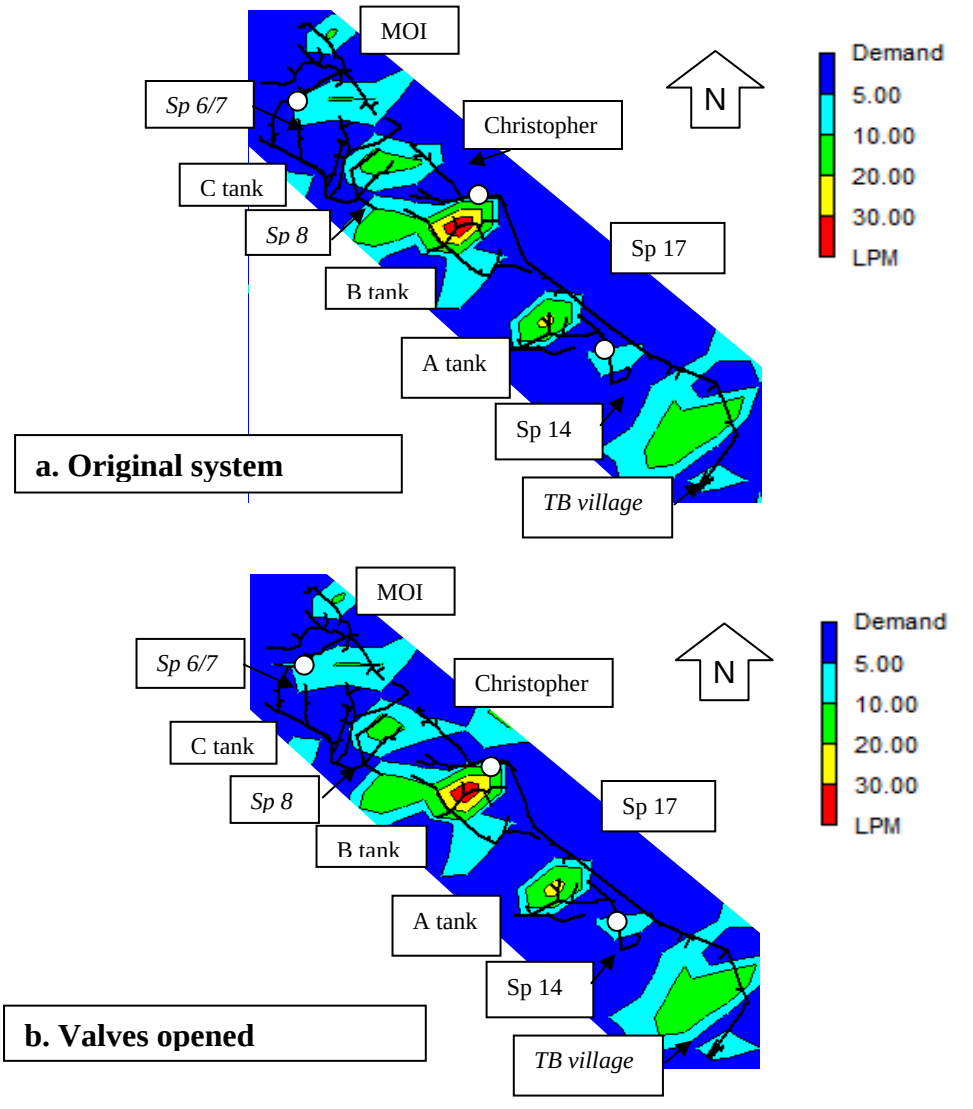

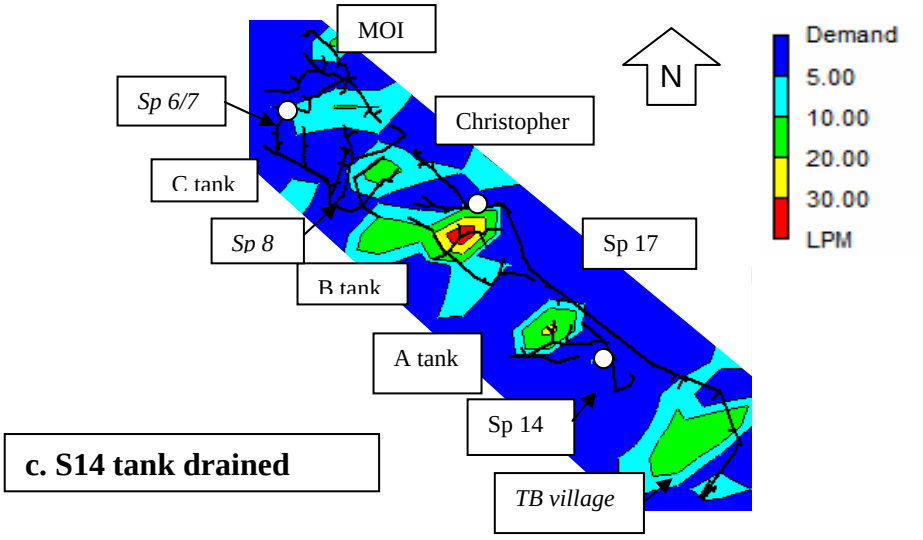

Figure 3-23. Evolution of flow distribution from opening system connecting valves

The frequency plot of pressure distribution in this scenario is very similar to that of the original scenario because it is showing pressure at hundreds of nodes and the difference is not noticeable. The demand distribution before and after the Spring 14 tank drainage are compared to the original scenario in Figure 3-24. The difference between the curves might seem minimal but it should be realized that each 2 percent increase or decrease from a threshold consists of about three taps that have varied. Hence a careful analysis is important considering that about 300 people are served by each tap on a daily basis.

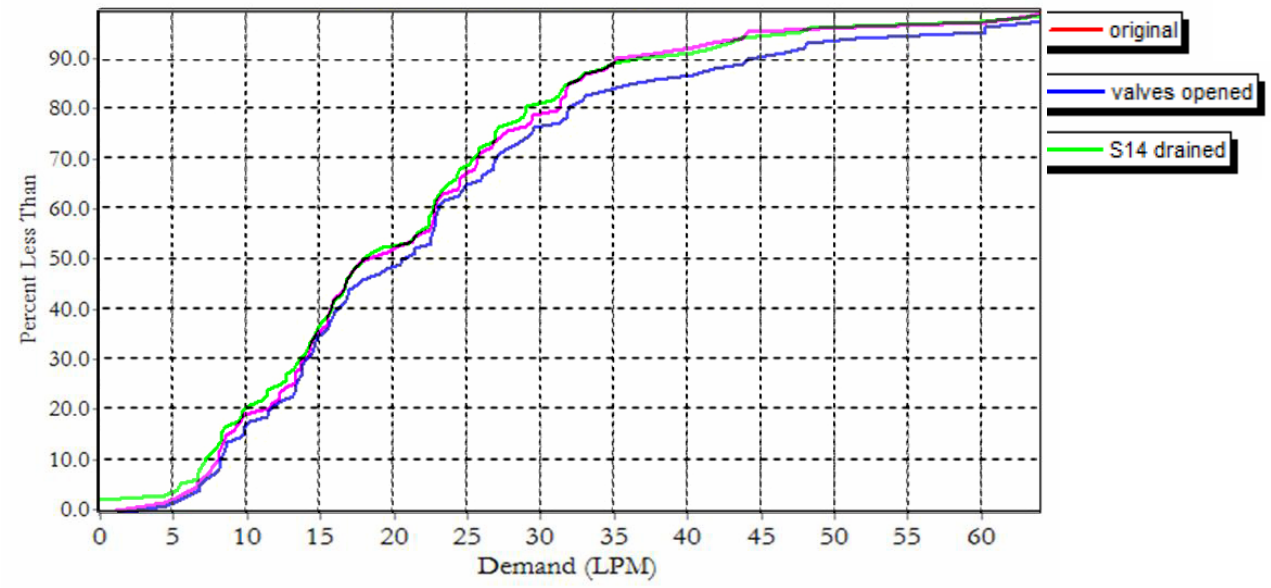

Figure 3-24. Numerical distribution of demand from opening system connecting valves

During the first hour of distribution after opening the valves (blue line in Figure 3-24), 17 percent of the taps provide less than 10 liters per minute (1 percent less than the original scenario), 34 percent provide 15 liters or less (the same as the original scenario) and 48 percent provide 20 liters per minute or less (3 percent less than the original scenario). Here, a lower percentage is a good result, indicating that a smaller percent of the population has lower than desired flow. After this hour, the percentages for 10, 15 and 20 liters per minute are 20 (2 percent more than the original scenario), 34 (the same) and 52 (1 percent more). These results, of course, are adverse in that more people have lower flow rates.

These statistics show that, during the first hour of distribution, opening the valves does provide a benefit to the low-flow taps. Looking at the blue line in Figure 3-24, the decrease in percentage of low-flow taps is particularly significant in the 16 to 22 liters per minute range by pushing 3 percent of them to higher flow rates. However, Figure 3-24 also shows that the bulk of the benefit in flow occurs for higher flow taps between 33 and 47 liters per minute by increasing their numbers closer to 6 percent. The downfall of this scenario occurs after the Spring 14 ring tanks drain, as illustrated by the green line in Figure 3-24: there are 2 percent more taps with flows under 15 liters per minute. Actually this 2 percent increase is a result of taps that are not receiving any water at all. Hence, this scenario benefits taps already with high flow and then completely cuts the water supply to specific taps and areas within the camp. This scenario should not be set in place.

III.3.C Connecting Pipes

Another simple analysis made was to consider adding connecting pipes between adjacent subsystems of high pressure and those of low pressures. We placed new pipes where systems were in closest proximity to minimize potential cost. Seven pipes were added to the system: two connect zones of high pressure from the C Tank subsystem to adjacent lower pressure MOI branches. One pipe connects a high pressure Christopher subsystem branch to the lower pressure B Tank subsystem which is then connected to low-pressure points in the Spring 17 subsystem with two pipes. Since the Spring 17 subsystem has some of the lowest pressures, two more pipes were added from the A Tank subsystem to the Spring 17 subsystem at varying locations. Figure 3-25 shows the evolution of pressure distribution from the original scenario to the pipe-connections scenario with the new pipes shown in white.

Figure 3-25 shows that the desired increase in pressure in the MOI subsystem was not achieved perhaps because the MOI system is located at higher elevations than the connecting portion of the C Tank system. Pressure in the B Tank subsystem does seem to have increased slightly and the connection from the A Tank subsystem to the Spring 17 subsystem did lead to higher pressure. It is comforting to see that at least, unlike the opening of system valves, this scenario does not exacerbate the pressure heterogeneity. Before recommending pipe connections, let us examine the variation of flow distribution, as illustrated in Figure 3-26. Despite the recorded increase in pressure because of added connections in parts of the Spring 17 subsystem, actual flow rates did not increase to any significant extent in that area. As mentioned in Section III.3.B, flow occurs from the Spring 17 Tank to the MaeLa 2 secondary collection tank which then redistributes the water. The flow from the points of connection in the Spring 17 subsystem is directed to the MaeLa 2 Tank and many of the taps connecting on the path to MaeLa 2 Tank are zero-use taps and cannot be outputting water even with increases in pressure.

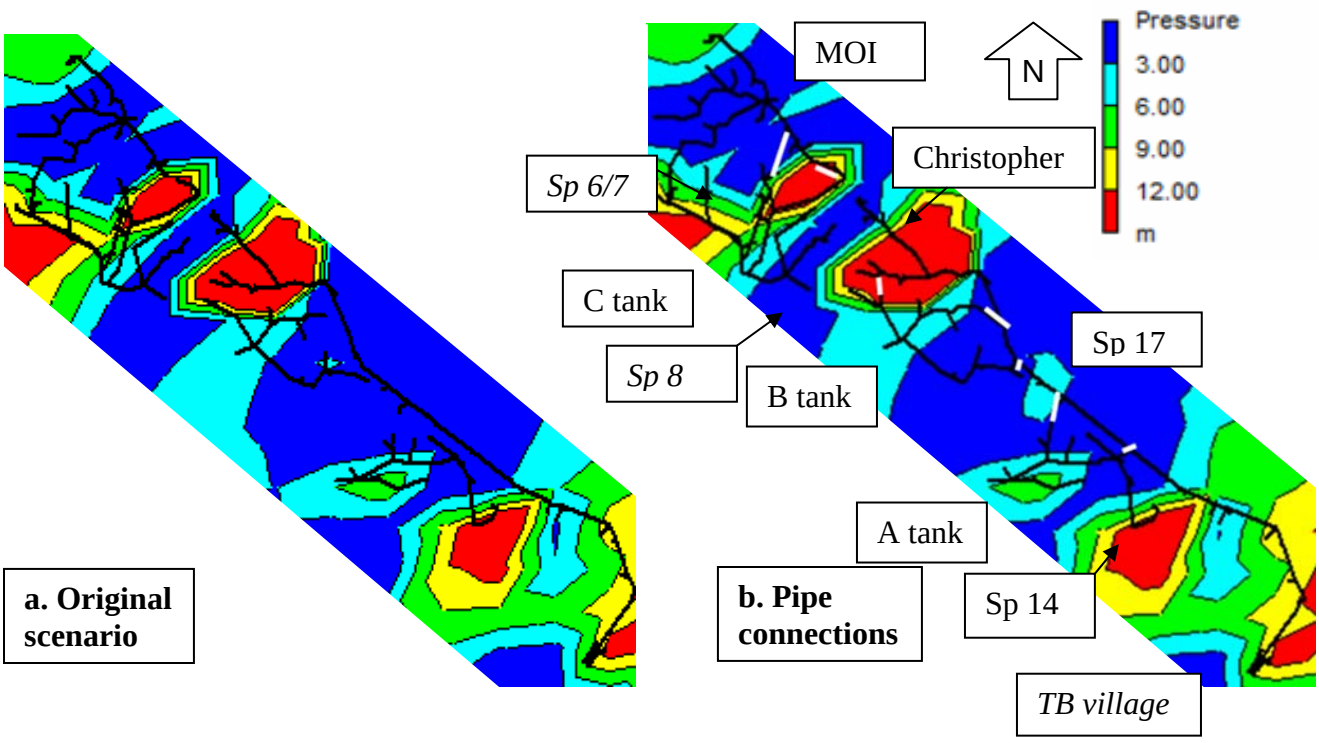

Figure 3-25. Geographical pressure distribution variation from adding pipe connections

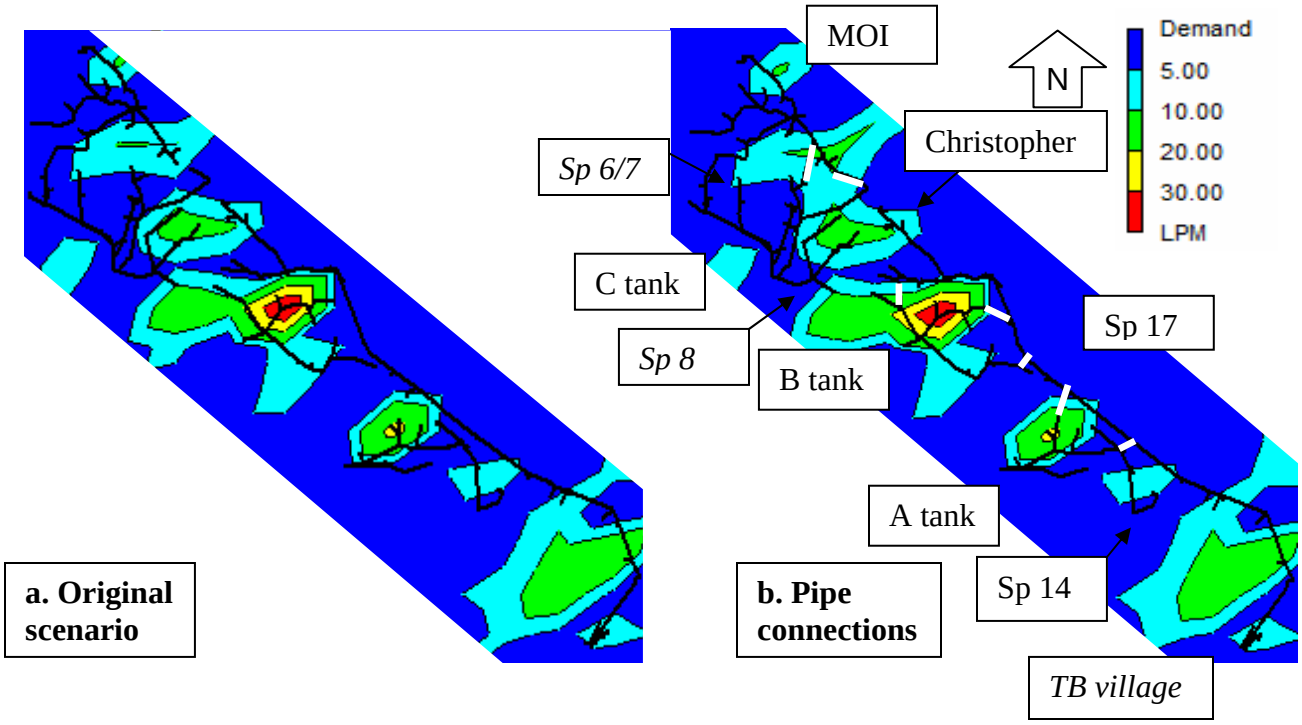

Figure 3-26. Geographical flow distribution from adding pipe connections

Flows are a bit higher in the B Tank subsystem thanks to water diverted from the Christopher subsystem, and it is surprising to see that even with no clear pressure differential between the C Tank and MOI subsystems, an increase in flow has taken place in regions with previously low flows in the MOI subsystem. Overall, recommended pipe connections that would justify the costs include the two connections from the C Tank to the MOI subsystem and the one connection from the Christopher to the B Tank subsystem.

In Figure 3-27, illustrating the quantitative flow distribution, the percentages corresponding to flows less than 10, 15 and 20 liters per minute are 16, 32 and 51 percent respectively. This compares to 18, 34 and 51 percent in the original scenario. Hence, even though the total number of taps under 20 liters per minute is still the same, there was an improvement in the lowest flow rates: 2 percent of the taps are no longer under 10 liters per minute and 2 percent as well are no longer under 15 liters per minute. These 2 percent have now moved to the 15 to 25 liters per minute range, a more reasonable flow rate. Also, taps with flows between 25 and 28 liters per minute have decreased by 2 percent. Hence, adding these pipe connections was generally a successful experiment, particularly from the Christopher Tank to the B Tank subsystem and from the C Tank to the MOI Tank subsystem. It would require a low investment and no added water supply.

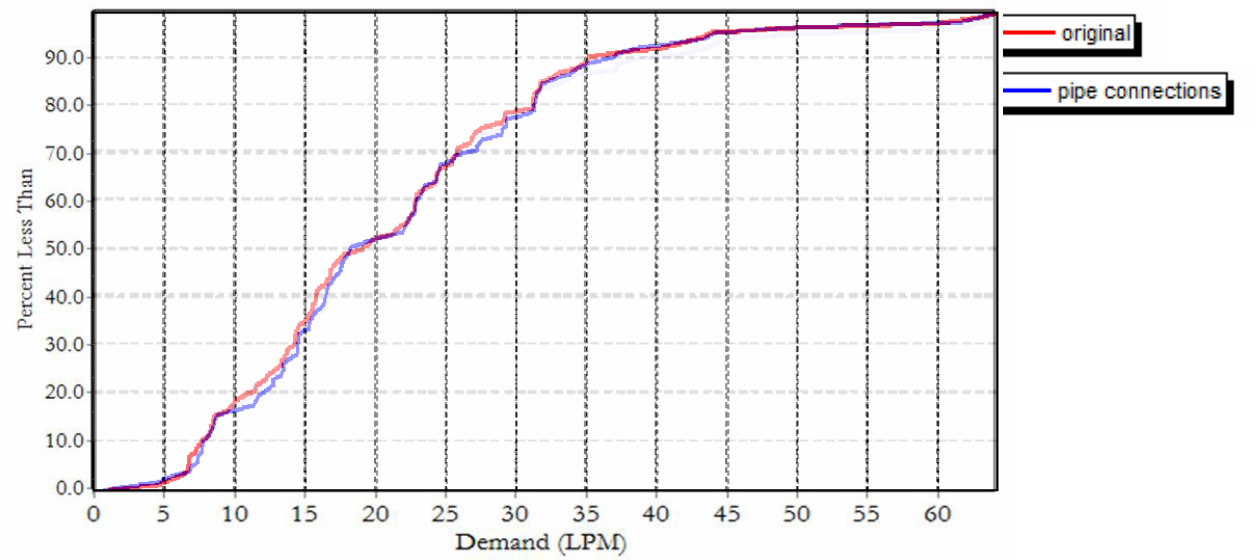

Figure 3-27. Numerical demand distribution under the adding pipe connections scenario

It should be noted however that the new flow rates resulting from such modifications also depend on the diameter of pipes installed. Here, considering the diameter of the pipes at the connecting junction, the pipes were chosen to follow the logic of the system. A larger diameter can significantly increase flow to the new parts of the system, but a trade-off between draining tanks faster and having more flow available has to be made.

III.3.D Geographical Coverage of Taps

Another analysis made for improvement of the water distribution system consisted in adding new taps at locations that did not have easy access to a public tap stand. A preliminary Geographical Information System (GIS) analysis was made of distance to the closest tap stand (Harding, 2008). It is found that over a distance of 100 meters from a household, the probability of traveling to fetch water reduces significantly. Hence, the goal of this exercise was to provide 100-meter radius access to water over the whole area of the camp by including new tap stands that would fill the gaps in the current system.

Ten new taps were chosen at specific locations in the camp using this process. Then, the decision of what respective subsystem would supply each tap was made using a number of criteria. The first one was pressure potential of the subsystem: any tap at a higher elevation than the supply

tank in a subsystem cannot be connected to that subsystem since no water would reach it through gravity feed. The second criterion was the capacity of the subsystem: ring tanks for example are not ideal suppliers of water because their volume is smaller than the major tanks and ring tank water supply (from springs) is not directly controlled and can quickly run short in the dry season. The third criterion was proximity of the subsystem, in order to minimize the cost of pipe but also to avoid laying long pipes across the camp. This would not only save unnecessary energy lost through high head-loss but it would also prevent a higher risk of damage of the pipe system.

Figure 3-28 shows the pressure distribution before and after addition of the taps with the tap locations identified by white stars. It clearly shows that the setup is capable of supplying large pressures to these new taps. The northern-most tap would need to be checked for flows because of its lower pressure. All four new taps to the northwest of the map were supplied by the C Tank subsystem, with appropriate head, proximity and high capacity. It was preferred over the Spring 6/7 ring tank because its supply is more predictable. The two center taps were supplied by the Christopher Tank subsystem and the Spring 17 subsystem via the MaeLa 2 Tank which possesses reasonable capacity and a better pressure than if the tap was tapping directly into the line.

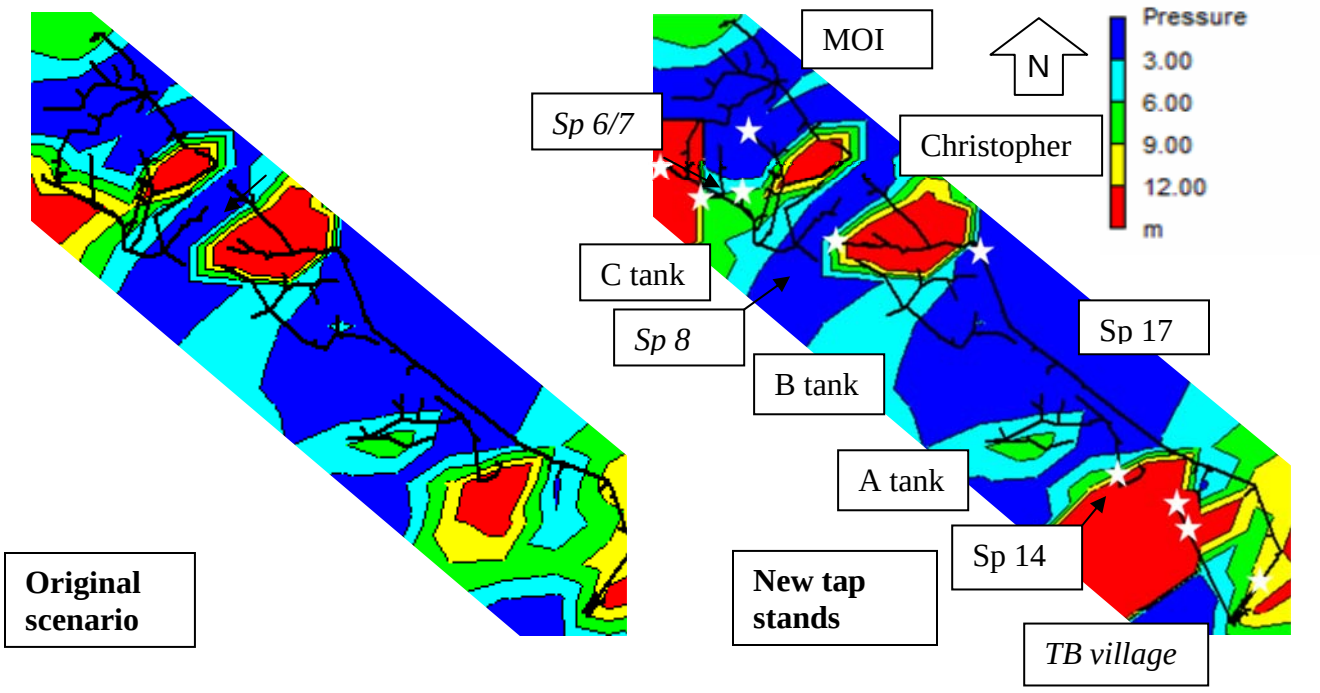

Figure 3-28. Geographical pressure distribution variation from adding new taps

The four taps at the south are at particularly high elevations which A Tank would have a hard time reaching. The three southern-most taps are supplied by the TB ring tanks with the highest head of all tanks. Even though this is a ring tank and its total volume is limited (it is estimated to drain within an hour and a half without refill), it is different than spring ring tanks in that its supply is actually derived from the productive and reliable Spring 17 which pours into the large capacity Spring 17 tank. Because the TB Village ring tanks are actually connected to the Spring 17 Tank and water is pumped to it even during distribution, it was chosen to supply the majority of the taps. The last tap is supplied by the Spring 14 ring tank which possesses a high enough pressure to supply water to this tap while at the same time possessing the needed water volume capacity. Since it is only supplying one tap (modeled as a public tap whereas it is actually used intermittently by the nearby temple and the border control office), EPANET predicts it to be able to handle this other tap. It would be wise however to build an extension of the TB pipeline to plan for possible drying out of the spring in the dry season.

Figure 3-29 illustrates the flow distribution after adding the new taps. It shows that reasonable flow rates can come out of all the new taps. This also includes the northern-most tap. Comparing the original scenario against the one with new tap stands, one can see that the latter covers a larger geographical area of the camp: it has a denser southeastern distribution as well as northwestern.

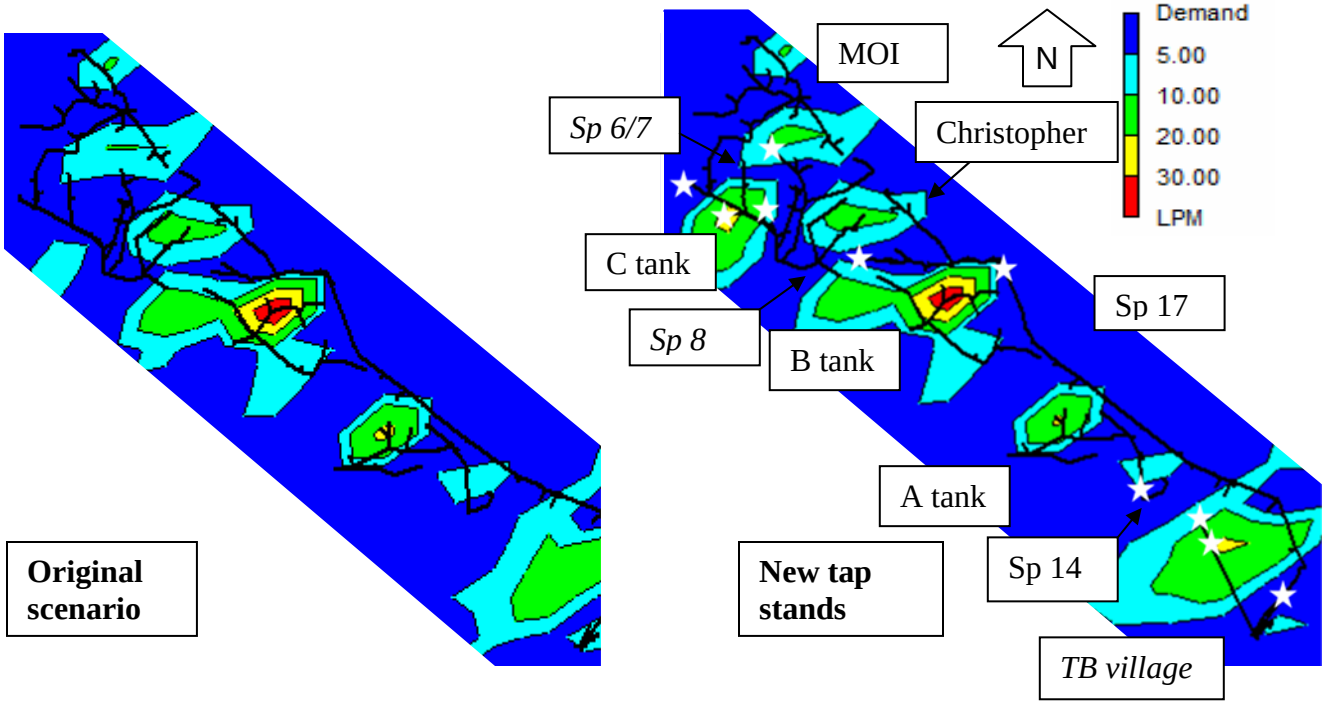

Figure 3-29. Geographical flow distribution from adding pipe connections

Adding tap stands to cover the camp area does not necessarily imply meeting the minimum flow required at each tap stand to provide sufficient water to the surrounding population. An analysis of flow required per tap stand would determine the needed diameter of pipes added and the number of faucets at each tap stand. The present analysis assumed one faucet per tap stand and followed the logic of using the diameter of the connecting pipe (and to not increase the pipe diameter downstream so that water velocity is maintained despite head losses). The pipe choice would also drive how fast the tanks would drain and the pumping costs. Hence, as discussed in Chapter IV, Recommendations, this analysis needs to be taken beyond a simple geographical coverage of the camp but in addition to that, a calculation of flow at each tap taking into account required flow per household, the number of households distribution within 100 meters of the tap, and the share of the flow each tap should provide if there were overlaps in areas.

III.3.E Tank Levels

An understanding of the tank levels is a final straightforward result that could lead to an improvement in the distribution of water around the camp. Currently, water cannot be distributed throughout the day because of limited river flow rate and tank size. Hence, understanding the capacity usage of the tanks could lead to increasing the distribution time.

Considering the present system as is, Figure 3-30 gives a representation of the tank levels throughout the three-hour distribution period. These results should be taken into account in the context of the assumptions made about the functioning of the system. The most relevant assumptions here are that all tanks start at their maximum levels and are not re-filled by any other system during distribution. As noted earlier in the discussion of the salt tracer test in Section III.2.C, TB rings and Spring 8 rings are re-filled during distribution and this second assumption is not perfect. Also it seemed that the levels to which the tanks are actually filled are not consistent and depends not only on the season (and variation of source potential for springs and for river), but also simply on the technician's judgment.

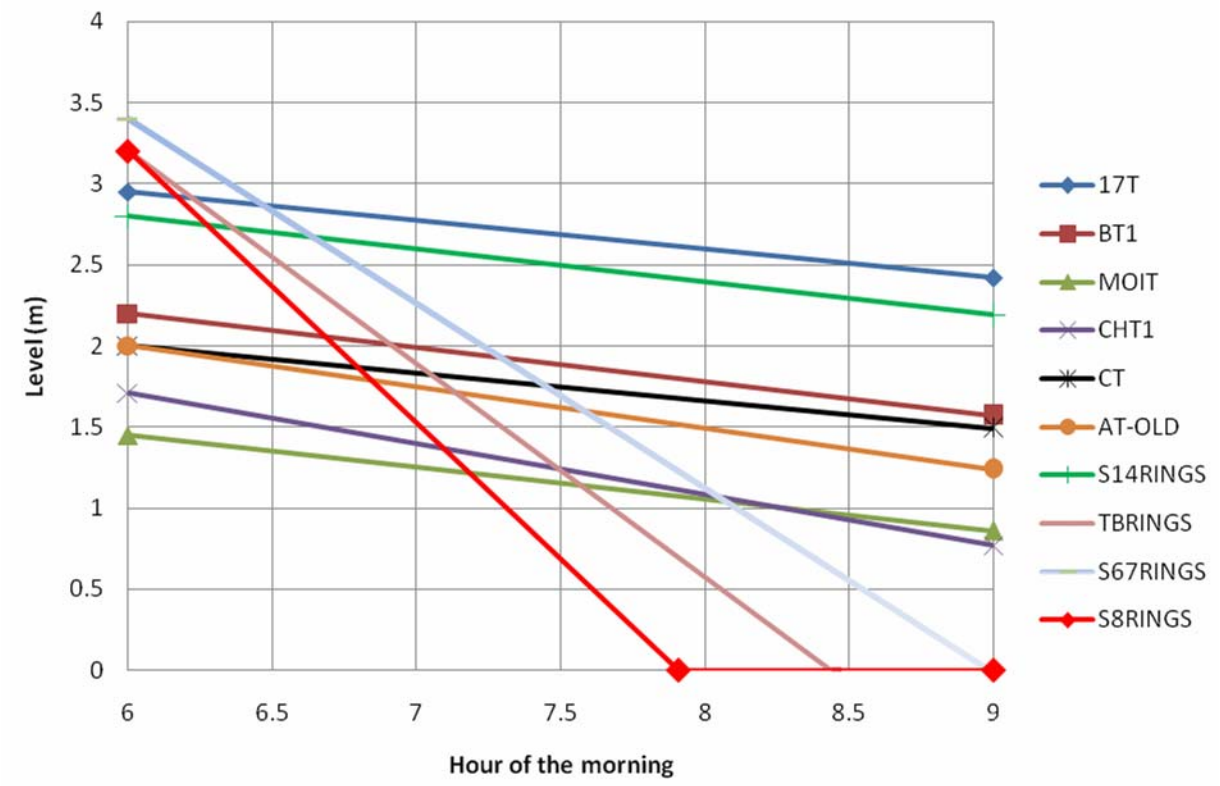

Figure 3-30. Tank levels during three-hour distribution period

Disregarding the ring tanks, which only make up about 5 percent of the total volume of water supplied, none of the major tanks drain fully after 3 hours of distribution. The tank whose capacity is used least is Spring 17 Tank which drains only about 17 percent of its total volume by the end of the distribution. The limiting tank with the most use of its capacity is the Christopher Tank which drains about 53 percent of its volume.

Hence the full capacity of these individual tanks is not used. In addition, we observed during the field study that the potential capacity of the system is even larger than that modeled: large compartments of tanks remain unused such as the second compartment of the Christopher Tank which would double its capacity, the new A Tank compartment, and the second B Tank compartment (which is rotated with the first tank but never used simultaneously). This additional potential storage will conservatively be ignored from the analysis however.

Higher need for water exists considering that demand in the camp is a function of the pressure available. Hence potential consumption is higher than the current supply. Assuming that the river could support such pumping rates (which would be crucial to investigate), and that there is funding for pumping costs and management, one could conservatively drain the limiting tank, Christopher,

down to about 10 percent of its volume. This would amount to a 0.17-meter final level and a distribution period of 4.8 hours, or, to be more conservative even, about 4 and a half hour of distribution.

If the political logistics of the camp, or the time in between distribution periods and pumping rate permit, an increased distribution time is only reasonable. This conclusion is reinforced because the assumption of constant pressure-driven demand used by the model is an overestimation of reality: Taps are opened and closed, and there are periods of the day, such as at 6 AM, when all taps are not in use, as observed during field work. But care should be taken to prevent potential downfalls. For example, if tanks were to drain and pipes were made empty, the water quality would diminish for the next round of distribution as biomass develops on the inside of the pipes.

IV RECOMMENDATIONS AND FUTURE WORK

IV.1 Elevation Error

Calibration results have shown reasonable accuracy of the model to predict parameters of importance for analysis and future expansion of the water distribution system. However, there is room for improvement particularly in the accuracy of pressure and flow predictions.

The calibration data showed an R^2 of close to 0.4 between calculations and measurements for both flow and pressure with a random error that was not a function of the methodology used. This error lies heavily in the accuracy of the elevations which was dependent on the accuracy of the GPS instruments used for surveying. Salt concentration calibration on the other hand showed a higher correlation because it is more dependent on mixing assumptions and lengths of pipes, which could be more accurately measured than elevations.

Despite the four-square-meter resolution of the DEM with a precision to the meter in elevation, calculation of elevations in a region such as MaeLa, located on steep hills, also requires precise X-Y coordinates to take advantage of the DEM. The horizontal accuracy of the GPS device was 15 meters on average (for X-Y coordinates) during field work (the device gives an error estimate). This is confirmed by Harding's (2008) analysis. Depending on the region of the camp this 15-meter horizontal error could amount to no vertical error or vertical error of up to 18 meters. On average, an error of about 3 meters was incurred because of the accuracy of the GPS devices. This vertical error likely caused the difference between calculated heads in the system and those measured.

This elevation error has caused the model to calculate negative pressures at points of low pressure in the system (refer to Appendix B for an EPANET output report). EPANET does point out negative pressures but they do not interfere with the calculations of flow rates at taps. The dilemma however is that one cannot distinguish between true negative pressures and those that are simply a result of the elevation error. Hence using EPANET for troubleshooting requires higher accuracy.

Precision of pressure is most important at taps because of its relation to flow. These negative pressures have caused some of the high-use tap stands to have no predicted water flow in the model. This is the case for T12-S17, TB4-S17, T13-BT, T9-BT, T1-MOI, TNEW-MOI, T10-AT and TEMT2-CT.

As to the influence of elevation error on flow rates at taps, it is relevant to understand that an average 3-meter pressure error in the system does not translate to a 3-meter pressure difference at a flowing faucet. The relationship between pressure and flow for a flowing tap-stand faucet is shown in Figure 2-6. An ideal tap actually has a pressure of zero out of it, but because of friction out of the taps the whole pressure head in the system cannot be used to provide flow. Similarly, because friction becomes more limiting as pressure increases, if more faucets were added at the tap stands of high pressure, the pressure and friction at the individual faucets would reduce; the tap stand would then produce a higher flow and take more advantage of the pressure in the system. The pressure at taps shown in EPANET is also that of a flowing tap with its assigned emitter curve: one can usually observe a much greater pressure just upstream of the tap..

Within the working range shown on Figure 2-6, an average pressure difference of three meters for a single flowing faucet could be incorrectly interpreted as a doubling of flow rate or no flow out. To correctly understand the influence of the three-meter elevation error on flow rates, one needs to compare it to the potential head at each tap, based on the elevation difference between the supplying tank and the tap of concern. Because the head is higher at taps with a larger elevation difference from the tank than taps closer to their supplying tank, this leads one to think that flow errors should be greater closer to the supplying tanks. This is because the elevation error would then make up a bigger portion of the potential head. Ironically, the measurements of elevation are also worse closer to the tanks because these are situated in steep areas higher on the hill: this fact exacerbates the problem.

Refining the model is hence an important and necessary task. More precise measuring instrumentation is needed to either collect more accurate X-Y coordinates to be used with the DEM or to measure the elevation directly. Such a task should focus on tap stand locations and give priority to those on steep hills closer to the tanks. Special care should also be given to getting the exact elevation of the supplying tanks because these affect pressure in the whole subsystem. Despite not being located in a steep area, the Spring 17 subsystem is also important because Tank 17 is located at a lower elevation than the other tanks and hence the pressure head potential is less and proportionally more prone to error from inaccurate elevation measurement.

An alternative method for obtaining this elevation data would be to acquire an aerial photograph of suffiently high enough resolution that tap stands would be visible and could be located accurately enough to use the DEM to its full extent and obtain elevations of 1-meter accuracy. This method would be more prone to human error however.

Finding more accurate elevations should be complemented by more calibration data to further correct the model. The current size of the sample data set is relatively small to be fully representative of the camp: further testing should take place that would cover most taps and particularly those on steep hills and with small head potential.

With a precise model, the minor head losses would then actually make a difference in the output and they should be included as part of the piping.

IV.2 Further Analysis

The current model focuses on the major subsystems supplied by pumped river water mainly. Flows from springs to tanks have not been modeled because they constitute only a small fraction of the total water volume distributed and they vary seasonally. Further refinement of the model could include these flows in EPANET and different models could be made to account for the variation between dry and rainy season.

Multiple smaller spring-based subsystems have not been modeled either, thus excluding a minor but important part of the camp's population. These include Springs 2, 4, 5, 9, 10, 11, 12 and 15 and their associated piping networks. Depending on the decisions of Solidarites, the organization that will manage the water system starting at the end of 2008, these systems could be given their due attention or the current river-based system could be extended to their area of supply.

To increase the distribution time period up to constant supply potentially, and to further understand the major river-based system, a worthwhile enterprise would include constructing an optimization model that would take into account constraints on pumping capacity, tank volumes, costs and river flow. Such a model would first require surveying the supply portion of the system from the river to the tanks. This portion of the system is currently being modified by the addition of a reservoir to the supply system, and this modification should be taken into account. The model should also consider the pump characteristics (such as the head versus flow curve or, if considered a constant energy device, the horsepower of each pump). The pump's operation would also be crucial, such as the duration of pumping and possible variation of pumping speed according to seasonal change or the tank levels. Assigning an efficiency curve and a schedule of energy prices, the energy consumption and cost of pumping could be calculated by EPANET. Calibration data would also need to be collected for comparison of pumping flows and costs. Then a survey of river flow throughout the year would be important to understand the environmental limits on the pumping capacity.

With information on the flow limits of the river, pumping costs and capital investment for new pumps or to expand tank capacity, one could form a linear programming problem to maximize distribution time. Distribution time would be based on the modeled distribution of water, and it could be revised with possible system expansions. Different scenarios could be modeled to maximize distribution: each would vary budgeting constraints and pumping and tank capacity. Innovative designs of system layout or system controls could also be included as potential scenarios. Management would then receive these different cases to decide on an optimal solution to increase drinking water distribution in MaeLa.

But increasing the distribution time to constant supply is not enough if the system does not cover the whole extent of the camp's population. Even if water does reach an area of the camp but the flow per person per day is still less than a determined threshold required, the optimization problem is still not useful. The problem needs to be well understood first, taking into account population distribution and conducting further surveys of demand for water. Then, with the help of GIS, one would conduct further analysis and devise appropriate goals of minimum flow per tap stand (including new taps). EPANET would then be used to modify the layout of the system by adding tap stands, modifying the number of taps at tap stands and changing pipe diameters to reach these goals; it is only then that an optimization model could be fully useful.

CONCLUSION

The purpose of this work was to develop a model that would represent the water distribution system in MaeLa. It would serve as an analysis tool to increase understanding of the complexities of the system and to plan improvements.

This project started with an exposure to the intricacies of the system and an analysis of its peculiarities such as the intermittent nature of flow and the decentralized sources of water. Data was collected through field surveying of the system and calibration testing. A model of the system was then assembled in EPANET and multiple controls were added to best represent the current functioning of this water system and to simulate the calibration tests. The model simulated field dynamics successfully despite its inaccuracies in elevation due to the imprecise instrumentation used for surveying. It also served as a great tool to understand operation of the system such as mixing in the tanks, connections between subsystems and control habits of the technicians.

The distribution system model was then used to evaluate three alternative scenarios to improve system performance. The objective of the first and second scenario was to increase the flow rate at taps of low supply; the third scenario aimed at adding taps to parts of the camp without easy access to running water. The first scenario consisted in opening valves to connect subsystems: it increased the flow rate at taps of large supply more so than at taps of low supply. This scenario was not recommended because it would quickly drain parts of the water supply. The second scenario consisted of adding connecting pipes between subsystems of high pressure and those of low pressure. It was recommended because it would increase the flow rate of low- and medium-supply taps. For the third scenario, areas of the camp without easy access to water were defined by using the results of mapping the current system and the population distribution in a Geographical Information System software. These new taps were successful in providing water to these areas without significantly affecting the rest of the system. An additional recommendation for increasing the water supply in the camp was found from analyzing tank level: because tanks would not drain by the end of the distribution period, it was recommended that the period of water supply be increased from 3 hour periods to 4½ hours.

This work is closely related to the mapping of the MaeLa water system completed by Harding (2008). One of the objectives for the model was to facilitate exchange of information between EPANET and the GIS software used by Harding. This exchange was realized successfully through the process of first importing elevations of surveyed points from a Digital Elevation Model in GIS

to EPANET. The input data of links and nodes was exported from EPANET into GIS as well. Results in the form of flows and pressure were also successfully exported. The combined analysis of EPANET results and GIS population distribution provided the locations of the new tap stands in the third scenario analyzed. The results were then again exported to GIS for evaluation.

It is hoped that this thesis will facilitate the work of improving the water distribution in MaeLa and that it will also assist in the transfer of management between AMI and Solidarites. Further work has been laid out: it should include a refining of the model through more precise elevation data and inclusion of springs. After re-defining the layout of the system to meet goals of distribution per household in the whole area of the camp, the next step would be to run an optimization model that could lead to an era of constant, accessible, drinking water supply.

References

3M. (2001). *Petrifilm® E. coli/Coliform Count Plate Interpretation Guide.* St. Paul, MN, USA: 3M Microbiology Products.

Aide Médicale Internationale (AMI). (2007). *Mae La Distribution Data.* Unpublished data. Thailand: Aide Médicale Internationale.

Aide Médicale Internationale (AMI). (2007). *Missions: Thailand.* Retrieved December 12, 2007 from http://www.amifrance.org/-Thailand-.html

Alekal, P., R. Baffrey, A. Franz, B. Loux, M. Pihulic, B. Robinson, and S. Young. 2005. Decentralized Household Water Treatment and Sanitation Systems. Unpublished Master of Engineering project report. Cambridge, MA, USA: Civil and Environmental Engineering Department, Massachusetts Institute of Technology. Retrieved November 17, 2007 from http://web.mit.edu/watsan/Docs/Student%20Reports/Kenya/Kenya%20Group%20Report%202005.pdf

Andey, P. & Kelkar, P. (2007). Performance of water distribution systems during intermittent versus continuous water supply. *Journal American Water Works Association*. 99:8:99.

Baffrey, R. (2005). *Development of program implementation, evaluation, and selection tools for household water treatment and safe storage systems in developing countries.* Master of Engineering Thesis. Civil and Environmental Engineering Department, Massachusetts Institute of Technology. Retrieved May 5, 2008 from http://hdl.handle.net/1721.1/28942

Batish, R. (2003). A New Approach to the Design of Intermittent Water Supply Networks. In: Bizier, P and DeBarry, P. (Eds.) *World Water Congress 2003, June 23–26, 2003, Philadelphia, Pennsylvania, USA.* American Society of Civil Engineers, Washington, D.C.

Bentley (2006). *Efficient Pressure Dependent Demand Model for Large Water Distribution System Analysis.* Haestad Methods Solution Center, Bentley Systems, Incorporated. Retrieved May 5, 2008 from ftp://ftp2.bentley.com/dist/collateral/whitepaper/WDSA2006_EfficientPDD_haestad_eng_lowres.pdf

Briere F. (1999). *Drinking-Water Distribution, Sewage and Rainfall Collection.* Paris, Presse Internationale Polytechnique.

Brinkhoff, T. (2007). *City Population: Thailand.* Retrieved October 12, 2007, from http://www.citypopulation.de/Thailand.html

Brizou, J. (2006). *Thailand Mission: Maela Camp Nov. 2005- Aug. 2006: Final Report.* Unpublished report. Aide Médicale Internationale. Paris, FRANCE.

CBS. (2007). *Country Fast Facts: Burma.* CBS Interactive Inc. Retrieved December 16, 2007 from http://www.cbsnews.com/stories/2007/10/04/country_facts.shtml

Coelho, S.T., James, S., Summa, N., Abu Jaish, A. & Chatila, J. (2003). Controlling Water Quality in Intermittent Supply Systems. *Journal Water Supply*, 3:1:119.

Eaton, A., Clesceri, L., and Greenberg, A. (Eds.). (2005). *Standard Methods for the Examination of Water and Wastewater.* (21st ed.). American Public Health Association, American Water Works Association, and Water Pollution Control Federation.

ESS. (2002). *Macro-scale, Multi-temporal Land Cover Assessment and Monitoring of Thailand.* Environmental Software and Services. Retrieved October 12, 2007, from http://www.ess.co.at/GAIA/CASES/TAI/chp1to3.html

Fogarty, P. (2007, October 10). Poverty driving Burmese workers east. *BBC News.* Retrieved December 12, 2007, from http://news.bbc.co.uk/go/pr/fr/-/2/hi/asia-pacific/70336633.stm

GOSIC. (2007). *Global Historic Climatology Network Daily – Mae Sot, Thailand.* Global Observing Systems Information Center. Retrieved November 26, 2007, from http://gosic.org/gcos/GSN/gsndatamatrix.htm

Google. (2007). *Google maps – Mae Sot, Tak, Thailand.* Retrieved October 12, 2007, from http://maps.google.com

Hofkes, E.H. (Ed.) 1983. *Small Community Water Supplies, Technology of Small Community Water Supply Systems in Developing Countries.* International Reference Centre for Community Water Supply and Sanitation Technical Paper Series No. 18, John Wiley and Sons, New York

KarenPeople. (2004). *Who Are The Karen?* Retrieved December 5, 2007, from http://www.karenpeople.org

Lantagne, D. (2007). *Water and Sanitation Assessment to Inform Case-Control Study of Cholera Outbreak in Mae La Refugee Camp, Thailand.* Unpublished presentation. Centers for Disease Control and Prevention, Atlanta, USA.

Lansner, T. (2006). A Brief History of Burma. *UC Berkley School of Journalism.* Retrieved December 17, 2007, from http://journalism.berkeley.edu/projects/burma/history.html

Maps-Thailand (2006). *Map of the Mekong river subregion*. Retrieved May 2nd 2008 from http://www.maps-thailand.com/map-mekong-subregion.php

McGeown, K. (2007). Life on the Burma-Thai border. *BBC News*. Retrieved December 8, 2007, from http://news.bbc.co.uk/2/hi/asia-pacific/6397243.stm

MWH. (2005). *Water Treatment: Principles and Design*. (2nd ed). USA: John Wiley and Sons.

Okun, D. and Schulz, C. (1984). *Surface Water Treatment for Communities in Developing Countries*. Great Britain: John Wiley and Sons.

Polprasert, C., Bergado, D., Koottatep, T., & Tawatchai, T. (2006, Auguest 15). *Report on Water and Environmental Sanitations Assessment of Mae La Temporary Shelter, Thasogyant District, Tak Province, Thailand.* Asian Institute of Technology (AIT).

Refugees International. (2007). *Thailand: Humanitarian Situation*. Retrieved December 15, 2007 from http://www.refugeesinternational.org/content/country/detail/2894/

Rossman, L.A. (2000). *EPANET2 USERS MANUAL*. Cincinnati, OH, USA: National Risk Management Research Laboratory. Available at: http://www.epa.gov/nrmrl/wswrd/dw/epanet.html

Sashikumar, N., Mohankumar, M.S. & Sridharan, K. (2003). Modelling an Intermittent Water Supply. In: Bizier, P and DeBarry, P. (Eds.) *World Water Congress 2003, June 23–26, 2003, Philadelphia*, Pennsylvania, USA. American Society of Civil Engineers, Washington, D.C.

Sawyer, C., McCarty, P., and Parkin, G. (2003). *Chemistry for Environmental Engineering and Science*. (5th ed). USA: McGraw-Hill.

Thailand Burma Border Consortium (TBBC). (No Date). *Mae Sot area*. Retrieved December 5, 2007, from http://www.tbbc.org/camps/mst.htm

Tokajian, S. & Hashwa, F. (2003). Water Quality Problems Associated with Intermittent Water Supply. *Water Science and Technology*. 47:3:229.

U.S. EPA. (2007). *National Primary Drinking Water Standards*. U.S. Environmental Protection Agency. Retrieved December 10, 2007, from http://www.epa.gov/safewater/contaminants/index.html#d_dbps

UN Thailand. (2006). *Thailand Info*. Retrieved October 12, 2007, from http://www.un.or.th/thailand/geography.html

UNHCR. (2007, May 27). *Resettlement of Myanmar refugees under way from northern Thai camp*. United Nations High Commissioner on Refugees. Retrieved December 5, 2007, from http://www.unhcr.org/news/NEWS/465430f04.html

UNHCR. (2006, September 20). *Myanmar Thailand border Age distribution of refugee population*. United Nations High Commissioner on Refugees. Retrieved December 5, 2007, from http://www.unhcr.org/publ/PUBL/3f7a9a2c4.pdf

Viessman W. Jr. and Hammer M.J. (1998). *Water Supply and Pollution Control*. Menlo Park, CA: Addison Wesley Longman.

Wagner, E. and Lanoix, J. (1959). *Water Supply for Rural Areas and Small Communities*. Geneva: World Health Organization - Monograph Series 42

WHO. (1993). *Drinking Water Standards*. World Health Organization. Retrieved December 10, 2007, from http://www.lenntech.com/WHO's-drinking-water-standards.htm

Appendix A: EPANET Input Parameters for Current System

[TITLE]

[JUNCTIONS]

;ID	Elev		Demand	Pattern
J-S17	230	0		;
T15-S17	229	0		;1 tap, small use, tank + latrine
JT-S17	230	0		;
JT2-S17	231	0		;
J3-S17	229	0		;
T14-S17	229	0		;1 tap (large use)
JT3-S17	238	0		;
J4-S17	231	0		;
T13-S17	234	0		;3 taps (large use) + elbow
T12-S17	238	0		;1 tap (large use)
JT4-S17	238	0		;
JT5-S17	238	0		;
J5-S17	235	0		;
TNEW-S17	235	0		;1 tap (large use)
JT6-S17	240	0		;
T11-S17	242	0		;latrine
T10-S17	241	0		;2 taps large use
JT7-S17	242	0		;
J6-S17	241	0		;
T8-S17	243	0		;2 taps latrine
JT8-S17	243	0		;
T7A-S17	243	0		;1 tap little use
T7B-S17	242	0		;latrine
JT9-S17	244	0		;
T9-S17	246	0		;2 taps latrine
T6-S17	243	0		;1 tap large use
JT11-S17	244	0		;
JT10-S17	244	0		;
J7-S17	244	0		;
T5-S17	244	0		;2 taps (large use)
JT12-S17	249	0		;
T4-S17	245	0		;1 tap not concrete large use?
J8-S17	245	0		;
JT13-S17	249	0		;
T3-S17	248	0		;not large use 2 ring tanks+2bends
T2-S17	261	0		;1 tap +1 joint+bends
JT14-S17	253	0		;
JB-S17	254	0		;
JT15-S17	264	0		;
T1A-S17	262	0		;latrine
T1B-S17	262	0		;latrine
J9-S17	268	0		;
PTBi	288	0		;
JT16-S17	335	0		;
TB1-S17	334	0		;1 tap washing
TB2-S17	326	0		;1 tap washing +bath
TB9-S17	308	0		;CP10 not used too much
TB4-S17	337	0		;hose to 1 ring
TB5-S17	331	0		;1 tap to ring
JT17-S17	335	0		;

JT18-S17	314	0		;
TB6-S17	316	0		;1 tap school small use
TB7-S17	316	0		;not working!
TB3-S17	313	0		;1 tap
TB10-S17	306	0		;used? reservoir 1 tap faucet
TB8-S17	310	0		;1 tap to ring washing...
J10-S17	308	0		;
T18-S17	224	0		;3 taps concrete Connected to CH system also intermittently
T4-BT	231	0		;2 taps concrete large use
J01-BT	233	0		;
V1i-BT	231	0		;
JT1-BT	240	0		;
T3-BT	241	0		;2 taps concrete
J2-BT	242	0		;
J3-BT	239	0		;
JT2-BT	242	0		;
V2i-BT	239	0		;
T2-BT	234	0		;2 taps concrete
JB2-BT	250	0		;
T13-BT	249	0		;1 tap concrete
JT3-BT	248	0		;
J4-BT	248	0		;
JT4-BT	250	0		;
T1-BT	246	0		;3 taps concrete
JT5-BT	247	0		;
T12-BT	248	0		;1 tap no concrete
Vi-branchT4-BT		267	0	;
J5-BT	265	0		;
Vi-branchT5-BT		267	0	;
T5-BT	241	0		;1 tap conrete Is this actually T6?
T6-BT	238	0		;2 taps concrete Is this actually T5?
Vi-branchT10-BT		266	0	;
JT6-BT	257	0		;
T11-BT	247	0		;1 tap no concrete
J6-BT	252	0		;
T7-BT	251	0		;2 taps concrete
J7-BT	251	0		;
JT7-BT	253	0		;
T8-BT	235	0		;2 taps concrete
T9-BT	245	0		;1 tap concrete
T10-BT	225	0		;3 taps concrete
T5A-MOI	218	0		;military
JT1-MOI	220	0		;
T5B-MOI	223	0		;latrine + 2 bends
J1-MOI	224	0		;
T4-MOI	237	0		;1 tap little use
JT2-MOI	226	0		;
T3-MOI	222	0		;2 taps concrete
JT3-MOI	228	0		;
T2-MOI	228	0		";2 latrines, 1 tap UN office
T1-MOI	233	0		;1 pipe to tank of 1000 L
T27-MOI	220	0		;1 tap large use
J2-MOI	208	0		;
JT4-MOI	209	0		;
T6-MOI	213	0		;1 tap to ring
JT5-MOI	210	0		;
T7-MOI	215	0		;2 taps oncrete full use

```
JT6-MOI         211     0                       ;
T30-MOI         209     0                       ;1 tap to drum
T31A-MOI        208     0                       ;latrine
T31B-MOI        212     0                       ;latrine
JT7-MOI         209     0                       ;
T32A-MOI        211     0                       ;valve to ring of 2
T32B-MOI        209     0                       ;drum
J1-CH           276     0                       ;
JT1-CH          274     0                       ;
J2-CH           272     0                       ;
JT2-CH          260     0                       ;
Vi-T2-CH        259     0                       ;
T2-CH           236     0                       ";Not in use (to 3 rings, 1 tap). The system continues to the
camp leader with personal taps
Vi-T3-CH        250     0                       ;
T1-CH           250     0                       ;1 tap concrete
T3-CH           217     0                       ;1 tap concrete
JT3-CH          270     0                       ;
T4-CH           268     0                       ;1 tap concrete
T5-CH           255     0                       ;1 tap large use
V5i-CH          220     0                       ;
Vi-brancT10-CH          218     0                       ;
T6-CH           214     0                       ;3 taps concrete
JT4-CH          218     0                       ;
T7-CH           221     0                       ;3 taps concrete
JT5-CH          218     0                       ;
JT6-CH          223     0                       ;
JT7-CH          225     0                       ;
T8-CH           229     0                       ;1 tap to ring (2)
T11-CH          224     0                       ;1 tap large use
J3-CH           227     0                       ;
Vi-T11-CH       223     0                       ;
JT8-CH          222     0                       ;
T9-CH           223     0                       ;UN office 1 tap
J4-CH           222     0                       ;
T10-CH          222     0                       ;3 taps concrete
V7i-CH          225     0                       ;
J3-MOI          230     0                       ;
T19-MOI         222     0                       ;2 taps concrete
J4-MOI          221     0                       ;
T153-MOI        218     0                       ;4 taps latrine
JT9-MOI         218     0                       ;
T151-MOI        218     0                       ;MOI office
T150-MOI        213     0                       ;1 tap large use
T23-MOI         213     0                       ;2 taps concrete
JT10-MOI        213     0                       ;
T24-MOI         209     0                       ;2 taps concrete
V1-MOI          216     0                       ;
J6-MOI          216     0                       ;
J5-MOI          209     0                       ;
JT12-MOI        209     0                       ;
T25-MOI         209     0                       ;3 taps concrete
T29-MOI         206     0                       ;1 tap large use
J7-MOI          209     0                       ;
T26-MOI         212     0                       ;2 taps concrete
J8-MOI          213     0                       ;
JT13-MOI        217     0                       ;
```

T20-MOI	219	0		;1 tap concrete
J9-MOI	211	0		;
T21-MOI	218	0		;1 tap concrete+ elbows
J10-MOI	223	0		;
JT8CHECK-MOI		225	0	;to T18 and T29
T15-MOI	216	0		;2 taps concrete
T16-MOI	216	0		;
J11-MOI	212	0		;
JT14-MOI	213	0		;
T17-MOI	214	0		;2 taps concrete
Vi-T17-MOI	215	0		;
JT15-MOI	213	0		;
T18-MOI	213	0		;3 taps concrete
B1-MOI	220	0		;
J12-MOI	228	0		;
JT16-MOI	231	0		;
T13-MOI	221	0		;3 taps concrete + reduce to 3/4
T14-MOI	212	0		;2 taps concrete
JT17-MOI	229	0		;
T8-MOI	217	0		;2 taps concrete
J13-MOI	216	0		;
JT18-MOI	217	0		;
T9-MOI	208	0		;2 taps concrete
T10-MOI	210	0		;1 tap large use
T11-MOI	215	0		;3 taps concrete
J14-MOI	215	0		;
J15-MOI	211	0		;
TNEW-MOI		219	0	;1 tap large use
T12-MOI	213	0		;3 taps concrete
JT19-MOI	212	0		;
T28-MOII	212	0		;2 taps large use
T3-S67	210	0		;3 taps concrete + T
T6-S67	203	0		;1 tap large use
JT1-S67	212	0		;
J1-S67	222	0		;
J2-S67	226	0		;
T2-S67	236	0		;2 taps concrete
J3-S67	241	0		;
T1-S67	244	0		;2 taps concrete
V1i-S67	247	0		;
T5-S67	207	0		;2 taps concrete + T to T18-MOI and bends
Vi-18-5	209	0		;
J4-S67	210	0		;
J5-S67	206	0		;
T7-S67	207	0		;1 tap large use
JT2-S67	209	0		;
TNEW-S67	203	0		;MaeLa1 1 tap to sink little use
T4-S67	203	0		;1 tap concrete
JT3-S67	206	0		;
V2i-S67	210	0		;
J6-S67	204	0		;
J7-S67	209	0		;
JT4-S67	207	0		;
T8-S67	214	0		;school (Tim house) 1 tap little use
V3i-S67	213	0		;
V4j-S67	211	0		;

```
J8-S67          241     0                       ;
JT1CHECK-CT             256     0                       ;altimeter:258
J1-CT           247     0                       ;
V1-CT           258     0                       ;
JT2-CT          239     0                       ;
TEMT1           242     0                       ;2 taps drinking use (little)
TEMT2           247     0                       ;2 taps to little tank
TEMT3           244     0                       ;1 tap hallway
JT3-CT          264     0                       ;
T1-CT           252     0                       ;1 tap concrete
J2-CT           250     0                       ;
JT4-CT          238     0                       ;
V2i-CT          234     0                       ;
T3-CT           224     0                       ;2 taps concrete
JT5-CT          235     0                       ;
V3j-CT          235     0                       ;
JT6-CT          233     0                       ;
V4j-CT          223     0                       ;
J3-CT           219     0                       ;
T9-CT           214     0                       ;2 taps large use
T4-CT           217     0                       ;2 taps concrete
J4-CT           229     0                       ;
T5-CT           230     0                       ;2 taps concrete large use
V5i-CT          228     0                       ;
J5-CT           210     0                       ;
J6-CT           224     0                       ;
JT7-CT          222     0                       ;
T6-CT           218     0                       ;2 taps concrete
J7-CT           222     0                       ;
T7-CT           223     0                       ;2 taps concrete
T8-CT           223     0                       ;3 taps concrete
T8-S8           214     0                       ;1 tap large use
JT1-S8          218     0                       ;
T3-S8           217     0                       ;2 taps large use
JT2-S8          225     0                       ;
TNEW-S8         225     0                       ;to small private tank
J1-S8           229     0                       ;
JT3-S8          232     0                       ;
T2-S8           230     0                       ;2 taps concrete large use
JT4-S8          256     0                       ;
T1-S8           239     0                       ;3 taps concrete
JT5-S8          258     0                       ;
J2-S8           265     0                       ;
T4-S8           255     0                       ;2 taps concrete
V6j-S8          254     0                       ;
T5-S8           236     0                       ;1 tap concrete + reduce from 1.5 to 3/4

J3-S8           222     0                       ;
JT6-S8          219     0                       ;
T6-S8           217     0                       ;2 taps concrete large use + B
T7-S8           208     0                       ;3 taps concrete + Bend
T6-AT           237     0                       ;2 taps concrete
B1-AT           233     0                       ;
JT1-AT          240     0                       ;
T5-AT           239     0                       ;2 taps concrete
J1-AT           242     0                       ;
J2-AT           251     0                       ;
```

JT2-AT	252	0	;
J3-AT	249	0	;
T10-AT	252	0	;2 taps concrete + Bend
JT3-AT	310	0	;
J4-AT	287	0	;
J5-AT	286	0	;
B2-AT	286	0	;
J6-AT	287	0	;
T2-AT	286	0	;2 taps to container temple (5x2.5x2.5) for drinking and washing and 1 more tap to border ring tank
JT4-AT	239	0	;
JT5-AT	256	0	;
T4-AT	256	0	;2 taps concrete
J7-AT	255	0	;
JT6-AT	267	0	;
T13-AT	251	0	;1 tap large use
J8-AT	245	0	;
T9-AT	246	0	;2 taps concrete
JT7-AT	326	0	;
T1-AT	290	0	;1 tap large use
J9-AT	300	0	;
JT8-AT	295	0	;
T2B-AT	300	0	;2 taps concrete
J10-AT	298	0	;
T11-AT	301	0	;1 tap large use
T3-AT	294	0	;2 taps concrete
JT9-AT	275	0	;
J11-AT	255	0	;
JT10-AT	254	0	;
T7-AT	245	0	;2 taps concrete
J12-AT	254	0	;
T12-AT	254	0	;1 tap large use
T8-AT	236	0	;2 taps concrete
J1-S17	226	0	;
J2-S17	227	0	;
J4T-S17	227	0	;
J5!-S17	235	0	;
J6!-S17	232	0	;
J7!-S17	234	0	;
T16-S17	230	0	;2 taps concrete
T17-S17	232	0	";special need school, small use
T19A-S17	226	0	;latrine
T19B-S17	227	0	;small tap to tank
T20-S17	226	0	;COERR ring tank small use
T21-S17	231	0	;latrine
V1j-S17	224	0	;
Vi-T18-S17	221	0	;
Vj-T18-S17	221	0	;
V1i-S17	224	0	;
Vi-ML2	227	0	;
Vj-ML2	227	0	;
Vi-T16-S17	234	0	;
Vi-T21-S17	231	0	;
Vi-T17-S17	235	0	;
Vi-T19	227	0	;
Vj-T19	227	0	;
Vj-T17-S17	235	0	;

```
Vj-T16-S17      234     0                       ;
Vj-T21-S17      231     0                       ;
Vi-T15-S17      231     0                       ;
Vj-T15-S17      231     0                       ;
Vj-T14-S17      231     0                       ;
Vi-T14-S17      231     0                       ;
Vi-T13-S17      238     0                       ;
Vj-T13-S17      238     0                       ;
Vi-T12-S17      238     0                       ;
Vj-T12-S17      238     0                       ;
Vi-TNEW-S17             235     0                       ;
Vj-TNEW         235     0                       ;
Vi-T11-S17      241     0                       ;
Vj-T11-S17      241     0                       ;
Vj-T10-S17      241     0                       ;
Vi-T10-S17      240     0                       ;
Vj-S17beforeT10 242     0                       ;
Vi-S17beforeT10 242     0                       ;
Vj-T7/8-S17     243     0                       ;
Vi-T7/8-S17     243     0                       ;
JT-T7/8-S17     243     0                       ;
Vi-T9-S17       244     0                       ;
Vj-T9-S17       244     0                       ;
Vj-T6-S17       244     0                       ;
Vi-T6-S17       244     0                       ;
Vj-T5-S17       244     0                       ;
Vi-T5-S17       244     0                       ;
Vi-T4-S17       249     0                       ;
Vj-T4-S17       249     0                       ;
Vi-T3-S17       249     0                       ;
Vj-T3-S17       249     0                       ;
Vi-T2-S17       253     0                       ;
Vj-T2-S17       253     0                       ;
JT-T1/2-S17     263     0                       ;
PTBj            288     0                       ;
Vi-PTB          288     0                       ;
JT-TB2-S17      336     0                       ;
Vj-TBR          336     0                       ;
Vi-TBR          336     0                       ;
JT-TB5-S17      331     0                       ;
JT-TB6/7-S17    318     0                       ;
JT-TB8-S17      313     0                       ;
V1j-BT          231     0                       ;
Vj-T3-BT        241     0                       ;
Vi-T3-BT        241     0                       ;
V2j-BT          239     0                       ;
Vi-T1-BT        250     0                       ;
Vj-T1-BT        250     0                       ;
Vj-branchT4-BT          267     0                       ;
JbranchT10-BT   266     0                       ;
Vj-branchT10-BT         266     0                       ;
JTbranches-BT   266     0                       ;
JT-branchT5-BT          266     0                       ;
Vj-branchT5-BT          267     0                       ;
JT-T5-BT        241     0                       ;
Vj-T13-BT       249     0                       ;255
Vi-T13-BT       249     0                       ;
```

Vj-T5-BT 241 0 ;
Vi-T5-BT 241 0 ;
Vj-T6-BT 237 0 ;
Vi-T6-BT 237 0 ;
JT-T7-BT 252 0 ;
Vj-T7-BT 251 0 ;
Vi-T7-BT 251 0 ;
Vi-T9/10-BT 250 0 ;
Vj-T9/10-BT 250 0 ;
Vj-T8-BT 235 0 ;
Vi-T8-BT 235 0 ;
Vj-T9-BT 245 0 ;
Vi-T9-BT 245 0 ;
JT-T9-BT 245 0 ;
Vj-T10-BT 225 0 ;
Vi-T10-BT 225 0 ;
JT-T4-MOI 237 0 ;
Vj-T3-MOI 222 0 ;
Vi-T3-MOI 222 0 ;
JT-T1-MOI 233 0 ;
JT-T27-MOI 220 0 ;
Vj-toT7-MOI 211 0 ;
Vi-toT7-MOI 211 0 ;
Vj-T7-MOI 214 0 ;
Vi-T7-MOI 214 0 ;
JT-T31B-MOI 212 0 ;
JT-T32-MOI 209 0 ;
Vj-JT7-MOI 209 0 ;
Vi-JT7-MOI 209 0 ;
Vi-brancT29-MOI 225 0 ;
Vj-brancT29-MOI 225 0 ;
JT-T19-MOI 222 0 ;
JT-T153-MOI 218 0 ;
JT-T26-MOI 220 0 ;
JT-T51-MOI 220 0 ;
Vi-T26-MOI 220 0 ;
Vj-T26-MOI 220 0 ;
Vj-JT9-MOI 220 0 ;
Vi-JT9-MOI 220 0 ;
Vi-T150-MOI 218 0 ;
Vj-T150-MOI 218 0 ;
JT-T23-MOI 213 0 ;
Vj-T24-MOI 209 0 ;
Vi-T24-MOI 209 0 ;
Vj-T25-MOI 209 0 ;
Vi-T25-MOI 209 0 ;
Vj-T20-MOI 219 0 ;
Vi-T20-MOI 219 0 ;
JT-T20-MOI 217 0 ;
Vj-T21-MOI 216 0 ;
Vi-T21-MOI 216 0 ;
Vj-T15-MOI 216 0 ;
Vi-T15-MOI 216 0 ;
JT-T15-MOI 216 0 ;
Vj-T16-MOI 216 0 ;
Vi-T16-MOI 216 0 ;
JT-T16-MOI 216 0 ;

```
Vj-T17-MOI      215     0                       ;
Vj-T18-MOI      213     0                       ;
Vi-T18-MOI      213     0                       ;
Vj-T13-MOI      221     0                       ;
Vi-T13-MOI      221     0                       ;
JT-T13-MOI      221     0                       ;
Vi-brancT12-MOI         227     0                       ;
Vj-brancT12-MOI         227     0                       ;
Vj-T14-MOI      212     0                       ;
Vi-T14-MOI      215     0                       ;
Vj-T8-MOI       217     0                       ;
Vi-T8-MOI       217     0                       ;
Vj-T9-MOI       208     0                       ;
Vi-T9-MOI       208     0                       ;
JT-T9-MOI       208     0                       ;
JT18!-MOI       215     0                       ;
Vj-T11-MOI      216     0                       ;
Vi-T11-MOI      216     0                       ;
JT-T11-MOI      216     0                       ;
Vj-T12-MOI      213     0                       ;
Vi-T12-MOI      213     0                       ;
Vi-brancT3-CH   274     0                       ;
Vj-brancT3-CH   273     0                       ;
Vj-T2-CH        259     0                       ;
Vj-T1-CH        251     0                       ;
Vi-T1-CH        251     0                       ;
JT-T1-CH        251     0                       ;
Vj-T3-CH        250     0                       ;
J2!-CH          273     0                       ;
Vj-T4-CH        268     0                       ;
Vi-T4-CH        268     0                       ;
Vi-JT3-CH       270     0                       ;
Vj-JT3-CH       270     0                       ;
Vj-T5-CH        255     0                       ;
Vi-T5-CH        255     0                       ;
JT-T5-CH        255     0                       ;
Vj-brancT10-CH          218     0                       ;
Vi-toT18-S17    218     0                       ;
Vj-toT18-S17    218     0                       ;
JT3!-CH         218     0                       ;
V5j-CH          220     0                       ;
Vj-T7-CH        221     0                       ;
Vi-T7-CH        221     0                       ;
Vj-T6-CH        214     0                       ;
Vi-T6-CH        214     0                       ;
Vj-T11-CH       223     0                       ;
Vj-T10-CH       222     0                       ;
Vi-T10-CH       222     0                       ;
V7j-CH          225     0                       ;
Vj-T6-AT        237     0                       ;
Vi-T6-AT        237     0                       ;
Vj-T5-AT        239     0                       ;
Vi-T5-AT        238     0                       ;
Vi-JT1-AT       240     0                       ;
Vj-JT1-AT       240     0                       ;
Vi-S14RING      310     0                       ;
Vj-S14RING      310     0                       ;
```

```
Vj-JT5-AT       256     0               ;
Vi-JT5-AT       256     0               ;
Vj-T13-AT       251     0               ;
Vi-T13-AT       251     0               ;
Vj-T9-AT        246     0               ;
Vi-T9-AT        246     0               ;
Vi-suggesT10-AT         252     0               ;
Vj-suggesT10-AT         253     0               ;
Vi-T1-AT        323     0               ;
Vj-T1-AT        323     0               ;
JT-T12-AT       253     0               ;
Vj-T7-AT        245     0               ;
Vi-T7-AT        245     0               ;
Vj-T8-AT        237     0               ;
Vi-T8-AT        237     0               ;
Vj-T2B-AT       300     0               ;
Vi-T2B-AT       300     0               ;
Vj-T11-AT       301     0               ;
Vi-T11-AT       301     0               ;
JT-T11-AT       301     0               ;
Vj-T3-AT        294     0               ;
Vi-T3-AT        294     0               ;
Vj-T2-S67       236     0               ;
Vi-T2-S67       236     0               ;
JT-T2-S67       235     0               ;
Vi-S67RING      248     0               ;
Vj-S67RING      248     0               ;
JT-S67RING      248     0               ;
V1j-S67         247     0               ;
Vj-T1-S67       244     0               ;
Vi-T1-S67       244     0               ;
Vj-toS67RING            256     0               ;
Vi-toS67RING            256     0               ;
J-toS67RING     247     0               ;
JT-toT5-CT      248     0               ;
Vi-pourS67RING          248     0               ;
Vj-pourS67RING          248     0               ;
JT-T5-S67       208     0               ;
Vj-18-5         210     0               ;
Vi-T5-S67       208     0               ;
Vj-T5-S67       208     0               ;
Vj-T7-S67       207     0               ;
Vi-T7-S67       207     0               ;
JT-T7-S67       207     0               ;
Vi-TNEW-S67             209     0               ;
Vj-TNEW-S67             209     0               ;
JT-T4-S67       203     0               ;
Vi-T4-S67       203     0               ;
Vj-T4-S67       203     0               ;
V2j-S67         210     0               ;
Vi-ML1-S67      206     0               ;
Vj-ML1-S67      206     0               ;
Vi-brancT5-S67  206     0               ;
Vj-brancT5-S67  206     0               ;
Vi-toML1        207     0               ;
Vj-toML1        207     0               ;
Vi-toTIMhouse   207     0               ;
```

```
Vj-toTIMhouse 207 0 ;
V3j-S67 215 0 ;
V4i-S67 211 0 ;
JT-TEMRIN3 239 0 ;
JT-TEMT3 240 0 ;
JT-TEMRIN1 240 0 ;
JT-TEMT2 237 0 ;
Vi-brancT8-CT 266 0 ;
Vj-brancT8-CT 266 0 ;
Vj-T1-CT 251 0 ;
Vi-T1-CT 252 0 ;
JT-T1-CT 252 0 ;
Vj-T3-CT 224 0 ;
Vi-T3-CT 224 0 ;
V2j-CT 234 0 ;
V3i-CT 235 0 ;
V4i-CT 223 0 ;
Vj-T4-CT 217 0 ;
Vi-T4-CT 217 0 ;
JT-T5-CT 230 0 ;
Vj-T5-CT 230 0 ;
Vi-T5-CT 230 0 ;
V5j-CT 228 0 ;
Vj-T6-CT 218 0 ;
Vi-T6-CT 218 0 ;
JT-T6-CT 218 0 ;
Vj-T7-CT 223 0 ;
Vi-T7-CT 223 0 ;
Vj-T8-CT 223 0 ;
Vi-T8-CT 223 0 ;
Vi-JT1-S8 219 0 ;
Vj-JT1-S8 219 0 ;
Vj-T3-S8 217 0 ;
Vi-T3-S8 217 0 ;
Vj-T2-S8 230 0 ;
Vi-T2-S8 230 0 ;
Vi-JT4-S8 256 0 ;
Vj-JT4-S8 256 0 ;
Vj-T1-S8 239 0 ;
Vi-T1-S8 239 0 ;
Vj-JT5-S8 258 0 ;
Vi-JT5-S8 258 0 ;
Vj-T4-S8 255 0 ;
Vi-T4-S8 255 0 ;
JT-T4-S8 255 0 ;
Vi-toS8RING 267 0 ;
Vj-toS8RING 266 0 ;
V6i-S8 254 0 ;
Vj-T5-S8 236 0 ;
Vi-T5-S8 236 0 ;
J-T5-S8 236 0 ;
JT-T5-S8 236 0 ;
Vj-T6-S8 217 0 ;
Vi-T6-S8 217 0 ;
Vi-JT6-S8 219 0 ;
Vj-JT6-S8 219 0 ;
Vi-CHT2 276 0 ;
```

```
Vj-CHT2         276     0                       ;
Vi-CHT1         276     0                       ;
Vi-CHTout       276     0                       ;
Vj-CHTout       276     0                       ;
Vi-BT1          268     0                       ;
Vj-BT1          268     0                       ;
Vi-BT2          268     0                       ;
Vj-BT2          268     0                       ;
Vj-BTout        268     0                       ;
Vj-CHT1         276     0                       ;
Vi-BTout        268     0                       ;
Vi-17Tout       275     0                       ;
Vj-17Tout       275     0                       ;
Vi-TBRINGSout           336     0                       ;
Vj-TBRINGSout           336     0                       ;
Vi-MOITout      227     0                       ;
Vj-MOITout      227     0                       ;
Vi-CTout        267     0                       ;
Vj-CTout        267     0                       ;
Vi-AT-OLDout            324     0                       ;
Vj-AT-OLDout            324     0                       ;
PSVi-MAELA2             227     0                       ;
PSVj-MAELA2             227     0                       ;
PSVi-ML1        208     0                       ;
PSVj-ML1        207     0                       ;
PSVi-TEMRIN2            240     0                       ;
PSVj-TEMRIN2            240     0                       ;
PSVj-TEMRIN3            235     0                       ;
PSVi-TEMRIN3            236     0                       ;
PSVi-TEMRIN1            242     0                       ;
PSVj-TEMRIN1            242     0                       ;
PSVi-S8RIN      257     0                       ;
PSVj-S8RIN      257     0                       ;
FCVi-CHT1       276     0                       ;
FCVj-CHT1       276     0                       ;
FCVi-AT-OLD             324     0                       ;
FCVj-AT-OLD             324     0                       ;
FCVi-MOIT       226     0                       ;
FCVj-MOIT       226     0                       ;
FCVi-17T        275     0                       ;
FCVj-17T        275     0                       ;
FCVi-CT         267     0                       ;
FCVj-CT         267     0                       ;
FCVi-BT         268     0                       ;
FCVj-BT         268     0                       ;
Vi-T23-MOI      213     0                       ;
Vj-T23-MOI      213     0                       ;

[RESERVOIRS]
;ID             Head            Pattern

[TANKS]
;ID             Elevation       InitLevel       MinLevel        MaxLevel        Diameter        MinVol
        VolCurve
 17T            275     2.96    0       2.96    9.23136 0                       ;3 compartments for a total
of 200 instead of 100
 TBRINGS        336     3.2     0       3.2     2.26    0                       ;8 rings x 4 of them
```

BT1 268 2.21 0 2.21 8.9818 0 ;actually twice the capacity marked (3 compartments each): other is 1.71*8.46*6.8 but they rotate between morning and evening
MOIT 226 1.45 0 1.45 13.1203 0 ";8 compartments total, with 2 new ones"""
CHT1 276 1.71 0 1.71 7.16773 0 ";2 tanks of 69 m3 (one has 2 compartments). (instead of 150, it is 138) one of them was not used during experiment"""
S67RING 248 3.4 0 3.4 2.76792 0 ;3x8 rings+ 3x9rings
CT 267 2 0 2 11.9758 0 ";all 4 tanks connected (25, 25 50, 50), but actual volume is 225 not 150"""
ML1RING 207 0 0 2.4 2.50348 0 ;2x6rings+7m3 tank
TEMRIN1 242 0 0 2 1.59806 0 ;2x5rings
TEMRIN2 241 0 0 2.4 1.59806 0 ;2x6rings
TEMRIN3 235 0 0 2 1.59806 0 ;2x5rings
S8RIN 257 3.2 0 3.2 2.76792 0 ;6 tanks of 8 rings
S14-RING 309 2.8 0 2.8 2.26 0 ;4 tanks of 7 rings
AT-NEW 308 2.1 0 2.1 8.90634 0 ";not working and wasn't used for experiment, 3 compartments"""
AT-OLD 324 2 0 2 8.5003 0 ;3 compartments
MAELA2-RIN 227 0 0 3.2 2.57895 0
";3x8rings+2.5m*1.9m diameter tank, 3 valves out, pouring from top"""
CHT2 276 1.71 0 1.71 7.16773 0 ";2 tanks of 69 m3 (one has 2 compartments). (instead of 150, it is 138) one of them was not used during experiment"""
BT2 268 2.21 0 2.21 8.9818 0 ;
Salt-CHT1 276 10 0 20 50 0 ;
Salt-AT-OLD 324 10 0 20 50 0 ;
Salt-MOIT 226 10 0 20 50 0 ;
Salt-17T 275 10 0 20 50 0 ;
Salt-CT 267 10 0 20 50 0 ;
Salt-BT1 268 10 0 20 50 0 ;

[PIPES]

;ID	Node1	Node2	Length	Diameter		Roughness	MinorLoss	Status
S17-1	Vi-T18-S17	T18-S17	6.5	19.05	150	0	CV	;
S17-2	V1i-S17	Vj-T18-S17	81.22	25.4	150	0	Open	;
S17-3	J1-S17	V1j-S17	38.44	25.4	150	0	Open	;
S17-4	Vi-ML2	J1-S17	8.8	38.1	150	0	Open	;
S17-5	MAELA2-RIN	Vj-ML2	0.72	38.1	150	0	Open	;
S17-6	J6!-S17	J7!-S17	26	50.8	150	0	Open	;
S17-7	J7!-S17	Vi-T16-S17	0.77	19.05	150	0	Open	;
S17-8	J6!-S17	Vi-T21-S17	0.86	12.7	150	0	Open	;
S17-9	J7!-S17	J5!-S17	98	50.8	150	0	Open	;
S17-10	J5!-S17	Vi-T17-S17	0.43	12.7	150	0	Open	;
S17-11	J4T-S17	T19A-S17	11.86	12.7	150	0	CV	;
S17-12	J4T-S17	T19B-S17	2.86	12.7	150	0	CV	;
S17-13	J4T-S17	T20-S17	41	12.7	150	0	CV	;
S17-15	J5!-S17	J2-S17	271.07	50.8	150	0	Open	;
S17-16	Vi-ML2	Vi-T19	44.82	38.1	150	0	Open	;
S17-17	Vj-T19	J4T-S17	0.84	12.7	150	0	Open	;
S17-18	JT-S17	J6!-S17	37	50.8	150	0	Open	;
S17-19	Vj-T17-S17	T17-S17	24.5	12.7	150	0	CV	;
S17-20	Vj-T16-S17	T16-S17	15	19.05	150	0	CV	;
S17-21	Vj-T21-S17	T21-S17	8	12.7	150	0	CV	;
S17-22	J-S17	T15-S17	7.5	12.7	150	0	CV	;
S17-23	JT2-S17	JT-S17	156	50.8	150	0	Open	;
S17-24	J3-S17	T14-S17	1.6	12.7	150	0	CV	;
S17-25	JT-S17	Vi-T15-S17	0.2	25.4	150	0	Open	;

```
S17-26  Vj-T15-S17      J-S17           4.5     25.4    150     0       Open    ;
S17-27  JT2-S17         Vi-T14-S17      0.2     19.05   150     0       Open    ;
S17-28  Vj-T14-S17      J3-S17          29      19.05   150     0       Open    ;
S17-29  JT3-S17         JT2-S17         113     50.8    150     0       Open    ;
S17-30  JT3-S17         Vi-T13-S17      0.2     25.4    150     0       Open    ;
S17-31  Vj-T13-S17      J4-S17          48      25.4    150     0       CV      ;
S17-32  J4-S17          T13-S17         29      19.05   150     0       Open    ;
S17-33  JT4-S17         JT3-S17         118     50.8    150     0       Open    ;
S17-34  JT4-S17         Vi-T12-S17      0.35    12.7    150     0       Open    ;
S17-35  Vj-T12-S17      T12-S17         5.2     12.7    150     0       CV      ;
S17-36  JT5-S17         JT4-S17         63.6    50.8    150     0       Open    ;
S17-37  JT5-S17         J5-S17          13      19.05   150     0       Open    ;
S17-38  J5-S17          Vi-TNEW-S17     4       12.7    150     0       Open    ;
S17-39  Vj-TNEW         TNEW-S17        0.19    12.7    150     0       CV      ;
S17-40  JT6-S17         JT5-S17         214     50.8    150     0       Open    ;
S17-41  JT6-S17         Vi-T11-S17      0.66    12.7    150     0       Open    ;
S17-42  Vj-T11-S17      T11-S17         6       12.7    150     0       CV      ;
S17-43  JT7-S17         JT6-S17         286     50.8    150     0       Open    ;
S17-44  JT7-S17         J6-S17          8       19.05   150     0       Open    ;
S17-45  J6-S17          Vi-T10-S17      14      12.7    150     0       Open    ;
S17-46  Vj-T10-S17      T10-S17         0.95    12.7    150     0       CV      ;
S17-47  Vj-S17beforeT10 JT7-S17         1.2     50.8    150     0       Open    ;
S17-48  JT8-S17         Vi-S17beforeT10 119     50.8    150     0       Open    ;
S17-49  JT8-S17         Vi-T7/8-S17     1.5     19.05   150     0       Open    ;
S17-50  Vj-T7/8-S17     T7B-S17         5       19.05   150     0       CV      ;
S17-51  Vj-T7/8-S17     JT-T7/8-S17     0.56    19.05   150     0       Open    ;
S17-52  JT-T7/8-S17     T7A-S17         0.81    19.05   150     0       CV      ;
S17-53  JT-T7/8-S17     T8-S17          4       19.05   150     0       CV      ;
S17-54  JT9-S17         JT8-S17         22      50.8    150     0       Open    ;
S17-55  JT9-S17         Vi-T9-S17       0.46    12.7    150     0       Open    ;
S17-56  Vj-T9-S17       T9-S17          53      12.7    150     0       CV      ;
S17-57  Vj-T5-S17       T5-S17          0.25    19.05   150     0       CV      ;
S17-58  Vj-T6-S17       T6-S17          0.5     19.05   150     0       CV      ;
S17-59  JT11-S17        JT9-S17         59      50.8    150     0       Open    ;
S17-60  JT11-S17        JT10-S17        15      25.4    150     0       Open    ;
S17-61  JT10-S17        Vi-T5-S17       22      19.05   150     0       Open    ;
S17-62  JT10-S17        J7-S17          3       25.4    150     0       Open    ;
S17-63  J7-S17          Vi-T6-S17       65.5    19.05   150     0       Open    ;
S17-64  JT12-S17        JT11-S17        227     50.8    150     0       Open    ;
S17-65  JT12-S17        Vi-T4-S17       0.23    25.4    150     0       Open    ;
S17-66  Vj-T4-S17       J8-S17          37      19.05   150     0       Open    ;
S17-67  J8-S17          T4-S17          16      12.7    150     0       CV      ;
S17-68  JT13-S17        JT12-S17        71      50.8    150     0       Open    ;
S17-69  JT13-S17        Vi-T3-S17       0.21    12.7    150     0       Open    ;
S17-70  Vj-T3-S17       T3-S17          13      12.7    150     0       CV      ;
S17-71  JT14-S17        JT13-S17        187     50.8    150     0       Open    ;
S17-72  JT14-S17        Vi-T2-S17       0.8     19.05   150     0       Open    ;
S17-73  Vj-T2-S17       T2-S17          39      19.05   150     0       CV      ;
S17-74  JB-S17          JT14-S17        85      50.8    150     0       Open    ;
S17-75  JT15-S17        JB-S17          26      50.8    150     0       Open    ;
S17-76  J9-S17          JT15-S17        1       50.8    150     0       Open    ;
S17-77  JT15-S17        JT-T1/2-S17     9       12.7    150     0       Open    ;
S17-78  JT-T1/2-S17     T1B-S17         1       12.7    150     0       CV      ;
S17-79  JT-T1/2-S17     T1A-S17         1       12.7    150     0       CV      ;
S17-80  Vj-17Tout       J9-S17          19      76.2    150     0       Open    ;
S17-81  17T             Vi-PTB          17.11   50.8    150     0       CV      ;
S17-82  JT16-S17        TB1-S17         20      12.7    150     0       CV      ;
```

S17-83	Vj-TBRINGSout	JT17-S17	17	25.4	150	0	Open	;
S17-84	JT17-S17	TB4-S17	3	12.7	150	0	CV	;
S17-85	JT16-S17	TB3-S17	115	25.4	150	0	CV	;
S17-86	Vj-TBRINGSout	JT-TB2-S17	4	25.4	150	0	Open	;
S17-87	JT-TB2-S17	JT16-S17	8	25.4	150	0	Open	;
S17-88	JT-TB2-S17	TB2-S17	42	12.7	150	0	CV	;
S17-89	Vj-TBR	TBRINGS	0.25	100	150	0	CV	;
S17-90	PTBj	Vi-TBR	384	50.8	150	0	Open	;
S17-91	JT17-S17	JT-TB5-S17	38	25.4	150	0	Open	;
S17-92	JT-TB5-S17	TB5-S17	24	12.7	150	0	CV	;
S17-93	JT-TB5-S17	JT18-S17	49	25.4	150	0	Open	;
S17-94	JT18-S17	JT-TB6/7-S17	4	12.7	150	0	Open	;
S17-95	JT-TB6/7-S17	TB6-S17	3	12.7	150	0	CV	;
S17-96	JT-TB6/7-S17	TB7-S17	4	12.7	150	0	CV	;
S17-97	JT18-S17	JT-TB8-S17	2.5	25.4	150	0	Open	;
S17-98	JT-TB8-S17	TB8-S17	12	12.7	150	0	CV	;
S17-99	JT-TB8-S17	J10-S17	8	19.05	150	0	Open	;
S17-100	J10-S17	TB10-S17	4	12.7	150	0	CV	;
S17-101	JT-TB8-S17	TB9-S17	10	19.05	150	0	CV	;
BT-1	J01-BT	T4-BT	62	19.05	150	0	Open	;
BT-2	V1i-BT	J01-BT	73	25.4	150	0	CV	;
BT-3	JT1-BT	V1j-BT	86	25.4	150	0	Open	;
BT-4	JT1-BT	Vi-T3-BT	14	19.05	150	0	Open	;
BT-5	Vj-T3-BT	T3-BT	0.3	12.7	150	0	CV	;
BT-6	J2-BT	JT1-BT	19	25.4	150	0	Open	;
BT-7	JT2-BT	J2-BT	1.5	38.1	150	0	Open	;
BT-8	V2j-BT	J3-BT	2	25.4	150	0	Open	;
BT-9	JT2-BT	V2i-BT	11	25.4	150	0	Open	;
BT-10	J3-BT	T2-BT	92	19.05	150	0	CV	;
BT-11	JB2-BT	JT2-BT	79	38.1	150	0	Open	;
BT-12	JT3-BT	JB2-BT	6	38.1	150	0	Open	;
BT-13	JT4-BT	JT3-BT	41	38.1	150	0	Open	;
BT-14	Vj-T1-BT	J4-BT	7	25.4	150	0	Open	;
BT-15	J4-BT	T1-BT	30	19.05	150	0	CV	;7 meters difference
BT-16	JT5-BT	JT4-BT	79	38.1	150	0	Open	;
BT-17	JT5-BT	T12-BT	12	12.7	150	0	CV	;
BT-18	J5-BT	Vj-branchT4-BT	6	38.1	150	0	Open	;
BT-19	JbranchT10-BT	Vi-branchT10-BT	18	38.1	150	0	Open	;
BT-20	JTbranches-BT	J5-BT	0.6	76.2	150	0	Open	;
BT-21	JTbranches-BT	JbranchT10-BT	0.6	76.2	150	0	Open	;
BT-22	JT-branchT5-BT	JTbranches-BT	0.6	76.2	150	0	Open	;
BT-23	JT-branchT5-BT	Vi-branchT5-BT	18	19.05	150	0	Open	;
BT-24	Vj-branchT5-BT	JT-T5-BT	148	19.05	150	0	Open	;
BT-25	Vj-T13-BT	T13-BT	0.03	12.7	150	0	CV	;
BT-26	Vi-T13-BT	JT3-BT	5	12.7	150	0	Open	;
BT-27	JT-T5-BT	Vi-T5-BT	1	12.7	150	0	Open	;
BT-28	Vj-T5-BT	T5-BT	0.04	12.7	150	0	CV	;
BT-29	Vj-T6-BT	T6-BT	0.31	12.7	150	0	CV	;
BT-30	JT-T5-BT	Vi-T6-BT	152	19.05	150	0	Open	;
BT-31	Vj-branchT10-BT	JT6-BT	125.5	38.1	150	0	Open	;
BT-32	Vi-branchT4-BT	JT5-BT	228	38.1	150	0	Open	;
BT-33	JT6-BT	T11-BT	70	12.7	150	0	CV	;
BT-34	Vj-T7-BT	T7-BT	0.05	12.7	150	0	CV	;
BT-35	JT-T7-BT	Vi-T7-BT	1	19.05	150	0	Open	;
BT-36	JT-T7-BT	J6-BT	11	38.1	150	0	Open	;
BT-37	JT6-BT	JT-T7-BT	54	38.1	150	0	Open	;

```
BT-38       J6-BT          JT7-BT          68      25.4    150     0       Open    ;
BT-39       JT7-BT         J7-BT           11      25.4    150     0       Open    ;
BT-40       J7-BT          Vi-T9/10-BT     2       19.05   150     0       Open    ;
BT-41       Vj-T8-BT       T8-BT           0.24    12.7    150     0       CV      ;
BT-42       JT7-BT         Vi-T8-BT        93      19.05   150     0       Open    ;
BT-43       Vj-T9-BT       T9-BT           0.1     12.7    150     0       CV      ;
BT-44       JT-T9-BT       Vi-T9-BT        0.54    19.05   150     0       Open    ;
BT-45       Vj-T9/10-BT    JT-T9-BT        54      19.05   150     0       Open    ;
BT-46       Vj-T10-BT      T10-BT          0.29    12.7    150     0       CV      ;
BT-47       JT-T9-BT       Vi-T10-BT       91      19.05   150     0       Open    ;
MOI-1       JT1-MOI        T5A-MOI         9.98    12.7    150     0       CV      ;
MOI-2       JT1-MOI        T5B-MOI         13.13   12.7    150     0       CV      ;
MOI-3       J1-MOI         JT1-MOI         14.69   25.4    150     0       Open    ;
MOI-4       JT2-MOI        JT-T4-MOI       33      38.1    150     0       Open    ;
MOI-5       JT-T4-MOI      T4-MOI          1.51    12.7    150     0       CV      ;
MOI-6       JT-T4-MOI      J1-MOI          23      38.1    150     0       Open    ;
MOI-7       JT3-MOI        JT2-MOI         47      38.1    150     0       Open    ;
MOI-8       JT3-MOI        T2-MOI          2.43    12.7    150     0       CV      ;
MOI-9       Vj-T3-MOI      T3-MOI          0.48    12.7    150     0       CV      ;
MOI-10      JT2-MOI        Vi-T3-MOI       28      12.7    150     0       Open    ;
MOI-11      JT-T1-MOI      JT3-MOI         30      38.1    150     0       Open    ;
MOI-12      JT-T1-MOI      T1-MOI          0.42    19.05   150     0       CV      ;
MOI-13      Vj-MOITout     JT-T1-MOI       46      38.1    150     0       Open    ;
MOI-14      JT1-MOI        JT-T27-MOI      43      25.4    150     0       Open    ;
MOI-15      JT-T27-MOI     T27-MOI         0.7     12.7    150     0       CV      ;
MOI-16      JT-T27-MOI     J2-MOI          105     25.4    150     0       Open    ;
MOI-17      Vj-toT7-MOI    JT4-MOI         0.32    19.05   150     0       Open    ;
MOI-18      J2-MOI         Vi-toT7-MOI     41      19.05   150     0       Open    ;
MOI-19      JT4-MOI        T6-MOI          16      12.7    150     0       CV      ;
MOI-20      JT4-MOI        JT5-MOI         25.5    19.05   150     0       Open    ;
MOI-21      Vj-T7-MOI      T7-MOI          0.35    12.7    150     0       CV      ;
MOI-22      JT5-MOI        Vi-T7-MOI       15      19.05   150     0       Open    ;
MOI-23      JT5-MOI        JT6-MOI         7.27    19.05   150     0       Open    ;
MOI-24      JT-T31B-MOI    T31B-MOI        0.04    12.7    150     0       CV      ;
MOI-25      JT6-MOI        JT-T31B-MOI     11.59   19.05   150     0       Open    ;
MOI-26      JT-T31B-MOI    T31A-MOI        29.01   19.05   150     0       CV      ;
MOI-27      JT7-MOI        T30-MOI         1.66    19.05   150     0       CV      ;
MOI-28      JT7-MOI        JT-T32-MOI      0.11    19.05   150     0       Open    ;
MOI-29      Vj-JT7-MOI     JT7-MOI         0.01    19.05   150     0       Open    ;
MOI-30      JT6-MOI        Vi-JT7-MOI      21.38   19.05   150     0       Open    ;
MOI-31      JT-T32-MOI     T32B-MOI        5.72    19.05   150     0       CV      ;
MOI-32      JT-T32-MOI     T32A-MOI        13.65   19.05   150     0       CV      ;
MOI-33      Vj-MOITout     JT8CHECK-MOI            7       76.2    150     0       Open    ;
MOI-34      JT8CHECK-MOI           Vi-brancT29-MOI         0.32    76.2    150     0       Open
    ;
MOI-35      Vj-brancT29-MOI        J3-MOI          19      76.2    150     0       Open    ;
MOI-36      J3-MOI         J4-MOI          55      63.5    150     0       Open    ;
MOI-37      JT-T19-MOI     T19-MOI         1       12.7    150     0       CV      ;
MOI-38      J4-MOI         JT-T19-MOI      12      38.1    150     0       Open    ;
MOI-39      JT-T153-MOI    T153-MOI        0.71    12.7    150     0       CV      ;
MOI-40      JT-T19-MOI     JT-T153-MOI     40      38.1    150     0       Open    ;
MOI-41      JT-T153-MOI    JT13-MOI        7.06    38.1    150     0       Open    ;
MOI-42      JT-T51-MOI     T151-MOI        7       19.05   150     0       CV      ;
MOI-43      JT-T51-MOI     JT-T26-MOI      1.57    38.1    150     0       Open    ;
MOI-44      JT13-MOI       JT-T51-MOI      14.05   38.1    150     0       Open    ;
MOI-45      JT-T26-MOI     Vi-T26-MOI      0.38    25.4    150     0       Open    ;
MOI-46      JT-T26-MOI     Vi-JT9-MOI      0.32    38.1    150     0       Open    ;
```

MOI-47	Vj-JT9-MOI	JT9-MOI	2.64	38.1	150	0	Open	;
MOI-48	JT9-MOI	Vi-T150-MOI	0.29	12.7	150	0	Open	;
MOI-49	Vj-T150-MOI	T150-MOI	11.56	12.7	150	0	CV	;
MOI-50	JT9-MOI	JT-T23-MOI	75	38.1	150	0	Open	;
MOI-51	JT-T23-MOI	Vi-T23-MOI	0.33	12.7	150	0	CV	;
MOI-52	JT-T23-MOI	JT10-MOI	75	38.1	150	0	Open	;
MOI-53	JT10-MOI	J5-MOI	48	19.05	150	0	Open	;
MOI-54	Vj-T24-MOI	T24-MOI	0.15	12.7	150	0	CV	;
MOI-55	J5-MOI	Vi-T24-MOI	8	12.7	150	0	Open	;
MOI-56	JT10-MOI	J6-MOI	44	38.1	150	0	Open	;
MOI-57	J6-MOI	V1-MOI	17	25.4	150	0	Open	;
MOI-58	V1-MOI	JT12-MOI	77	25.4	150	0	Open	;
MOI-59	J7-MOI	T29-MOI	101	12.7	150	0	Open	;
MOI-60	JT12-MOI	J7-MOI	5	25.4	150	0	CV	;
MOI-61	Vj-T25-MOI	T25-MOI	0.32	19.05	150	0	CV	;
MOI-62	JT12-MOI	Vi-T25-MOI	19	19.05	150	0	Open	;
MOI-63	Vj-T20-MOI	T20-MOI	0.11	12.7	150	0	CV	;
MOI-64	JT-T20-MOI	Vi-T20-MOI	1	12.7	150	0	Open	;
MOI-65	JT13-MOI	JT-T20-MOI	52	25.4	150	0	Open	;
MOI-66	JT-T20-MOI	J9-MOI	9	25.4	150	0	Open	;
MOI-67	Vj-T21-MOI	T21-MOI	0.32	12.7	150	0	CV	;
MOI-68	J9-MOI	Vi-T21-MOI	51	19.05	150	0	Open	;
MOI-69	Vj-T26-MOI	J8-MOI	85	25.4	150	0	Open	;
MOI-70	J8-MOI	T26-MOI	79	19.05	150	0	CV	;
MOI-71	JT8CHECK-MOI	J10-MOI	14	63.5	150	0	Open	;
MOI-72	JT-T15-MOI	Vi-T15-MOI	2	12.7	150	0	Open	;
MOI-73	Vj-T15-MOI	T15-MOI	0.35	12.7	150	0	CV	;
MOI-74	J10-MOI	JT-T15-MOI	115	38.1	150	0	Open	;
MOI-75	JT-T16-MOI	Vi-T16-MOI	0.53	12.7	150	0	Open	;
MOI-76	Vj-T16-MOI	T16-MOI	0.44	12.7	150	0	CV	;
MOI-77	JT-T15-MOI	JT-T16-MOI	49	38.1	150	0	Open	;
MOI-78	JT-T16-MOI	J11-MOI	38	25.4	150	0	Open	;
MOI-79	J11-MOI	JT14-MOI	22	25.4	150	0	Open	;
MOI-80	JT14-MOI	Vi-T17-MOI	57	19.05	150	0	Open	;
MOI-81	Vj-T17-MOI	T17-MOI	22	19.05	150	0	CV	;
MOI-82	JT14-MOI	JT15-MOI	68	25.4	150	0	Open	;
MOI-83	Vj-T18-MOI	T18-MOI	0.07	12.7	150	0	CV	;
MOI-84	JT15-MOI	Vi-T18-MOI	9	12.7	150	0	Open	;
MOI-85	JT16-MOI	J12-MOI	6	38.1	150	0	Open	;
MOI-86	J12-MOI	B1-MOI	74	25.4	150	0	Open	;
MOI-87	Vj-T13-MOI	T13-MOI	0.38	12.7	150	0	CV	;
MOI-88	JT-T13-MOI	Vi-T13-MOI	0.23	12.7	150	0	Open	;
MOI-89	B1-MOI	JT-T13-MOI	4.5	25.4	150	0	Open	;
MOI-90	Vj-MOITout	Vi-brancT12-MOI	0.78	76.2	150	0	Open	;
MOI-91	Vj-brancT12-MOI	JT16-MOI	7	76.2	150	0	Open	;
MOI-92	Vj-T14-MOI	T14-MOI	0.45	12.7	150	0	CV	;
MOI-93	JT-T13-MOI	Vi-T14-MOI	69	19.05	150	0	Open	;
MOI-94	JT16-MOI	JT17-MOI	8.97	76.2	150	0	Open	;
MOI-95	Vj-T8-MOI	T8-MOI	0.24	12.7	150	0	CV	;
MOI-96	JT17-MOI	Vi-T8-MOI	50	19.05	150	0	Open	;
MOI-97	JT17-MOI	J13-MOI	41	50.8	150	0	Open	;
MOI-98	Vj-T9-MOI	T9-MOI	1.5	19.05	150	0	CV	;
MOI-99	JT-T9-MOI	Vi-T9-MOI	0.21	19.05	150	0	Open	;
MOI-100	J13-MOI	JT-T9-MOI	81	38.1	150	0	Open	;
MOI-101	JT-T9-MOI	JT18-MOI	79	38.1	150	0	Open	;
MOI-102	JT18-MOI	T10-MOI	66	19.05	150	0	CV	;
MOI-103	JT18-MOI	JT18!-MOI	4	38.1	150	0	Open	;

MOI-104	Vj-T11-MOI	T11-MOI	0.58	19.05	150	0	CV	;
MOI-105	JT-T11-MOI	Vi-T11-MOI	0.52	19.05	150	0	Open	;
MOI-106	JT18!-MOI	JT-T11-MOI	18	19.05	150	0	Open	;
MOI-107	JT-T11-MOI	TNEW-MOI		14	19.05	150	0	CV ;
MOI-108	JT18!-MOI	J14-MOI	18	38.1	150	0	Open	;
MOI-109	J14-MOI	JT19-MOI	24	25.4	150	0	Open	;
MOI-110	JT19-MOI	J15-MOI	6	25.4	150	0	Open	;
MOI-111	JT19-MOI	T28-MOII	53	12.7	150	0	CV	;
MOI-112	Vj-T12-MOI	T12-MOI	0.34	19.05	150	0	CV	;
MOI-113	J15-MOI	Vi-T12-MOI	50	19.05	150	0	Open	;
CH-1	J1-CH	JT1-CH	6	50.8	150	0	Open	;
CH-2	JT1-CH	Vi-brancT3-CH	2.5	25.4	150	0	Open	;
CH-3	Vj-brancT3-CH	J2-CH	29	25.4	150	0	Open	;
CH-4	J2-CH	JT2-CH	47	19.05	150	0	Open	;
CH-5	JT2-CH	Vi-T2-CH	6	12.7	150	0	Open	;
CH-6	Vj-T2-CH	T2-CH	93.21	12.7	150	0	CV	;
CH-7	Vj-T1-CH	T1-CH	0.15	12.7	150	0	CV	;
CH-8	JT-T1-CH	Vi-T1-CH	0.14	12.7	150	0	Open	;
CH-9	JT2-CH	JT-T1-CH	37	19.05	150	0	Open	;
CH-10	JT-T1-CH	Vi-T3-CH	3	19.05	150	0	Open	;
CH-11	Vj-T3-CH	T3-CH	92	12.7	150	0	CV	;
CH-12	JT1-CH	J2!-CH	3	50.8	150	0	Open	;
CH-13	J2!-CH	JT3-CH	14	38.1	150	0	Open	;
CH-14	JT3-CH	Vi-T4-CH	17	12.7	150	0	Open	;
CH-15	Vj-T4-CH	T4-CH	0.6	12.7	150	0	CV	;
CH-16	JT3-CH	Vi-JT3-CH	0.13	38.1	150	0	Open	;
CH-17	JT-T5-CH	Vi-T5-CH	0.12	12.7	150	0	Open	;
CH-18	Vj-T5-CH	T5-CH	0.09	12.7	150	0	CV	;
CH-19	Vj-JT3-CH	JT-T5-CH	48	38.1	150	0	Open	;
CH-20	Vj-brancT10-CH	JT3!-CH	0.58	38.1	150	0	Open	;
CH-21	JT3!-CH	Vi-toT18-S17	0.5	38.1	150	0	Open	;
CH-22	JT-T5-CH	Vi-brancT10-CH	74	38.1	150	0	Open	;
CH-23	JT3!-CH	V5i-CH	8	38.1	150	0	Open	;
CH-24	V5j-CH	JT4-CH	141	38.1	150	0	Open	;
CH-25	JT4-CH	JT5-CH	130	38.1	150	0	Open	;
CH-26	JT5-CH	JT6-CH	101	38.1	150	0	Open	;
CH-27	JT6-CH	T8-CH	51	12.7	150	0	CV	;
CH-28	Vj-T7-CH	T7-CH	0.37	19.05	150	0	CV	;
CH-29	JT5-CH	Vi-T7-CH	8	19.05	150	0	Open	;
CH-30	JT4-CH	Vi-T6-CH	14	12.7	150	0	Open	;
CH-31	Vj-T6-CH	T6-CH	0.42	12.7	150	0	CV	;
CH-32	JT6-CH	JT7-CH	37.54	38.1	150	0	Open	;
CH-33	JT7-CH	Vi-T11-CH	10	19.05	150	0	Open	;
CH-34	Vj-T11-CH	J3-CH	33	19.05	150	0	Open	;
CH-35	J3-CH	T11-CH	17	12.7	150	0	CV	;
CH-36	JT7-CH	JT8-CH	105	25.4	150	0	Open	;
CH-37	JT8-CH	T9-CH	33	12.7	150	0	CV	;
CH-38	JT8-CH	J4-CH	4	25.4	150	0	Open	;
CH-39	Vj-T10-CH	T10-CH	0.22	19.05	150	0	CV	;
CH-40	J4-CH	Vi-T10-CH	11	19.05	150	0	Open	;
CH-41	V7j-CH	T18-S17	0.67	38.1	150	0	CV	;
CH-42	Vj-toT18-S17	V7i-CH	69.15	38.1	150	0	Open	;
AT-1	Vj-T6-AT	T6-AT	0.58	12.7	150	0	CV	;
AT-2	B1-AT	Vi-T6-AT	4	19.05	150	0	Open	;
AT-3	Vj-T5-AT	T5-AT	0.94	19.05	150	0	CV	;
AT-4	JT1-AT	Vi-T5-AT	24	19.05	150	0	Open	;
AT-5	JT4-AT	JT1-AT	27	25.4	150	0	Open	;

AT-6	JT4-AT	B1-AT	170	25.4	150	0	Open	;
AT-7	JT1-AT	Vi-JT1-AT	3	25.4	150	0	Open	;
AT-8	Vj-JT1-AT	J1-AT	15	25.4	150	0	Open	;
AT-9	J1-AT	JT2-AT	61	38.1	150	0	Open	;
AT-10	JT2-AT	J2-AT	24	38.1	150	0	Open	;
AT-11	J2-AT	J3-AT	17	25.4	150	0	Open	;
AT-12	J3-AT	T10-AT	13	19.05	150	0	CV	;
AT-13	S14-RING	Vi-S14RING	2	38.1	150	0	Open	;
AT-14	Vj-S14RING	JT3-AT	0.5	38.1	150	0	Open	;
AT-15	JT3-AT	J4-AT	34	25.4	150	0	Open	;
AT-16	J4-AT	J5-AT	59	12.7	150	0	Open	;
AT-17	J5-AT	B2-AT	50	19.05	150	0	Open	;
AT-18	B2-AT	J6-AT	24	19.05	150	0	Open	;
AT-19	J6-AT	T2-AT	4	12.7	150	0	CV	;
AT-20	JT5-AT	Vj-JT5-AT	0.74	25.4	150	0	Open	;
AT-21	JT5-AT	T4-AT	4	19.05	150	0	CV	;
AT-22	Vi-JT5-AT	JT4-AT	69	25.4	150	0	Open	;
AT-23	J7-AT	JT5-AT	8	25.4	150	0	Open	;
AT-24	JT6-AT	J7-AT	152	38.1	150	0	Open	;
AT-25	Vj-T13-AT	T13-AT	3	12.7	150	0	CV	;
AT-26	JT6-AT	Vi-T13-AT	45	19.05	150	0	Open	;
AT-27	Vi-T13-AT	J8-AT	74	19.05	150	0	Open	;
AT-28	Vj-T9-AT	T9-AT	0.21	12.7	150	0	CV	;
AT-29	J8-AT	Vi-T9-AT	24	12.7	150	0	Open	;
AT-30	JT2-AT	Vi-suggesT10-AT	0.72	38.1	150	0	Open	;
AT-31	Vj-suggesT10-AT	JT3-AT	212	38.1	150	0	Open	;
AT-32	Vj-AT-OLDout	JT7-AT		109	38.1	150	0	Open ;
AT-33	JT7-AT	Vi-T1-AT	0.73	19.05	150	0	Open	;
AT-34	Vj-T1-AT	T1-AT	37	19.05	150	0	CV	;
AT-35	JT7-AT	JT9-AT	205	38.1	150	0	Open	;
AT-36	JT9-AT	JT6-AT	81	38.1	150	0	Open	;
AT-37	JT-T12-AT	T12-AT	0.74	12.7	150	0	CV	;
AT-38	JT9-AT	JT10-AT	59	25.4	150	0	Open	;
AT-39	JT10-AT	J11-AT	1	25.4	150	0	Open	;
AT-40	Vj-T7-AT	T7-AT	0.45	12.7	150	0	CV	;
AT-41	J11-AT	Vi-T7-AT	75	19.05	150	0	Open	;
AT-42	JT10-AT	JT-T12-AT	17	25.4	150	0	Open	;
AT-43	JT-T12-AT	J12-AT	8	25.4	150	0	Open	;
AT-44	Vj-T8-AT	T8-AT	0.68	12.7	150	0	CV	;
AT-45	J12-AT	Vi-T8-AT	57	19.05	150	0	Open	;
AT-46	Vj-AT-OLDout	J9-AT		166	38.1	150	0	Open ;
AT-47	J9-AT	JT8-AT	19	19.05	150	0	Open	;
AT-48	Vj-T2B-AT	T2B-AT	0.51	12.7	150	0	CV	;
AT-49	JT8-AT	Vi-T2B-AT	17	19.05	150	0	Open	;
AT-50	JT-T11-AT	Vi-T11-AT	0.22	19.05	150	0	Open	;
AT-51	Vj-T11-AT	T11-AT	6	12.7	150	0	CV	;
AT-52	Vi-T2B-AT	JT-T11-AT	97	25.4	150	0	Open	;
AT-53	JT-T11-AT	J10-AT	15	25.4	150	0	Open	;
AT-54	Vj-T3-AT	T3-AT	0.38	12.7	150	0	CV	;
AT-55	J10-AT	Vi-T3-AT	103	19.05	150	0	Open	;
S67-1	JT1-S67	T6-S67	85	12.7	150	0	CV	;
S67-2	JT1-S67	T3-S67	6	19.05	150	0	CV	;
S67-3	J1-S67	JT1-S67	38	19.05	150	0	Open	;
S67-4	J2-S67	J1-S67	78	25.4	150	0	Open	;
S67-5	Vj-T2-S67	T2-S67	0.2	12.7	150	0	CV	;
S67-6	JT-T2-S67	Vi-T2-S67	3	19.05	150	0	Open	;
S67-7	JT-T2-S67	J2-S67	99	38.1	150	0	Open	;

S67-8	S67RING	Vi-S67RING	0.74	38.1	150	0	Open	;
S67-9	Vj-S67RING	JT-S67RING	0.24	38.1	150	0	Open	;
S67-10	JT-S67RING	JT-T2-S67	79	38.1	150	0	Open	;
S67-11	JT-S67RING	V1i-S67	18	25.4	150	0	Open	;
S67-12	V1j-S67	J3-S67	30	25.4	150	0	Open	;
S67-13	Vj-T1-S67	T1-S67	0.09	12.7	150	0	CV	;
S67-14	J3-S67	Vj-T1-S67	48	19.05	150	0	Open	;
S67-15	JT1CHECK-CT	Vi-toS67RING	0.41	50.8	150	0	Open	;
S67-16	Vj-toS67RING	J-toS67RING	23	50.8	150	0	Open	;
S67-17	Vj-CTout	JT1CHECK-CT	60	50.8	150	0	CV	;
S67-18	Vj-pourS67RING	S67RING	0.41	100	150	0	CV	;
S67-19	Vi-pourS67RING	JT-toT5-CT	0.4	38.1	150	0	Open	;
S67-20	J-toS67RING	JT-toT5-CT	10	38.1	150	0	Open	;
S67-21	JT-T5-S67	T5-S67	2	12.7	150	0	CV	;
S67-22	Vi-T18-MOI	Vi-18-5	51.29	12.7	150	0	Open	;
S67-23	Vj-18-5	JT-T5-S67	93	12.7	150	0	Open	;
S67-24	Vj-T5-S67	JT-T5-S67	0.52	12.7	150	0	Open	;
S67-25	J4-S67	Vi-T5-S67	5	12.7	150	0	Open	;
S67-26	JT-T7-S67	Vi-T7-S67	0.5	12.7	150	0	Open	;
S67-27	Vj-T7-S67	T7-S67	0.5	12.7	150	0	CV	;
S67-28	JT-T7-S67	J4-S67	126	19.05	150	0	Open	;
S67-29	J5-S67	JT-T7-S67	40	19.05	150	0	Open	;
S67-30	JT2-S67	J5-S67	14	25.4	150	0	Open	;
S67-31	JT2-S67	Vi-TNEW-S67	5	12.7	150	0	Open	;
S67-32	Vj-TNEW-S67	TNEW-S67	23	12.7	150	0	CV	;
S67-33	JT-T4-S67	Vi-T4-S67	1	12.7	150	0	Open	;
S67-34	Vj-T4-S67	T4-S67	0.47	12.7	150	0	CV	;
S67-35	JT-T4-S67	JT2-S67	71	25.4	150	0	Open	;
S67-36	V2i-S67	JT-T4-S67	32	25.4	150	0	Open	;
S67-37	Vi-ML1-S67	JT3-S67	0.25	25.4	150	0	Open	;
S67-38	JT3-S67	Vi-brancT5-S67	0.12	25.4	150	0	Open	;
S67-39	Vj-brancT5-S67	V2j-S67	19	25.4	150	0	Open	;
S67-40	JT4-S67	Vi-toTIMhouse	0.36	25.4	150	0	Open	;
S67-41	JT4-S67	Vi-toML1	0.28	25.4	150	0	Open	;
S67-42	JT4-S67	Vj-ML1-S67	18	25.4	150	0	Open	;
S67-43	Vj-toTIMhouse	J6-S67	49	25.4	150	0	Open	;
S67-44	J6-S67	J7-S67	17	19.05	150	0	Open	;
S67-45	V3j-S67	T8-S67	14	12.7	150	0	CV	;
S67-46	V3i-S67	J7-S67	7	12.7	150	0	Open	;
S67-47	V4i-S67	Vj-toML1	74	25.4	150	0	Open	;
S67-49	J8-S67	JT3-S67	335.88	25.4	150	0	Open	;
S67-50	JT-toT5-CT	J8-S67	61	38.1	150	0	Open	;
CT-1	JT1CHECK-CT	V1-CT	16	25.4	150	0	Open	;
CT-2	V1-CT	J1-CT	81	25.4	150	0	Open	;
CT-3	J1-CT	JT2-CT	220	19.05	150	0	Open	;
CT-4	JT2-CT	JT-TEMT2	1	12.7	150	0	Open	;
CT-5	JT-TEMT2	JT-TEMRIN1	5	12.7	150	0	Open	;
CT-7	JT-TEMRIN1	JT-TEMT3	0.5	12.7	150	0	Open	;
CT-8	JT-TEMT3	TEMT3	32	12.7	150	0	CV	;
CT-9	JT-TEMT3	JT-TEMRIN3	2.63	12.7	150	0	Open	;
CT-12	JT2-CT	TEMT1	28	12.7	150	0	CV	;
CT-13	JT-TEMT2	TEMT2	3	12.7	150	0	CV	;
CT-14	Vj-CTout	Vi-brancT8-CT	1.29	76.2	150	0	Open	;
CT-15	Vj-brancT8-CT	JT3-CT	5	76.2	150	0	Open	;
CT-16	Vj-T1-CT	T1-CT	0.82	12.7	150	0	CV	;
CT-17	JT-T1-CT	Vi-T1-CT	0.71	12.7	150	0	Open	;
CT-18	JT3-CT	JT-T1-CT	74	76.2	150	0	Open	;

```
CT-19   JT-T1-CT    J2-CT       13      76.2    150     0       Open    ;
CT-20   J2-CT       JT4-CT      178     50.8    150     0       Open    ;
CT-21   JT4-CT      V2i-CT      32.7    19.05   150     0       Open    ;
CT-22   Vj-T3-CT    T3-CT       0.55    12.7    150     0       CV      ;
CT-23   V2j-CT      Vi-T3-CT    44      19.05   150     0       Open    ;
CT-24   JT4-CT      JT5-CT      51.2    50.8    150     0       Open    ;
CT-25   JT5-CT      V3i-CT      100     25.4    150     0       Open    ;
CT-26   V3j-CT      JT6-CT      66      25.4    150     0       Open    ;
CT-27   JT6-CT      V4i-CT      32      19.05   150     0       Open    ;
CT-28   V4j-CT      J3-CT       14      19.05   150     0       Open    ;
CT-29   J3-CT       T9-CT       16      12.7    150     0       CV      ;
CT-30   Vj-T4-CT    T4-CT       1.22    12.7    150     0       CV      ;
CT-31   JT6-CT      Vi-T4-CT    42      19.05   150     0       Open    ;
CT-32   JT5-CT      J4-CT       8       50.8    150     0       Open    ;
CT-33   Vj-T5-CT    T5-CT       0.12    12.7    150     0       CV      ;
CT-34   JT-T5-CT    Vi-T5-CT    2       12.7    150     0       Open    ;
CT-35   J4-CT       JT-T5-CT    16      38.1    150     0       Open    ;
CT-36   JT-T5-CT    V5i-CT      8.67    38.1    150     0       Open    ;
CT-37   V5j-CT      J5-CT       164     38.1    150     0       Open    ;
CT-38   Vj-T6-CT    T6-CT       0.54    12.7    150     0       CV      ;
CT-39   JT-T6-CT    Vi-T6-CT    0.85    12.7    150     0       Open    ;
CT-40   J5-CT       JT-T6-CT    118     25.4    150     0       Open    ;
CT-41   JT-T6-CT    JT7-CT      57      25.4    150     0       Open    ;
CT-42   JT7-CT      J6-CT       50      25.4    150     0       Open    ;
CT-43   Vj-T7-CT    T7-CT       0.42    12.7    150     0       CV      ;
CT-44   J6-CT       Vi-T7-CT    44      19.05   150     0       Open    ;
CT-45   JT7-CT      J7-CT       2       25.4    150     0       Open    ;
CT-46   Vj-T8-CT    T8-CT       0.14    12.7    150     0       CV      ;
CT-47   J7-CT       Vi-T8-CT    14      19.05   150     0       Open    ;
S8-1    JT2-S8      JT1-S8      21      19.05   150     0       Open    ;
S8-2    JT2-S8      TNEW-S8     12      19.05   150     0       CV      ;
S8-3    JT1-S8      Vi-JT1-S8   5       12.7    150     0       Open    ;
S8-4    Vj-JT1-S8   T8-S8       100     12.7    150     0       CV      ;
S8-5    Vj-T3-S8    T3-S8       0.25    12.7    150     0       CV      ;
S8-6    JT2-S8      TNEW-S8     5.93    12.7    150     0       CV      ;
S8-7    J1-S8       JT2-S8      30      19.05   150     0       Open    ;
S8-8    JT3-S8      J1-S8       15      25.4    150     0       Open    ;
S8-9    Vj-T2-S8    T2-S8       0.7     12.7    150     0       CV      ;
S8-10   JT3-S8      Vi-T2-S8    16      19.05   150     0       Open    ;
S8-11   JT4-S8      Vi-JT4-S8   3       25.4    150     0       Open    ;
S8-12   Vj-JT4-S8   JT3-S8      144     25.4    150     0       Open    ;
S8-13   Vj-T1-S8    T1-S8       0.34    12.7    150     0       CV      ;
S8-14   JT4-S8      Vi-T1-S8    145     19.05   150     0       Open    ;
S8-15   JT5-S8      JT4-S8      8       25.4    150     0       Open    ;
S8-16   Vj-JT5-S8   JT5-S8      0.67    38.1    150     0       Open    ;
S8-17   Vj-T4-S8    T4-S8       0.06    12.7    150     0       CV      ;
S8-18   JT-T4-S8    Vi-T4-S8    6       19.05   150     0       Open    ;
S8-19   JT5-S8      JT-T4-S8    39      38.1    150     0       Open    ;
S8-20   S8RIN       Vi-JT5-S8   5       38.1    150     0       Open    ;
S8-21   Vj-CTout    Vi-toS8RING 0.46    76.2    150     0       Open    ;
S8-22   Vj-toS8RING J2-S8       130.9   76.2    150     0       Open    ;
S8-24   JT-T4-S8    V6i-S8      6       38.1    150     0       Open    ;
S8-25   Vj-T5-S8    T5-S8       0.27    12.7    150     0       CV      ;
S8-26   J-T5-S8     Vi-T5-S8    0.49    19.05   150     0       Open    ;
S8-27   JT-T5-S8    J-T5-S8     0.54    25.4    150     0       Open    ;
S8-28   V6j-S8      JT-T5-S8    153     38.1    150     0       Open    ;
S8-29   JT-T5-S8    J3-S8       52.5    25.4    150     0       Open    ;
```

```
S8-30           J3-S8           JT6-S8          68.5    25.4    150     0       Open    ;
S8-31           Vj-T6-S8        T6-S8           0.41    12.7    150     0       CV      ;
S8-32           JT6-S8          Vi-T6-S8        7       12.7    150     0       Open    ;
S8-33           JT6-S8          Vi-JT6-S8       0.22    19.05   150     0       Open    ;
S8-34           Vj-JT6-S8       T7-S8           115     19.05   150     0       CV      ;
S8-35           JT1-S8          Vi-T3-S8        5       12.7    150     0       Open    ;
CH-43           CHT2            Vi-CHT2         1       76.2    150     0       Open    ;
CH-44           Vj-CHT2         Vi-CHTout       5       76.2    150     0       Open    ;
CH-45           CHT1            Vi-CHT1         0.5     76.2    150     0       Open    ;
CH-46           Vj-CHTout       J1-CH           6       76.2    150     0       Open    ;
BT-48           BT2             Vi-BT2          1       76.2    150     0       Open    ;
BT-49           Vj-BT2          Vj-BT1          10      76.2    150     0       Open    ;
BT-50           BT1             Vi-BT1          1       76.2    150     0       Open    ;
BT-51           Vj-BTout        JT-branchT5-BT  80      76.2    150     0       Open    ;
BT-14!          JT4-BT          Vi-T1-BT        0.1     25.4    150     0       Open    ;
CH-44!          Vj-CHT1         Vi-CHTout       0.1     76.2    150     0       Open    ;
BT-49!          Vj-BT1          Vi-BTout        0.1     76.2    150     0       Open    ;
S17-01          17T             Vi-17Tout       2       76.2    150     0       Open    ;
TB-01           TBRINGS         Vi-TBRINGSout           0.5     25.4    150     0       Open    ;
MOI-01          MOIT            Vi-MOITout      0.5     76.2    150     0       Open    ;
CT-01           CT              Vi-CTout        0.5     76.2    150     0       Open    ;
AT-OLD01        AT-OLD          Vi-AT-OLDout            0.5     38.1    150     0       Open    ;
S17-0           PSVj-MAELA2             MAELA2-RIN              1       100     150     0       Open
        ;
S17-0!          J2-S17          PSVi-MAELA2             28      50.8    150     0       Open    ;
S67-0!          PSVj-ML1        ML1RING         1       100     150     0       Open    ;
S67-0           V4j-S67         PSVi-ML1        6       25.4    150     0       CV      ;
CT-11!!         PSVj-TEMRIN2            TEMRIN2         1       100     150     0       Open    ;
CT11!           JT-TEMRIN3      PSVi-TEMRIN2            27      12.7    150     0       CV      ;
CT-10!          JT-TEMRIN3      PSVi-TEMRIN3            36      12.7    150     0       CV      ;
CT-10!!         PSVj-TEMRIN3            TEMRIN3         1       100     150     0       Open    ;
CT-6!           JT-TEMRIN1      PSVi-TEMRIN1            1       12.7    150     0       CV      ;
CT-6!!          PSVj-TEMRIN1            TEMRIN1         0.1     100     150     0       Open    ;
S8-23!          J2-S8           PSVi-S8RIN      65.42   50.8    150     0       CV      ;
S8-23!!         PSVj-S8RIN      S8RIN           1       100     150     0       Open    ;
3       Salt-CHT1       FCVi-CHT1       0.0001  100     150     0       Open    ;
4       FCVj-CHT1       CHT1            0.0001  100     150     0       Open    ;
5       FCVj-AT-OLD             AT-OLD          0.0001  100     150     0       Open    ;
6       Salt-AT-OLD     FCVi-AT-OLD             0.0001  100     150     0       Open    ;
8       Salt-MOIT       FCVi-MOIT       0.0001  100     150     0       Open    ;
9       FCVj-MOIT       MOIT            0.0001  100     150     0       Open    ;
10      FCVj-17T        17T             0.0001  100     150     0       Open    ;
11      Salt-17T        FCVi-17T        0.0001  100     150     0       Open    ;
12      FCVj-CT         CT              0.0001  100     150     0       Open    ;
13      Salt-CT         FCVi-CT         0.0001  100     150     0       Open    ;
14      FCVj-BT         BT1             0.0001  100     150     0       Open    ;
15      Salt-BT1        FCVi-BT         0.0001  100     150     0       Open    ;
MOI-51!         Vj-T23-MOI      T23-MOI         0.1     12.7    150     0       Open    ;

[PUMPS]
;ID             Node1           Node2           Parameters
 PTB            PTBi            PTBj            HEAD PTB        ;

[VALVES]
;ID             Node1           Node2           Diameter        Type    Setting         MinorLoss

 V-T18-S17      Vj-T18-S17      Vi-T18-S17      25.4    PRV     0       0       ;
```

```
V1-S17          V1j-S17         V1i-S17         25.4    PRV     0       0       ;
V-ML2           Vj-ML2          Vi-ML2          38.1    PRV     0       0       ;
V-T19-S17       Vi-T19          Vj-T19          38.1    PRV     0       0       ;
V-T17-S17       Vi-T17-S17      Vj-T17-S17      12.7    PRV     0       0       ;
V-T16-S17       Vi-T16-S17      Vj-T16-S17      19.05   PRV     0       0       ;
V-T21-S17       Vi-T21-S17      Vj-T21-S17      12.7    PRV     0       0       ;
V-T15-S17       Vi-T15-S17      Vj-T15-S17      25.4    PRV     0       0       ;
V-T14-S17       Vi-T14-S17      Vj-T14-S17      19.05   PRV     0       0       ;
V-T13-S17       Vi-T13-S17      Vj-T13-S17      25.4    PRV     0       0       ;
V-T12-S17       Vi-T12-S17      Vj-T12-S17      12.7    PRV     0       0       ;
V-TNEW-S17      Vi-TNEW-S17     Vj-TNEW         12.7    PRV     0       0       ;
V-T11-S17       Vi-T11-S17      Vj-T11-S17      12.7    PRV     0       0       ;
V-T10-S17       Vi-T10-S17      Vj-T10-S17      12.7    PRV     0       0       ;
V-S17beforeT10  Vi-S17beforeT10 Vj-S17beforeT10 50.8    PRV     0       0       ;
V-T7/8-S17      Vi-T7/8-S17     Vj-T7/8-S17     19.05   PRV     0       0       ;
V-T9-S17        Vi-T9-S17       Vj-T9-S17       12.7    PRV     0       0       ;
V-T6-S17        Vi-T6-S17       Vj-T6-S17       19.05   PRV     0       0       ;
V-T5-S17        Vi-T5-S17       Vj-T5-S17       19.05   PRV     0       0       ;
V-T4-S17        Vi-T4-S17       Vj-T4-S17       25.4    PRV     0       0       ;
V-T3-S17        Vi-T3-S17       Vj-T3-S17       12.7    PRV     0       0       ;
V-T2-S17        Vi-T2-S17       Vj-T2-S17       19.05   PRV     0       0       ;
V-PTB           Vi-PTB          PTBi            50.8    PRV     0       0       ;
V-TBR           Vj-TBR          Vi-TBR          50.8    PSV     0       0       ;
V1-BT           V1j-BT          V1i-BT          25.4    PRV     0       0       ;
V-T3-BT         Vi-T3-BT        Vj-T3-BT        19.05   PRV     0       0       ;
V2-BT           V2i-BT          V2j-BT          25.4    PRV     0       0       ;
V-T1-BT         Vi-T1-BT        Vj-T1-BT        25.4    PRV     0       0       ;
V-branchT4-BT   Vj-branchT4-BT  Vi-branchT4-BT  38.1    PRV     0       0       ;
V-branchT10-BT  Vi-branchT10-BT Vj-branchT10-BT 38.1    PRV     0       0
        ;
V-branchT5-BT   Vi-branchT5-BT  Vj-branchT5-BT  19.05   PRV     0       0       ;
V-T13-BT        Vi-T13-BT       Vj-T13-BT       12.7    PRV     0       0       ;
V-T5-BT         Vi-T5-BT        Vj-T5-BT        12.7    PRV     0       0       ;
V-T6-BT         Vi-T6-BT        Vj-T6-BT        19.05   PRV     0       0       ;
V-T7-BT         Vi-T7-BT        Vj-T7-BT        19.05   PRV     0       0       ;
V-T9/10-BT      Vi-T9/10-BT     Vj-T9/10-BT     19.05   PRV     0       0       ;
V-T8-BT         Vi-T8-BT        Vj-T8-BT        19.05   PRV     0       0       ;
V-T9-BT         Vi-T9-BT        Vj-T9-BT        19.05   PRV     0       0       ;
V-T10-BT        Vi-T10-BT       Vj-T10-BT       19.05   PRV     0       0       ;
V-T3-MOI        Vi-T3-MOI       Vj-T3-MOI       12.7    PRV     0       0       ;
V-toT7-MOI      Vi-toT7-MOI     Vj-toT7-MOI     19.05   PRV     0       0       ;
V-T7-MOI        Vi-T7-MOI       Vj-T7-MOI       19.05   PRV     0       0       ;
V-JT7-MOI       Vi-JT7-MOI      Vj-JT7-MOI      19.05   PRV     0       0       ;
V-brancT29-MOI  Vi-brancT29-MOI Vj-brancT29-MOI 76.2    PRV     0       0
        ;
V-T26-MOI       Vi-T26-MOI      Vj-T26-MOI      25.4    PRV     0       0       ;
V-JT9-MOI       Vi-JT9-MOI      Vj-JT9-MOI      38.1    PRV     0       0       ;
V-T150-MOI      Vi-T150-MOI     Vj-T150-MOI     12.7    PRV     0       0       ;
V-T24-MOI       Vi-T24-MOI      Vj-T24-MOI      12.7    PRV     0       0       ;
V-T25-MOI       Vi-T25-MOI      Vj-T25-MOI      19.05   PRV     0       0       ;
V-T20-MOI       Vi-T20-MOI      Vj-T20-MOI      12.7    PRV     0       0       ;
V-T21-MOI       Vi-T21-MOI      Vj-T21-MOI      19.05   PRV     0       0       ;
V-T15-MOI       Vi-T15-MOI      Vj-T15-MOI      12.7    PRV     0       0       ;
V-T16-MOI       Vi-T16-MOI      Vj-T16-MOI      12.7    PRV     0       0       ;
V-T17-MOI       Vi-T17-MOI      Vj-T17-MOI      19.05   PRV     0       0       ;
V-T18-MOI       Vi-T18-MOI      Vj-T18-MOI      12.7    PRV     0       0       ;
V-T13-MOI       Vi-T13-MOI      Vj-T13-MOI      12.7    PRV     0       0       ;
```

```
V-brancT12-MOI Vi-brancT12-MOI Vj-brancT12-MOI 76.2 PRV 0 0
;
V-T14-MOI Vi-T14-MOI Vj-T14-MOI 19.05 PRV 0 0 ;
V-T8-MOI Vi-T8-MOI Vj-T8-MOI 12.7 PRV 0 0 ;
V-T9-MOI Vi-T9-MOI Vj-T9-MOI 19.05 PRV 0 0 ;
V-T11-MOI Vi-T11-MOI Vj-T11-MOI 19.05 PRV 0 0 ;
V-T12-MOI Vi-T12-MOI Vj-T12-MOI 19.05 PRV 0 0 ;
V-bracT3-CH Vi-brancT3-CH Vj-brancT3-CH 25.4 PRV 0 0 ;
V-T2-CH Vj-T2-CH Vi-T2-CH 12.7 PRV 0 0 ;
V-T1-CH Vi-T1-CH Vj-T1-CH 12.7 PRV 0 0 ;
V-T3-CH Vi-T3-CH Vj-T3-CH 19.05 PRV 0 0 ;
V-JT3-CH Vi-JT3-CH Vj-JT3-CH 38.1 PRV 0 0 ;
V-T4-CH Vi-T4-CH Vj-T4-CH 12.7 PRV 0 0 ;
V-T5-CH Vi-T5-CH Vj-T5-CH 12.7 PRV 0 0 ;
V-brancT10-CH Vi-brancT10-CH Vj-brancT10-CH 38.1 PRV 0 0 ;
V-toT18-S17 Vi-toT18-S17 Vj-toT18-S17 38.1 PRV 0 0 ;
V5-CH V5i-CH V5j-CH 38.1 PRV 0 0 ;
V-T7-CH Vi-T7-CH Vj-T7-CH 19.05 PRV 0 0 ;
V-T6-CH Vi-T6-CH Vj-T6-CH 12.7 PRV 0 0 ;
V-T11-CH Vi-T11-CH Vj-T11-CH 19.05 PRV 0 0 ;
V-T10-CH Vi-T10-CH Vj-T10-CH 19.05 PRV 0 0 ;
V-T6-AT Vi-T6-AT Vj-T6-AT 19.05 PRV 0 0 ;
V-T5-AT Vi-T5-AT Vj-T5-AT 19.05 PRV 0 0 ;
V-JT1-AT Vi-JT1-AT Vj-JT1-AT 25.4 PRV 0 0 ;
V-S14RING Vi-S14RING Vj-S14RING 38.1 PRV 0 0 ;
V-JT5-AT Vj-JT5-AT Vi-JT5-AT 25.4 PRV 0 0 ;
V-T13-AT Vi-T13-AT Vj-T13-AT 19.05 PRV 0 0 ;
V-T9-AT Vi-T9-AT Vj-T9-AT 12.7 PRV 0 0 ;
V-T10-AT Vi-suggesT10-AT Vj-suggesT10-AT 38.1 PRV 0 0 ;
V-T1-AT Vi-T1-AT Vj-T1-AT 19.05 PRV 0 0 ;
V-T7-AT Vi-T7-AT Vj-T7-AT 19.05 PRV 0 0 ;
V-T8-AT Vi-T8-AT Vj-T8-AT 19.05 PRV 0 0 ;
V-T2B-AT Vi-T2B-AT Vj-T2B-AT 19.05 PRV 0 0 ;
V-T11-AT Vi-T11-AT Vj-T11-AT 19.05 PRV 0 0 ;
V-T3-AT Vi-T3-AT Vj-T3-AT 19.05 PRV 0 0 ;
V-T2-S67 Vi-T2-S67 Vj-T2-S67 19.05 PRV 0 0 ;
V-S67RING Vi-S67RING Vj-S67RING 38.1 PRV 0 0 ;
V1-S67 V1i-S67 V1j-S67 25.4 PRV 0 0 ;
V-T1-S67 Vi-T1-S67 Vj-T1-S67 19.05 PRV 0 0 ;
V-toS67RING Vi-toS67RING Vj-toS67RING 50.8 PRV 0 0 ;
V-pourS67RING Vi-pourS67RING Vj-pourS67RING 38.1 PSV 0 0
;
V7-CH V7i-CH V7j-CH 38.1 PRV 0 0 ;
V-18-5 Vi-18-5 Vj-18-5 12.7 PRV 0 0 ;
V-T5-S67 Vi-T5-S67 Vj-T5-S67 12.7 PRV 0 0 ;
V-T7-S67 Vi-T7-S67 Vj-T7-S67 12.7 PRV 0 0 ;
V-TNEW-S67 Vi-TNEW-S67 Vj-TNEW-S67 12.7 PRV 0 0 ;
V-T4-S67 Vi-T4-S67 Vj-T4-S67 12.7 PRV 0 0 ;
V2-S67 V2j-S67 V2i-S67 25.4 PRV 0 0 ;
V-ML1-S67 Vi-ML1-S67 Vj-ML1-S67 25.4 PRV 0 0 ;
V-brancT5-S67 Vi-brancT5-S67 Vj-brancT5-S67 25.4 PRV 0 0 ;
V-toTIMhouse Vi-toTIMhouse Vj-toTIMhouse 25.4 PRV 0 0 ;
V-toML1 Vi-toML1 Vj-toML1 25.4 PRV 0 0 ;
V3-S67 V3i-S67 V3j-S67 12.7 PRV 0 0 ;
V4-S67 V4i-S67 V4j-S67 25.4 PRV 0 0 ;
V-brancT8-CT Vi-brancT8-CT Vj-brancT8-CT 76.2 PRV 0 0 ;
V-T1-CT Vi-T1-CT Vj-T1-CT 12.7 PRV 0 0 ;
```

```
V-T3-CT         Vi-T3-CT        Vj-T3-CT        19.05   PRV     0       0       ;
V2-CT           V2i-CT          V2j-CT          19.05   PRV     0       0       ;
V3-CT           V3i-CT          V3j-CT          25.4    PRV     0       0       ;
V4-CT           V4i-CT          V4j-CT          19.05   PRV     0       0       ;
V-T4-CT         Vi-T4-CT        Vj-T4-CT        19.05   PRV     0       0       ;
V-T5-CT         Vi-T5-CT        Vj-T5-CT        12.7    PRV     0       0       ;
V5-CT           V5i-CT          V5j-CT          38.1    PRV     0       0       ;
V-T6-CT         Vi-T6-CT        Vj-T6-CT        12.7    PRV     0       0       ;
V-T7-CT         Vi-T7-CT        Vj-T7-CT        19.05   PRV     0       0       ;
V-T8-CT         Vi-T8-CT        Vj-T8-CT        19.05   PRV     0       0       ;
V-JT1-S8        Vi-JT1-S8       Vj-JT1-S8       12.7    PRV     0       0       ;
V-T3-S8         Vi-T3-S8        Vj-T3-S8        12.7    PRV     0       0       ;
V-T2-S8         Vi-T2-S8        Vj-T2-S8        19.05   PRV     0       0       ;
V-JT4-S8        Vi-JT4-S8       Vj-JT4-S8       25.4    PRV     0       0       ;
V-T1-S8         Vi-T1-S8        Vj-T1-S8        19.05   PRV     0       0       ;
V-JT5-S8        Vi-JT5-S8       Vj-JT5-S8       38.1    PRV     0       0       ;
V-T4-S8         Vi-T4-S8        Vj-T4-S8        19.05   PRV     0       0       ;
V-toS8RING      Vi-toS8RING     Vj-toS8RING     76.2    PRV     0       0       ;
V6-S8           V6i-S8          V6j-S8          38.1    PRV     0       0       ;
V-T5-S8         Vi-T5-S8        Vj-T5-S8        19.05   PRV     0       0       ;
V-T6-S8         Vi-T6-S8        Vj-T6-S8        12.7    PRV     0       0       ;
V-JT6-S8        Vi-JT6-S8       Vj-JT6-S8       19.05   PRV     0       0       ;
V-CHT2          Vi-CHT2         Vj-CHT2         76.2    PRV     0       0       ;
V-CHT1          Vi-CHT1         Vj-CHT1         76.2    PRV     0       0       ;
V-CHTout        Vi-CHTout       Vj-CHTout       76.2    PRV     0       0       ;
V-BT2           Vi-BT2          Vj-BT2          76.2    PRV     0       0       ;
V-BT1           Vi-BT1          Vj-BT1          76.2    PRV     0       0       ;
V-Btout         Vi-BTout        Vj-BTout        76.2    PRV     0       0       ;
V-17Tout        Vi-17Tout       Vj-17Tout       76.2    PRV     0       0       ;
V-TBRINGSout    Vi-TBRINGSout   Vj-TBRINGSout   25.4    PRV     0       0
        ;
V-MOITout       Vi-MOITout      Vj-MOITout      76.2    PRV     0       0       ;
V-CTout         Vi-CTout        Vj-CTout        76.2    PRV     0       0       ;
V-AT-OLDout     Vi-AT-OLDout    Vj-AT-OLDout    38.1    PRV     0       0
        ;
PSV-MAELA2      PSVi-MAELA2     PSVj-MAELA2     30.5    PSV     0       0
        ;
PSV-ML1         PSVi-ML1        PSVj-ML1        25.4    PRV     0       0       ;
PSV-TEMRIN2     PSVi-TEMRIN2    PSVj-TEMRIN2    12.7    PSV     0       0
        ;
PSV-TEMRIN3     PSVi-TEMRIN3    PSVj-TEMRIN3    12.7    PSV     0       0
        ;
PSV-TEMRIN1     PSVi-TEMRIN1    PSVj-TEMRIN1    12.7    PSV     0       0
        ;
PSV-S8RIN       PSVi-S8RIN      PSVj-S8RIN      50.8    PSV     0       0       ;
FCV-CHT1        FCVi-CHT1       FCVj-CHT1       100     FCV     0.1     0       ;
FCV-AT-OLD      FCVi-AT-OLD     FCVj-AT-OLD     100     FCV     0.1     0
        ;
FCV-MOIT        FCVi-MOIT       FCVj-MOIT       100     FCV     0.1     0       ;
FCV-17T         FCVi-17T        FCVj-17T        100     FCV     0.1     0       ;
FCV-CT          FCVi-CT         FCVj-CT         100     FCV     0.1     0       ;
FCV-BT          FCVi-BT         FCVj-BT         100     FCV     0.1     0       ;
V-T23-MOI       Vi-T23-MOI      Vj-T23-MOI      12.7    PRV     0       0       ;

[TAGS]
 NODE T18-S17           3tapsSANWAlargeuse
```

[DEMANDS]
;Junction Demand Pattern Category

[STATUS]
;ID Status/Setting
V-T18-S17 Open
V1-S17 Open
V-ML2 Closed
V-T19-S17 Open
V-T17-S17 Open
V-T16-S17 Open
V-T21-S17 Open
V-T15-S17 Open
V-T14-S17 Open
V-T13-S17 Open
V-T12-S17 Open
V-TNEW-S17 Open
V-T11-S17 Open
V-T10-S17 Open
V-S17beforeT10 Open
V-T7/8-S17 Open
V-T9-S17 Open
V-T6-S17 Open
V-T5-S17 Open
V-T4-S17 Open
V-T3-S17 Open
V-T2-S17 Open
V-PTB Closed
V-TBR Open
V1-BT Open
V-T3-BT Open
V2-BT Open
V-T1-BT Open
V-branchT4-BT Open
V-branchT10-BT Open
V-branchT5-BT Open
V-T13-BT Open
V-T5-BT Open
V-T6-BT Open
V-T7-BT Open
V-T9/10-BT Open
V-T8-BT Open
V-T9-BT Open
V-T10-BT Open
V-T3-MOI Open
V-toT7-MOI Open
V-T7-MOI Open
V-JT7-MOI Open
V-brancT29-MOI Open
V-T26-MOI Open
V-JT9-MOI Open
V-T150-MOI Open
V-T24-MOI Open
V-T25-MOI Open
V-T20-MOI Open
V-T21-MOI Open
V-T15-MOI Open

V-T16-MOI	Open
V-T17-MOI	Open
V-T18-MOI	Open
V-T13-MOI	Open
V-brancT12-MOI	Open
V-T14-MOI	Open
V-T8-MOI	Open
V-T9-MOI	Open
V-T11-MOI	Open
V-T12-MOI	Open
V-bracT3-CH	Open
V-T2-CH	Open
V-T1-CH	Open
V-T3-CH	Open
V-JT3-CH	Open
V-T4-CH	Open
V-T5-CH	Open
V-brancT10-CH	Open
V-toT18-S17	Open
V5-CH	Open
V-T7-CH	Open
V-T6-CH	Open
V-T11-CH	Open
V-T10-CH	Open
V-T6-AT	Open
V-T5-AT	Open
V-JT1-AT	Open
V-S14RING	Closed
V-JT5-AT	Open
V-T13-AT	Open
V-T9-AT	Open
V-T10-AT	Closed
V-T1-AT	Open
V-T7-AT	Open
V-T8-AT	Open
V-T2B-AT	Open
V-T11-AT	Open
V-T3-AT	Open
V-T2-S67	Open
V-S67RING	Closed
V1-S67	Open
V-T1-S67	Open
V-toS67RING	Open
V-pourS67RING	Closed
V7-CH	Closed
V-18-5	Closed
V-T5-S67	Open
V-T7-S67	Open
V-TNEW-S67	Open
V-T4-S67	Open
V2-S67	Open
V-ML1-S67	Open
V-brancT5-S67	Open
V-toTIMhouse	Open
V-toML1	Open
V3-S67	Open
V4-S67	Open

```
V-brancT8-CT    Open
V-T1-CT         Open
V-T3-CT         Open
V2-CT           Open
V3-CT           Open
V4-CT           Open
V-T4-CT         Open
V-T5-CT         Open
V5-CT           Open
V-T6-CT         Open
V-T7-CT         Open
V-T8-CT         Open
V-JT1-S8        Open
V-T3-S8         Open
V-T2-S8         Open
V-JT4-S8        Open
V-T1-S8         Open
V-JT5-S8        Closed
V-T4-S8         Open
V-toS8RING      Closed
V6-S8           Open
V-T5-S8         Open
V-T6-S8         Open
V-JT6-S8        Open
V-CHT2          Closed
V-CHT1          Closed
V-CHTout        Open
V-BT2           Closed
V-BT1           Closed
V-Btout         Open
V-17Tout        Closed
V-TBRINGSout            Closed
V-MOITout       Closed
V-CTout         Closed
V-AT-OLDout             Closed
V-T23-MOI       Open

[PATTERNS]
;ID             Multipliers
;
1       0       0       0       0       0       0
1       1       1       1       0       0       0
1       0       0       0       1       1       1
1       0       0       0       0       0       0
;
 17T            0       0       0       0       0       0
 17T            0       0       0       0       0       0
 17T            0       0       0       0       0       0
 17T            0       0       0       0       0       0
 17T            0       0       0       0       0       0
 17T            0       0       0       0       0       0
 17T            0       0       0       0       0       0
 17T            0       0       0       0       0       0
 17T            0       0       0       0       0       0
 17T            0       0       0       0       0       0
 17T            0       0       0       0       0       0
 17T            0       0       0       0       0       0
```

```
 17T             0       0       0       0       1       1
 17T             1       1       0       0       0       0
 17T             0       0       0       0       0       0
 17T             0       0       0       0       0       0
 17T             0       0       0       0       0       0
 17T             0       0       0       0       0       0
;
 MOIT            0       0       0       0       0       0
 MOIT            0       0       0       0       0       0
 MOIT            0       0       0       0       0       0
 MOIT            0       0       0       0       0       0
 MOIT            0       0       0       0       0       0
 MOIT            0       0       0       0       0       0
 MOIT            0       0       0       0       0       0
 MOIT            0       0       0       0       0       0
 MOIT            0       0       0       0       0       0
 MOIT            0       0       0       0       0       0
 MOIT            0       0       0       0       0       0
 MOIT            0       0       0       0       0       0
 MOIT            0       0       0       0       1       1
 MOIT            1       1       1       1       1       1
 MOIT            0       0       0       0       0       0
 MOIT            0       0       0       0       0       0
 MOIT            0       0       0       0       0       0
 MOIT            0       0       0       0       0       0
 MOIT            0
;
 AT              0       0       0       0       0       0
 AT              0       0       0       0       0       0
 AT              0       0       0       0       0       0
 AT              0       0       0       0       0       0
 AT              0       0       0       0       0       0
 AT              0       0       0       0       0       0
 AT              0       0       0       0       0       0
 AT              0       0       0       0       0       0
 AT              0       0       0       0       0       0
 AT              0       0       0       0       0       0
 AT              0       0       0       0       0       0
 AT              0       0       0       0       0       0
 AT              0       0       0       0       0       0
 AT              0       0       0       0       1       1
 AT              1       0       0       0       0       0
 AT              0       0       0       0       0       0
 AT              0       0       0       0       0       0
 AT              0       0       0       0       0       0
 AT              0       0       0       0       0       0
 AT              0
;
 CHT             0       0       0       0       0       0
 CHT             0       0       0       0       0       0
 CHT             0       0       0       0       0       0
 CHT             0       0       0       0       0       0
 CHT             0       0       0       0       0       0
 CHT             0       0       0       0       0       0
 CHT             0       0       0       0       0       0
 CHT             0       0       0       0       0       0
 CHT             0       0       0       0       0       0
 CHT             0       0       0       0       0       0
```

```
 CHT             0       0       0       0       0       0
 CHT             0       0       0       0       0       0
 CHT             0       0       0       0       1       1
 CHT             0       0       0       0       0       0
 CHT             0       0       0       0       0       0
 CHT             0       0       0       0       0       0
 CHT             0       0       0       0       0       0
 CHT             0       0       0       0       0       0
;
 CT              0       0       0       0       0       0
 CT              0       0       0       0       0       0
 CT              0       0       0       0       0       0
 CT              0       0       0       0       0       0
 CT              0       0       0       0       0       0
 CT              0       0       0       0       0       0
 CT              0       0       0       0       0       0
 CT              0       0       0       0       0       0
 CT              0       0       0       0       0       0
 CT              0       0       0       0       0       0
 CT              0       0       0       0       0       0
 CT              0       0       0       0       0       0
 CT              0       0       0       0       0       0
 CT              0       0       0       0       1       1
 CT              1       1       1       1       0       0
 CT              0       0       0       0       0       0
 CT              0       0       0       0       0       0
 CT              0       0       0       0       0       0
 CT              0       0       0       0       0       0
 CT              0
;
 BT              0       0       0       0       0       0
 BT              0       0       0       0       0       0
 BT              0       0       0       0       0       0
 BT              0       0       0       0       0       0
 BT              0       0       0       0       0       0
 BT              0       0       0       0       0       0
 BT              0       0       0       0       0       0
 BT              0       0       0       0       0       0
 BT              0       0       0       0       0       0
 BT              0       0       0       0       0       0
 BT              0       0       0       0       0       0
 BT              0       0       0       0       0       0
 BT              0       0       0       0       0       0
 BT              0       0       0       0       1       1
 BT              1       0       0       0       0       0
 BT              0       0       0       0       0       0
 BT              0       0       0       0       0       0
 BT              0       0       0       0       0       0
 BT              0       0       0       0       0       0

[CURVES]
;ID             X-Value         Y-Value
;PUMP:          made up
 PTB             20      10

[CONTROLS]
LINK V-17Tout OPEN AT CLOCKTIME 5:59 AM
LINK V-17Tout CLOSED AT CLOCKTIME 9:01 AM
```

LINK V-17Tout OPEN AT CLOCKTIME 2:59 PM
LINK V-17Tout CLOSED AT CLOCKTIME 6:01 PM
LINK V-TBRINGSout OPEN AT CLOCKTIME 5:59 AM
LINK V-TBRINGSout CLOSED AT CLOCKTIME 9:01 AM
LINK V-TBRINGSout OPEN AT CLOCKTIME 2:59 PM
LINK V-TBRINGSout CLOSED AT CLOCKTIME 6:01 PM
LINK V-MOITout OPEN AT CLOCKTIME 5:59 AM
LINK V-MOITout CLOSED AT CLOCKTIME 9:01 AM
LINK V-MOITout OPEN AT CLOCKTIME 2:59 PM
LINK V-MOITout CLOSED AT CLOCKTIME 6:01 PM
LINK V-ML2 OPEN AT CLOCKTIME 5:59 AM
LINK V-ML2 CLOSED AT CLOCKTIME 9:01 AM
LINK V-ML2 OPEN AT CLOCKTIME 2:59 PM
LINK V-ML2 CLOSED AT CLOCKTIME 6:01 PM
LINK V-CTout OPEN AT CLOCKTIME 5:59 AM
LINK V-CTout CLOSED AT CLOCKTIME 9:01 AM
LINK V-CTout OPEN AT CLOCKTIME 2:59 PM
LINK V-CTout CLOSED AT CLOCKTIME 6:01 PM
LINK V-JT5-S8 OPEN AT CLOCKTIME 5:59 AM
LINK V-JT5-S8 CLOSED AT CLOCKTIME 9:01 AM
LINK V-JT5-S8 OPEN AT CLOCKTIME 2:59 PM
LINK V-JT5-S8 CLOSED AT CLOCKTIME 6:01 PM
LINK V-S67RING OPEN AT CLOCKTIME 5:59 AM
LINK V-S67RING CLOSED AT CLOCKTIME 9:01 AM
LINK V-S67RING OPEN AT CLOCKTIME 2:59 PM
LINK V-S67RING CLOSED AT CLOCKTIME 6:01 PM
LINK V-BT1 OPEN AT CLOCKTIME 5:59 AM
LINK V-BT1 CLOSED AT CLOCKTIME 9:01 AM
LINK V-BT2 OPEN AT CLOCKTIME 2:59 PM
LINK V-BT2 CLOSED AT CLOCKTIME 6:01 PM
LINK V-AT-OLDout OPEN AT CLOCKTIME 5:59 AM
LINK V-AT-OLDout CLOSED AT CLOCKTIME 9:01 AM
LINK V-AT-OLDout OPEN AT CLOCKTIME 2:59 PM
LINK V-AT-OLDout CLOSED AT CLOCKTIME 6:01 PM
LINK V-CHT1 OPEN AT CLOCKTIME 5:59 AM
LINK V-CHT1 CLOSED AT CLOCKTIME 9:01 AM
LINK V-CHT2 OPEN AT CLOCKTIME 2:59 PM
LINK V-CHT2 CLOSED AT CLOCKTIME 6:01 PM
LINK V-S14RING OPEN AT CLOCKTIME 5:59 AM
LINK V-S14RING CLOSED AT CLOCKTIME 9:01 AM
LINK V-S14RING OPEN AT CLOCKTIME 2:59 PM
LINK V-S14RING CLOSED AT CLOCKTIME 6:01 PM
LINK V-T25-MOI CLOSED AT CLOCKTIME 3:00 PM
LINK V-T25-MOI OPEN AT CLOCKTIME 3:02 PM
LINK MOI-59 CLOSED AT CLOCKTIME 3:02 PM
LINK MOI-59 OPEN AT CLOCKTIME 3:04 PM
LINK V-T24-MOI CLOSED AT CLOCKTIME 3:04 PM
LINK V-T24-MOI OPEN AT CLOCKTIME 3:06 PM
LINK V-T23-MOI CLOSED AT CLOCKTIME 3:06 PM
LINK V-T23-MOI OPEN AT CLOCKTIME 3:08 PM
LINK V-T16-S17 CLOSED AT CLOCKTIME 3:00 PM
LINK V-T16-S17 OPEN AT CLOCKTIME 3:02 PM
LINK BT-1 CLOSED AT CLOCKTIME 3:00 PM
LINK BT-1 OPEN AT CLOCKTIME 3:02 PM
LINK V-T5-AT CLOSED AT CLOCKTIME 3:00 PM
LINK V-T5-AT OPEN AT CLOCKTIME 3:02 PM
LINK V-T6-CH CLOSED AT CLOCKTIME 3:00 PM

LINK V-T6-CH OPEN AT CLOCKTIME 3:02 PM
LINK V-T7-CH CLOSED AT CLOCKTIME 3:02 PM
LINK V-T7-CH OPEN AT CLOCKTIME 3:04 PM
LINK V-T10-CH CLOSED AT CLOCKTIME 3:04 PM
LINK V-T10-CH OPEN AT CLOCKTIME 3:06 PM
LINK S17-32 CLOSED AT CLOCKTIME 3:02 PM
LINK S17-32 OPEN AT CLOCKTIME 3:04 PM
LINK V-T10-BT CLOSED AT CLOCKTIME 3:02 PM
LINK V-T10-BT OPEN AT CLOCKTIME 3:04 PM
LINK V-T3-BT CLOSED AT CLOCKTIME 3:04 PM
LINK V-T3-BT OPEN AT CLOCKTIME 3:06 PM
LINK V-T12-MOI CLOSED AT CLOCKTIME 3:08 PM
LINK V-T12-MOI OPEN AT CLOCKTIME 3:10 PM
LINK V-T11-MOI CLOSED AT CLOCKTIME 3:10 PM
LINK V-T11-MOI OPEN AT CLOCKTIME 3:12 PM

[RULES]

[ENERGY]

Global Efficiency	75
Global Price	0
Demand Charge	0

[EMITTERS]

;Junction	Coefficient
T15-S17	0
T14-S17	8.948
T13-S17	26.844
T12-S17	8.948
TNEW-S17	8.948
T11-S17	0
T10-S17	17.896
T8-S17	0
T7A-S17	0
T7B-S17	0
T9-S17	0
T6-S17	8.948

T5-S17	17.896
T4-S17	8.948
T3-S17	0
T2-S17	8.948
T1A-S17	0
T1B-S17	0
TB1-S17	8.948
TB2-S17	8.948
TB9-S17	0
TB4-S17	8.948
TB5-S17	8.948
TB6-S17	0
TB7-S17	0
TB3-S17	8.948
TB10-S17	0
TB8-S17	8.948
T18-S17	26.844
T4-BT	17.896
T3-BT	17.896
T2-BT	17.896
T13-BT	8.948
T1-BT	26.844
T12-BT	8.948
T5-BT	8.948
T6-BT	17.896
T11-BT	8.948
T7-BT	17.896
T8-BT	17.896
T9-BT	8.948
T10-BT	26.844
T5A-MOI	0
T5B-MOI	0
T4-MOI	0
T3-MOI	17.896
T2-MOI	0
T1-MOI	8.948
T27-MOI	8.948
T6-MOI	0
T7-MOI	17.896
T30-MOI	0
T31A-MOI	0
T31B-MOI	0
T32A-MOI	0
T32B-MOI	0
T2-CH	0
T1-CH	8.948
T3-CH	8.948
T4-CH	8.948
T5-CH	8.948
T6-CH	26.844
T7-CH	26.844
T8-CH	0
T11-CH	8.948
T9-CH	0
T10-CH	26.844
T19-MOI	17.896
T153-MOI	0

T151-MOI	0	
T150-MOI	8.948	
T23-MOI	17.896	
T24-MOI	17.896	
T25-MOI	26.844	
T29-MOI	8.948	
T26-MOI	17.896	
T20-MOI	8.948	
T21-MOI	8.948	
T15-MOI	17.896	
T16-MOI	17.896	
T17-MOI	17.896	
T18-MOI	26.844	
T13-MOI	26.844	
T14-MOI	17.896	
T8-MOI	17.896	
T9-MOI	17.896	
T10-MOI	8.948	
T11-MOI	26.844	
TNEW-MOI		8.948
T12-MOI	26.844	
T28-MOII	17.896	
T3-S67	26.844	
T6-S67	8.948	
T2-S67	17.896	
T1-S67	17.896	
T5-S67	17.896	
T7-S67	8.948	
TNEW-S67	0	
T4-S67	8.948	
T8-S67	0	
TEMT1	0	
TEMT2	17.896	
TEMT3	0	
T1-CT	8.948	
T3-CT	17.896	
T9-CT	17.896	
T4-CT	17.896	
T5-CT	17.896	
T6-CT	17.896	
T7-CT	17.896	
T8-CT	26.844	
T8-S8	8.948	
T3-S8	17.896	
TNEW-S8	0	
T2-S8	17.896	
T1-S8	26.844	
T4-S8	17.896	
T5-S8	8.948	
T6-S8	17.896	
T7-S8	26.844	
T6-AT	17.896	
T5-AT	17.896	
T10-AT	17.896	
T2-AT	17.896	
T4-AT	17.896	
T13-AT	8.948	

T9-AT	17.896
T1-AT	8.948
T2B-AT	17.896
T11-AT	8.948
T3-AT	17.896
T7-AT	17.896
T12-AT	8.948
T8-AT	17.896
T16-S17	17.896
T17-S17	0
T19A-S17	0
T19B-S17	0
T20-S17	0
T21-S17	0

[QUALITY]

;Node	InitQual
J-S17	448.9
T15-S17	448.9
JT-S17	448.9
JT2-S17	448.9
J3-S17	448.9
T14-S17	448.9
JT3-S17	448.9
J4-S17	448.9
T13-S17	448.9
T12-S17	448.9
JT4-S17	448.9
JT5-S17	448.9
J5-S17	448.9
TNEW-S17	448.9
JT6-S17	448.9
T11-S17	448.9
T10-S17	448.9
JT7-S17	448.9
J6-S17	448.9
T8-S17	448.9
JT8-S17	448.9
T7A-S17	448.9
T7B-S17	448.9
JT9-S17	448.9
T9-S17	448.9
T6-S17	448.9
JT11-S17	448.9
JT10-S17	448.9
J7-S17	448.9
T5-S17	448.9
JT12-S17	448.9
T4-S17	448.9
J8-S17	448.9
JT13-S17	448.9
T3-S17	448.9
T2-S17	448.9
JT14-S17	448.9
JB-S17	448.9
JT15-S17	448.9
T1A-S17	448.9

T1B-S17	448.9	
J9-S17	448.9	
PTBi	448.9	
JT16-S17	448.9	
TB1-S17	448.9	
TB2-S17	448.9	
TB9-S17	448.9	
TB4-S17	448.9	
TB5-S17	448.9	
JT17-S17	448.9	
JT18-S17	448.9	
TB6-S17	448.9	
TB7-S17	448.9	
TB3-S17	448.9	
TB10-S17	448.9	
TB8-S17	448.9	
J10-S17	448.9	
T18-S17	448.9	
T4-BT	160.8	
J01-BT	160.8	
V1i-BT	160.8	
JT1-BT	160.8	
T3-BT	160.8	
J2-BT	160.8	
J3-BT	160.8	
JT2-BT	160.8	
V2i-BT	160.8	
T2-BT	160.8	
JB2-BT	160.8	
T13-BT	160.8	
JT3-BT	160.8	
J4-BT	160.8	
JT4-BT	160.8	
T1-BT	160.8	
JT5-BT	160.8	
T12-BT	160.8	
Vi-branchT4-BT		160.8
J5-BT	160.8	
Vi-branchT5-BT		160.8
T5-BT	160.8	
T6-BT	160.8	
Vi-branchT10-BT		160.8
JT6-BT	160.8	
T11-BT	160.8	
J6-BT	160.8	
T7-BT	160.8	
J7-BT	160.8	
JT7-BT	160.8	
T8-BT	160.8	
T9-BT	160.8	
T10-BT	160.8	
T5A-MOI	167.5	
JT1-MOI	167.5	
T5B-MOI	167.5	
J1-MOI	167.5	
T4-MOI	167.5	
JT2-MOI	167.5	

T3-MOI	167.5	
JT3-MOI	167.5	
T2-MOI	167.5	
T1-MOI	167.5	
T27-MOI	167.5	
J2-MOI	167.5	
JT4-MOI	167.5	
T6-MOI	167.5	
JT5-MOI	167.5	
T7-MOI	167.5	
JT6-MOI	167.5	
T30-MOI	167.5	
T31A-MOI	167.5	
T31B-MOI	167.5	
JT7-MOI	167.5	
T32A-MOI	167.5	
T32B-MOI	167.5	
J1-CH	154.1	
JT1-CH	154.1	
J2-CH	154.1	
JT2-CH	154.1	
Vi-T2-CH	154.1	
T2-CH	154.1	
Vi-T3-CH	154.1	
T1-CH	154.1	
T3-CH	154.1	
JT3-CH	154.1	
T4-CH	154.1	
T5-CH	154.1	
V5i-CH	154.1	
Vi-brancT10-CH		154.1
T6-CH	154.1	
JT4-CH	154.1	
T7-CH	154.1	
JT5-CH	154.1	
JT6-CH	154.1	
JT7-CH	154.1	
T8-CH	154.1	
T11-CH	154.1	
J3-CH	154.1	
Vi-T11-CH	154.1	
JT8-CH	154.1	
T9-CH	154.1	
J4-CH	154.1	
T10-CH	154.1	
V7i-CH	154.1	
J3-MOI	167.5	
T19-MOI	167.5	
J4-MOI	167.5	
T153-MOI	167.5	
JT9-MOI	167.5	
T151-MOI	167.5	
T150-MOI	167.5	
T23-MOI	167.5	
JT10-MOI	167.5	
T24-MOI	167.5	
V1-MOI	167.5	

J6-MOI	167.5	
J5-MOI	167.5	
JT12-MOI	167.5	
T25-MOI	167.5	
T29-MOI	167.5	
J7-MOI	167.5	
T26-MOI	167.5	
J8-MOI	167.5	
JT13-MOI	167.5	
T20-MOI	167.5	
J9-MOI	167.5	
T21-MOI	167.5	
J10-MOI	167.5	
JT8CHECK-MOI		167.5
T15-MOI	167.5	
T16-MOI	167.5	
J11-MOI	167.5	
JT14-MOI	167.5	
T17-MOI	167.5	
Vi-T17-MOI	167.5	
JT15-MOI	167.5	
T18-MOI	167.5	
B1-MOI	167.5	
J12-MOI	167.5	
JT16-MOI	167.5	
T13-MOI	167.5	
T14-MOI	167.5	
JT17-MOI	167.5	
T8-MOI	167.5	
J13-MOI	167.5	
JT18-MOI	167.5	
T9-MOI	167.5	
T10-MOI	167.5	
T11-MOI	167.5	
J14-MOI	167.5	
J15-MOI	167.5	
TNEW-MOI		167.5
T12-MOI	167.5	
JT19-MOI	167.5	
T28-MOII	167.5	
T3-S67	237.6	
T6-S67	237.6	
JT1-S67	237.6	
J1-S67	237.6	
J2-S67	237.6	
T2-S67	237.6	
J3-S67	237.6	
T1-S67	237.6	
V1i-S67	237.6	
T5-S67	237.6	
Vi-18-5	237.6	
J4-S67	237.6	
J5-S67	237.6	
T7-S67	237.6	
JT2-S67	237.6	
TNEW-S67	237.6	
T4-S67	237.6	

JT3-S67	237.6	
V2i-S67	237.6	
J6-S67	237.6	
J7-S67	237.6	
JT4-S67	237.6	
T8-S67	237.6	
V3i-S67	237.6	
V4j-S67	237.6	
J8-S67	237.6	
JT1CHECK-CT		160.8
J1-CT	160.8	
V1-CT	160.8	
JT2-CT	160.8	
TEMT1	160.8	
TEMT2	160.8	
TEMT3	160.8	
JT3-CT	160.8	
T1-CT	160.8	
J2-CT	160.8	
JT4-CT	160.8	
V2i-CT	160.8	
T3-CT	160.8	
JT5-CT	160.8	
V3j-CT	160.8	
JT6-CT	160.8	
V4j-CT	160.8	
J3-CT	160.8	
T9-CT	160.8	
T4-CT	160.8	
J4-CT	160.8	
T5-CT	160.8	
V5i-CT	160.8	
J5-CT	160.8	
J6-CT	160.8	
JT7-CT	160.8	
T6-CT	160.8	
J7-CT	160.8	
T7-CT	160.8	
T8-CT	160.8	
T8-S8	234.5	
JT1-S8	234.5	
T3-S8	234.5	
JT2-S8	234.5	
TNEW-S8	234.5	
J1-S8	234.5	
JT3-S8	234.5	
T2-S8	234.5	
JT4-S8	234.5	
T1-S8	234.5	
JT5-S8	234.5	
J2-S8	234.5	
T4-S8	234.5	
V6j-S8	234.5	
T5-S8	234.5	
J3-S8	234.5	
JT6-S8	234.5	
T6-S8	234.5	

T6-AT	201
B1-AT	201
JT1-AT	201
T5-AT	201
J1-AT	201
J2-AT	201
JT2-AT	201
J3-AT	201
T10-AT	201
JT3-AT	201
J4-AT	201
J5-AT	201
B2-AT	201
J6-AT	201
T2-AT	201
JT4-AT	201
JT5-AT	201
T4-AT	201
J7-AT	201
JT6-AT	201
T13-AT	201
J8-AT	201
T9-AT	201
JT7-AT	201
T1-AT	201
J9-AT	201
JT8-AT	201
T2B-AT	201
J10-AT	201
T11-AT	201
T3-AT	201
JT9-AT	201
J11-AT	201
JT10-AT	201
T7-AT	201
J12-AT	201
T12-AT	201
T8-AT	201
J1-S17	448.9
J2-S17	448.9
J4T-S17	448.9
J5!-S17	448.9
J6!-S17	448.9
J7!-S17	448.9
T16-S17	448.9
T17-S17	448.9
T19A-S17	448.9
T19B-S17	448.9
T20-S17	448.9
T21-S17	448.9
V1j-S17	448.9
Vi-T18-S17	448.9
Vj-T18-S17	448.9
V1i-S17	448.9
Vi-ML2	448.9
Vj-ML2	448.9
Vi-T16-S17	448.9

Vi-T21-S17	448.9	
Vi-T17-S17	448.9	
Vi-T19	448.9	
Vj-T19	448.9	
Vj-T17-S17	448.9	
Vj-T16-S17	448.9	
Vj-T21-S17	448.9	
Vi-T15-S17	448.9	
Vj-T15-S17	448.9	
Vj-T14-S17	448.9	
Vi-T14-S17	448.9	
Vi-T13-S17	448.9	
Vj-T13-S17	448.9	
Vi-T12-S17	448.9	
Vj-T12-S17	448.9	
Vi-TNEW-S17		448.9
Vj-TNEW	448.9	
Vi-T11-S17	448.9	
Vj-T11-S17	448.9	
Vj-T10-S17	448.9	
Vi-T10-S17	448.9	
Vj-S17beforeT10	448.9	
Vi-S17beforeT10	448.9	
Vj-T7/8-S17	448.9	
Vi-T7/8-S17	448.9	
JT-T7/8-S17	448.9	
Vi-T9-S17	448.9	
Vj-T9-S17	448.9	
Vj-T6-S17	448.9	
Vi-T6-S17	448.9	
Vj-T5-S17	448.9	
Vi-T5-S17	448.9	
Vi-T4-S17	448.9	
Vj-T4-S17	448.9	
Vi-T3-S17	448.9	
Vj-T3-S17	448.9	
Vi-T2-S17	448.9	
Vj-T2-S17	448.9	
JT-T1/2-S17	448.9	
PTBj	448.9	
Vi-PTB	448.9	
JT-TB2-S17	448.9	
Vj-TBR	448.9	
Vi-TBR	448.9	
JT-TB5-S17	448.9	
JT-TB6/7-S17	448.9	
JT-TB8-S17	448.9	
V1j-BT	160.8	
Vj-T3-BT	160.8	
Vi-T3-BT	160.8	
V2j-BT	160.8	
Vi-T1-BT	160.8	
Vj-T1-BT	160.8	
Vj-branchT4-BT		160.8
JbranchT10-BT	160.8	
Vj-branchT10-BT		160.8
JTbranches-BT	160.8	

JT-branchT5-BT		160.8
Vj-branchT5-BT		160.8
JT-T5-BT	160.8	
Vj-T13-BT	160.8	
Vi-T13-BT	160.8	
Vj-T5-BT	160.8	
Vi-T5-BT	160.8	
Vj-T6-BT	160.8	
Vi-T6-BT	160.8	
JT-T7-BT	160.8	
Vj-T7-BT	160.8	
Vi-T7-BT	160.8	
Vi-T9/10-BT	160.8	
Vj-T9/10-BT	160.8	
Vj-T8-BT	160.8	
Vi-T8-BT	160.8	
Vj-T9-BT	160.8	
Vi-T9-BT	160.8	
JT-T9-BT	160.8	
Vj-T10-BT	160.8	
Vi-T10-BT	160.8	
JT-T4-MOI	167.5	
Vj-T3-MOI	167.5	
Vi-T3-MOI	167.5	
JT-T1-MOI	167.5	
JT-T27-MOI	167.5	
Vj-toT7-MOI	167.5	
Vi-toT7-MOI	167.5	
Vj-T7-MOI	167.5	
Vi-T7-MOI	167.5	
JT-T31B-MOI		167.5
JT-T32-MOI	167.5	
Vj-JT7-MOI	167.5	
Vi-JT7-MOI	167.5	
Vi-brancT29-MOI		167.5
Vj-brancT29-MOI		167.5
JT-T19-MOI	167.5	
JT-T153-MOI	167.5	
JT-T26-MOI	167.5	
JT-T51-MOI	167.5	
Vi-T26-MOI	167.5	
Vj-T26-MOI	167.5	
Vj-JT9-MOI	167.5	
Vi-JT9-MOI	167.5	
Vi-T150-MOI	167.5	
Vj-T150-MOI	167.5	
JT-T23-MOI	167.5	
Vj-T24-MOI	167.5	
Vi-T24-MOI	167.5	
Vj-T25-MOI	167.5	
Vi-T25-MOI	167.5	
Vj-T20-MOI	167.5	
Vi-T20-MOI	167.5	
JT-T20-MOI	167.5	
Vj-T21-MOI	167.5	
Vi-T21-MOI	167.5	
Vj-T15-MOI	167.5	

Vi-T15-MOI	167.5	
JT-T15-MOI	167.5	
Vj-T16-MOI	167.5	
Vi-T16-MOI	167.5	
JT-T16-MOI	167.5	
Vj-T17-MOI	167.5	
Vj-T18-MOI	167.5	
Vi-T18-MOI	167.5	
Vj-T13-MOI	167.5	
Vi-T13-MOI	167.5	
JT-T13-MOI	167.5	
Vi-brancT12-MOI		167.5
Vj-brancT12-MOI		167.5
Vj-T14-MOI	167.5	
Vi-T14-MOI	167.5	
Vj-T8-MOI	167.5	
Vi-T8-MOI	167.5	
Vj-T9-MOI	167.5	
Vi-T9-MOI	167.5	
JT-T9-MOI	167.5	
JT18!-MOI	167.5	
Vj-T11-MOI	167.5	
Vi-T11-MOI	167.5	
JT-T11-MOI	167.5	
Vj-T12-MOI	167.5	
Vi-T12-MOI	167.5	
Vi-brancT3-CH	154.1	
Vj-brancT3-CH	154.1	
Vj-T2-CH	154.1	
Vj-T1-CH	154.1	
Vi-T1-CH	154.1	
JT-T1-CH	154.1	
Vj-T3-CH	154.1	
J2!-CH	154.1	
Vj-T4-CH	154.1	
Vi-T4-CH	154.1	
Vi-JT3-CH	154.1	
Vj-JT3-CH	154.1	
Vj-T5-CH	154.1	
Vi-T5-CH	154.1	
JT-T5-CH	154.1	
Vj-brancT10-CH		154.1
Vi-toT18-S17	154.1	
Vj-toT18-S17	154.1	
JT3!-CH	154.1	
V5j-CH	154.1	
Vj-T7-CH	154.1	
Vi-T7-CH	154.1	
Vj-T6-CH	154.1	
Vi-T6-CH	154.1	
Vj-T11-CH	154.1	
Vj-T10-CH	154.1	
Vi-T10-CH	154.1	
V7j-CH	154.1	
JT-TEMRIN3		160.8
JT-TEMT3	160.8	
JT-TEMRIN1		160.8

JT-TEMT2	160.8
Vi-brancT8-CT	160.8
Vj-brancT8-CT	160.8
Vj-T1-CT	160.8
Vi-T1-CT	160.8
JT-T1-CT	160.8
Vj-T3-CT	160.8
Vi-T3-CT	160.8
V2j-CT	160.8
V3i-CT	160.8
V4i-CT	160.8
Vj-T4-CT	160.8
Vi-T4-CT	160.8
JT-T5-CT	160.8
Vj-T5-CT	160.8
Vi-T5-CT	160.8
V5j-CT	160.8
Vj-T6-CT	160.8
Vi-T6-CT	160.8
JT-T6-CT	160.8
Vj-T7-CT	160.8
Vi-T7-CT	160.8
Vj-T8-CT	160.8
Vi-T8-CT	160.8
Vi-JT1-S8	234.5
Vj-JT1-S8	234.5
Vj-T3-S8	234.5
Vi-T3-S8	234.5
Vj-T2-S8	234.5
Vi-T2-S8	234.5
Vi-JT4-S8	234.5
Vj-JT4-S8	234.5
Vj-T1-S8	234.5
Vi-T1-S8	234.5
Vj-JT5-S8	234.5
Vi-JT5-S8	234.5
Vj-T4-S8	234.5
Vi-T4-S8	234.5
JT-T4-S8	234.5
Vi-toS8RING	234.5
Vj-toS8RING	234.5
V6i-S8	234.5
Vj-T5-S8	234.5
Vi-T5-S8	234.5
J-T5-S8	234.5
JT-T5-S8	234.5
Vj-T6-S8	234.5
Vi-T6-S8	234.5
Vi-JT6-S8	234.5
Vj-JT6-S8	234.5
17T	448.9
TBRINGS	455.6
BT1	160.8
MOIT	167.5
CHT1	154.1
S67RING	237.6
CT	160.8

```
 S8RIN              234.5
 AT-OLD             201

[SOURCES]
;Node               Type            Quality         Pattern
 Salt-CHT1          MASS            583000  CHT
 Salt-AT-OLD        MASS            583000  AT
 Salt-MOIT          MASS            583000  MOIT
 Salt-17T           MASS            583000  17T
 Salt-CT            MASS            583000  CT
 Salt-BT1           MASS            583000  BT

[REACTIONS]
;Type     Pipe/Tank          Coefficient


[REACTIONS]
 Order Bulk                 1
 Order Tank                 1
 Order Wall                 1
 Global Bulk                0
 Global Wall                0
 Limiting Potential         0
 Roughness Correlation      0

[MIXING]
;Tank               Model
 17T                2Comp           0.12
 BT1                2Comp           0.12
 MOIT               2Comp           0.12
 CHT1               2Comp           0.12
 CT                 2Comp           0.12
 AT-OLD             2Comp           0.12



[TIMES]
 Duration           18:05
 Hydraulic Timestep         0:05
 Quality Timestep           0:05
 Pattern Timestep           0:05
 Pattern Start      0:00
 Report Timestep            0:05
 Report Start       0:00
 Start ClockTime            12:00 AM
 Statistic          NONE

[REPORT]
 Status             Yes
 Summary            No
 Page               0

[OPTIONS]
 Units              LPM
 Headloss           H-W
 Specific Gravity   0.998
 Viscosity          1
```

Trials	10000
Accuracy	0.03
Unbalanced	Continue 10
Pattern	1
Demand Multiplier	1
Emitter Exponent	0.52
Quality	Salt mg/L
Diffusivity	0
Tolerance	0.01

[COORDINATES]

;Node	X-Coord	Y-Coord
J-S17	434981.63	1893210.27
T15-S17	434976.1	1893210.45
JT-S17	434986.55	1893210.11
JT2-S17	435099.54	1893118.65
J3-S17	435079.66	1893105.9
T14-S17	435078.42	1893105.03
JT3-S17	435203.44	1893045.48
J4-S17	435163.23	1893023.77
T13-S17	435161.46	1892997.77
T12-S17	435286.98	1892973.74
JT4-S17	435288.42	1892980.42
JT5-S17	435337.18	1892939.59
J5-S17	435325.59	1892932.66
TNEW-S17	435321.19	1892932.63
JT6-S17	435492.42	1892815.97
T11-S17	435490.78	1892807.99
T10-S17	435736.54	1892618.07
JT7-S17	435726.05	1892640.6
J6-S17	435728.75	1892634.49
T8-S17	435834.13	1892590
JT8-S17	435836.58	1892593.38
T7A-S17	435835.97	1892589.72
T7B-S17	435835.8	1892586.23
JT9-S17	435858.63	1892576.92
T9-S17	435842.44	1892530.76
T6-S17	435882.45	1892495.97
JT11-S17	435918.97	1892563.34
JT10-S17	435912.73	1892552.69
J7-S17	435910.64	1892548.09
T5-S17	435929	1892538.44
JT12-S17	436131.79	1892471.51
T4-S17	436083.98	1892423.38
J8-S17	436095.54	1892436.76
JT13-S17	436159.32	1892408.32
T3-S17	436146.89	1892395.38
T2-S17	436187.55	1892246.39
JT14-S17	436223.35	1892233.56
JB-S17	436259.17	1892161.75
JT15-S17	436239.21	1892151.65
T1A-S17	436247.21	1892150.64
T1B-S17	436250.23	1892149.24
J9-S17	436238.2	1892151.03
PTBi	436228.9	1892118.58
JT16-S17	436014.78	1891841.28
TB1-S17	436002.64	1891835.7

TB2-S17	436044.32	1891866.67
TB9-S17	436103.11	1891897.66
TB4-S17	436040.44	1891820.92
TB5-S17	436058.21	1891838.53
JT17-S17	436032.77	1891829.37
JT18-S17	436084.95	1891884.21
TB6-S17	436093.41	1891884.15
TB7-S17	436096.85	1891871.21
TB3-S17	436072.31	1891938.83
TB10-S17	436111.74	1891901.24
TB8-S17	436088.34	1891897.27
J10-S17	436112.34	1891894.02
T18-S17	434671.1	1893608.16
T4-BT	435012.55	1893138.89
J01-BT	434952.39	1893172.12
V1i-BT	434906.22	1893186.49
JT1-BT	434836.02	1893182.32
T3-BT	434831.27	1893175.18
J2-BT	434804.48	1893184.12
J3-BT	434805.36	1893194.51
JT2-BT	434803.07	1893184.07
V2i-BT	434804.78	1893193.07
T2-BT	434823.11	1893281.21
JB2-BT	434757.34	1893121.59
T13-BT	434758.43	1893117.3
JT3-BT	434751.25	1893118.67
J4-BT	434714.7	1893137.88
JT4-BT	434713.68	1893130.08
T1-BT	434715.26	1893160.97
JT5-BT	434645.54	1893165.99
T12-BT	434646.06	1893162.86
Vi-branchT4-BT	434488.67	1893312.47
J5-BT	434480.99	1893305.24
Vi-branchT5-BT	434471.01	1893315.15
T5-BT	434390.76	1893446.71
T6-BT	434249.01	1893527.37
Vi-branchT10-BT	434495.08	1893320.14
JT6-BT	434562.83	1893408.6
T11-BT	434550.14	1893481.89
J6-BT	434626.69	1893440.95
T7-BT	434613.86	1893435.8
J7-BT	434700.79	1893427.06
JT7-BT	434684.58	1893431.07
T8-BT	434725.15	1893343.51
T9-BT	434727.67	1893448.98
T10-BT	434821.91	1893449.73
T5A-MOI	433802.92	1894510.91
JT1-MOI	433809.68	1894518.25
T5B-MOI	433811.56	1894505.25
J1-MOI	433814.59	1894504.41
T4-MOI	433822.24	1894484.87
JT2-MOI	433830.88	1894456.94
T3-MOI	433820.71	1894432.52
JT3-MOI	433867.22	1894436.49
T2-MOI	433869.4	1894437.57
T1-MOI	433879.44	1894411.01
T27-MOI	433779.15	1894549.72

J2-MOI	433702.07	1894615.69
JT4-MOI	433672.5	1894640.58
T6-MOI	433682.03	1894652.98
JT5-MOI	433647.61	1894640.63
T7-MOI	433634.59	1894645.79
JT6-MOI	433645.29	1894633.74
T30-MOI	433626.08	1894621.09
T31A-MOI	433608.08	1894617.49
T31B-MOI	433634.65	1894629.14
JT7-MOI	433627.64	1894621.66
T32A-MOI	433639.8	1894627.69
T32B-MOI	433621.85	1894622.26
J1-CH	434475.42	1893559.94
JT1-CH	434477.84	1893564.01
J2-CH	434455.64	1893586.42
JT2-CH	434413.93	1893594.27
Vi-T2-CH	434408.56	1893596.41
T2-CH	434332.07	1893651.67
Vi-T3-CH	434371.79	1893587.16
T1-CH	434375.21	1893591.35
T3-CH	434279.38	1893609.7
JT3-CH	434494.55	1893578.19
T4-CH	434488.64	1893584.4
T5-CH	434538.41	1893574.28
V5i-CH	434595.03	1893590.36
Vi-brancT10-CH	434601.83	1893588.9
T6-CH	434530.66	1893680.55
JT4-CH	434532.64	1893686.31
T7-CH	434440.32	1893759.65
JT5-CH	434442.32	1893764.5
JT6-CH	434392.43	1893821.32
JT7-CH	434363.74	1893845.53
T8-CH	434401.91	1893865.58
T11-CH	434320.64	1893827.94
J3-CH	434311.79	1893840.2
Vi-T11-CH	434357.02	1893852.26
JT8-CH	434292.76	1893905.99
T9-CH	434319.97	1893912.37
J4-CH	434287.85	1893922.86
T10-CH	434294.88	1893933.14
V7i-CH	434670.08	1893607.92
J3-MOI	433838.24	1894375.21
T19-MOI	433775.74	1894382.54
J4-MOI	433783.18	1894392.64
T153-MOI	433734.49	1894397.39
JT9-MOI	433710.44	1894406.28
T151-MOI	433728.1	1894406.28
T150-MOI	433708.93	1894418.28
T23-MOI	433633.18	1894403.43
JT10-MOI	433586.11	1894341.56
T24-MOI	433547.51	1894378.95
V1-MOI	433558.66	1894295.38
J6-MOI	433576.99	1894296.45
J5-MOI	433549.15	1894374.09
JT12-MOI	433508.21	1894278.7
T25-MOI	433489.27	1894282.85
T29-MOI	433387.58	1894285.73

J7-MOI	433479.23	1894290.37
T26-MOI	433610.6	1894519.19
J8-MOI	433664.46	1894453.84
JT13-MOI	433727.96	1894399.75
T20-MOI	433754.81	1894449.9
J9-MOI	433746.72	1894450.03
T21-MOI	433729.53	1894499.49
J10-MOI	433853.06	1894351.02
JT8CHECK-MOI	433852.98	1894357.38
T15-MOI	433736.62	1894297.87
T16-MOI	433696.22	1894249.14
J11-MOI	433669.55	1894248.49
JT14-MOI	433658.74	1894231.78
T17-MOI	433605.71	1894252.45
Vi-T17-MOI	433620.16	1894252.9
JT15-MOI	433644.77	1894165.24
T18-MOI	433646.29	1894161.28
B1-MOI	433860.13	1894301.63
J12-MOI	433876.22	1894354.52
JT16-MOI	433870.82	1894359.85
T13-MOI	433867.17	1894296.64
T14-MOI	433833.88	1894266.88
JT17-MOI	433879.73	1894360.86
T8-MOI	433930.38	1894366.92
J13-MOI	433928.68	1894313.06
JT18-MOI	434018.35	1894183.38
T9-MOI	433973.17	1894250.01
T10-MOI	433979.58	1894130.55
T11-MOI	434019.46	1894165
J14-MOI	434025.43	1894160.7
J15-MOI	434045.47	1894136.58
TNEW-MOI	434002.57	1894156.7
T12-MOI	434081.96	1894099.41
JT19-MOI	434042	1894141.33
T28-MOII	434083.93	1894172.14
T3-S67	433637.24	1893960.49
T6-S67	433613.51	1894068.42
JT1-S67	433618.91	1893950.58
J1-S67	433618.02	1893897.77
J2-S67	433632.63	1893813.68
T2-S67	433718.08	1893776.77
J3-S67	433798.57	1893729.38
T1-S67	433835.8	1893731.94
V1i-S67	433785.48	1893711.96
T5-S67	433505.77	1894174.44
Vi-18-5	433596.71	1894174.55
J4-S67	433508.26	1894169.8
J5-S67	433462.79	1894051.09
T7-S67	433460.27	1894080.9
JT2-S67	433462.24	1894041.87
TNEW-S67	433427.12	1894028.95
T4-S67	433447.42	1893947.94
JT3-S67	433460.09	1893910.56
V2i-S67	433462.88	1893921.04
J6-S67	433466.78	1893950.02
J7-S67	433470.39	1893975.89
JT4-S67	433452.32	1893905.23

T8-S67	433488	1893979.28
V3i-S67	433478.61	1893971.55
V4j-S67	433379.38	1893950.87
J8-S67	433757.37	1893754.22
JT1CHECK-CT	433773.53	1893664.17
J1-CT	433814.64	1893726
V1-CT	433786.98	1893662.96
JT2-CT	433870.89	1893913.09
TEMT1	433888.24	1893915.6
TEMT2	433880.82	1893912.29
TEMT3	433898.47	1893926.64
JT3-CT	433796.31	1893594.81
T1-CT	433842.76	1893655.32
J2-CT	433850.52	1893644.58
JT4-CT	433892.97	1893831
V2i-CT	433861.98	1893841.45
T3-CT	433827.99	1893857.06
JT5-CT	433915.94	1893876.76
V3j-CT	433895.74	1893971.16
JT6-CT	433873.77	1894013.85
V4j-CT	433909.71	1894037.67
J3-CT	433917	1894039.45
T9-CT	433936.36	1894044.44
T4-CT	433859.17	1894084.08
J4-CT	433927.59	1893877.84
T5-CT	433930.67	1893882.97
V5i-CT	433939.72	1893881.64
J5-CT	434092.39	1893926.5
J6-CT	434192.82	1894054.18
JT7-CT	434229.64	1894020.48
T6-CT	434184.54	1893986.02
J7-CT	434230.37	1894021.73
T7-CT	434135.08	1894080.82
T8-CT	434231.8	1894029.91
T8-S8	434183.36	1893814
JT1-S8	434128.84	1893746.24
T3-S8	434155.04	1893738.46
JT2-S8	434093.05	1893743.58
TNEW-S8	434097.18	1893739.32
J1-S8	434082.42	1893710.47
JT3-S8	434065.06	1893713.16
T2-S8	434055.29	1893720.76
JT4-S8	433968	1893596.87
T1-S8	434074.37	1893523.11
JT5-S8	433969.61	1893588.78
J2-S8	433898.24	1893561.51
T4-S8	433964.45	1893600.84
V6j-S8	433964.82	1893610
T5-S8	433923.49	1893764.57
J3-S8	433963.99	1893789.97
JT6-S8	434017.8	1893823.63
T6-S8	434025.86	1893825.34
T7-S8	434101.23	1893892.37
T6-AT	435309.49	1892873.47
B1-AT	435292.95	1892889.85
JT1-AT	435439.11	1892762.99
T5-AT	435457.27	1892768.6

J1-AT	435447.12	1892745.04
J2-AT	435491.74	1892684.08
JT2-AT	435479.91	1892698.36
J3-AT	435494.43	1892670.34
T10-AT	435504.37	1892666.17
JT3-AT	435501.43	1892474.36
J4-AT	435544.09	1892487.82
J5-AT	435584.71	1892508.9
B2-AT	435611.61	1892549.76
J6-AT	435594.34	1892565.02
T2-AT	435584.02	1892573.99
JT4-AT	435423.72	1892785.52
JT5-AT	435353.86	1892770.6
T4-AT	435356.21	892770.66
J7-AT	435360.32	1892763.19
JT6-AT	435212.55	1892758.22
T13-AT	435211.86	1892808.17
J8-AT	435233.64	1892860.52
T9-AT	435235.07	1892873.6
JT7-AT	434961.62	1892691.17
T1-AT	434927.85	1892742.04
J9-AT	435059.83	1892676.66
JT8-AT	435065.56	1892697.93
T2B-AT	435072.83	1892681.97
J10-AT	435167.44	1892653.24
T11-AT	435155.96	1892642.39
T3-AT	435277.38	1892687.66
JT9-AT	435129.68	1892775.18
J11-AT	435126.82	1892826.46
JT10-AT	435128.87	1892829.94
T7-AT	435084.21	1892866.77
J12-AT	435123.09	1892850.56
T12-AT	435115.89	1892847.32
T8-AT	435131.95	1892901.6
J1-S17	434786.12	1893608.87
J2-S17	434823.45	1893604.39
J4T-S17	434832.81	1893586.01
J5!-S17	434925.72	1893360.58
J6!-S17	434961.16	1893256.48
J7!-S17	434949.61	1893281.28
T16-S17	434937.38	1893284.01
T17-S17	434910.91	1893385.37
T19A-S17	434820.95	1893585.97
T19B-S17	434830.44	1893587.59
T20-S17	434865.61	1893547.54
T21-S17	434951.53	1893251.68
V1j-S17	434753.91	1893587.92
Vi-T18-S17	434681.41	1893606.96
Vj-T18-S17	434681.96	1893606.73
V1i-S17	434753.43	1893587.94
Vi-ML2	434794.22	1893610.82
Vj-ML2	434794.39	1893610.88
Vi-T16-S17	434948.84	1893281.39
Vi-T21-S17	434960.42	1893256.05
Vi-T17-S17	434925.53	1893360.96
Vi-T19	434832.18	1893586.99
Vj-T19	434832.39	1893586.74

Vj-T17-S17	434925.44	1893361.14
Vj-T16-S17	434948.62	1893281.41
Vj-T21-S17	434960.33	1893256
Vi-T15-S17	434986.21	1893210.12
Vj-T15-S17	434986.01	1893210.14
Vj-T14-S17	435098.8	1893118.2
Vi-T14-S17	435099.02	1893118.33
Vi-T13-S17	435200.74	1893043.99
Vj-T13-S17	435200.35	1893043.68
Vi-T12-S17	435288.34	1892980.08
Vj-T12-S17	435288.3	1892979.79
Vi-TNEW-S17	435321.64	1892932.62
Vj-TNEW	435321.38	1892932.63
Vi-T11-S17	435492.26	1892815.32
Vj-T11-S17	435492.22	1892814.94
Vj-T10-S17	435736.48	1892619.02
Vi-T10-S17	435736.48	1892619.39
Vj-S17beforeT10	435727.21	1892640.31
Vi-S17beforeT10	435727.4	1892640.22
Vj-T7/8-S17	435836.57	1892590.7
Vi-T7/8-S17	435836.57	1892590.99
JT-T7/8-S17	435836.04	1892590.53
Vi-T9-S17	435858.42	1892576.51
Vj-T9-S17	435858.3	1892576.33
Vj-T6-S17	435882.93	1892496.85
Vi-T6-S17	435882.98	1892497.03
Vj-T5-S17	435928.75	1892538.46
Vi-T5-S17	435928.6	1892538.47
Vi-T4-S17	436131.67	1892471.32
Vj-T4-S17	436131.27	1892470.88
Vi-T3-S17	436159.18	1892408.16
Vj-T3-S17	436159.12	1892408.07
Vi-T2-S17	436222.55	1892233.64
Vj-T2-S17	436221.51	1892233.95
JT-T1/2-S17	436248.14	1892148.55
PTBj	436228.84	1892118.49
Vi-PTB	436228.94	1892118.64
JT-TB2-S17	436020.15	1891834.9
Vj-TBR	436024.91	1891834.37
Vi-TBR	436025.03	1891834.37
JT-TB5-S17	436049.56	1891847.32
JT-TB6/7-S17	436091.11	1891879.01
JT-TB8-S17	436093.39	1891888.57
V1j-BT	434906.05	1893186.48
Vj-T3-BT	434831.36	1893175.46
Vi-T3-BT	434831.44	1893175.68
V2j-BT	434804.82	1893193.21
Vi-T1-BT	434713.69	1893130.23
Vj-T1-BT	434713.69	1893130.32
Vj-branchT4-BT	434488.45	1893312.2
JbranchT10-BT	434480.1	1893306.05
Vj-branchT10-BT	434495.2	1893320.22
JTbranches-BT	434480.52	1893305.64
JT-branchT5-BT	434480.18	1893305.34
Vj-branchT5-BT	434470.97	1893315.22
JT-T5-BT	434391.6	1893447.19
Vj-T13-BT	434758.4	1893117.31

Vi-T13-BT	434758.37	1893117.31
Vj-T5-BT	434390.79	1893446.73
Vi-T5-BT	434390.81	1893446.74
Vj-T6-BT	434249.27	1893527.2
Vi-T6-BT	434249.41	1893527.08
JT-T7-BT	434614.1	1893435.15
Vj-T7-BT	434613.87	1893435.75
Vi-T7-BT	434613.88	1893435.72
Vi-T9/10-BT	434702.7	1893426.65
Vj-T9/10-BT	434702.91	1893426.58
Vj-T8-BT	434725.03	1893343.72
Vi-T8-BT	434724.97	1893343.83
Vj-T9-BT	434727.66	1893448.88
Vi-T9-BT	434727.66	1893448.78
JT-T9-BT	434727.68	1893448.23
Vj-T10-BT	434821.62	1893449.74
Vi-T10-BT	434821.35	1893449.75
JT-T4-MOI	433823.61	1894485.5
Vj-T3-MOI	433821.01	1894432.89
Vi-T3-MOI	433821.18	1894433.07
JT-T1-MOI	433879.78	1894411.25
JT-T27-MOI	433779.76	1894550.05
Vj-toT7-MOI	433672.76	1894640.39
Vi-toT7-MOI	433672.92	1894640.24
Vj-T7-MOI	433634.91	1894645.65
Vi-T7-MOI	433635.07	1894645.55
JT-T31B-MOI	433634.67	1894629.1
JT-T32-MOI	433627.54	1894621.7
Vj-JT7-MOI	433627.65	1894621.66
Vi-JT7-MOI	433627.65	1894621.67
Vi-brancT29-MOI	433852.66	1894357.38
Vj-brancT29-MOI	433852.03	1894357.9
JT-T19-MOI	433774.73	1894383.11
JT-T153-MOI	433734.81	1894398.03
JT-T26-MOI	433713.18	1894404.74
JT-T51-MOI	433714.57	1894404
Vi-T26-MOI	433713.41	1894405.05
Vj-T26-MOI	433713.58	1894405.34
Vj-JT9-MOI	433712.75	1894404.98
Vi-JT9-MOI	433712.91	1894404.9
Vi-T150-MOI	433710.4	1894406.56
Vj-T150-MOI	433710.37	1894406.81
JT-T23-MOI	433633.06	1894403.74
Vj-T24-MOI	433547.55	1894378.81
Vi-T24-MOI	433547.58	1894378.75
Vj-T25-MOI	433489.58	1894282.76
Vi-T25-MOI	433489.72	1894282.73
Vj-T20-MOI	433754.75	1894449.81
Vi-T20-MOI	433754.68	1894449.69
JT-T20-MOI	433754.61	1894449.59
Vj-T21-MOI	433729.61	1894499.18
Vi-T21-MOI	433729.66	1894498.89
Vj-T15-MOI	433736.84	1894297.59
Vi-T15-MOI	433737.04	1894297.29
JT-T15-MOI	433737.27	1894296.96
Vj-T16-MOI	433695.96	1894249.5
Vi-T16-MOI	433695.74	1894249.74

JT-T16-MOI	433695.4	1894250.15
Vj-T17-MOI	433619.57	1894252.89
Vj-T18-MOI	433646.28	1894161.32
Vi-T18-MOI	433646.27	1894161.38
Vj-T13-MOI	433867.53	1894296.77
Vi-T13-MOI	433867.72	1894296.86
JT-T13-MOI	433867.92	1894296.97
Vi-brancT12-MOI	433886.09	1894367.56
Vj-brancT12-MOI	433885.93	1894367.42
Vj-T14-MOI	433834.13	1894267.25
Vi-T14-MOI	433834.45	1894267.55
Vj-T8-MOI	433930.14	1894366.92
Vi-T8-MOI	433930.02	1894366.9
Vj-T9-MOI	433972.61	1894250.9
Vi-T9-MOI	433972.47	1894251.12
JT-T9-MOI	433972.38	1894251.31
JT18!-MOI	434020.66	1894180.24
Vj-T11-MOI	434019.5	1894165.57
Vi-T11-MOI	434019.57	1894166.11
JT-T11-MOI	434019.63	1894166.62
Vj-T12-MOI	434081.73	1894099.66
Vi-T12-MOI	434081.56	1894099.79
Vi-brancT3-CH	434476.5	1893565.3
Vj-brancT3-CH	434476.15	1893565.62
Vj-T2-CH	434407.36	1893596.71
Vj-T1-CH	434375.33	1893591.25
Vi-T1-CH	434375.41	1893591.16
JT-T1-CH	434375.49	1893591.04
Vj-T3-CH	434371.71	1893587.05
J2!-CH	434480.56	1893566.38
Vj-T4-CH	434489.02	1893583.94
Vi-T4-CH	434489.72	1893583.17
Vi-JT3-CH	434494.64	1893578.29
Vj-JT3-CH	434494.68	1893578.32
Vj-T5-CH	434538.4	1893574.19
Vi-T5-CH	434538.4	1893574.11
JT-T5-CH	434538.4	1893573.99
Vj-brancT10-CH	434602.18	1893588.91
Vi-toT18-S17	434603.27	1893588.84
Vj-toT18-S17	434603.62	1893588.83
JT3!-CH	434602.76	1893588.84
V5j-CH	434594.67	1893590.58
Vj-T7-CH	434440.42	1893760
Vi-T7-CH	434440.48	1893760.15
Vj-T6-CH	434530.74	1893680.97
Vi-T6-CH	434530.87	1893681.23
Vj-T11-CH	434356.87	1893852.43
Vj-T10-CH	434294.74	1893932.96
Vi-T10-CH	434294.58	1893932.79
V7j-CH	434670.44	1893608.05
Vj-T6-AT	435309.08	1892873.88
Vi-T6-AT	435308.63	1892874.34
Vj-T5-AT	435456.53	1892769.18
Vi-T5-AT	435456.26	1892769.52
Vi-JT1-AT	435440.12	1892761.52
Vj-JT1-AT	435440.24	1892761.34
Vi-S14RING	435501.43	1892473.18

Vj-S14RING	435501.4	1892473.45
Vj-JT5-AT	435354.43	1892771.07
Vi-JT5-AT	435354.52	1892771.15
Vj-T13-AT	435212.56	1892808.09
Vi-T13-AT	435212.92	1892807.97
Vj-T9-AT	435235.03	1892873.39
Vi-T9-AT	435235	1892873.26
Vi-suggesT10-AT	435479.85	1892697.64
Vj-suggesT10-AT	435479.85	1892697.27
Vi-T1-AT	434961.48	1892691.88
Vj-T1-AT	434961.25	1892692.45
JT-T12-AT	435116.62	1892847.17
Vj-T7-AT	435084.55	1892866.48
Vi-T7-AT	435084.81	1892866.2
Vj-T8-AT	435131.78	1892900.94
Vi-T8-AT	435131.52	1892900.57
Vj-T2B-AT	435072.64	1892682.44
Vi-T2B-AT	435072.47	1892682.82
Vj-T11-AT	435155.88	1892642.94
Vi-T11-AT	435155.86	1892643.1
JT-T11-AT	435155.83	1892643.32
Vj-T3-AT	435277.02	1892687.52
Vi-T3-AT	435276.7	1892687.29
Vj-T2-S67	433717.75	1893776.73
Vi-T2-S67	433717.37	1893776.73
JT-T2-S67	433714.6	1893776.46
Vi-S67RING	433774.47	1893709.47
Vj-S67RING	433774.33	1893710
JT-S67RING	433774.26	1893710.23
V1j-S67	433785.66	1893711.97
Vj-T1-S67	433835.71	1893731.92
Vi-T1-S67	433835.64	1893731.92
Vj-toS67RING	433773.54	1893664.73
Vi-toS67RING	433773.54	1893664.58
J-toS67RING	433774.93	1893699
JT-toT5-CT	433774.75	1893707.81
Vi-pourS67RING	433774.75	1893708.21
Vj-pourS67RING	433774.74	1893708.37
JT-T5-S67	433507.42	1894174.23
Vj-18-5	433595.13	1894174.61
Vi-T5-S67	433507.47	1894173.5
Vj-T5-S67	433507.47	1894173.72
Vj-T7-S67	433460.56	1894080.76
Vi-T7-S67	433460.79	1894080.64
JT-T7-S67	433461.05	1894080.52
Vi-TNEW-S67	433458.55	1894041.26
Vj-TNEW-S67	433457.76	1894040.79
JT-T4-S67	433448.38	1893947.91
Vi-T4-S67	433448.15	1893947.91
Vj-T4-S67	433447.89	1893947.93
V2j-S67	433462.95	1893920.87
Vi-ML1-S67	433459.87	1893910.44
Vj-ML1-S67	433459.71	1893910.32
Vi-brancT5-S67	433460.12	1893910.68
Vj-brancT5-S67	433460.13	1893910.77
Vi-toML1	433452.04	1893905.25
Vj-toML1	433451.88	1893905.29

Vi-toTIMhouse	433452.34	1893905.58
Vj-toTIMhouse	433452.34	1893905.79
V3j-S67	433479.02	1893971.55
V4i-S67	433379.45	1893950.78
JT-TEMRIN3	433866.18	1893932.45
JT-TEMT3	433866.48	1893929.84
JT-TEMRIN1	433866.58	1893927.43
JT-TEMT2	433870.89	1893915.19
Vi-brancT8-CT	433775.82	1893605.05
Vj-brancT8-CT	433776.36	1893604.21
Vj-T1-CT	433842.63	1893654.51
Vi-T1-CT	433842.44	1893653.86
JT-T1-CT	433842.16	1893653.2
Vj-T3-CT	433828.5	1893856.85
Vi-T3-CT	433828.91	1893856.71
V2j-CT	433861.4	1893841.67
V3i-CT	433895.75	1893969.92
V4i-CT	433909.25	1894037.49
Vj-T4-CT	433859.29	1894082.86
Vi-T4-CT	433859.29	1894081.95
JT-T5-CT	433931.05	1893881.31
Vj-T5-CT	433930.7	1893882.85
Vi-T5-CT	433930.72	1893882.74
V5j-CT	433939.81	1893881.64
Vj-T6-CT	434184.27	1893985.55
Vi-T6-CT	434184.06	1893985.09
JT-T6-CT	434183.7	1893984.32
Vj-T7-CT	434135.35	1894080.49
Vi-T7-CT	434135.61	1894080.14
Vj-T8-CT	434231.75	1894029.78
Vi-T8-CT	434231.7	1894029.66
Vi-JT1-S8	434132.45	1893751.37
Vj-JT1-S8	434133.6	1893752.95
Vj-T3-S8	434154.8	1893738.49
Vi-T3-S8	434154.61	1893738.58
Vj-T2-S8	434055.86	1893720.35
Vi-T2-S8	434056.03	1893720.15
Vi-JT4-S8	433969.06	1893598.8
Vj-JT4-S8	433969.26	1893599.09
Vj-T1-S8	434074.12	1893523.34
Vi-T1-S8	434073.92	1893523.54
Vj-JT5-S8	433969.16	1893588.28
Vi-JT5-S8	433968.72	1893587.77
Vj-T4-S8	433964.48	1893600.79
Vi-T4-S8	433964.52	1893600.73
JT-T4-S8	433962.79	1893598.55
Vi-toS8RING	433774.82	1893605.43
Vj-toS8RING	433774.82	1893605.13
V6i-S8	433964.79	1893609.9
Vj-T5-S8	433923.53	1893764.31
Vi-T5-S8	433923.59	1893764.08
J-T5-S8	433923.62	1893763.59
JT-T5-S8	433923.67	1893763.06
Vj-T6-S8	434025.45	1893825.35
Vi-T6-S8	434025.15	1893825.38
Vi-JT6-S8	434017.92	1893823.82
Vj-JT6-S8	434017.96	1893823.95

Vi-CHT2	434469.08	1893554.85
Vj-CHT2	434469.02	1893554.86
Vi-CHT1	434466.36	1893555.07
Vi-CHTout	434466.41	1893555.12
Vj-CHTout	434466.43	1893555.16
Vi-BT1	434400.18	1893268.1
Vj-BT1	434400.28	1893268.15
Vi-BT2	434400.43	1893267.61
Vj-BT2	434400.43	1893267.71
Vj-BTout	434400.38	1893268.23
Vj-CHT1	434466.41	1893555.12
Vi-BTout	434400.29	1893268.16
Vi-17Tout	436238.9	1892132.69
Vj-17Tout	436238.9	1892132.77
Vi-TBRINGSout	436024.63	1891834.34
Vj-TBRINGSout	436024.6	1891834.29
Vi-MOITout	433886.55	1894368.18
Vj-MOITout	433886.45	1894368.25
Vi-CTout	433774.88	1893605.88
Vj-CTout	433774.9	1893605.86
Vi-AT-OLDout	434862.53	1892676.01
Vj-AT-OLDout	434863.05	1892676.03
PSVi-MAELA2	434802.12	1893610.07
PSVj-MAELA2	434800.93	1893610.32
PSVi-ML1	433385.03	1893961.2
PSVj-ML1	433385.39	1893961.91
PSVi-TEMRIN2	433866.02	1893948.23
PSVj-TEMRIN2	433866.02	1893948.72
PSVj-TEMRIN3	433840.38	1893947.16
PSVi-TEMRIN3	433840.7	1893946.88
PSVi-TEMRIN1	433868.97	1893926.19
PSVj-TEMRIN1	433869.22	1893926
PSVi-S8RIN	433958.49	1893582.55
PSVj-S8RIN	433959.01	1893582.63
FCVi-CHT1	434466.17	1893554.96
FCVj-CHT1	434466.21	1893554.97
FCVi-AT-OLD	434861.62	1892675.96
FCVj-AT-OLD	434861.71	1892675.97
FCVi-MOIT	433886.91	1894368
FCVj-MOIT	433886.81	1894368.03
FCVi-17T	436239.07	1892132.53
FCVj-17T	436239.01	1892132.53
FCVi-CT	433774.68	1893605.89
FCVj-CT	433774.75	1893605.89
FCVi-BT	434399.85	1893268.04
FCVj-BT	434399.91	1893268.06
Vi-T23-MOI	433633.17	1894403.45
Vj-T23-MOI	433633.18	1894403.44
17T	436238.9	1892132.55
TBRINGS	436024.66	1891834.37
BT1	434400.05	1893268.08
MOIT	433886.64	1894368.11
CHT1	434466.26	1893554.98
S67RING	433774.74	1893708.78
CT	433774.84	1893605.89
ML1RING	433385.72	1893963.19
TEMRIN1	433869.69	1893925.53

```
 TEMRIN2        433865.86       1893949.64
 TEMRIN3        433839.73       1893947.87
 S8RIN          433959.9 1893583.36
 S14-RING       435501.51       1892470.71
 AT-NEW         434865.15       1892692.85
 AT-OLD         434861.93       1892676
 MAELA2-RIN             434794.85       1893611.05
 CHT2           434469.19       1893554.83
 BT2            434400.41       1893267.49
 Salt-CHT1      434466.12       1893554.94
 Salt-AT-OLD    434861.51       1892675.95
 Salt-MOIT      433887.04       1894367.98
 Salt-17T       436239.14       1892132.52
 Salt-CT        433774.57       1893605.89
 Salt-BT1       434399.71       1893268.03

[VERTICES]
;Link           X-Coord         Y-Coord
 S17-5          434794.82       1893611.04
 CH-16          434494.6 1893578.25

[LABELS]
;X-Coord        Y-Coord         Label & Anchor Node

[BACKDROP]
 DIMENSIONS             431735.03       1891688.93      436654.99       1895352.45

 UNITS          Meters
 FILE           C:\Users\Myself\Documents\project\EPANET\background2 copy.bmp

 OFFSET         0       0

[END]
```

Appendix B: EPANET Report for 6:05 AM

```
******************************************************************
*                    E P A N E T                    *
*              Hydraulic and Water Quality           *
*              Analysis for Pipe Networks            *
*                   Version 2.0                      *
******************************************************************

Node Results at 6:05 Hrs:
----------------------------------------------------------------
Node            Demand      Head  Pressure   Quality
ID              LPM         m     m          mg/L
----------------------------------------------------------------
J-S17           0.00    231.19      1.18    448.90
T15-S17         0.00    231.19      2.18    448.90
JT-S17          0.00    231.19      1.18    448.90
JT2-S17         0.00    232.84      1.83    448.90
J3-S17          0.00    231.64      2.64    448.90
T14-S17         13.37   231.17      2.16    448.90
JT3-S17         0.00    234.41     -3.59    448.90
J4-S17          0.00    234.30      3.30    448.90
T13-S17         5.78    234.05      0.05    448.90
T12-S17         0.00    238.00      0.00      0.00
JT4-S17         0.00    236.23     -1.77    448.90
JT5-S17         0.00    237.21     -0.79    448.90
J5-S17          0.00    236.91      1.90    448.90
TNEW-S17        9.84    236.20      1.20    448.90
JT6-S17         0.00    241.11      1.11    448.90
T11-S17         0.00    241.11     -0.88    448.90
T10-S17         13.38   241.57      0.57    448.90
JT7-S17         0.00    246.33      4.32    448.90
J6-S17          0.00    246.00      4.99    448.90
T8-S17          0.00    249.03      6.01    448.90
JT8-S17         0.00    249.03      6.01    448.90
T7A-S17         0.00    249.03      6.01    448.90
T7B-S17         0.00    249.03      7.01    448.90
JT9-S17         0.00    249.52      5.51    448.90
T9-S17          0.00    249.52      3.51    448.90
T6-S17          15.58   245.91      2.91    448.90
JT11-S17        0.00    250.84      6.83    448.90
JT10-S17        0.00    249.55      5.54    448.90
J7-S17          0.00    249.51      5.50    448.90
T5-S17          26.96   246.20      2.20    448.90
JT12-S17        0.00    259.52     10.50    448.90
T4-S17          17.90   248.80      3.79    448.90
J8-S17          0.00    256.92     11.89    448.90
JT13-S17        0.00    262.79     13.77    448.90
T3-S17          0.00    262.79     14.76    448.90
T2-S17          22.75   267.03      6.02    448.90
JT14-S17        0.00    271.40     18.37    448.90

Page 2163
Node Results at 6:05 Hrs: (continued)
----------------------------------------------------------------
```

Node ID	Demand LPM	Head m	Pressure m	Quality mg/L
JB-S17	0.00	276.24	22.19	448.90
JT15-S17	0.00	277.72	13.69	448.90
T1A-S17	0.00	277.72	15.69	448.90
T1B-S17	0.00	277.72	15.69	448.90
J9-S17	0.00	277.78	9.76	0.00
PTBi	0.00	325.71	37.64	448.90
JT16-S17	0.00	337.40	2.39	448.90
TB1-S17	8.41	334.89	0.89	448.90
TB2-S17	12.15	327.81	1.80	448.90
TB9-S17	0.00	332.93	24.88	448.90
TB4-S17	4.88	337.31	0.31	448.90
TB5-S17	8.51	331.91	0.91	448.90
JT17-S17	0.00	337.45	2.44	0.00
JT18-S17	0.00	333.03	18.99	448.90
TB6-S17	0.00	333.03	17.00	448.90
TB7-S17	0.00	333.03	17.00	448.90
TB3-S17	38.15	329.30	16.26	448.90
TB10-S17	0.00	332.93	26.88	448.90
TB8-S17	28.00	318.99	8.97	448.90
J10-S17	0.00	332.93	24.88	448.90
T18-S17	19.34	224.46	0.46	0.00
T4-BT	23.47	232.69	1.68	160.80
J01-BT	0.00	239.90	6.89	160.80
V1i-BT	0.00	241.99	10.97	160.80
JT1-BT	0.00	244.46	4.45	160.80
T3-BT	23.08	242.63	1.63	160.80
J2-BT	0.00	246.39	4.38	160.80
J3-BT	0.00	246.05	7.04	160.80
JT2-BT	0.00	246.41	4.40	160.80
V2i-BT	0.00	246.11	7.09	160.80
T2-BT	23.13	235.64	1.64	160.80
JB2-BT	0.00	248.77	-1.23	160.80
T13-BT	0.00	249.00	0.00	0.00
JT3-BT	0.00	248.95	0.95	160.80
J4-BT	0.00	249.98	1.98	160.80
JT4-BT	0.00	250.17	0.17	160.80
T1-BT	22.63	246.72	0.72	160.80
JT5-BT	0.00	254.14	7.12	160.80
T12-BT	13.89	250.33	2.33	160.80
Vi-branchT4-BT	0.00	268.98	1.98	160.80
J5-BT	0.00	269.37	4.36	160.80
Vi-branchT5-BT	0.00	266.63	-0.37	160.80
T5-BT	14.79	243.63	2.63	160.80
T6-BT	12.41	238.50	0.49	160.80
Vi-branchT10-BT	0.00	268.21	2.21	160.80
JT6-BT	0.00	260.13	3.13	160.80
T11-BT	9.92	248.22	1.22	160.80

Page 2164
Node Results at 6:05 Hrs: (continued)

Node ID	Demand LPM	Head m	Pressure m	Quality mg/L

J6-BT	0.00	257.05	5.04	160.80
T7-BT	44.28	256.72	5.71	160.80
J7-BT	0.00	248.33	-2.66	160.80
JT7-BT	0.00	248.74	-4.25	160.80
T8-BT	24.47	236.83	1.83	160.80
T9-BT	0.00	245.00	0.00	0.00
T10-BT	26.90	226.01	1.00	160.80
T5A-MOI	0.00	224.97	6.96	167.50
JT1-MOI	0.00	224.97	4.96	167.50
T5B-MOI	0.00	224.97	1.97	167.50
J1-MOI	0.00	225.70	1.69	167.50
T4-MOI	0.00	225.85	-11.12	167.50
JT2-MOI	0.00	226.08	0.08	167.50
T3-MOI	8.74	222.25	0.25	167.50
JT3-MOI	0.00	226.59	-1.41	167.50
T2-MOI	0.00	226.59	-1.41	167.50
T1-MOI	0.00	233.00	0.00	0.00
T27-MOI	14.68	222.59	2.59	167.50
J2-MOI	0.00	221.21	13.18	167.50
JT4-MOI	0.00	218.60	9.58	167.50
T6-MOI	0.00	218.60	5.59	167.50
JT5-MOI	0.00	217.00	6.98	167.50
T7-MOI	16.85	215.89	0.89	167.50
JT6-MOI	0.00	217.00	5.98	167.50
T30-MOI	0.00	217.00	7.98	167.50
T31A-MOI	0.00	217.00	8.98	167.50
T31B-MOI	0.00	217.00	4.99	167.50
JT7-MOI	0.00	217.00	7.98	167.50
T32A-MOI	0.00	217.00	5.98	167.50
T32B-MOI	0.00	217.00	7.98	167.50
J1-CH	0.00	277.62	1.62	0.00
JT1-CH	0.00	277.24	3.24	154.10
J2-CH	0.00	275.34	3.34	154.10
JT2-CH	0.00	263.84	3.83	154.10
Vi-T2-CH	0.00	263.84	4.83	154.10
T2-CH	0.00	263.84	27.79	154.10
Vi-T3-CH	0.00	254.63	4.62	154.10
T1-CH	19.79	254.61	4.60	154.10
T3-CH	15.28	219.80	2.80	154.10
JT3-CH	0.00	274.50	4.50	154.10
T4-CH	12.51	269.91	1.90	154.10
T5-CH	31.59	266.34	11.31	154.10
V5i-CH	0.00	257.32	37.24	154.10
Vi-brancT10-CH	0.00	258.29	40.21	154.10
T6-CH	35.27	215.69	1.69	0.00
JT4-CH	0.00	241.40	23.35	154.10
T7-CH	64.44	226.40	5.39	154.10

Page 2165
Node Results at 6:05 Hrs: (continued)

Node ID	Demand LPM	Head m	Pressure m	Quality mg/L
JT5-CH	0.00	232.72	14.69	154.10
JT6-CH	0.00	231.47	8.46	154.10
JT7-CH	0.00	231.01	6.00	154.10

T8-CH	0.00	231.47	2.47	154.10
T11-CH	11.73	225.69	1.68	154.10
J3-CH	0.00	229.63	2.62	154.10
Vi-T11-CH	0.00	230.69	7.67	154.10
JT8-CH	0.00	225.82	3.81	154.10
T9-CH	0.00	225.82	2.81	154.10
J4-CH	0.00	225.62	3.61	154.10
T10-CH	31.52	223.36	1.36	154.10
V7i-CH	0.00	258.22	33.15	154.10
J3-MOI	0.00	227.25	-2.74	167.50
T19-MOI	26.28	224.10	2.09	167.50
J4-MOI	0.00	226.67	5.66	167.50
T153-MOI	0.00	221.51	3.51	167.50
JT9-MOI	0.00	219.65	1.65	167.50
T151-MOI	0.00	219.91	1.90	167.50
T150-MOI	14.55	215.55	2.55	167.50
T23-MOI	33.02	216.25	3.25	0.00
JT10-MOI	0.00	215.96	2.96	167.50
T24-MOI	16.06	209.81	0.81	167.50
V1-MOI	0.00	215.02	-0.97	167.50
J6-MOI	0.00	215.71	-0.28	167.50
J5-MOI	0.00	213.20	4.19	167.50
JT12-MOI	0.00	211.90	2.89	167.50
T25-MOI	22.96	209.74	0.74	167.50
T29-MOI	5.37	206.38	0.37	0.00
J7-MOI	0.00	211.89	2.88	167.50
T26-MOI	17.60	212.97	0.97	167.50
J8-MOI	0.00	218.36	5.35	167.50
JT13-MOI	0.00	220.88	3.87	167.50
T20-MOI	8.43	219.89	0.89	167.50
J9-MOI	0.00	219.99	8.97	167.50
T21-MOI	8.83	218.98	0.97	167.50
J10-MOI	0.00	227.28	4.27	167.50
JT8CHECK-MOI	0.00	227.34	2.33	0.00
T15-MOI	29.61	218.64	2.63	167.50
T16-MOI	32.02	219.07	3.06	167.50
J11-MOI	0.00	218.87	6.86	167.50
JT14-MOI	0.00	217.92	4.91	167.50
T17-MOI	13.57	214.59	0.59	167.50
Vi-T17-MOI	0.00	215.52	0.51	167.50
JT15-MOI	0.00	216.99	3.98	167.50
T18-MOI	15.74	213.36	0.36	167.50
B1-MOI	0.00	221.94	1.93	167.50
J12-MOI	0.00	227.30	-0.70	167.50

Page 2166
Node Results at 6:05 Hrs: (continued)

Node ID	Demand LPM	Head m	Pressure m	Quality mg/L
JT16-MOI	0.00	227.36	-3.63	167.50
T13-MOI	15.87	221.36	0.36	167.50
T14-MOI	22.87	213.61	1.60	167.50
JT17-MOI	0.00	227.32	-1.67	167.50
T8-MOI	27.45	219.28	2.28	167.50
J13-MOI	0.00	226.46	10.44	167.50

JT18-MOI	0.00	217.62	0.62	167.50
T9-MOI	60.42	218.40	10.38	167.50
T10-MOI	16.94	213.42	3.41	167.50
T11-MOI	21.59	215.66	0.66	167.50
J14-MOI	0.00	217.49	2.48	167.50
J15-MOI	0.00	216.68	5.66	167.50
TNEW-MOI	0.00	219.00	0.00	0.00
T12-MOI	17.09	213.42	0.42	167.50
JT19-MOI	0.00	216.77	4.76	167.50
T28-MOII	6.91	212.16	0.16	167.50
T3-S67	44.01	212.59	2.59	237.60
T6-S67	8.52	203.91	0.91	237.60
JT1-S67	0.00	214.83	2.82	237.60
J1-S67	0.00	234.48	12.46	237.60
J2-S67	0.00	244.41	18.38	237.60
T2-S67	52.32	243.88	7.87	237.60
J3-S67	0.00	250.05	9.03	237.60
T1-S67	21.15	245.38	1.38	237.59
V1i-S67	0.00	250.76	3.75	0.00
T5-S67	7.69	207.20	0.20	0.00
Vi-18-5	0.00	213.39	4.38	237.60
J4-S67	0.00	208.00	-2.00	237.60
J5-S67	0.00	214.03	8.02	237.60
T7-S67	14.44	209.52	2.51	237.60
JT2-S67	0.00	214.39	5.38	237.60
TNEW-S67	0.00	214.39	11.37	237.60
T4-S67	31.28	214.12	11.10	0.00
JT3-S67	0.00	222.94	16.90	237.60
V2i-S67	0.00	220.42	10.40	0.00
J6-S67	0.00	222.94	18.90	237.60
J7-S67	0.00	222.94	13.91	237.60
JT4-S67	0.00	222.94	15.90	237.60
T8-S67	0.00	222.94	8.92	237.60
V3i-S67	0.00	222.94	9.92	237.60
V4j-S67	0.00	222.94	11.91	237.60
J8-S67	0.00	267.08	26.03	237.60
JT1CHECK-CT	0.00	268.48	12.45	160.80
J1-CT	0.00	266.29	19.25	160.80
V1-CT	0.00	268.12	10.10	160.80
JT2-CT	0.00	246.12	7.11	160.80
TEMT1	0.00	246.12	4.12	160.80

Page 2167
Node Results at 6:05 Hrs: (continued)

Node ID	Demand LPM	Head m	Pressure m	Quality mg/L
TEMT2	0.00	247.00	0.00	0.00
TEMT3	0.00	242.04	-1.96	160.80
JT3-CT	0.00	268.90	4.89	160.80
T1-CT	34.50	265.42	13.40	160.80
J2-CT	0.00	267.93	17.89	160.80
JT4-CT	0.00	256.50	18.46	160.80
V2i-CT	0.00	245.40	11.38	160.80
T3-CT	41.84	229.13	5.12	160.80
JT5-CT	0.00	254.25	19.22	160.80

V3j-CT	0.00	240.53	5.52	160.80
JT6-CT	0.00	231.47	-1.53	160.80
V4j-CT	0.00	228.29	5.28	160.80
J3-CT	0.00	226.89	7.88	160.80
T9-CT	21.56	215.43	1.43	160.80
T4-CT	33.14	220.28	3.27	160.80
J4-CT	0.00	254.07	25.02	160.80
T5-CT	63.39	241.41	11.38	160.80
V5i-CT	0.00	252.37	24.32	160.80
J5-CT	0.00	248.11	38.03	160.80
J6-CT	0.00	224.04	0.04	160.80
JT7-CT	0.00	224.25	2.24	160.80
T6-CT	40.42	222.80	4.79	160.80
J7-CT	0.00	224.22	2.22	160.80
T7-CT	8.35	223.23	0.23	160.80
T8-CT	15.95	223.37	0.37	160.80
T8-S8	6.90	214.61	0.61	234.50
JT1-S8	0.00	223.74	5.72	234.50
T3-S8	24.77	218.87	1.87	234.50
JT2-S8	0.00	227.99	2.98	234.50
TNEW-S8	0.00	227.99	2.98	234.50
J1-S8	0.00	234.07	5.06	234.50
JT3-S8	0.00	234.82	2.81	234.50
T2-S8	25.46	231.97	1.97	234.50
JT4-S8	0.00	256.69	0.69	234.50
T1-S8	23.30	239.76	0.76	234.50
JT5-S8	0.00	258.94	0.94	234.50
J2-S8	0.00	260.01	-4.98	234.50
T4-S8	16.90	255.90	0.89	234.50
V6j-S8	0.00	256.01	2.00	234.50
T5-S8	32.42	247.91	11.89	234.50
J3-S8	0.00	240.16	18.12	234.50
JT6-S8	0.00	229.33	10.30	234.50
T6-S8	29.79	219.67	2.66	234.50
T7-S8	29.25	209.18	1.18	0.00
T6-AT	27.46	239.28	2.28	0.00
B1-AT	0.00	240.56	7.54	201.00
JT1-AT	0.00	245.91	5.90	200.98

Page 2168
Node Results at 6:05 Hrs: (continued)

Node ID	Demand LPM	Head m	Pressure m	Quality mg/L
T5-AT	29.19	241.57	2.56	197.86
J1-AT	0.00	245.91	3.90	201.00
J2-AT	0.00	245.91	-5.08	201.00
JT2-AT	0.00	245.91	-6.08	17.02
J3-AT	0.00	245.91	-3.08	201.00
T10-AT	0.00	252.00	0.00	0.00
JT3-AT	0.00	311.77	1.77	0.00
J4-AT	0.00	311.38	24.33	201.00
J5-AT	0.00	291.47	5.46	201.00
B2-AT	0.00	289.13	3.12	201.00
J6-AT	0.00	288.01	1.00	201.00
T2-AT	14.36	286.66	0.65	201.00

JT4-AT	0.00	247.07	8.05	0.00
JT5-AT	0.00	257.29	1.28	201.00
T4-AT	17.91	257.00	1.00	0.00
J7-AT	0.00	259.23	4.23	201.00
JT6-AT	0.00	264.37	-2.62	201.00
T13-AT	17.35	254.58	3.57	194.72
J8-AT	0.00	253.19	8.18	201.00
T9-AT	12.86	246.53	0.53	197.86
JT7-AT	0.00	302.89	-23.06	0.00
T1-AT	25.79	297.67	7.65	201.00
J9-AT	0.00	322.82	22.77	0.00
JT8-AT	0.00	312.79	17.75	7.72
T2B-AT	31.97	303.06	3.05	201.00
J10-AT	0.00	301.30	3.29	6.18
T11-AT	4.60	301.28	0.28	201.00
T3-AT	16.55	294.86	0.86	201.00
JT9-AT	0.00	269.51	-5.48	201.00
J11-AT	0.00	256.87	1.87	201.00
JT10-AT	0.00	256.90	2.89	201.00
T7-AT	24.71	246.86	1.86	200.99
J12-AT	0.00	254.81	0.81	0.00
T12-AT	9.70	255.17	1.17	0.00
T8-AT	35.08	239.66	3.65	0.00
J1-S17	0.00	227.04	1.04	448.90
J2-S17	0.00	227.31	0.31	448.90
J4T-S17	0.00	227.06	0.06	448.90
J5!-S17	0.00	229.67	-5.32	448.90
J6!-S17	0.00	230.79	-1.20	448.90
J7!-S17	0.00	230.52	-3.47	448.90
T16-S17	8.51	230.24	0.24	448.90
T17-S17	0.00	229.67	-2.33	448.90
T19A-S17	0.00	227.06	1.06	448.90
T19B-S17	0.00	227.06	0.06	448.90
T20-S17	0.00	227.06	1.06	448.90
T21-S17	0.00	230.79	-0.20	448.90

Page 2169
Node Results at 6:05 Hrs: (continued)

Node ID	Demand LPM	Head m	Pressure m	Quality mg/L
V1j-S17	0.00	226.36	2.36	448.90
Vi-T18-S17	0.00	224.93	3.92	0.00
Vj-T18-S17	0.00	224.93	3.92	0.00
V1i-S17	0.00	226.36	2.36	448.90
Vi-ML2	0.00	227.06	0.06	448.90
Vj-ML2	0.00	227.06	0.06	448.90
Vi-T16-S17	0.00	230.51	-3.49	448.90
Vi-T21-S17	0.00	230.79	-0.20	448.90
Vi-T17-S17	0.00	229.67	-5.32	448.90
Vi-T19	0.00	227.06	0.06	448.90
Vj-T19	0.00	227.06	0.06	448.90
Vj-T17-S17	0.00	229.67	-5.32	448.90
Vj-T16-S17	0.00	230.51	-3.49	448.90
Vj-T21-S17	0.00	230.79	-0.20	448.90
Vi-T15-S17	0.00	231.19	0.19	448.90

Vj-T15-S17	0.00	231.19	0.19	448.90
Vj-T14-S17	0.00	232.83	1.83	448.90
Vi-T14-S17	0.00	232.83	1.83	448.90
Vi-T13-S17	0.00	234.41	-3.59	448.90
Vj-T13-S17	0.00	234.41	-3.59	448.90
Vi-T12-S17	0.00	236.23	-1.77	448.90
Vj-T12-S17	0.00	236.23	-1.77	448.90
Vi-TNEW-S17	0.00	236.24	1.23	448.90
Vj-TNEW	0.00	236.24	1.23	448.90
Vi-T11-S17	0.00	241.11	0.11	448.90
Vj-T11-S17	0.00	241.11	0.11	448.90
Vj-T10-S17	0.00	241.85	0.85	448.90
Vi-T10-S17	0.00	241.85	1.85	448.90
Vj-S17beforeT10	0.00	246.36	4.35	448.90
Vi-S17beforeT10	0.00	246.36	4.35	448.90
Vj-T7/8-S17	0.00	249.03	6.01	448.90
Vi-T7/8-S17	0.00	249.03	6.01	448.90
JT-T7/8-S17	0.00	249.03	6.01	448.90
Vi-T9-S17	0.00	249.52	5.51	448.90
Vj-T9-S17	0.00	249.52	5.51	448.90
Vj-T6-S17	0.00	245.94	1.94	448.90
Vi-T6-S17	0.00	245.94	1.94	448.90
Vj-T5-S17	0.00	246.24	2.24	448.90
Vi-T5-S17	0.00	246.24	2.24	448.90
Vi-T4-S17	0.00	259.52	10.50	448.90
Vj-T4-S17	0.00	259.52	10.50	448.90
Vi-T3-S17	0.00	262.79	13.77	448.90
Vj-T3-S17	0.00	262.79	13.77	448.90
Vi-T2-S17	0.00	271.31	18.28	448.90
Vj-T2-S17	0.00	271.31	18.28	448.90
JT-T1/2-S17	0.00	277.72	14.69	448.90
PTBj	0.00	339.05	50.95	448.90

Page 2170
Node Results at 6:05 Hrs: (continued)

Node ID	Demand LPM	Head m	Pressure m	Quality mg/L
Vi-PTB	0.00	277.94	-10.04	448.90
JT-TB2-S17	0.00	338.21	2.21	0.00
Vj-TBR	0.00	339.05	3.04	448.90
Vi-TBR	0.00	339.05	3.04	448.90
JT-TB5-S17	0.00	334.98	3.97	448.90
JT-TB6/7-S17	0.00	333.03	15.00	448.90
JT-TB8-S17	0.00	332.93	19.89	448.90
V1j-BT	0.00	241.99	10.97	160.80
Vj-T3-BT	0.00	242.88	1.87	160.80
Vi-T3-BT	0.00	242.88	1.87	160.80
V2j-BT	0.00	246.11	7.09	160.80
Vi-T1-BT	0.00	250.17	0.17	160.80
Vj-T1-BT	0.00	250.17	0.17	160.80
Vj-branchT4-BT	0.00	268.98	1.98	160.80
JbranchT10-BT	0.00	269.37	3.36	160.80
Vj-branchT10-BT	0.00	268.21	2.21	160.80
JTbranches-BT	0.00	269.37	3.37	160.80
JT-branchT5-BT	0.00	269.38	3.37	160.80

Vj-branchT5-BT	0.00	266.63	-0.37	160.80
JT-T5-BT	0.00	244.01	3.00	160.80
Vj-T13-BT	0.00	248.95	-0.05	160.80
Vi-T13-BT	0.00	248.95	-0.05	160.80
Vj-T5-BT	0.00	243.65	2.64	160.80
Vi-T5-BT	0.00	243.65	2.64	160.80
Vj-T6-BT	0.00	238.58	1.57	160.80
Vi-T6-BT	0.00	238.58	1.57	160.80
JT-T7-BT	0.00	257.24	5.22	160.80
Vj-T7-BT	0.00	256.86	5.85	160.80
Vi-T7-BT	0.00	256.86	5.85	160.80
Vi-T9/10-BT	0.00	248.03	-1.96	160.80
Vj-T9/10-BT	0.00	248.03	-1.96	160.80
Vj-T8-BT	0.00	237.05	2.04	160.80
Vi-T8-BT	0.00	237.05	2.04	160.80
Vj-T9-BT	0.00	239.95	-5.04	160.80
Vi-T9-BT	0.00	239.95	-5.04	160.80
JT-T9-BT	0.00	239.95	-5.04	160.80
Vj-T10-BT	0.00	226.32	1.32	160.80
Vi-T10-BT	0.00	226.32	1.32	160.80
JT-T4-MOI	0.00	225.85	-11.12	167.50
Vj-T3-MOI	0.00	222.32	0.32	167.50
Vi-T3-MOI	0.00	222.32	0.32	167.50
JT-T1-MOI	0.00	226.91	-6.07	167.50
JT-T27-MOI	0.00	222.84	2.83	167.50
Vj-toT7-MOI	0.00	218.62	7.61	167.50
Vi-toT7-MOI	0.00	218.62	7.61	167.50
Vj-T7-MOI	0.00	216.05	2.05	167.50
Vi-T7-MOI	0.00	216.05	2.05	167.50

Page 2171
Node Results at 6:05 Hrs: (continued)

Node ID	Demand LPM	Head m	Pressure m	Quality mg/L
JT-T31B-MOI	0.00	217.00	4.99	167.50
JT-T32-MOI	0.00	217.00	7.98	167.50
Vj-JT7-MOI	0.00	217.00	7.98	167.50
Vi-JT7-MOI	0.00	217.00	7.98	167.50
Vi-brancT29-MOI	0.00	227.34	2.33	167.50
Vj-brancT29-MOI	0.00	227.34	2.33	167.50
JT-T19-MOI	0.00	225.13	3.12	167.50
JT-T153-MOI	0.00	221.51	3.51	167.50
JT-T26-MOI	0.00	219.80	-0.20	167.50
JT-T51-MOI	0.00	219.91	-0.09	167.50
Vi-T26-MOI	0.00	219.79	-0.21	167.50
Vj-T26-MOI	0.00	219.79	-0.21	167.50
Vj-JT9-MOI	0.00	219.78	-0.22	167.50
Vi-JT9-MOI	0.00	219.78	-0.22	167.50
Vi-T150-MOI	0.00	219.55	1.55	167.50
Vj-T150-MOI	0.00	219.55	1.55	167.50
JT-T23-MOI	0.00	216.93	3.92	167.50
Vj-T24-MOI	0.00	209.88	0.87	167.50
Vi-T24-MOI	0.00	209.88	0.87	167.50
Vj-T25-MOI	0.00	209.78	0.78	167.50
Vi-T25-MOI	0.00	209.78	0.78	167.50

Vj-T20-MOI	0.00	219.91	0.91	167.50
Vi-T20-MOI	0.00	219.91	0.91	167.50
JT-T20-MOI	0.00	220.03	3.03	167.50
Vj-T21-MOI	0.00	219.02	3.01	167.50
Vi-T21-MOI	0.00	219.02	3.01	167.50
Vj-T15-MOI	0.00	219.09	3.08	167.50
Vi-T15-MOI	0.00	219.09	3.08	167.50
JT-T15-MOI	0.00	221.67	5.65	167.50
Vj-T16-MOI	0.00	219.72	3.72	167.50
Vi-T16-MOI	0.00	219.72	3.72	167.50
JT-T16-MOI	0.00	220.51	4.50	167.50
Vj-T17-MOI	0.00	215.52	0.51	167.50
Vj-T18-MOI	0.00	213.39	0.39	167.50
Vi-T18-MOI	0.00	213.39	0.39	167.50
Vj-T13-MOI	0.00	221.52	0.52	167.50
Vi-T13-MOI	0.00	221.52	0.52	167.50
JT-T13-MOI	0.00	221.61	0.61	167.50
Vi-brancT12-MOI	0.00	227.41	0.41	0.00
Vj-brancT12-MOI	0.00	227.41	0.41	167.50
Vj-T14-MOI	0.00	213.96	1.96	167.50
Vi-T14-MOI	0.00	213.96	-1.03	167.50
Vj-T8-MOI	0.00	219.55	2.54	167.50
Vi-T8-MOI	0.00	219.55	2.54	167.50
Vj-T9-MOI	0.00	219.41	11.38	167.50
Vi-T9-MOI	0.00	219.41	11.38	167.50
JT-T9-MOI	0.00	219.55	11.52	167.50

Page 2172
Node Results at 6:05 Hrs: (continued)

Node ID	Demand LPM	Head m	Pressure m	Quality mg/L
JT18!-MOI	0.00	217.56	2.56	167.50
Vj-T11-MOI	0.00	215.72	-0.28	167.50
Vi-T11-MOI	0.00	215.72	-0.28	167.50
JT-T11-MOI	0.00	215.77	-0.23	167.50
Vj-T12-MOI	0.00	213.44	0.44	167.50
Vi-T12-MOI	0.00	213.44	0.44	167.50
Vi-brancT3-CH	0.00	277.09	3.09	154.10
Vj-brancT3-CH	0.00	277.09	4.08	154.10
Vj-T2-CH	0.00	263.84	4.83	154.10
Vj-T1-CH	0.00	254.70	3.69	154.10
Vi-T1-CH	0.00	254.70	3.69	154.10
JT-T1-CH	0.00	254.79	3.78	154.10
Vj-T3-CH	0.00	254.63	4.62	154.10
J2!-CH	0.00	277.10	4.10	154.10
Vj-T4-CH	0.00	270.06	2.06	154.10
Vi-T4-CH	0.00	270.06	2.06	154.10
Vi-JT3-CH	0.00	274.48	4.47	154.10
Vj-JT3-CH	0.00	274.48	4.47	154.10
Vj-T5-CH	0.00	266.47	11.44	154.10
Vi-T5-CH	0.00	266.47	11.44	154.10
JT-T5-CH	0.00	266.64	11.62	154.10
Vj-brancT10-CH	0.00	258.29	40.21	154.10
Vi-toT18-S17	0.00	258.22	40.14	154.10
Vj-toT18-S17	0.00	258.22	40.14	154.10

JT3!-CH	0.00	258.22	40.14	154.10
V5j-CH	0.00	257.32	37.24	154.10
Vj-T7-CH	0.00	226.68	5.67	154.10
Vi-T7-CH	0.00	226.68	5.67	154.10
Vj-T6-CH	0.00	216.44	2.44	0.00
Vi-T6-CH	0.00	216.44	2.44	154.10
Vj-T11-CH	0.00	230.69	7.67	154.10
Vj-T10-CH	0.00	223.41	1.41	154.10
Vi-T10-CH	0.00	223.41	1.41	154.10
V7j-CH	0.00	224.46	-0.54	154.10
Vj-T6-AT	0.00	239.93	2.93	0.00
Vi-T6-AT	0.00	239.93	2.93	201.00
Vj-T5-AT	0.00	241.73	2.73	0.00
Vi-T5-AT	0.00	241.73	3.72	0.00
Vi-JT1-AT	0.00	245.91	5.90	0.00
Vj-JT1-AT	0.00	245.91	5.90	0.00
Vi-S14RING	0.00	311.78	1.77	0.00
Vj-S14RING	0.00	311.78	1.77	0.00
Vj-JT5-AT	0.00	257.18	1.17	0.00
Vi-JT5-AT	0.00	257.18	1.17	0.00
Vj-T13-AT	0.00	256.02	5.01	0.00
Vi-T13-AT	0.00	256.02	5.01	201.00
Vj-T9-AT	0.00	246.59	0.59	0.00

Page 2173
Node Results at 6:05 Hrs: (continued)

Node ID	Demand LPM	Head m	Pressure m	Quality mg/L
Vi-T9-AT	0.00	246.59	0.59	201.00
Vi-suggesT10-AT	0.00	245.91	-6.08	0.01
Vj-suggesT10-AT	0.00	311.77	58.66	0.00
Vi-T1-AT	0.00	302.79	-20.17	201.00
Vj-T1-AT	0.00	302.79	-20.17	201.00
JT-T12-AT	0.00	255.29	2.29	201.00
Vj-T7-AT	0.00	247.28	2.27	0.00
Vi-T7-AT	0.00	247.28	2.27	201.00
Vj-T8-AT	0.00	240.85	3.85	0.00
Vi-T8-AT	0.00	240.85	3.85	0.00
Vj-T2B-AT	0.00	303.82	3.81	97.91
Vi-T2B-AT	0.00	303.82	3.81	201.00
Vj-T11-AT	0.00	301.52	0.52	201.00
Vi-T11-AT	0.00	301.52	0.52	6.18
JT-T11-AT	0.00	301.53	0.52	0.00
Vj-T3-AT	0.00	295.03	1.03	200.80
Vi-T3-AT	0.00	295.03	1.03	201.00
Vj-T2-S67	0.00	244.62	8.61	237.60
Vi-T2-S67	0.00	244.62	8.61	0.00
JT-T2-S67	0.00	246.16	11.14	0.00
Vi-S67RING	0.00	251.21	3.20	237.60
Vj-S67RING	0.00	251.21	3.20	237.60
JT-S67RING	0.00	251.19	3.18	0.00
V1j-S67	0.00	250.76	3.75	237.60
Vj-T1-S67	0.00	245.44	1.44	237.60
Vi-T1-S67	0.00	245.44	1.44	237.59
Vj-toS67RING	0.00	268.48	12.45	160.80

Vi-toS67RING	0.00	268.48	12.45	160.80
J-toS67RING	0.00	268.37	21.33	160.80
JT-toT5-CT	0.00	268.19	20.15	0.00
Vi-pourS67RING	0.00	268.19	20.15	0.00
Vj-pourS67RING	0.00	251.27	3.27	0.00
JT-T5-S67	0.00	207.41	-0.59	0.00
Vj-18-5	0.00	207.41	-2.58	0.00
Vi-T5-S67	0.00	207.47	-0.53	234.84
Vj-T5-S67	0.00	207.47	-0.53	0.00
Vj-T7-S67	0.00	209.69	2.68	4.97
Vi-T7-S67	0.00	209.69	2.68	0.00
JT-T7-S67	0.00	209.86	2.85	237.60
Vi-TNEW-S67	0.00	214.39	5.38	237.60
Vj-TNEW-S67	0.00	214.39	5.38	237.60
JT-T4-S67	0.00	216.22	13.19	0.00
Vi-T4-S67	0.00	214.79	11.77	0.00
Vj-T4-S67	0.00	214.79	11.77	0.00
V2j-S67	0.00	220.42	10.40	237.60
Vi-ML1-S67	0.00	222.94	16.90	237.60
Vj-ML1-S67	0.00	222.94	16.90	237.60

Page 2174
Node Results at 6:05 Hrs: (continued)

Node ID	Demand LPM	Head m	Pressure m	Quality mg/L
Vi-brancT5-S67	0.00	222.92	16.89	237.60
Vj-brancT5-S67	0.00	222.92	16.89	237.60
Vi-toML1	0.00	222.94	15.90	0.00
Vj-toML1	0.00	222.94	15.90	0.00
Vi-toTIMhouse	0.00	222.94	15.90	237.60
Vj-toTIMhouse	0.00	222.94	15.90	237.60
V3j-S67	0.00	222.94	7.92	237.60
V4i-S67	0.00	222.94	11.91	237.60
JT-TEMRIN3	0.00	241.41	2.40	0.01
JT-TEMT3	0.00	242.04	2.04	0.01
JT-TEMRIN1	0.00	242.16	2.16	160.80
JT-TEMT2	0.00	245.46	8.45	160.80
Vi-brancT8-CT	0.00	268.96	2.95	0.00
Vj-brancT8-CT	0.00	268.96	2.95	160.80
Vj-T1-CT	0.00	266.83	15.80	160.80
Vi-T1-CT	0.00	266.83	14.80	160.80
JT-T1-CT	0.00	268.04	16.01	160.80
Vj-T3-CT	0.00	230.48	6.46	160.80
Vi-T3-CT	0.00	230.48	6.46	160.80
V2j-CT	0.00	245.40	11.38	160.80
V3i-CT	0.00	240.53	5.52	160.80
V4i-CT	0.00	228.29	5.28	160.80
Vj-T4-CT	0.00	222.21	5.20	160.80
Vi-T4-CT	0.00	222.21	5.20	160.80
JT-T5-CT	0.00	252.60	22.55	160.80
Vj-T5-CT	0.00	242.04	12.02	160.80
Vi-T5-CT	0.00	242.04	12.02	160.80
V5j-CT	0.00	252.37	24.32	160.80
Vj-T6-CT	0.00	224.04	6.03	160.80
Vi-T6-CT	0.00	224.04	6.03	160.80

JT-T6-CT	0.00	225.99	7.97	160.80
Vj-T7-CT	0.00	223.28	0.28	160.80
Vi-T7-CT	0.00	223.28	0.28	160.80
Vj-T8-CT	0.00	223.43	0.42	160.80
Vi-T8-CT	0.00	223.43	0.42	160.80
Vi-JT1-S8	0.00	223.30	4.29	234.50
Vj-JT1-S8	0.00	223.30	4.29	234.50
Vj-T3-S8	0.00	219.10	2.10	234.50
Vi-T3-S8	0.00	219.10	2.10	234.50
Vj-T2-S8	0.00	232.66	2.65	234.50
Vi-T2-S8	0.00	232.66	2.65	234.50
Vi-JT4-S8	0.00	256.25	0.25	234.50
Vj-JT4-S8	0.00	256.25	0.25	234.50
Vj-T1-S8	0.00	240.04	1.04	234.50
Vi-T1-S8	0.00	240.04	1.04	234.50
Vj-JT5-S8	0.00	259.06	1.06	234.50
Vi-JT5-S8	0.00	259.06	1.06	234.50

Page 2175
Node Results at 6:05 Hrs: (continued)

Node ID	Demand LPM	Head m	Pressure m	Quality mg/L
Vj-T4-S8	0.00	255.92	0.92	234.50
Vi-T4-S8	0.00	255.92	0.92	234.50
JT-T4-S8	0.00	256.30	1.30	234.50
Vi-toS8RING	0.00	268.97	1.97	234.49
Vj-toS8RING	0.00	260.01	-5.98	234.50
V6i-S8	0.00	256.01	2.00	234.50
Vj-T5-S8	0.00	248.32	12.30	234.50
Vi-T5-S8	0.00	248.32	12.30	234.50
J-T5-S8	0.00	248.43	12.40	234.50
JT-T5-S8	0.00	248.46	12.43	234.50
Vj-T6-S8	0.00	220.20	3.20	234.50
Vi-T6-S8	0.00	220.20	3.20	234.50
Vi-JT6-S8	0.00	229.29	10.27	234.50
Vj-JT6-S8	0.00	229.29	10.27	234.50
Vi-CHT2	0.00	277.71	1.71	0.00
Vj-CHT2	0.00	277.67	1.67	0.00
Vi-CHT1	0.00	277.67	1.67	153.47
Vi-CHTout	0.00	277.67	1.67	0.00
Vj-CHTout	0.00	277.67	1.67	0.00
Vi-BT1	0.00	270.18	2.17	160.46
Vj-BT1	0.00	270.18	2.17	0.00
Vi-BT2	0.00	270.21	2.21	0.00
Vj-BT2	0.00	270.18	2.17	0.00
Vj-BTout	0.00	270.18	2.17	0.00
Vj-CHT1	0.00	277.67	1.67	0.00
Vi-BTout	0.00	270.18	2.17	0.00
Vi-17Tout	0.00	277.93	2.92	448.25
Vj-17Tout	0.00	277.93	2.92	0.00
Vi-TBRINGSout	0.00	338.84	2.83	455.60
Vj-TBRINGSout	0.00	338.84	2.83	455.60
Vi-MOITout	0.00	227.41	0.41	167.26
Vj-MOITout	0.00	227.41	0.41	0.00
Vi-CTout	0.00	268.97	1.97	160.59

Vj-CTout	0.00	268.97	1.97	0.00
Vi-AT-OLDout	0.00	325.81	1.81	200.50
Vj-AT-OLDout	0.00	325.81	1.81	200.66
PSVi-MAELA2	0.00	227.06	0.06	448.90
PSVj-MAELA2	0.00	227.06	0.06	0.01
PSVi-ML1	0.00	222.94	14.91	0.01
PSVj-ML1	0.00	207.00	0.00	0.00
PSVi-TEMRIN2	0.00	241.01	1.01	0.00
PSVj-TEMRIN2	0.00	241.01	1.01	0.00
PSVj-TEMRIN3	0.00	235.03	0.03	0.00
PSVi-TEMRIN3	0.00	236.00	0.00	0.01
PSVi-TEMRIN1	0.00	242.03	0.03	0.01
PSVj-TEMRIN1	0.00	242.03	0.03	0.00
PSVi-S8RIN	0.00	260.01	3.00	0.00

Page 2176
Node Results at 6:05 Hrs: (continued)

Node ID	Demand LPM	Head m	Pressure m	Quality mg/L	
PSVj-S8RIN	0.00	260.01	3.00	0.00	
FCVi-CHT1	0.00	286.00	9.98	0.00	
FCVj-CHT1	0.00	277.68	1.67	0.00	
FCVi-AT-OLD	0.00	334.00	9.98	0.00	
FCVj-AT-OLD	0.00	325.97	1.97	0.00	
FCVi-MOIT	0.00	236.00	9.98	0.00	
FCVj-MOIT	0.00	227.43	1.43	0.00	
FCVi-17T	0.00	285.00	9.98	0.00	
FCVj-17T	0.00	277.94	2.94	0.00	
FCVi-CT	0.00	277.00	9.98	0.00	
FCVj-CT	0.00	268.98	1.98	0.00	
FCVi-BT	0.00	278.00	9.98	0.00	
FCVj-BT	0.00	270.19	2.18	0.00	
Vi-T23-MOI	0.00	216.41	3.41	167.50	
Vj-T23-MOI	0.00	216.41	3.41	0.00	
17T	-210.40	277.94	2.94	448.27	Tank
TBRINGS	-100.12	339.05	3.04	455.60	Tank
BT1	-238.90	270.19	2.18	160.48	Tank
MOIT	-473.38	227.43	1.43	167.28	Tank
CHT1	-222.06	277.68	1.67	153.54	Tank
S67RING	-126.01	251.27	3.27	237.60	Tank
CT	-333.11	268.98	1.98	160.60	Tank
ML1RING	0.00	207.00	0.00	0.00	Tank
TEMRIN1	8.70	242.03	0.03	0.00	Tank
TEMRIN2	2.66	241.01	0.01	0.00	Tank
TEMRIN3	9.26	235.03	0.03	0.00	Tank
S8RIN	-188.81	260.01	3.00	234.50	Tank
S14-RING	-14.36	311.78	2.77	0.00	Tank
AT-NEW	0.00	310.10	2.10	0.00	Tank
AT-OLD	-253.05	325.97	1.97	200.54	Tank
MAELA2-RIN	57.03	227.06	0.06	0.00	Tank
CHT2	0.00	277.71	1.71	0.00	Tank
BT2	0.00	270.21	2.21	0.00	Tank
Salt-CHT1	-0.10	286.00	9.98	0.00	Tank
Salt-AT-OLD	-0.10	334.00	9.98	0.00	Tank
Salt-MOIT	-0.10	236.00	9.98	0.00	Tank

Salt-17T	-0.10	285.00	9.98	0.00 Tank
Salt-CT	-0.10	277.00	9.98	0.00 Tank
Salt-BT1	-0.10	278.00	9.98	0.00 Tank

Page 2177
Link Results at 6:05 Hrs:

Link ID	Flow LPM	Velocity m/s	Unit Headloss m/km	Status
S17-1	19.34	1.13	71.68	Open
S17-2	19.33	0.64	17.65	Open
S17-3	19.33	0.64	17.65	Open
S17-4	19.33	0.28	2.45	Open
S17-5	19.34	0.28	2.45	Open
S17-6	84.89	0.70	10.59	Open
S17-7	8.51	0.50	17.76	Open
S17-8	0.00	0.00	0.00	Open
S17-9	76.38	0.63	8.71	Open
S17-10	0.00	0.00	0.00	Open
S17-11	0.00	0.00	0.00	Open
S17-12	0.00	0.00	0.00	Open
S17-13	0.00	0.00	0.00	Open
S17-15	76.38	0.63	8.71	Open
S17-16	0.01	0.00	0.00	Open
S17-17	0.01	0.00	0.00	Open
S17-18	84.89	0.70	10.59	Open
S17-19	0.00	0.00	0.00	Open
S17-20	8.51	0.50	17.75	Open
S17-21	0.00	0.00	0.00	Open
S17-22	0.00	0.00	0.00	Open
S17-23	84.90	0.70	10.59	Open
S17-24	13.37	1.76	295.52	Open
S17-25	0.00	0.00	0.00	Open
S17-26	0.00	0.00	0.00	Open
S17-27	13.37	0.78	41.02	Open
S17-28	13.37	0.78	41.01	Open
S17-29	98.26	0.81	13.88	Open
S17-30	5.78	0.19	2.14	Open
S17-31	5.78	0.19	2.14	Open
S17-32	5.78	0.34	8.68	Open
S17-33	104.05	0.86	15.43	Open
S17-34	0.00	0.00	0.00	Open
S17-35	0.00	0.00	0.00	Closed
S17-36	104.05	0.86	15.43	Open
S17-37	9.85	0.58	23.28	Open
S17-38	9.85	1.30	167.79	Open
S17-39	9.84	1.30	167.73	Open
S17-40	113.89	0.94	18.25	Open
S17-41	0.00	0.00	0.00	Open
S17-42	0.00	0.00	0.00	Open
S17-43	113.90	0.94	18.25	Open
S17-44	13.39	0.78	41.12	Open
S17-45	13.39	1.76	296.36	Open
S17-46	13.38	1.76	296.21	Open
S17-47	127.28	1.05	22.42	Open

S17-48	127.28	1.05	22.42	Open

Page 2178
Link Results at 6:05 Hrs: (continued)

Link ID	Flow LPM	Velocity m/s	Unit Headloss m/km	Status
S17-49	0.00	0.00	0.00	Open
S17-50	0.00	0.00	0.00	Open
S17-51	0.00	0.00	0.00	Open
S17-52	0.00	0.00	0.00	Open
S17-53	0.00	0.00	0.00	Open
S17-54	127.29	1.05	22.42	Open
S17-55	0.00	0.00	0.00	Open
S17-56	0.00	0.00	0.00	Open
S17-57	26.96	1.58	150.39	Open
S17-58	15.58	0.91	54.47	Open
S17-59	127.29	1.05	22.42	Open
S17-60	42.55	1.40	86.21	Open
S17-61	26.96	1.58	150.39	Open
S17-62	15.59	0.51	13.42	Open
S17-63	15.59	0.91	54.50	Open
S17-64	169.84	1.40	38.24	Open
S17-65	17.89	0.59	17.31	Open
S17-66	17.90	1.05	70.39	Open
S17-67	17.90	2.35	507.25	Open
S17-68	187.73	1.54	46.04	Open
S17-69	0.00	0.00	0.00	Open
S17-70	0.00	0.00	0.00	Open
S17-71	187.74	1.54	46.04	Open
S17-72	22.75	1.33	109.81	Open
S17-73	22.75	1.33	109.83	Open
S17-74	210.49	1.73	56.90	Open
S17-75	210.49	1.73	56.90	Open
S17-76	210.50	1.73	56.91	Open
S17-77	0.01	0.00	0.00	Open
S17-78	0.00	0.00	0.00	Open
S17-79	0.00	0.00	0.00	Open
S17-80	210.50	0.77	7.90	Open
S17-81	-0.00	0.00	0.00	Open
S17-82	8.41	1.11	125.35	Open
S17-83	41.39	1.36	81.89	Open
S17-84	4.88	0.64	45.39	Open
S17-85	38.15	1.25	70.45	Open
S17-86	58.72	1.93	156.55	Open
S17-87	46.57	1.53	101.89	Open
S17-88	12.15	1.60	247.77	Open
S17-89	-0.01	0.00	0.00	Open
S17-90	-0.00	0.00	0.00	Open
S17-91	36.51	1.20	64.92	Open
S17-92	8.51	1.12	127.92	Open
S17-93	28.00	0.92	39.72	Open
S17-94	0.00	0.00	0.00	Open
S17-95	0.00	0.00	0.00	Closed

Page 2179
Link Results at 6:05 Hrs: (continued)

Link ID	Flow LPM	Velocity m/s	Unit Headloss m/km	Status
S17-96	0.00	0.00	0.00	Closed
S17-97	28.00	0.92	39.72	Open
S17-98	28.00	3.68	1162.20	Open
S17-99	0.00	0.00	0.00	Open
S17-100	0.00	0.00	0.00	Closed
S17-101	0.00	0.00	0.00	Closed
BT-1	23.47	1.37	116.33	Open
BT-2	23.47	0.77	28.65	Open
BT-3	23.48	0.77	28.66	Open
BT-4	23.08	1.35	112.79	Open
BT-5	23.08	3.04	812.60	Open
BT-6	46.56	1.53	101.86	Open
BT-7	46.56	0.68	14.14	Open
BT-8	23.13	0.76	27.88	Open
BT-9	23.13	0.76	27.88	Open
BT-10	23.13	1.35	113.16	Open
BT-11	69.69	1.02	29.83	Open
BT-12	69.69	1.02	29.83	Open
BT-13	69.69	1.02	29.83	Open
BT-14	22.63	0.74	26.77	Open
BT-15	22.63	1.32	108.70	Open
BT-16	92.32	1.35	50.21	Open
BT-17	13.89	1.83	317.16	Open
BT-18	106.21	1.55	65.09	Open
BT-19	105.58	1.54	64.39	Open
BT-20	106.21	0.39	2.23	Open
BT-21	105.58	0.39	2.20	Open
BT-22	211.79	0.77	8.00	Open
BT-23	27.20	1.59	152.84	Open
BT-24	27.20	1.59	152.84	Open
BT-25	0.00	0.00	0.00	Closed
BT-26	-0.00	0.00	0.00	Open
BT-27	14.79	1.95	356.50	Open
BT-28	14.79	1.95	356.26	Open
BT-29	12.41	1.63	257.33	Open
BT-30	12.41	0.73	35.73	Open
BT-31	105.58	1.54	64.39	Open
BT-32	106.21	1.55	65.09	Open
BT-33	9.92	1.31	170.14	Open
BT-34	44.28	5.83	2716.49	Open
BT-35	44.28	2.59	376.94	Open
BT-36	51.38	0.75	16.96	Open
BT-37	95.66	1.40	53.63	Open
BT-38	51.38	1.69	122.23	Open
BT-39	26.90	0.88	36.88	Open
BT-40	26.90	1.57	149.75	Open
BT-41	24.47	3.22	905.60	Open

Page 2180
Link Results at 6:05 Hrs: (continued)

Link ID	Flow LPM	Velocity m/s	Unit Headloss m/km	Status

BT-42	24.48	1.43	125.71	Open
BT-43	0.00	0.00	0.00	Closed
BT-44	0.00	0.00	0.00	Open
BT-45	26.90	1.57	149.75	Open
BT-46	26.90	3.54	1078.94	Open
BT-47	26.90	1.57	149.74	Open
MOI-1	0.00	0.00	0.00	Open
MOI-2	0.00	0.00	0.00	Open
MOI-3	31.54	1.04	49.53	Open
MOI-4	31.54	0.46	6.87	Open
MOI-5	0.00	0.00	0.00	Open
MOI-6	31.54	0.46	6.87	Open
MOI-7	40.28	0.59	10.81	Open
MOI-8	0.00	0.00	0.00	Open
MOI-9	8.74	1.15	134.41	Open
MOI-10	8.74	1.15	134.46	Open
MOI-11	40.28	0.59	10.81	Open
MOI-12	0.00	0.00	0.00	Closed
MOI-13	40.28	0.59	10.81	Open
MOI-14	31.54	1.04	49.51	Open
MOI-15	14.68	1.93	351.26	Open
MOI-16	16.86	0.55	15.53	Open
MOI-17	16.87	0.99	63.08	Open
MOI-18	16.86	0.99	63.06	Open
MOI-19	0.00	0.00	0.00	Open
MOI-20	16.87	0.99	63.07	Open
MOI-21	16.85	2.22	453.77	Open
MOI-22	16.85	0.99	62.96	Open
MOI-23	0.02	0.00	0.00	Open
MOI-24	0.00	0.00	0.00	Open
MOI-25	0.01	0.00	0.00	Open
MOI-26	0.00	0.00	0.00	Open
MOI-27	0.00	0.00	0.00	Open
MOI-28	0.01	0.00	0.00	Open
MOI-29	0.01	0.00	0.00	Open
MOI-30	0.01	0.00	0.00	Open
MOI-31	0.00	0.00	0.00	Open
MOI-32	0.00	0.00	0.00	Open
MOI-33	244.05	0.89	10.38	Open
MOI-34	153.11	0.56	4.36	Open
MOI-35	153.11	0.56	4.38	Open
MOI-36	153.11	0.81	10.64	Open
MOI-37	26.28	3.46	1033.28	Open
MOI-38	153.11	2.24	128.15	Open
MOI-39	0.00	0.00	0.00	Open
MOI-40	126.83	1.85	90.42	Open
MOI-41	126.83	1.85	90.42	Open

Page 2181
Link Results at 6:05 Hrs: (continued)

Link ID	Flow LPM	Velocity m/s	Unit Headloss m/km	Status
MOI-42	0.00	0.00	0.00	Open
MOI-43	109.57	1.60	68.95	Open

MOI-44	109.57	1.60	68.96	Open
MOI-45	17.60	0.58	16.84	Open
MOI-46	91.97	1.34	49.88	Open
MOI-47	91.97	1.34	49.86	Open
MOI-48	14.55	1.91	345.96	Open
MOI-49	14.55	1.91	345.83	Open
MOI-50	77.41	1.13	36.24	Open
MOI-51	33.02	4.34	1577.47	Open
MOI-52	44.39	0.65	12.94	Open
MOI-53	16.06	0.94	57.61	Open
MOI-54	16.06	2.11	414.98	Open
MOI-55	16.06	2.11	415.18	Open
MOI-56	28.33	0.41	5.63	Open
MOI-57	28.33	0.93	40.59	Open
MOI-58	28.33	0.93	40.59	Open
MOI-59	5.37	0.71	54.60	Open
MOI-60	5.37	0.18	1.87	Open
MOI-61	22.96	1.34	111.68	Open
MOI-62	22.96	1.34	111.67	Open
MOI-63	8.43	1.11	125.83	Open
MOI-64	8.43	1.11	125.74	Open
MOI-65	17.26	0.57	16.21	Open
MOI-66	8.83	0.29	4.69	Open
MOI-67	8.83	1.16	137.03	Open
MOI-68	8.83	0.52	19.03	Open
MOI-69	17.60	0.58	16.81	Open
MOI-70	17.60	1.03	68.26	Open
MOI-71	90.94	0.48	4.06	Open
MOI-72	29.60	3.90	1288.61	Open
MOI-73	29.61	3.90	1288.59	Open
MOI-74	90.94	1.33	48.83	Open
MOI-75	32.02	4.21	1490.07	Open
MOI-76	32.02	4.21	1489.93	Open
MOI-77	61.33	0.90	23.55	Open
MOI-78	29.31	0.96	43.23	Open
MOI-79	29.31	0.96	43.23	Open
MOI-80	13.57	0.79	42.15	Open
MOI-81	13.57	0.79	42.16	Open
MOI-82	15.74	0.52	13.67	Open
MOI-83	15.74	2.07	400.24	Open
MOI-84	15.74	2.07	400.17	Open
MOI-85	38.74	0.57	10.06	Open
MOI-86	38.74	1.27	72.46	Open
MOI-87	15.87	2.09	406.05	Open
MOI-88	15.87	2.09	406.20	Open

Page 2182
Link Results at 6:05 Hrs: (continued)

Link ID	Flow LPM	Velocity m/s	Unit Headloss m/km	Status
MOI-89	38.74	1.27	72.46	Open
MOI-90	189.15	0.69	6.46	Open
MOI-91	189.15	0.69	6.48	Open
MOI-92	22.87	3.01	798.71	Open
MOI-93	22.87	1.34	110.83	Open
MOI-94	150.41	0.55	4.24	Open
MOI-95	27.45	3.61	1120.24	Open
MOI-96	27.45	1.61	155.46	Open
MOI-97	122.95	1.01	21.03	Open
MOI-98	60.42	3.53	670.07	Open
MOI-99	60.42	3.53	670.08	Open
MOI-100	122.95	1.80	85.37	Open
MOI-101	62.54	0.91	24.41	Open
MOI-102	16.94	0.99	63.60	Open
MOI-103	45.60	0.67	13.59	Open
MOI-104	21.59	1.26	99.66	Open
MOI-105	21.59	1.26	99.67	Open
MOI-106	21.59	1.26	99.67	Open
MOI-107	0.00	0.00	0.00	Closed
MOI-108	24.00	0.35	4.14	Open
MOI-109	24.00	0.79	29.86	Open
MOI-110	17.10	0.56	15.93	Open
MOI-111	6.91	0.91	87.00	Open
MOI-112	17.09	1.00	64.62	Open
MOI-113	17.10	1.00	64.67	Open
CH-1	222.15	1.83	62.88	Open
CH-2	35.08	1.15	60.28	Open
CH-3	35.07	1.15	60.27	Open
CH-4	35.07	2.05	244.73	Open
CH-5	0.00	0.00	0.00	Open
CH-6	0.00	0.00	0.00	Open
CH-7	19.79	2.60	611.06	Open
CH-8	19.79	2.60	610.99	Open
CH-9	35.07	2.05	244.70	Open
CH-10	15.28	0.89	52.55	Open
CH-11	15.28	2.01	378.54	Open
CH-12	187.08	1.54	45.75	Open
CH-13	187.08	2.73	185.73	Open
CH-14	12.50	1.65	261.17	Open
CH-15	12.51	1.65	261.26	Open
CH-16	174.57	2.55	163.28	Open
CH-17	31.59	4.16	1453.40	Open
CH-18	31.59	4.16	1453.35	Open
CH-19	174.57	2.55	163.39	Open
CH-20	142.98	2.09	112.87	Open
CH-21	0.00	0.00	0.00	Open
CH-22	142.98	2.09	112.89	Open

Page 2183
Link Results at 6:05 Hrs: (continued)

Link ID	Flow LPM	Velocity m/s	Unit Headloss m/km	Status
CH-23	142.97	2.09	112.88	Open
CH-24	142.97	2.09	112.88	Open
CH-25	107.70	1.57	66.79	Open
CH-26	43.25	0.63	12.33	Open
CH-27	0.00	0.00	0.00	Closed
CH-28	64.44	3.77	755.10	Open
CH-29	64.44	3.77	755.11	Open
CH-30	35.28	4.64	1782.77	Open
CH-31	35.27	4.64	1782.62	Open
CH-32	43.25	0.63	12.33	Open
CH-33	11.73	0.69	32.18	Open
CH-34	11.73	0.69	32.17	Open
CH-35	11.73	1.54	231.86	Open
CH-36	31.53	1.04	49.47	Open
CH-37	0.00	0.00	0.00	Open
CH-38	31.52	1.04	49.46	Open
CH-39	31.52	1.84	200.83	Open
CH-40	31.52	1.84	200.84	Open
CH-41	0.00	0.00	0.00	Open
CH-42	0.00	0.00	0.00	Open
AT-1	27.46	3.61	1121.34	Open
AT-2	27.46	1.61	155.59	Open
AT-3	29.19	1.71	174.16	Open
AT-4	29.19	1.71	174.22	Open
AT-5	29.19	0.96	42.89	Open
AT-6	27.46	0.90	38.32	Open
AT-7	-0.01	0.00	0.00	Open
AT-8	-0.00	0.00	0.00	Open
AT-9	-0.00	0.00	0.00	Open
AT-10	0.00	0.00	0.00	Open
AT-11	0.00	0.00	0.00	Open
AT-12	0.00	0.00	0.00	Closed
AT-13	14.36	0.21	1.60	Open
AT-14	14.36	0.21	1.60	Open
AT-15	14.36	0.47	11.53	Open
AT-16	14.36	1.89	337.47	Open
AT-17	14.36	0.84	46.83	Open
AT-18	14.36	0.84	46.83	Open
AT-19	14.36	1.89	337.48	Open
AT-20	56.65	1.86	146.49	Open
AT-21	17.91	1.05	70.47	Open
AT-22	56.65	1.86	146.47	Open
AT-23	74.56	2.45	243.61	Open
AT-24	74.56	1.09	33.80	Open
AT-25	17.35	2.28	479.05	Open
AT-26	30.21	1.77	185.65	Open
AT-27	12.86	0.75	38.18	Open

Page 2184
Link Results at 6:05 Hrs: (continued)

Link ID	Flow LPM	Velocity m/s	Unit Headloss m/km	Status

AT-28	12.86	1.69	275.07	Open
AT-29	12.86	1.69	275.16	Open
AT-30	-0.00	0.00	0.00	Open
AT-31	-0.00	0.00	0.00	Open
AT-32	200.03	2.92	210.25	Open
AT-33	25.78	1.51	138.43	Open
AT-34	25.79	1.51	138.44	Open
AT-35	174.25	2.55	162.83	Open
AT-36	104.77	1.53	63.47	Open
AT-37	9.70	1.28	163.08	Open
AT-38	69.48	2.29	213.77	Open
AT-39	24.70	0.81	31.50	Open
AT-40	24.71	3.25	921.74	Open
AT-41	24.70	1.44	127.89	Open
AT-42	44.77	1.47	94.74	Open
AT-43	35.08	1.15	60.29	Open
AT-44	35.08	4.61	1764.02	Open
AT-45	35.08	2.05	244.79	Open
AT-46	53.11	0.78	18.04	Open
AT-47	53.11	3.11	527.81	Open
AT-48	31.97	4.21	1485.55	Open
AT-49	53.11	3.11	527.81	Open
AT-50	4.60	0.27	5.67	Open
AT-51	4.60	0.60	40.92	Open
AT-52	21.14	0.70	23.61	Open
AT-53	16.55	0.54	15.00	Open
AT-54	16.55	2.18	438.75	Open
AT-55	16.55	0.97	60.89	Open
S67-1	8.52	1.12	128.42	Open
S67-2	44.01	2.57	372.59	Open
S67-3	52.53	3.07	517.16	Open
S67-4	52.53	1.73	127.37	Open
S67-5	52.32	6.88	3698.84	Open
S67-6	52.32	3.06	513.28	Open
S67-7	52.53	0.77	17.67	Open
S67-8	126.01	1.84	89.35	Open
S67-9	126.01	1.84	89.30	Open
S67-10	104.85	1.53	63.56	Open
S67-11	21.16	0.70	23.64	Open
S67-12	21.16	0.70	23.64	Open
S67-13	21.15	2.78	691.43	Open
S67-14	21.16	1.24	95.98	Open
S67-15	53.43	0.44	4.49	Open
S67-16	53.43	0.44	4.49	Open
S67-17	74.07	0.61	8.22	Open
S67-18	0.00	0.00	0.00	Open
S67-19	0.00	0.00	0.00	Open

Page 2185
Link Results at 6:05 Hrs: (continued)

Link ID	Flow LPM	Velocity m/s	Unit Headloss m/km	Status
S67-20	53.43	0.78	18.24	Open
S67-21	7.69	1.01	106.24	Open

S67-22	0.00	0.00	0.00	Open
S67-23	0.00	0.00	0.00	Open
S67-24	7.69	1.01	106.22	Open
S67-25	7.70	1.01	106.37	Open
S67-26	14.44	1.90	340.97	Open
S67-27	14.44	1.90	341.00	Open
S67-28	7.70	0.45	14.76	Open
S67-29	22.14	1.29	104.39	Open
S67-30	22.14	0.73	25.71	Open
S67-31	0.00	0.00	0.00	Open
S67-32	0.00	0.00	0.00	Closed
S67-33	31.28	4.12	1427.11	Open
S67-34	31.28	4.12	1426.81	Open
S67-35	22.14	0.73	25.71	Open
S67-36	53.42	1.76	131.40	Open
S67-37	-0.00	0.00	0.00	Open
S67-38	53.43	1.76	131.31	Open
S67-39	53.43	1.76	131.41	Open
S67-40	0.00	0.00	0.00	Open
S67-41	0.00	0.00	0.00	Open
S67-42	-0.01	0.00	0.00	Open
S67-43	0.00	0.00	0.00	Open
S67-44	0.00	0.00	0.00	Open
S67-45	0.00	0.00	0.00	Closed
S67-46	-0.00	0.00	0.00	Open
S67-47	-0.00	0.00	0.00	Open
S67-49	53.43	1.76	131.43	Open
S67-50	53.43	0.78	18.24	Open
CT-1	20.64	0.68	22.57	Open
CT-2	20.64	0.68	22.58	Open
CT-3	20.64	1.21	91.67	Open
CT-4	20.64	2.72	660.61	Open
CT-5	20.64	2.72	660.61	Open
CT-7	11.94	1.57	239.72	Open
CT-8	0.00	0.00	0.00	Closed
CT-9	11.94	1.57	239.70	Open
CT-12	0.00	0.00	0.00	Open
CT-13	0.00	0.00	0.00	Closed
CT-14	259.15	0.95	11.61	Open
CT-15	259.15	0.95	11.60	Open
CT-16	34.50	4.54	1710.48	Open
CT-17	34.50	4.54	1710.48	Open
CT-18	259.15	0.95	11.61	Open
CT-19	224.65	0.82	8.91	Open
CT-20	224.65	1.85	64.20	Open

Page 2186
Link Results at 6:05 Hrs: (continued)

Link ID	Flow LPM	Velocity m/s	Unit Headloss m/km	Status
CT-21	41.84	2.45	339.29	Open
CT-22	41.84	5.50	2445.18	Open
CT-23	41.84	2.45	339.29	Open
CT-24	182.81	1.50	43.83	Open
CT-25	54.70	1.80	137.27	Open
CT-26	54.70	1.80	137.28	Open

CT-27	21.56	1.26	99.40	Open
CT-28	21.56	1.26	99.40	Open
CT-29	21.56	2.84	716.32	Open
CT-30	33.14	4.36	1587.63	Open
CT-31	33.14	1.94	220.34	Open
CT-32	128.11	1.05	22.69	Open
CT-33	63.39	8.34	5278.90	Open
CT-34	63.39	8.34	5279.01	Open
CT-35	128.11	1.87	92.12	Open
CT-36	64.72	0.95	26.01	Open
CT-37	64.72	0.95	26.01	Open
CT-38	40.42	5.32	2294.09	Open
CT-39	40.42	5.32	2294.03	Open
CT-40	64.72	2.13	187.44	Open
CT-41	24.30	0.80	30.54	Open
CT-42	8.35	0.27	4.23	Open
CT-43	8.35	1.10	123.58	Open
CT-44	8.35	0.49	17.16	Open
CT-45	15.95	0.52	14.01	Open
CT-46	15.95	2.10	409.68	Open
CT-47	15.95	0.93	56.85	Open
S8-1	31.68	1.85	202.66	Open
S8-2	0.00	0.00	0.00	Open
S8-3	6.91	0.91	86.97	Open
S8-4	6.90	0.91	86.92	Open
S8-5	24.77	3.26	926.31	Open
S8-6	0.00	0.00	0.00	Open
S8-7	31.68	1.85	202.66	Open
S8-8	31.68	1.04	49.91	Open
S8-9	25.46	3.35	974.48	Open
S8-10	25.46	1.49	135.23	Open
S8-11	57.14	1.88	148.81	Open
S8-12	57.14	1.88	148.81	Open
S8-13	23.30	3.07	827.31	Open
S8-14	23.31	1.36	114.83	Open
S8-15	80.44	2.65	280.42	Open
S8-16	188.81	2.76	188.92	Open
S8-17	16.90	2.22	455.79	Open
S8-18	16.91	0.99	63.26	Open
S8-19	108.37	1.58	67.56	Open
S8-20	188.81	2.76	188.93	Open

Page 2187
Link Results at 6:05 Hrs: (continued)

Link ID	Flow LPM	Velocity m/s	Unit Headloss m/km	Status
S8-21	0.00	0.00	0.00	Open
S8-22	0.00	0.00	0.00	Open
S8-24	91.46	1.34	49.35	Open
S8-25	32.42	4.27	1524.66	Open
S8-26	32.42	1.90	211.59	Open
S8-27	32.42	1.07	52.12	Open
S8-28	91.46	1.34	49.35	Open
S8-29	59.04	1.94	158.11	Open
S8-30	59.04	1.94	158.11	Open

S8-31	29.79	3.92	1303.20	Open
S8-32	29.79	3.92	1303.16	Open
S8-33	29.25	1.71	174.87	Open
S8-34	29.25	1.71	174.83	Open
S8-35	24.77	3.26	926.23	Open
CH-43	0.00	0.00	0.00	Open
CH-44	0.00	0.00	0.00	Open
CH-45	222.15	0.81	8.71	Open
CH-46	222.15	0.81	8.73	Open
BT-48	-0.00	0.00	0.00	Open
BT-49	0.00	0.00	0.00	Open
BT-50	238.99	0.87	9.99	Open
BT-51	238.99	0.87	9.99	Open
BT-14!	22.63	0.74	26.79	Open
CH-44!	222.15	0.81	8.74	Open
BT-49!	238.99	0.87	10.05	Open
S17-01	210.50	0.77	7.90	Open
TB-01	100.11	3.29	420.51	Open
MOI-01	473.47	1.73	35.46	Open
CT-01	333.21	1.22	18.49	Open
AT-OLD01	253.14	3.70	325.19	Open
S17-0	76.38	0.16	0.33	Open
S17-0!	76.38	0.63	8.71	Open
S67-0!	0.00	0.00	0.00	Open
S67-0	0.00	0.00	0.00	Open
CT-11!!	2.66	0.01	0.00	Open
CT11!	2.66	0.35	14.87	Open
CT-10!	9.28	1.22	150.26	Open
CT-10!!	9.26	0.02	0.00	Open
CT-6!	8.70	1.14	133.41	Open
CT-6!!	8.70	0.02	0.00	Open
S8-23!	0.00	0.00	0.00	Open
S8-23!!	-0.00	0.00	0.00	Open
3	0.10	0.00	0.00	Open
4	0.10	0.00	0.00	Open
5	0.10	0.00	0.00	Open
6	0.10	0.00	0.00	Open
8	0.10	0.00	0.00	Open

Page 2188
Link Results at 6:05 Hrs: (continued)

Link ID	Flow LPM	Velocity m/s	Unit Headloss m/km	Status
9	0.10	0.00	0.00	Open
10	0.10	0.00	0.00	Open
11	0.10	0.00	0.00	Open
12	0.10	0.00	0.00	Open
13	0.10	0.00	0.00	Open
14	0.10	0.00	0.00	Open
15	0.10	0.00	0.00	Open
MOI-51!	33.02	4.34	1577.58	Open
PTB	-0.00	0.00	-13.33	Open Pump
V-T18-S17	19.33	0.64	0.00	Open Valve
V1-S17	19.34	0.64	0.00	Open Valve
V-ML2	19.34	0.28	0.00	Open Valve

V-T19-S17	0.01	0.00	0.00	Open Valve
V-T17-S17	0.00	0.00	0.00	Open Valve
V-T16-S17	8.51	0.50	0.00	Open Valve
V-T21-S17	0.00	0.00	0.00	Open Valve
V-T15-S17	0.00	0.00	0.00	Open Valve
V-T14-S17	13.37	0.78	0.00	Open Valve
V-T13-S17	5.78	0.19	0.00	Open Valve
V-T12-S17	0.00	0.00	0.00	Open Valve
V-TNEW-S17	9.85	1.30	0.00	Open Valve
V-T11-S17	0.00	0.00	0.00	Open Valve
V-T10-S17	13.39	1.76	0.00	Open Valve
V-S17beforeT10	127.29	1.05	0.00	Open Valve
V-T7/8-S17	0.00	0.00	0.00	Open Valve
V-T9-S17	0.00	0.00	0.00	Open Valve
V-T6-S17	15.59	0.91	0.00	Open Valve
V-T5-S17	26.96	1.58	0.00	Open Valve
V-T4-S17	17.89	0.59	0.00	Open Valve
V-T3-S17	0.00	0.00	0.00	Open Valve
V-T2-S17	22.75	1.33	0.00	Open Valve
V-PTB	0.00	0.00	0.00	Closed Valve
V-TBR	0.00	0.00	0.00	Open Valve
V1-BT	23.47	0.77	0.00	Open Valve
V-T3-BT	23.08	1.35	0.00	Open Valve
V2-BT	23.13	0.76	0.00	Open Valve
V-T1-BT	22.63	0.74	0.00	Open Valve
V-branchT4-BT	106.21	1.55	0.00	Open Valve
V-branchT10-BT	105.58	1.54	0.00	Open Valve
V-branchT5-BT	27.20	1.59	0.00	Open Valve
V-T13-BT	-0.00	0.00	0.00	Open Valve
V-T5-BT	14.79	1.95	0.00	Open Valve
V-T6-BT	12.41	0.73	0.00	Open Valve
V-T7-BT	44.28	2.59	0.00	Open Valve
V-T9/10-BT	26.90	1.57	0.00	Open Valve
V-T8-BT	24.47	1.43	0.00	Open Valve
V-T9-BT	0.00	0.00	0.00	Open Valve

Page 2189
Link Results at 6:05 Hrs: (continued)

Link ID	Flow LPM	Velocity m/s	Unit Headloss m/km	Status
V-T10-BT	26.90	1.57	0.00	Open Valve
V-T3-MOI	8.74	1.15	0.00	Open Valve
V-toT7-MOI	16.87	0.99	0.00	Open Valve
V-T7-MOI	16.85	0.99	0.00	Open Valve
V-JT7-MOI	0.01	0.00	0.00	Open Valve
V-brancT29-MOI	153.11	0.56	0.00	Open Valve
V-T26-MOI	17.60	0.58	0.00	Open Valve
V-JT9-MOI	91.97	1.34	0.00	Open Valve
V-T150-MOI	14.55	1.91	0.00	Open Valve
V-T24-MOI	16.06	2.11	0.00	Open Valve
V-T25-MOI	22.96	1.34	0.00	Open Valve
V-T20-MOI	8.43	1.11	0.00	Open Valve
V-T21-MOI	8.83	0.52	0.00	Open Valve
V-T15-MOI	29.61	3.90	0.00	Open Valve
V-T16-MOI	32.02	4.21	0.00	Open Valve

V-T17-MOI	13.57	0.79	0.00	Open Valve
V-T18-MOI	15.75	2.07	0.00	Open Valve
V-T13-MOI	15.87	2.09	0.00	Open Valve
V-brancT12-MOI	189.15	0.69	0.00	Open Valve
V-T14-MOI	22.87	1.34	0.00	Open Valve
V-T8-MOI	27.45	3.61	0.00	Open Valve
V-T9-MOI	60.42	3.53	0.00	Open Valve
V-T11-MOI	21.59	1.26	0.00	Open Valve
V-T12-MOI	17.10	1.00	0.00	Open Valve
V-bracT3-CH	35.08	1.15	0.00	Open Valve
V-T2-CH	-0.00	0.00	0.00	Open Valve
V-T1-CH	19.79	2.60	0.00	Open Valve
V-T3-CH	15.28	0.89	0.00	Open Valve
V-JT3-CH	174.57	2.55	0.00	Open Valve
V-T4-CH	12.50	1.65	0.00	Open Valve
V-T5-CH	31.59	4.16	0.00	Open Valve
V-brancT10-CH	142.98	2.09	0.00	Open Valve
V-toT18-S17	0.00	0.00	0.00	Open Valve
V5-CH	142.97	2.09	0.00	Open Valve
V-T7-CH	64.44	3.77	0.00	Open Valve
V-T6-CH	35.28	4.64	0.00	Open Valve
V-T11-CH	11.73	0.69	0.00	Open Valve
V-T10-CH	31.52	1.84	0.00	Open Valve
V-T6-AT	27.46	1.61	0.00	Open Valve
V-T5-AT	29.19	1.71	0.00	Open Valve
V-JT1-AT	-0.00	0.00	0.00	Open Valve
V-S14RING	14.36	0.21	0.00	Open Valve
V-JT5-AT	56.65	1.86	0.00	Open Valve
V-T13-AT	17.35	1.01	0.00	Open Valve
V-T9-AT	12.86	1.69	0.00	Open Valve
V-T10-AT	0.00	0.00	0.00	Closed Valve
V-T1-AT	25.79	1.51	0.00	Open Valve

Page 2190
Link Results at 6:05 Hrs: (continued)

Link ID	Flow LPM	Velocity m/s	Unit Headloss m/km	Status
V-T7-AT	24.70	1.44	0.00	Open Valve
V-T8-AT	35.08	2.05	0.00	Open Valve
V-T2B-AT	31.97	1.87	0.00	Open Valve
V-T11-AT	4.59	0.27	0.00	Open Valve
V-T3-AT	16.55	0.97	0.00	Open Valve
V-T2-S67	52.32	3.06	0.00	Open Valve
V-S67RING	126.01	1.84	0.00	Open Valve
V1-S67	21.16	0.70	0.00	Open Valve
V-T1-S67	-0.00	0.00	0.00	Open Valve
V-toS67RING	53.43	0.44	0.00	Open Valve
V-pourS67RING	0.00	0.00	0.00	Closed Valve
V7-CH	0.00	0.00	0.00	Closed Valve
V-18-5	0.00	0.00	0.00	Closed Valve
V-T5-S67	7.70	1.01	0.00	Open Valve
V-T7-S67	14.44	1.90	0.00	Open Valve
V-TNEW-S67	0.00	0.00	0.00	Open Valve
V-T4-S67	31.28	4.12	0.00	Open Valve
V2-S67	53.42	1.76	0.00	Open Valve

V-ML1-S67	0.01	0.00	0.00	Open Valve
V-brancT5-S67	53.43	1.76	0.00	Open Valve
V-toTIMhouse	0.00	0.00	0.00	Open Valve
V-toML1	0.00	0.00	0.00	Open Valve
V3-S67	0.00	0.00	0.00	Open Valve
V4-S67	0.00	0.00	0.00	Open Valve
V-brancT8-CT	259.15	0.95	0.00	Open Valve
V-T1-CT	34.50	4.54	0.00	Open Valve
V-T3-CT	41.84	2.45	0.00	Open Valve
V2-CT	41.84	2.45	0.00	Open Valve
V3-CT	54.70	1.80	0.00	Open Valve
V4-CT	21.56	1.26	0.00	Open Valve
V-T4-CT	33.14	1.94	0.00	Open Valve
V-T5-CT	63.39	8.34	0.00	Open Valve
V5-CT	64.72	0.95	0.00	Open Valve
V-T6-CT	40.42	5.32	0.00	Open Valve
V-T7-CT	8.35	0.49	0.00	Open Valve
V-T8-CT	15.95	0.93	0.00	Open Valve
V-JT1-S8	6.91	0.91	0.00	Open Valve
V-T3-S8	24.77	3.26	0.00	Open Valve
V-T2-S8	25.46	1.49	0.00	Open Valve
V-JT4-S8	57.13	1.88	0.00	Open Valve
V-T1-S8	23.31	1.36	0.00	Open Valve
V-JT5-S8	188.81	2.76	0.00	Open Valve
V-T4-S8	16.90	0.99	0.00	Open Valve
V-toS8RING	0.00	0.00	0.00	Closed Valve
V6-S8	91.46	1.34	0.00	Open Valve
V-T5-S8	32.42	1.90	0.00	Open Valve
V-T6-S8	29.79	3.92	0.00	Open Valve

Page 2191
Link Results at 6:05 Hrs: (continued)

Link ID	Flow LPM	Velocity m/s	Unit Headloss m/km	Status
V-JT6-S8	29.25	1.71	0.00	Open Valve
V-CHT2	0.00	0.00	0.00	Closed Valve
V-CHT1	222.15	0.81	0.00	Open Valve
V-CHTout	222.15	0.81	0.00	Open Valve
V-BT2	0.00	0.00	0.00	Closed Valve
V-BT1	238.99	0.87	0.00	Open Valve
V-Btout	238.99	0.87	0.00	Open Valve
V-17Tout	210.50	0.77	0.00	Open Valve
V-TBRINGSout	100.11	3.29	0.00	Open Valve
V-MOITout	473.47	1.73	0.00	Open Valve
V-CTout	333.22	1.22	0.00	Open Valve
V-AT-OLDout	253.14	3.70	0.00	Open Valve
PSV-MAELA2	76.38	1.74	0.00	Open Valve
PSV-ML1	0.00	0.00	0.00	Closed Valve
PSV-TEMRIN2	2.66	0.35	0.00	Open Valve
PSV-TEMRIN3	9.26	1.22	0.97	Active Valve
PSV-TEMRIN1	8.70	1.14	0.00	Open Valve
PSV-S8RIN	0.00	0.00	0.00	Open Valve
FCV-CHT1	0.10	0.00	8.32	Active Valve
FCV-AT-OLD	0.10	0.00	8.03	Active Valve
FCV-MOIT	0.10	0.00	8.57	Active Valve

FCV-17T	0.10	0.00	7.06	Active Valve
FCV-CT	0.10	0.00	8.02	Active Valve
FCV-BT	0.10	0.00	7.81	Active Valve
V-T23-MOI	33.02	4.34	0.00	Open Valve

Appendix C: Calibration Files

; Flow test measurements (LPM)
;Location Time Value
T2-AT 7:30 18.0514 ;because of the peculiarity of point (one tap to container and other to border tank), I'm assuming that this measurement includes both taps
T16-S17 7:30 26.6148 ;2 taps - pipeline was broken previous night near tap 4 and so couldn't get measurements for all times
T7-MOI 7:30 7.57098 ;2 taps - security guard closed valve to get more to him
T25-MOI 7:30 41.8605 ;3 taps - large variations
T10-AT 7:30 67.1328 ;2 taps
T16-S17 7:30 26.4706 ;2 taps - afternoon, started late
T7-S8 7:30 12.9497 ;3 taps - afternoon no CTank connection, so finished at 16:00 PM
T10-BT 7:30 23.6842 ;3 taps - afternoon
T3-CH 7:30 29.4479 ;1 tap - afternoon
T7-BT 7:30 42.1053 ;2 taps - afternoon
T3-S67 7:30 78.2609 ;3 taps - afternoon
T8-CT 7:30 22.7129 ;3 taps - afternoon
T4-CT 7:30 34.7826 ;2 taps - afternoon
T10-CH 7:30 33.6449 ;3 taps - afernoon
T4-BT 7:30 30.2521 ;2 taps - afternoon
T18-MOI 7:00 22.1311 ;3 taps
T8-AT 7:00 15.142 ;2 taps
T12-MOI 7:00 24.1071 ;3 taps
TB5-S17 7:00 3.52595 ;1 tap

; times were all moved to morning to allow for comparison. Pressure difference is minimal throughout distibution

; Pressure test measurements (m)
;Location Time Value
Vi-T25-MOI 15:01 8.5; T25-MOI
J7-MOI 15:03 9;T29-MOI
Vi-T24-MOI 15:05 7; T24-MOI
Vi-T23-MOI 15:07 5.5; T23-MOI
Vi-T16-S17 15:01 4; T16-S17
J01-BT 15:01 22.5;T4-BT
Vi-T5-AT 15:01 22; T5-AT
;------- first data set taken with 10 bar pressure gage (1 bar = 10 meters = 1 kg/square cm) in morning. Second data set in afternoon with 3 bar gage
Vi-T6-CH 15:01 23; T6-CH
Vi-T7-CH 15:03 21; T7-CH
Vi-T10-CH 15:05 11; T10-CH
;AT T10, T5, T6 are more than 30 meters
Vi-T8-CT 15:01 9; T8-CT
Vi-T7-CT 15:03 9; T7-CT
J4-S17 15:03 2;T13-S17
Vi-T10-BT 15:03 19; T10-BT
Vi-T3-BT 15:05 10; T3-BT
Vi-T12-MOI 15:09 9; T12-MOI
Vi-T11-MOI 15:11 5; T11-MOI

;times were changed for comparison and non-interference with 6 to 9 AM distribution period. Valves were closed at these times to simulate the same kind of testing done on the field

;Salt tracer test results (with background levels) and using a factor of 0.67 between microsiemens/cm and mg/L (tested)

;Location	Time	Value
T16-S17	8:12	448.9
T16-S17	8:15	448.9
T16-S17	8:30	797.3
T16-S17	8:45	676.7
T16-S17	9:00	716.9
T7-MOI	6:45	167.5
T7-MOI	7:00	227.8
T7-MOI	7:15	288.1
T7-MOI	7:30	716.9
T7-MOI	7:45	757.1
T7-MOI	8:00	609.7
T7-MOI	8:15	529.3
T7-MOI	8:30	502.5
T7-MOI	8:45	428.8
T7-MOI	9:00	408.7
T12-MOI	6:05	167.5
T12-MOI	6:15	174.2
T12-MOI	6:30	174.2
T12-MOI	6:45	174.2
T12-MOI	7:00	335
T12-MOI	7:15	676.7
T12-MOI	7:30	737
T12-MOI	7:45	670
T12-MOI	8:00	569.5
T12-MOI	8:15	515.9
T12-MOI	8:30	448.9
T12-MOI	8:45	388.6
T12-MOI	9:00	341.7
TB5-S17	6:00	455.6
TB5-S17	6:15	455.6
TB5-S17	6:30	455.6
TB5-S17	6:45	455.6
TB5-S17	7:00	1112.2
TB5-S17	7:15	850.9
TB5-S17	7:30	830.8
TB5-S17	7:45	536
TB5-S17	8:00	710.2
TB5-S17	8:15	737
TB5-S17	8:30	690.1
TB5-S17	8:45	683.4
TB5-S17	9:00	670
T10-AT	6:08	335
T10-AT	6:15	201
T10-AT	6:30	201
T10-AT	6:45	194.3
T10-AT	7:00	1058.6
T10-AT	7:15	743.7
T10-AT	7:30	616.4
T10-AT	7:45	489.1
T10-AT	8:00	361.8
T10-AT	8:15	301.5

T10-AT	8:30	268	
T10-AT	8:45	201	
T10-AT	9:00	455.6	
T18-MOI		6:00	174.2
T18-MOI		6:15	180.9
T18-MOI		6:30	442.2
T18-MOI		6:45	817.4
T18-MOI		7:00	368.5
T18-MOI		7:15	341.7
T18-MOI		7:30	368.5
T18-MOI		7:45	375.2
T18-MOI		8:00	314.9
T18-MOI		8:15	281.4
T18-MOI		8:30	261.3
T18-MOI		8:45	241.2
T18-MOI		9:00	227.8
T2B-AT	6:00	201	
T2B-AT	6:30	201	
T2B-AT	6:45	938	
T2B-AT	7:00	757.1	
T2B-AT	7:15	603	
T2B-AT	7:30	462.3	
T2B-AT	7:45	368.5	
T2B-AT	8:00	294.8	
T2B-AT	8:15	274.7	
T2B-AT	8:30	247.9	
T2B-AT	8:45	234.5	
T2B-AT	9:00	221.1	
T25-MOI		6:30	281.4
T25-MOI		6:45	469
T25-MOI		7:00	455.6
T25-MOI		7:15	408.7
T25-MOI		7:30	408.7
T25-MOI		7:45	395.3
T25-MOI		8:00	375.2
T25-MOI		8:15	435.5
T25-MOI		8:30	335
T25-MOI		8:45	301.5
T25-MOI		9:00	274.7
T8-AT	6:00	201	
T8-AT	6:15	201	
T8-AT	6:30	201	
T8-AT	6:45	1065.3	
T8-AT	7:00	804	
T8-AT	7:15	629.8	
T8-AT	7:30	489.1	
T8-AT	7:45	375.2	
T8-AT	8:00	321.6	
T8-AT	8:15	281.4	
T8-AT	8:30	247.9	
T8-AT	8:45	234.5	
T8-AT	9:00	214.4	
T10-BT	6:00	154.1	
T10-BT	6:15	154.1	
T10-BT	6:30	160.8	
T10-BT	6:45	475.7	
T10-BT	7:00	703.5	

T10-BT	7:15	569.5
T10-BT	7:30	515.9
T10-BT	7:45	408.7
T10-BT	8:00	335
T10-BT	8:15	281.4
T10-BT	8:30	241.2
T10-BT	8:45	221.1
T10-BT	9:00	201
T3-CH	6:00	160.8
T3-CH	6:15	154.1
T3-CH	6:30	154.1
T3-CH	6:45	797.3
T3-CH	7:00	435.5
T3-CH	7:15	294.8
T3-CH	7:30	221.1
T3-CH	7:45	194.3
T3-CH	8:00	180.9
T3-CH	8:15	174.2
T3-CH	8:30	174.2
T3-CH	8:45	180.9
T3-CH	9:00	234.5
T7-BT	6:00	167.5
T7-BT	6:15	160.8
T7-BT	6:30	160.8
T7-BT	6:45	790.6
T7-BT	7:00	690.1
T7-BT	7:15	636.5
T7-BT	7:30	489.1
T7-BT	7:45	381.9
T7-BT	8:00	321.6
T7-BT	8:15	268
T7-BT	8:30	234.5
T7-BT	8:45	214.4
T7-BT	9:00	194.3
T3-S67	6:00	241.2
T3-S67	6:15	241.2
T3-S67	6:30	234.5
T3-S67	6:45	227.8
T3-S67	7:00	234.5
T3-S67	7:15	241.2
T3-S67	7:30	247.9
T3-S67	7:45	241.2
T3-S67	8:00	241.2
T3-S67	8:15	234.5
T3-S67	8:30	234.5
T3-S67	8:45	241.2
T3-S67	9:00	227.8
T8-CT	6:00	160.8
T8-CT	6:15	160.8
T8-CT	6:30	160.8
T8-CT	6:45	160.8
T8-CT	7:00	676.7
T8-CT	7:15	469
T8-CT	7:30	381.9
T8-CT	7:45	314.9
T8-CT	8:00	261.3
T8-CT	8:15	247.9

T8-CT	8:30	221.1
T8-CT	8:45	207.7
T8-CT	9:00	201
T4-CT	6:00	154.1
T4-CT	6:15	154.1
T4-CT	6:30	160.8
T4-CT	6:45	214.4
T4-CT	7:00	469
T4-CT	7:15	435.5
T4-CT	7:30	355.1
T4-CT	7:45	288.1
T4-CT	8:00	247.9
T4-CT	8:15	227.8
T4-CT	8:30	214.4
T4-CT	8:45	187.6
T4-CT	9:00	180.9
T10-CH	6:00	154.1
T10-CH	6:15	154.1
T10-CH	6:30	154.1
T10-CH	6:45	1299.8
T10-CH	7:00	629.8
T10-CH	7:15	375.2
T10-CH	7:30	268
T10-CH	7:45	221.1
T10-CH	8:00	187.6
T10-CH	8:15	180.9
T10-CH	8:30	180.9
T10-CH	8:45	180.9
T10-CH	9:00	187.6
T4-BT	6:30	160.8
T4-BT	6:45	623.1
T4-BT	7:00	643.2
T4-BT	7:15	609.7
T4-BT	7:30	549.4
T4-BT	7:45	428.8
T4-BT	8:00	355.1
T4-BT	8:15	301.5
T4-BT	8:30	247.9
T4-BT	8:45	214.4
T4-BT	9:00	214.4
T7-S8	6:15	314.9
T7-S8	6:30	442.2
T7-S8	6:45	234.5
T7-S8	7:00	288.1
T16-S17	8:00	576.2
T16-S17	8:15	716.9
T16-S17	8:30	670
T16-S17	8:45	656.6
T16-S17	9:00	629.8

Appendix D: Dispersion Calculations

Calculation of dispersion from Tank 17 to T16-S17

ID	Length (m)	Diameter (mm)	Avg velocity (m/s)	Head loss (m/1000m)	Avearge shear stress (N/m²)	Shear velocity (m/s)	Dispersion (m² /s)
S17-01	2	76.2	0.77	7.81	1.458	0.038	0.015
S17-80	19	76.2	0.77	7.82	1.460	0.038	0.015
S17-76	1	50.8	1.72	56.35	7.013	0.084	0.021
S17-75	26	50.8	1.72	56.35	7.013	0.084	0.021
S17-74	85	50.8	1.72	56.35	7.013	0.084	0.021
S17-71	187	50.8	1.54	45.65	5.682	0.075	0.019
S17-68	71	50.8	1.54	45.64	5.680	0.075	0.019
S17-64	227	50.8	1.32	37.91	4.718	0.069	0.018
S17-59	59	50.8	1.04	22.18	2.761	0.053	0.013
S17-54	22	50.8	1.04	22.18	2.761	0.053	0.013
S17-48	119	50.8	1.04	22.18	2.761	0.053	0.013
S17-43	286	50.8	0.93	18.02	2.243	0.047	0.012
S17-40	214	50.8	0.93	18.02	2.243	0.047	0.012
S17-36	63.6	50.8	0.85	15.14	1.884	0.043	0.011
S17-33	118	50.8	0.85	15.14	1.884	0.043	0.011
S17-29	113	50.8	0.79	13.26	1.650	0.041	0.010
S17-23	156	50.8	0.67	9.93	1.236	0.035	0.009
S17-18	37	50.8	0.67	9.93	1.236	0.035	0.009
S17-6	26	50.8	0.67	9.93	1.236	0.035	0.009
S17-20	15	19.05	0.67	31.18	1.455	0.038	0.004

Average dispersion: 0.014 m^2/s

Total length: 1846.6 m
Average velocity: 1.06 m/s
Average time of travel: 29 min

Standard deviation of mass distribution

$$D = \frac{\sigma^2}{2t}$$

$$\Leftrightarrow \sigma = \sqrt{D \cdot 2t}$$
$$\Leftrightarrow \sigma = 6.95\ m$$